

STRESS CONCENTRATIONS
IN LOAD BEARING
BRICKWORK DETAILS

THESIS SUBMITTED FOR THE DEGREE

OF

DOCTOR OF PHILOSOPHY

OF THE

UNIVERSITY OF EDINBURGH

by

Duncan J. Rutherford, B.Sc., M.Sc.

May 1968



ACKNOWLEDGEMENTS

The author wishes to thank Professor A.W. Hendry for providing the opportunity to carry out this research under his personal supervision.

The British Ceramic Research Association is thanked for providing the model bricks used.

The Brick Development Association is thanked for its general financial assistance.

The help of Miss Isabel McCabe in typing the thesis, and of Miss Pauline Anderson for photographic work is gratefully acknowledged.

Thanks are also given to the technical staff of the department.

CONTENTS

	<u>Page</u>
<u>Acknowledgements</u>	(i)
<u>Contents</u>	(ii)
<u>Synopsis</u>	(xv)
<u>Chapter 1</u>	
<u>An introduction to the problem of stress concentrations in load bearing brickwork</u>	
1. Brickwork as a structural medium	1
2. A review of previous work	
2.1 Early investigations	4
2.2 Bearing capacity research	5
2.3 Swiss wall tests and research	9
2.4 The experimental and theoretical work of Hast	9
2.5 The theoretical investigations of Vogt, Haller and Sinha	13
2.6 Recent Russian research	15
2.7 Local stress concentrations at a lintel support	16
2.8 British standard code of practice	17
3. The scope of the present investigation	
3.1 Theoretical investigations	19
3.2 Experimental investigations	20
<u>Chapter 2</u>	
<u>A review of previous theoretical and experimental work on stress concentrations</u>	
1. Introduction	22
2. Boussinesq's stress distribution theory	23
3. Flamant's contribution	25

	<u>Page</u>
4. Any vertical loading of a straight boundary	27
5. A force acting on the end of a wedge	
5.1 The generalised case	30
5.2 A force acting on a 90° wedge	31
6. Coker and Filon's contribution	
6.1 The theoretical solution of stress concentrations	33
6.2 The stress distribution in a long rectangular plate subjected to a concentrated loading	34
6.3 The stress distribution in short rectangular blocks subjected to a concentrated load	35
7. Shepherd's contribution	35
8. Theoretical solutions for concentrated forces applied to members of finite size	
8.1 Introduction	36
8.2 Morsch's theory	37
8.3 Bortsch's theory	37
8.4 Magnel's theory	38
8.5 Chaikes' theory	38
8.6 Guyon's theory	39
8.7 Bleich's theory	39
8.8 Gerstner and Zienkiewicz's contribution	39
8.9 Sundara Raja Iyengar's elastic solution	40
8.10 A solution by lattice analogy	41
9. A comparison of the two dimensional solutions	41
10. Three dimensional solutions	

	<u>Page</u>
10.1 Guyon's solution	42
10.2 Sievers' theory	42
10.3 Douglas and Trahair's contribution	42
10.4 Iyengar's and Yogananda's elastic theory	43
11. A comparison of the three dimensional analyses	44
12. Experimental investigations of concentric concentrated loadings	
12.1 The work of Christodoulides	44
12.2 The work of Ban, Nugurama and Ogaki	45
12.3 The experiments of Douglas and Trahair	45
12.4 The experiments of Zielinski and Rowe	46
12.5 Bauschinger's tests on sandstone cubes	48
12.6 Meyerhof's tests and theory	49
12.7 The work of Au and Baird	51
12.8 The work of Shelson	52
12.9 The work of Campbell-Allen, Middendorf, Lin and Hawkins	53
13. Experimental investigations of eccentrically applied concentrated loadings	
13.1 The tests of Kriz and Rath	53
13.2 Campbell-Allen's investigation	55
13.3 The work of Adams, Baron and Plewes	55
14. A summary of the results of tests carried out on concrete blocks	56

	<u>Page</u>
15. Ghosh's investigation of beams supported on bearing blocks	
15.1 Object and types of test conducted	56
15.2 Test results	57
16. Design specifications in current codes of practice	
16.1 Introduction	58
16.2 Information given by codes of practice	58
16.3 Recommended design specifications	60
16.4 Comments on specifications and recommendations	62
17. A discussion of the theoretical and experimental investigations outlined above	62
18. A photo-elastic investigation of the stress distribution due to arbitrarily placed concentrated loadings on rectangular plates	63
19. A photo-elastic investigation of the stresses in brickwork subjected to a uniformly distributed load	65
20. The application of theoretical and experimental results to brickwork	66

Chapter 3

Full-scale brickwork tests

1. Scope of the investigations	69
2. The failure stresses of, and strain distributions in, brick walls subject to stress concentrations	69

	<u>Page</u>
2.1 Introduction	70
2.2 Materials used	70
2.3 Preparation of specimens	71
2.4 Testing equipment	73
2.5 Pier tests	73
2.6 Results	74
2.7 Discussion of results	75
2.8 Central loading tests	86
2.9 Conclusions	87
3. The effect of the variation of the bearing plate position on the strain distribution in a brickwork pier	
3.1 Introduction	90
3.2 Scope of the test programme	91
3.3 Test procedure	93
3.4 Test results	93
3.5 Discussion of results	96
3.6 A comparison of the results with photo-elastic tests	100
3.7 Conclusions	101

Chapter 4

Model Work

1. A review of previous investigations of the model technique applied to load bearing brick structures	
1.1 Introduction	105

	<u>Page</u>
1.2 Benjamin and Williams	105
1.3 Vogt	106
1.4 Murthy	107
1.5 Sinha	110
1.6 General conclusions	111
2. The scope of the model investigation undertaken	
2.1 The basic aims	112
2.2 Materials used	113
2.3 The physical and structural properties of the bricks and mortar	113
2.4 The elastic properties of the bricks and mortar	113
2.5 The elastic properties of the brickwork	114
2.6 The strength and elastic properties of brickwork cubes	114
2.7 Failure stresses under concentrated load	114
2.8 The strain distribution under concentrated load	114
2.9 The effect of edge distance	114
2.10 Cavity wall tests	114

Chapter 5

The physical, structural and elastic properties of the materials used for the model tests

1. The physical and structural properties of the bricks, sand and mortar	
1.1 Bricks	116
1.2 Sand	119

	<u>Page</u>
1.3 Mortar	119
2. The elastic properties of the bricks and mortar	
2.1 Bricks	119
2.2 Mortar	120
3. The elastic properties of the brickwork	
3.1 1/6th scale	121
3.2 1/3rd scale - type I bricks	121
3.3 1/3rd scale - type II bricks	122
4. Model brickwork cubes	
4.1 Discussion of the brickwork cube test	122
4.2 Elastic properties of the 9" brickwork cube	124
4.3 The scope of the test programme	125
4.4 Test results and observations	126
4.5 Discussion of results	128

Chapter 6.

Concentrated loading on model brick walls.

1. The scope of the investigation	
1.1 The variation of bearing plate length	134
1.2 The effect of edge distance	134
1.3 Age factor	134
1.4 Strain measurement	134
2. The test programme	
2.1 Models constructed	134
2.2 Series I tests	135
2.3 Series II tests	135

	<u>Page</u>
3. Materials used	
3.1 Bricks	136
3.2 Sand	136
3.3 Mortar	136
4. Dimensions of models	136
5. Method of model construction	137
6. The curing of specimens	137
7. The method of testing	
7.1 Preparation of the specimens	137
7.2 Loading conditions	138
7.3 Bearing plates	138
7.4 The rate of load application	138
8. The results of tests	
8.1 1/6th scale tests	139
8.2 1/3rd scale tests	140
8.3 Edge distance effects	140
8.4 Strain measurements	140
8.5 Modes of failure	141
9. Discussion of test results	
9.1 End bearing tests	141
9.2 Central bearing tests	142
9.3 A comparison of central and end bearing plate results	143
9.4 Statistical aspects of the results obtained	144
9.5 A comparison of test results and code requirements	145

	<u>Page</u>
9.6 Edge distance effects	148
9.7 Initial cracking stress	149
9.8 Modes of failure	150
9.9 Strain measurements	152
10. Conclusions	155

Chapter 7

Cavity walls - an introduction.

1. General considerations	192
2. Previous experimental investigations	
2.1 Wall tie tests	194
2.2 Load distribution tests	196
3. A theoretical investigation of the stress distribution in a cavity wall	
3.1 Assumptions	202
3.2 Calculation of stresses	202

Chapter 8.

The cavity wall test programme.

1. The objective of the test programme	205
2. The materials used	
2.1 Bricks	205
2.2 Mortar	205
2.3 Floor slab or lintel	205
2.4 Wall ties	206
2.5 Wall construction	206

	<u>Page</u>
3. The scope of the investigation	
3.1 Nature of test programme	207
3.2 Distributed load investigation	208
3.3 Concentrated load investigation	208
3.4 Lateral deflection profiles	208
4. Method of strain measurement	209
5. Experimental details	
5.1 Test arrangement	209
5.2 Load application	209
5.3 Load range	210
5.4 Zero readings	211

Chapter 9

Preliminary investigations of the strain distribution in a cavity wall

1. The cavity wall under test	212
2. Types of loading	
2.1 Uniformly distributed load	212
2.2 Concentrated central loading	212
2.3 Concentrated eccentric loading	212
3. Measurements taken	
3.1 Strain measurements	213
3.2 Lateral deflection measurements	213
4. Results of the test programme	
4.1 Stress/strain characteristics with distributed applied load	213

	<u>Page</u>
4.2 Stress/strain characteristics with concentrated applied load	215
4.3 Lateral deflection profile	216
5. Discussion of test results	
5.1 Distributed loadings	216
5.2 Concentrated loadings	222
5.3 Lateral deflection profile	226
6. Conclusions	
6.1 Transfer of bending moment	227
6.2 Strain distribution	227
6.3 Elastic properties	228

Chapter 10

A detailed investigation of the strain distribution in the leaves of a cavity wall

1. The cavity wall under investigation	229
2. Types of loading	
2.1 Uniformly distributed load	229
2.2 Concentrated loadings	229
3. The strain measurements made	
3.1 Measurements on the faces of the leaves	230
3.2 Measurements on the ends of the leaves	230
4. Lateral deflection measurements	230
5. The results of the test programme	
5.1 Strain measurements on the faces of the leaves	231

	<u>Page</u>
5.2 Strain measurements on the ends of the leaves	232
5.3 Lateral deflection profiles	232
6. Discussion of results	
6.1 Strains on the faces of the leaves	233
6.2 Strains on the ends of the leaves	234
6.3 Lateral deflection profiles	235
7. An analysis of the behaviour of the cavity walls tested	
7.1 The neutral axis of the cavity wall	237
7.2 The behaviour of the walls as units	237
8. Conclusions	239
 <u>Chapter 11</u>	
 <u>Conclusions</u>	
1. Introduction	241
2. Bearing stresses	
2.1 Experimental results	241
2.2 The correlation of test results with theoretical concepts and other experimental work	244
3. The load distribution at a stress concentration	
3.1 Single leaf walls	247
3.2 Cavity walls	248
4. The deformation characteristics of brickwork	250
5. Summary	251

References

- Tables - are presented at the end of each chapter.
- Figures - are presented where relevant in the text.
- Plates - are presented where relevant in the text.

SYNOPSIS

The problem of stress concentrations in brickwork is of increasing importance if brickwork is to be used as a designed engineering material in multi-storey construction.

The work described in this thesis was mainly of an experimental nature, and the results obtained have been compared with various other theoretical and experimental investigations, reviewed in Chapter 2.

Two investigations of full-scale brickwork walls subjected to stress concentrations are described in Chapter 3. The strain distributions and the failure stresses were investigated, when the walls were subject to central or end loadings of various lengths, applied through a rigid metal plate. The strain distribution was also investigated for any position of loading. The use of a model technique for brickwork is discussed in Chapter 4, and a series of preliminary tests on the model materials, and the brickwork constructed from them, are described in Chapter 5. 1/6th and 1/3rd scale model bricks were used.

The full-scale tests described in Chapter 3 were extended, using 1/6th and 1/3rd scale models, and the results of the full-scale, 1/6th scale and 1/3rd scale were found to correlate, when compared non-dimensionally. Results are described in Chapter 6.

From the full-scale, 1/6th scale and 1/3rd scale tests certain conclusions have been reached concerning the effect of the bearing plate length and its position on the failure stresses. A comparison of the results and the requirements of the code (C.P.111:1964) has

been made, in Chapters 6 and 11.

The cavity wall, as a structural unit, is discussed in Chapter 7, and the results of two series of non-destructive tests investigating the application of concentrated loads to a cavity wall are described in Chapters 9 and 10. The tests were concerned with the strain distributions in the cavity wall, particularly when the walls were subject to eccentric loading. The strain was investigated on the leaves, and across the leaves of the wall.

The mode of behaviour of brickwork subjected to a stress concentration was found to be similar to that of an elastic homogeneous material, but theoretically predicted failure stresses were greater than the experimental values. The trends of theoretical and experimental values were similar.

CHAPTER 1.

AN INTRODUCTION TO THE PROBLEM OF STRESS
CONCENTRATIONS IN LOAD BEARING BRICKWORK.

1. BRICKWORK AS A STRUCTURAL MEDIUM.

As recently as 1950 it seemed likely that brickwork had been superseded as a structural medium by steelwork and latterly by reinforced concrete.

At this time many new structural mediums started to come onto the market, and the advantages of prefabricated and system building were realised. Indeed, even the use of brickwork as a curtain wall in framed buildings was threatened by the advent of metal and glass curtain walling.

The reduction in the status of brickwork from that of a structural medium to that of one used mainly for the construction of single and two storey domestic dwellings may have passed partially unnoticed by the brick manufacturing industries, as it occurred during a period of increased domestic dwelling programmes, and general industrial expansion, which reached their climax in the brick shortage of 1964.

Since 1964, however, it has become increasingly obvious that competition in the housing sector, from industrialised system building, is going to pose an increasing problem in the future.

The reason for the reduction in the use of brickwork has mainly been a lack of knowledge about its structural capacities, and about design procedures which will enable it to be used for multi-storey buildings. At the present time, civil engineering undergraduates are taught the principles of design for reinforced concrete, structural

steelwork, prestressed concrete and shells but very few learn of brickwork as a structural medium.

The structural capacity and behaviour of brickwork units, considered singly, and of combinations of units in the form of a brickwork structure, with reinforced concrete floor slabs, may only be determined by experimental tests. These tests should be carried out initially on the single units, and then on combinations of the units. The structural interaction of units or groups of units is very important from the design point of view, particularly in multi-storey structures.

When the experimental behaviour has been investigated it may be possible to correlate the results obtained with known theoretical modes of behaviour of structures constructed of more homogeneous materials.

The practical difficulties involved in testing brick units must, however, be realised as the load capacities required are high, and the type of loading required or shape of the unit, often unsuitable for standard testing machines. Frequently these difficulties have led to the construction of special test frames etc. at a high capital cost, and requiring continual maintenance and supervisory staff.

The advantage that a model analysis would have has been realised for some time, and considerable work has been carried out to justify the model technique. Model work has been carried out on units ranging from single brick tensile specimens, to single wall units, and then to multi-storey structures simulating blocks of flats. In all cases the tests have elucidated the properties of the brickwork, and have clarified the validity of the assumptions used for design.

As in the past brickwork structures were designed by rule of thumb methods the research carried out has generally shown the methods used to be very conservative, although some cases have occurred where while being conservative at certain applied loads the assumptions led to smaller safety factors at other loads, which were not necessarily higher.

Research and testing led to the revision of the British code of practice, C.P.111, which appeared in a revised form in 1964.⁽¹⁾

As design techniques have become more refined the safety factors have, of course, been reduced to more reasonable proportions, and the permissible design stresses consequently increased considerably.

A classic example of this reduction in safety factors is given by a comparison of the Monadnock building with a recent Danish structure. The Monadnock building, constructed in Chicago in 1891, was thought to be the ultimate achievement of a masonry structure. It was sixteen storeys high, and had walls 6'-0" thick at the base, the design procedure being to allow so much extra wall thickness at the base for every storey added. The Danish structure, built in 1963, was also sixteen storeys high, but, by designing on allowable stresses, for walls, built using a particular unit, the wall thickness was reduced to 14" at the base, a reduction of 80% in the quantity of brickwork required in the first storey walls.

With the reduction of safety factors problems which were previously unimportant may become critical. The size of elements decreases with more rational design and the problems of overstressing and the attendant cracking or failure of the structure due to the presence of

concentrated loadings becomes more likely.

Very little experimental work has investigated the factors affecting the failure of a brickwork member subject to a stress concentration. Investigations have been limited to one series of tests conducted between 1930-38. The nature and results of this test series are described in the next section of this Chapter, but it should be said that only a few of the variables involved were thoroughly investigated.

The code of practice, C.P. 111: 1964, is vague on stress concentrations, but allows a 50% increase in the basic permissible stress for a unit, providing the stress caused by the load concentrations can be calculated.

It may be said that the rational design of load bearing brickwork structures has developed considerably over recent years but there are some factors which now require detailed investigation if the designer is to have complete confidence in brickwork as a structural medium. The concentration of stress is one of these factors, and the work described in this thesis is intended to clarify the behaviour of brickwork structures subjected to stress concentrations of various types.

2. A REVIEW OF PREVIOUS WORK.

2.1 EARLY INVESTIGATIONS.

During the present century work has been progressing to elucidate not only the basic properties of the bricks and brickwork, but also the structural interaction of components in a load bearing brickwork structure. The latter is of particular importance, if the design of a brickwork structure is to be based on structural principles, and not

merely rule of thumb and approximate methods that are known to be conservative.

The testing of brick masonry piers started in the U.S.A. in 1882.⁽²⁾ These tests led to the recognition of the influence of the brick unit strength and the mortar strength, on brickwork.

In 1915 a series of tests was carried out at the National Bureau of Standards (U.S.A.). These tests included series on brick piers and walls, and the ultimate strength of brickwork was related to the brick unit strength by a statistical method. The relationship was judged to be linear.

In G.B. from 1926-1934, extensive research was carried out, largely at the Building Research Station.⁽³⁾ This work consisted of loading tests on square brickwork piers, constructed of units of various strengths etc., and the results obtained formed the basis of the 1948 code of practice.

2.2 BEARING CAPACITY RESEARCH.

Towards the end of 1930, the Science Committee of the Institution of Structural Engineers directed their Masonry Sectional Committee to investigate the safe bearing pressure on brickwork carrying a heavy load applied through a steel plate bedded directly onto the brickwork. Work was carried out from 1930-38, and a final report produced⁽⁴⁾. This investigation tried to determine the effect of using bearing plates of different thicknesses, beneath the load, of using stronger bricks in the top courses, and of building in the section through which the load was applied to the bearing plate (an "I" section). The investigation also covered the effect of slenderness

ratio and the deflection of the lintel applying the load.

The number of tests conducted was statistically small, and the results led to no definite conclusions.

Initial bearing tests were carried out on wallettes, 2'-3" x 9" x 18" high and 3'-0" x 9" x 18" high, constructed in Old English bond using Fletton bricks of an unspecified compressive strength (from data available giving Fletton brick strengths it seems likely that the compressive strength was of the order of 3,900 p f. s. i.) A 1:3 (Portland cement: sand), by weight, mortar was used.

Three different types of central load application were investigated.

- a) Load applied through a 6" x 5" x 25 lb. B.S.B. whose flange (5 ins. wide) rested on a mortar bed on the wallette surface.
- b) Load applied through the B.S.B. as in a), but inserting a 10" x 7" x $\frac{1}{2}$ " thick M.S. plate beneath the beam.
- c) As in a) and b) but increasing the M.S. plate thickness to 1".

In cases b) and c) the M.S. plate was set back 1" from the front and rear faces of the wallettes.

In some tests the B.S.B. was built into the wall, and sometimes Staffordshire blue bricks (a high strength brick) were used directly beneath the bearing plate.

The average failure stresses for a), b), c), above were 2,763 pf. s. i., 1,861 pf. s. i., and 2,115 pf. s. i. respectively, indicating that as the 'wall length/bearing plate length' ratio decreases the failure stress also decreases. The result from loading b) 1,863 pfs.i. is difficult to analyse as it would appear that the $\frac{1}{2}$ " thick bearing plate was not giving a rigid bearing condition, and hence the actual effective bearing

plate length could not be determined. Assuming a linear decrease in bearing capacity as the bearing plate size increases a length of rigid bearing of approx. 7 - 7.5" may be obtained for this intermediate condition. The calculation is only approximate as no account has been taken of the effect of the 1" edge distance on the results obtained for the 10" x 7" plates. The edge distance has been shown to be an important factor, and an experimental investigation is described in Chapter 6.

The effect of building in the B.S.B., and using a $\frac{1}{2}$ " thick bearing plate was found to be similar to that of using the 1" bearing plate, and a failure stress of 2,105 p.f.s.i. was observed.

Staffordshire blues were included in the first course, the first two courses, or the first three courses, below the B.S.B. When incorporated into only the first course, the failure stress showed an unexpected decrease of 19.5%. When incorporated into the first and second courses, or the first, second, and third courses the failure stresses were increased by only 3.5% and 6.8% respectively.

The mode of failure of all the wallettes tested included the formation of vertical and diagonal cracks, originating below the point of load concentration.

The effect of slenderness ratio on the failure strength of walls subject to a load concentration was investigated by testing walls 4' and 5' high and $4\frac{1}{2}$ " thick. No discernible weakening of the wallettes was noted in the slenderness ratio range considered, (up to 13.5).

In order to investigate the effect of eccentric loading, caused for example, by a loaded beam spanning into a wall, six walls were

constructed. The dimensions were, 18" long, 4'-0" high and $4\frac{1}{2}$ " thick. These were tested in pairs, with a 10" x 6" R.S.J. spanning 6'-0", and resting on the two walls, perpendicular to their length.

The average failure stress obtained was 1,510 pf. s. i. and failure occurred due to local crushing beneath the bearing, and vertical splitting down the section.

A further series of six walls were constructed and were 3'-0" long, 8'-9" high, and $4\frac{1}{2}$ " thick. Four of the walls contained expanded metal reinforcement in the top four mortar joints, below the R.S.J., which was built in for this series of tests. For the reinforced walls the beam span was increased to 9'-6".

The failure stresses obtained were 1,510 pf. s. i. (unreinforced) and 2,360 pf. s. i. (reinforced). The failure mode was one of vertical splitting below the R.S.J. in all cases, and in one wall the crack appeared to originate in the tenth course down.

Having conducted the considerable number of tests indicated above the Committee came to certain conclusions. Although results indicated that well built brickwork, even in thin walls, acts as a unified mass, and is capable of sustaining load considerably greater than those permitted in the current codes, (1936) they concluded that permissible stresses should not be increased.

They gave two reasons for this decision. The first was the rigid foundation they had adopted, and the second, the high quality of workmanship in the specimens constructed.

They concluded that thin bearing plates were of little use, as was the provision of stronger bricks in only a few courses below the load.

Building the beam into the wall was, however, considered to increase the load capacity of the wall. No comment is made about the effectiveness of rigid bearing plates although their tests indicated that these increased the load capacity of the wall.

The effect of the wall height on the resistance to eccentric loading was not found to be important in the tests conducted, although strains measured on the wall faces were found to indicate much higher compression on the more heavily loaded faces.

2.3 SWISS WALL TESTS AND RESEARCH.

Tests were carried out on 1,600 wall specimens at the Swiss Federal Materials Testing and Research Institution in the late 1940's⁽⁵⁾. These investigations led to the rapid development of brickwork as a load bearing medium, and a thirteen storey load bearing brickwork apartment block was constructed in Basle in 1953. The same design technique led to the construction of an 18 storey high slab block in 1957.

Switzerland has no resources of iron ore, and so steel or reinforced concrete construction has obvious drawbacks.

2.4 THE EXPERIMENTAL AND THEORETICAL WORK OF HAST.

Nils Hast has conducted a large amount of experimental work to determine the causes of rupture in brickwork⁽⁶⁾. The high strength of brickwork constructed with weak mortars was of special interest.

In his work he used load measuring cells to determine the stress at different points in a brick used in construction, or in the mortar bed. The diameter of the load cells used was only 8 mm., and they were approximately the same length. The cells were either inserted and cemented into drilled holes in the brick, at various positions on its

face, or placed horizontally in the mortar bed between bricks. When placed in a brick, the brick was then built into a wallette, using the mortar under investigation.

Several cycles of uniform compressive load were applied to the wallettes, increasing the maximum load in each cycle, and the compressive stresses at the load cells were noted.

The tests conducted led to several observations being made, and these are summarised below.

1) The stresses measured by the cells were found to increase as the edge distance of the cells increased. This was particularly true if no attempt was made to pack the mortar at the exposed joints.

2) The stresses registered by the outer load cells decreased with the successive load cycles.

3) The horizontal stresses in the mortar joints were compressive, but were not appreciable unless the normal pressure applied was greater than 140 pf. s. i.

These observations led to the conclusion that four factors governed the rupture of brickwork, and these are described below.

FACTOR A - The same as in any solid material. The material strains, in the direction of the applied load, on being loaded, and eventually the maximum elongation of the material is reached (as suggested by St. Venant's classical theory). This process would occur if the brickwork consisted of only perfectly dimensioned bricks. The brickwork would in this case fail at the prismatic strength of the brick.

FACTOR B - Once the inherent compressive strength of the mortar has been exceeded considerable lateral forces must exist in the mortar

joint if complete failure is not to take place. These forces are, therefore, compressive, and are balanced by the restraint offered by the adjacent bricks, which keep the mortar in equilibrium, and are therefore subject to tension. If the compressive strength of the mortar is high, then the tensile stresses in the brick will only occur at high stresses. Similarly if the mortar joint is thin then the stresses will be relatively small. The above would indicate that the tensile strength of the brick is relatively more important than the compressive strength, when weak mortars and thick joints are used. Badly cracked bricks will obviously give poor results.

FACTOR C - If the mortar is weak then the load is not distributed through the mortar towards the edge of the brickwork, reducing the effective bearing area.

FACTOR D - The bricks may be subject to additional bending or shearing stresses, caused by uneven bedding or unsymmetrical bonding, and these stresses will combine to produce failure at a lower load. These secondary stresses are dismissed as being the main cause of failure, since vertical cracks were found to occur at points other than those subject to bending stresses.

It is of interest to mention here that work initiated by Vogt and Haller, and developed by Sinha has argued that the tensile forces caused in the brick are due to the restrained lateral expansion of the mortar. Their theories are based on the elastic constants of the brick and mortar and their relative free horizontal strains, without any breakdown of the mortar.

However it seems likely that the elastic constants vary with the

compressive strength of the brick and mortar and hence for weak mortars both theories predict high tensile stresses in the brick, whilst for strong mortars these stresses are relatively small. The effect of joint thickness is the same in both theories.

Hast is justified by the fact that his experiments showed that the stresses only became critical after the inherent mortar strength was reached.

Further experiments investigated the slenderness ratio of pillars, and concluded that the height/width ratio did not affect the rupture factors, where deflections of the pillar were not encountered.

Tests were carried out to determine the elastic properties of the bricks and mortar used and vertical and horizontal strains were measured in individual bricks or mortar prisms under uniform compressive load. To determine the properties of mortar prisms compressive cells were inbedded in the mortar, in longitudinal and transverse directions.

To determine the elastic properties of brick, the longitudinal strain was measured using external tensioned wires coupled with a modified load cell. The transverse strain was measured by drilling a small hole through the brick, and placing a tensioned wire in the hole, coupled with an external load cell.

For bricks of average types the "E" values obtained ranged from $1.85 - 2.0 \times 10^6$ pf.s.i. For a highly porous brick the value was 0.24×10^6 pf.s.i., whilst for aerated concrete the value was 0.29×10^6 pf.s.i.

For lime mortar an "E" value of 0.25×10^6 pf.s.i. was obtained.

The "E" value was found to decrease with applied stress.

The poisson's ratio (μ) for all the bricks tested ranged from 0.25 - 0.14. For lime mortar a value of approx. $\mu = 0.05$ was found. The poisson's ratio was found to increase with increased stress.

The work of Hast is of considerable interest, as it represents the only experimental investigation which has been conducted into the actual stresses occurring in the brick and mortar units, during a loading test. In recent research, stresses have been measured in individual bricks, using either resistance gauges⁽⁷⁾ or photo-elastic stress meters⁽⁸⁾, but the state of stress in the mortar, with particular reference to the horizontal stress, has been ignored.

2.5 THE THEORETICAL INVESTIGATIONS OF VOGT, HALLER, AND SINHA.

Vogt⁽⁹⁾ and Haller⁽¹⁰⁾ suggested, and Sinha⁽¹¹⁾ developed a theoretical approach for the stresses existing in a brickwork element subjected to a uniformly applied compressive load.

Sinha's analysis was based on the assumption that the brick and mortar layers expand laterally by different amounts (the poisson's ratios being different), if free to do so. (This mode of behaviour follows simply from the accepted theories of elasticity). In practice frictional forces and bond forces exist, and prevent relative movement between the two elements.

In general for normal types of brick and mortar it may be said that tensile stresses are set up in the brick, and compressive stresses in the mortar joint. Due to the frictional surface forces acting the brick layers and mortar joints are subject to shear forces, and these were incorporated in the analysis. When, on the point of failure, the maximum

shear stress is acting, then its value is μX the vertical compressive stress, where μ is the coefficient of friction.

Equations were derived from the conditions of strain in the brick, the mortar, and the brickwork as a whole, and also from the equilibrium of forces.

These equations allow the determination of the actual stresses acting, and from these stresses the principal stresses may be calculated, and also the maximum shear stress.

The principal stresses and maximum shear stress were given in terms of the elastic moduli, the poisson's ratios, the coefficient of friction between brick and mortar, and the relative thicknesses of the brick and mortar layers.

If the values of the terms given above are known, then all the stresses acting may be calculated, in terms of the applied compressive stress. Knowing the compressive strength, the tensile strength, and the shear strength of the brick the mode of failure may then be predicted.

A theoretical analysis of the results, obtained by varying the properties etc., indicated that the poisson's ratio effect is negligible compared with the effect of the shear forces, and may be ignored.

Thus this analysis leads to similar conclusions as to the nature of brickwork behaviour as the work of Nils Hast.

Experimental tests on two or three courses high brick piers, capped with top and bottom mortar, gave failure stresses in agreement with the theoretical concepts, and are suggested as a quality control test for brickwork. The failure stresses referred to above were those noted when initial cracking occurred.

2.6 RECENT RUSSIAN RESEARCH.

In recent years a considerable amount of research has been carried out in the U.S.S.R., into the properties of brickwork. Large scale experimental programmes have been initiated, and have led to theoretical relationships being proposed⁽¹²⁾, linking the various brickwork properties.

Polyakov⁽¹³⁾ carried out a comprehensive investigation of the strength and stiffness of masonry in filling in framed buildings.

Research has been carried out, to investigate the strength and stability of large panel brickwork constructions, and allied structures. This work has been reported by Sementov and Kameiko⁽¹⁴⁾. Tests were performed at the Central Research Institute for Building Construction of the U.S.S.R. Academy of Building and Architecture.

The rapid introduction of vibrated brick panels into the construction industry in the U.S.S.R. necessitated a large scale investigation of the factors affecting the load bearing properties of such elements.

Sementov concluded that the most important factor affecting the strength of brickwork is the quality of the mortar in filling of the brickwork joints. If an ideal mortar joint can be obtained with a uniform thickness and density, along the joint, and no voids between the surfaces of the mortar and the bricks, then it is possible to obtain a brickwork strength very nearly equal to that of the brick itself. This high strength brickwork can only be obtained if the mortar strength is equal to that of the brick, and its elastic properties are the same.

Tests have shown that the strength of hand laid brickwork cannot

approach that of the brick alone, as the joint filling cannot attain a high enough standard. The imperfections of laying lead to considerable bending and shear stresses, and these cause failure at stresses below the inherent compressive strength of the brick itself.

The compressive strength of hand laid brickwork, constructed with high strength bricks, was found to be 0.35 - 0.4 times the brick compressive strength.

When brickwork panels were manufactured by laying the bricks on horizontal form work, and vibrating mortar, to fill the joints completely, the brickwork strength was found to increase by approximately 40%.

LOCAL STRESS CONCENTRATIONS AT A LINTEL SUPPORT.

R. H. Wood⁽⁷⁾ has investigated the stresses at a lintel bearing, and in the lintel itself, when the lintel supports a brickwork panel, subjected to concentrated loadings.

It is customary in practice to design beams and lintels carrying brickwork so as to be capable of supporting a triangular load of brickwork, where the base of the triangle is the span of the beam. The triangular loading considered is that given by an equilateral triangle, in British practice, compared with a rightangled triangle with two angles of 45° , considered by American design practice. The design load is therefore 73% higher by British practice.

If any load is superimposed on the wall, above the apex of the triangle, then no particular recommendations exist as to what proportions of this load should be taken into account, and it is frequently ignored. C.P. 111: 1964, Clause 302, Load Dispersion, states that "the angle of dispersion of loading of walls should be taken as not more than 45°

from the direction of such loading".

In the tests conducted the lintel spanned 10'-6", and supported a double-leaf wall.

The tests led to several interesting conclusions which are summarised below.

(a) The stresses in the lintel indicated that arching action was occurring in the brickwork, and that the lintel was supporting little load.

(b) The rotation at the supports was low, and hence the full bearing length was effective. Thus the concentration of stress at the support expected in such a configuration does not appear to be serious at working loads.

2.8 BRITISH STANDARD CODE OF PRACTICE.

C.P. 111: 1964 ⁽¹⁾ Structural Recommendations for Load bearing Walls is vague where concentrations of stress are concerned.

Paragraph 302, Load Dispersion, states that "The angle of dispersion of loading of walls should be taken as not more than 45° from the direction of such loading".

Paragraph 315, c, Walls Subjected to Concentrated Loads, states "Additional stresses of a purely local nature, as at girder bearings, column bases, lintels or other concentrated loadings are to be calculated and the maximum stress resulting from a combination of these with those provided in subclause c and d should not exceed the permissible stress given by subclause c by more than 50%". Sub-clauses c and d deal with axial loads, eccentric loads and/or lateral forces, but which would normally be considered as uniformly

distributed on the unit. Subclause c also gives a reduction factor for stress, which is dependent on the slenderness ratio and the eccentricity of the loading.

The product of the basic stress for the unit and the reduction factor gives the allowable stress.

For a concentrated loading the stress should therefore be calculated and combined with any distributed loading, the resulting stress not exceeding the provisions of clause c of the code by more than 50%.

Paragraph 315, c, of the code allows for cases in which it may be impossible to calculate the stress due to a load concentration. "Where indeterminate but very high stresses occur, such as at the outer edge of a wall supporting a cantilever, a spreader should be provided".

The American⁽¹⁵⁾ concept of the distribution of a concentrated load allows only a dispersal of stress at 30° compared with the British 45°.

The code makes no differentiation between the various possible positions or types of loading. Experiment has shown that when the position of the load concentration on a brickwork unit, and the relative size of the area through which the load is transmitted to the unit, are varied, then the failure stress of the unit also varies. The movement of the load progressively further from the edge of the unit leads to increased failure stress, as does an increase of the "area of brickwork unit/area of bearing" ratio. (A_c/A_b).

Some continental and other codes have made allowances for an increase in the A_c/A_b , and these are reviewed in Ch. 2. No account has yet been taken of the effect of eccentricity from the lateral axis

of the unit.

In America many different building codes exist, and these suggest various empirical rules for distributing stress concentrations.

The City of Long Beach suggests that for calculating wall stresses concentrated loads may be assumed to be distributed over a length of wall not exceeding the centre to centre distance between loads, nor one half of the height of the wall, measured from the floor to the bearing plate.

The Los Angeles building code contains the same centre to centre distance requirement as above, and also states that where the concentrated loads are not distributed through a structural element the length of wall considered shall not exceed the width of the bearing plus four times the wall thickness.

The San Francisco Municipal code states that masonry above openings shall be supported by well buttressed arches or adequately anchored lintels of metal, reinforced masonry or reinforced concrete, which shall have a minimum bearing of four ins. Beams, joists and girders, or other concentrated loads, supported by a wall or pier, shall have a bearing at least three inches in length, upon solid masonry not less than four inches thick, or upon a metal bearing plate of adequate design and dimensions to distribute the loads safely on the wall or pier, or upon a continuous reinforced masonry member projecting not less than three inches from the face of the wall.

3. THE SCOPE OF THE PRESENT INVESTIGATION.

3.1 THEORETICAL INVESTIGATIONS.

The theoretical approaches to stress concentrations, adopted by

various investigators , have been surveyed, both for semi-infinite plates or bodies, and also for structures with specified boundary conditions.

The results indicated by the various theoretical approaches have been compared with experimental results obtained from tests on concrete and other structural materials.

3.2 EXPERIMENTAL INVESTIGATIONS.

The failure stresses, strain distributions, and failure modes of full-scale brickwork piers, subjected to stress concentrations, have been investigated. The bearing plate length was varied, and end, central and intermediate positions of loading were considered for the strain distributions.

The failure stresses, strain distributions, and modes of failure of model Brickwork piers were investigated. $1/6$ th and $1/3$ rd. scale piers were constructed and tested to ascertain certain properties. $1/3$ rd. scale piers were utilised to determine other properties. Basically the full-scale tests outlined above were repeated, testing a larger number of model piers, for statistical reasons, and widening the range of bearing plate length used, where thought necessary.

The elastic and structural properties of the model bricks, mortar and the various model brickwork structures utilised were investigated.

The structural behaviour of $1/3$ rd. scale model cavity walls, subjected to eccentric loading of various types, was investigated. The strain distribution was investigated on the faces of the two leaves, and across the leaves. The lateral deflections of the leaves of the wall were also investigated.

The basic aims of all the tests conducted were to ascertain the failure stresses in brickwork structures subjected to load concentrations and to determine the nature of the distribution of the concentrated load in the structure, prior to failure.

CHAPTER 2.

A REVIEW OF PREVIOUS THEORETICAL AND EXPERIMENTAL
WORK ON STRESS CONCENTRATIONS.

1. INTRODUCTION.

The problem of the application of a concentrated force to the boundary of a brickwork structure is one which presents almost insuperable problems for the solution of the stress distribution. The reasons for the difficulties arising are many, and include the non-homogeneity of brickwork, the anisotropic structure of the brickwork, and the difficulty in obtaining the elastic properties of the brick, mortar, and brickwork.

The solution of the concentrated stress problem for a body of finite dimensions, the properties of which are known, has proved difficult, and many solutions proposed have been shown to bear little relation to experimentally obtained results. In all cases the classical solutions have seriously underestimated the stresses occurring. A recent approach ⁽¹⁶⁾ by K. T. Iyengar and C. V. Yogananda claims to have formulated an elasticity solution, satisfying all the boundary conditions, and giving the solution for a cylinder with a co-axial cable duct.

As a theoretical solution for even a simple case is difficult to obtain, it seems reasonable to assume that experimental measurements of the strain distribution are likely to yield more reliable results. From the experimental results a theoretical procedure may be justified, if one can be found. If no theoretical solution is found, then the experimental results may be used as the basis of an empirical design method.

2. BOUSSINESQ'S STRESS DISTRIBUTION THEORY.

Boussinesq's stress distribution theory (17) is based on the results given by the mathematical theory of elasticity for the simplest case of loading of a solid, homogeneous, elastic-isotropic, semi-infinite medium, namely the case of a single, vertical, point load applied at a point on the horizontal boundary surface. Certain other assumptions are made, the most important being that the material is weightless, and follows the law of proportionality between stress and strain.

The principles of the derivation of Boussinesq's theory equations are: there are six unknown quantities in the stress distribution problem, namely:

the normal stresses : σ_y , σ_t , and σ_R

the shear stress : τ and

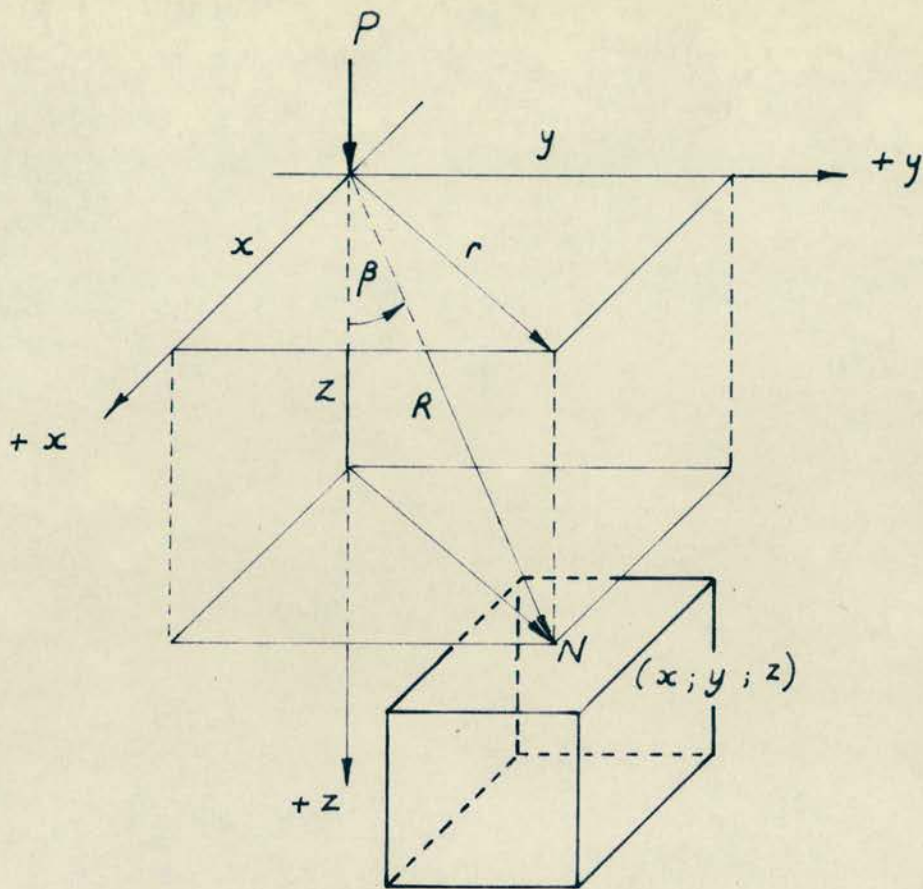
displacements : S_i (radial component) and
 S_v (Vertical component)

Hence the solution requires six independent equations. The equilibrium conditions of an elementary material prism renders two equations for the axi-symmetrical stress condition. The relationship between stress and strain and the continuity equations render the other four equations.

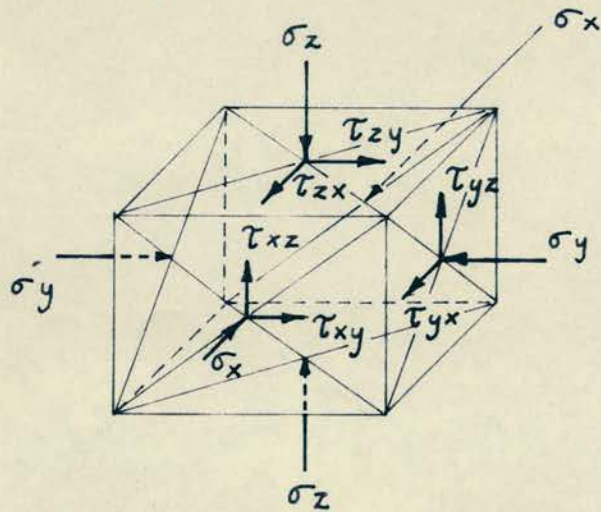
Fig. 2-1(a) illustrates the co-ordinate system for the stresses, a single concentrated force P , acting at the origin of the co-ordinates. Fig. 2-1(b) shows the stresses at a point N , defined in position by Fig. 2-1(a).

DESIGNATION OF STRESSES.

In the orthogonal co-ordinate system, the stressed condition of



(a) Coordinate System



(b) Normal and Shear Stresses at Point $N(x; y; z)$

Orthogonal Stresses - Boussinesq

an elementary cube, the faces of which are parallel to the planes of co-ordinates, is characterised by the following stresses, Fig.2-1(b)

a) Normal stresses

σ_z - vertical stress

σ_x and σ_y - horizontal normal stresses acting along or parallel to the x and y axes of co-ordinates respectively.

b) Shear stresses

τ_{xy} and τ_{yx} - shear stresses acting in the planes of a cube, planes which are parallel to the Z-axis of co-ordinates. These two shear stresses are acting in mutually perpendicular directions.

τ_{yz} and τ_{zy} - shear stresses acting in planes parallel to the x - axis.

τ_{zx} and τ_{xz} - shear stresses acting in planes parallel to the y axis.

The first subscript of the shear stress indicates the direction of the plane in which the shear stress τ acts, whereas the second subscript indicates the direction in which τ acts.

According to Boussinesq's theory the various stresses caused in the semi-infinite medium by a single concentrated load have the functions summarised as follows :

$$\sigma_z = \frac{3Pz^3}{2\pi R^5} = \frac{3P}{2\pi R^2} \cos^3 \beta$$

$$\sigma_x = \frac{P}{2\pi} \left[\frac{3x^2z}{R^5} - \frac{m-2}{m} \left\{ \frac{x^2-y^2}{Rr^2(R+z)} + \frac{y^2z}{R^3r^2} \right\} \right]$$

$$\sigma_y = \frac{P}{2\pi} \left[\frac{3y^2z}{R^5} - \frac{m-2}{m} \left\{ \frac{y^2-x^2}{Rr^2(R+r)} + \frac{x^2z}{R^3r^2} \right\} \right]$$

$$\sigma_r = \frac{P}{2\pi} \left[\frac{r^2z}{R^5} - \frac{m-2}{m} \left(\frac{R-z}{Rr^2} \right) \right]$$

$$\sigma_t = \frac{P}{2\pi} \left[\frac{m-2}{m} \left\{ \frac{1}{r^2} - \frac{z}{R^3} - \frac{z}{Rr^2} \right\} \right]$$

$$\tau_{rt} = \tau_{zt} = 0$$

$$\tau_{rz} = \frac{3P}{2\pi} \cdot \frac{rz^2}{R^5}$$

$$\tau_{zx} = \frac{3P \cdot z^2 \cdot x}{2\pi R^5}$$

$$\tau_{zy} = \frac{3P}{2\pi} \cdot \frac{z^2 \cdot y}{R^5}$$

$$\mu = 1/m = \text{Poisson's Ratio.}$$

3. FLAMANT'S CONTRIBUTION.

Flamant⁽¹⁸⁾ developed the three-dimensional theory of Boussinesq to solve the case of a concentrated vertical force acting on a horizontal straight boundary of an infinitely large plate. The thickness of the plate is taken as unity, and the load uniformly distributed across the width.

The distribution of stress is a simple radial distribution, Fig.2-2(i)a, any element A, at a distance R from the point of application of the load being subjected to a simple compression in the radial direction, the radial stress being

$$\sigma_R = \frac{2P}{\pi} \cdot \frac{\cos\theta}{R}$$

The tangential stress σ_θ , and the shearing stress $\tau_{R\theta}$ are zero.

The resultant of the forces acting on a cylindrical surface of radius R must balance P. Summing the vertical components,

find

$$2 \int_0^{\frac{\pi}{2}} \sigma_R \cos\theta \cdot R d\theta = - \frac{4P}{\pi} \int_0^{\frac{\pi}{2}} \cos^2\theta d\theta = -P$$

The solution $\sigma_R = \frac{2P}{\pi} \cdot \frac{\cos \theta}{R}$ is derived from the stress function $\phi = -\frac{P}{\pi} R \theta \sin \theta$

From the equilibrium equations in the radial and tangential directions for an element,

$$\sigma_R = \frac{1}{R} \frac{\partial \phi}{\partial R} + \frac{1}{R^2} \frac{\partial^2 \phi}{\partial \theta^2} = -\frac{2P \cos \theta}{\pi R}$$

$$\sigma_\theta = \frac{\partial^2 \phi}{\partial R^2} = 0$$

$$\tau_{R\theta} = -\frac{\partial}{\partial R} \left\{ \frac{1}{R} \cdot \frac{\partial \phi}{\partial \theta} \right\} = 0$$

These results coincide with those obtained above. Substituting the stress function $\phi = -\frac{P}{\pi} R \theta \sin \theta$, in the compatibility equation,

$$\left\{ \frac{\partial^2}{\partial R^2} + \frac{1}{R} \frac{\partial}{\partial R} + \frac{1}{R^2} \frac{\partial^2}{\partial \theta^2} \right\} \left\{ \frac{\partial^2 \phi}{\partial R^2} + \frac{1}{R} \frac{\partial}{\partial R} + \frac{1}{R^2} \frac{\partial^2 \phi}{\partial \theta^2} \right\} = 0$$

the equation is satisfied, and this is therefore the true stress function.

Taking a horizontal plane, at distance 'a' from the straight edge of the plate, the normal and shearing components of the stress on this plane, at any point, R_1 from the point of load application, are calculated from the simple compression in the radial direction,

$$\sigma_x = \sigma_{R_1} \cos^2 \theta_1 = -\frac{2P}{\pi} \cdot \frac{\cos^3 \theta_1}{R_1} = -\frac{2P \cos^4 \theta_1}{\pi R_1}$$

$$\sigma_y = \sigma_{R_1} \sin^2 \theta_1 = -\frac{2P}{\pi a} \sin^2 \theta_1 \cos^2 \theta_1$$

N.B. when $\theta_1 = 0$, $\sigma_y = 0$.

$$\tau_{xy} = \sigma_{R_1} \sin \theta_1 \cos \theta_1 = -\frac{2P}{\pi} \frac{\sin \theta_1 \cos^2 \theta_1}{R_1} = -\frac{2P \sin \theta_1 \cos^3 \theta_1}{\pi R_1}$$

where θ_1 is the angle from the point of load application to the point under consideration.

In Fig. 2-2(i)b the distribution of stresses σ_x , and τ_{xy} along the

horizontal plane mn is represented graphically.

At the point of load application the radial stress is theoretically infinitely large. In practice, at the point of load application there is always a certain yielding of material and as a result the load will be distributed over a finite area.

4. ANY VERTICAL LOADING OF A STRAIGHT BOUNDARY.

The curves for σ_x and τ_{xy} can be used as influence lines. If several forces $P_1, P_2, P_3,$ act on the boundary, then by moving the curves, to new origins, where the forces act, the stresses at particular points may be calculated by multiplying the force $P_1,$ etc., by the ordinate of the appropriate diagram. This produces the same result as multiplying the force by the ordinate of the diagram for the unit load applied immediately above the point under consideration.

Eg. for point D, Fig. 2-2(i)b, the value of σ_x , caused by $P_1, P_2,$ etc. is $P_1 \cdot \overline{H_1 K_1} + P_2 \cdot \overline{H_2 K_2} + \dots$ etc. This can only be applied if the curves are drawn for a unit force.

Similarly for a uniformly distributed load, the stress produced may be determined by multiplying the intensity of loading by the area under the influence diagram.

Another approach to the problem of distributed loading may be made by introducing a stress function in the form

$$\phi = A R^2 \theta$$

in which A is a constant. The corresponding stress components are

$$\sigma_R = \frac{1}{R} \frac{\partial \phi}{\partial R} + \frac{1}{R^2} \frac{\partial^2 \phi}{\partial \theta^2} = 2 A \theta$$

$$\sigma_\theta = \frac{\partial^2 \phi}{\partial R^2} = 2 A \theta$$

$$\tau_{R\theta} = -\frac{\partial}{\partial R} \left(\frac{1}{R} \frac{\partial \phi}{\partial \theta} \right) = -A$$

Applying this to a semi-infinite plate we arrive at the load distribution shown in Fig. 2-2(i)c. On the straight edge of the plate there acts a uniformly distributed shearing force of intensity - A, and a uniformly distributed normal load of the intensity $A \pi$, abruptly changing sign at the origin 0. By moving the origin to O1, and changing the sign of the stress function ϕ , we arrive at the stress distribution shown in Fig. 2-2(ii)d.

Superposing the two cases of load distribution we obtain the case of a uniform loading of a portion of the straight boundary of the semi-infinite plate shown in Fig. 2-2(ii)e. To obtain the given intensity q, of uniform load, we take

$$2 A \pi = q, \quad A = \frac{1}{2 \pi} \cdot q$$

The stress at any point of the plate is then given by the stress function (19).

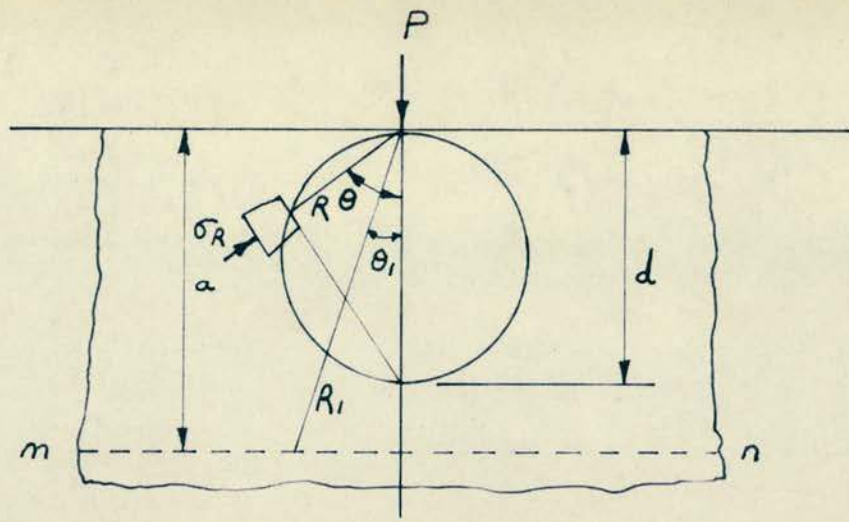
$$\phi = A (R^2 \theta - R_1^2 \theta_1) = \frac{q}{2 \pi} (R^2 \theta - R_1^2 \theta_1)$$

The first term of the stress function gives at any point M, Fig. 2-2(ii)f, a uniform tension in all directions in the plane of the plate equal to $2A \theta$ and a pure shear - A. In the same manner, the second term of the function gives a uniform compression - $2A \theta_1$ and a pure shear A. The uniform tension and compression can be simply added together, and we find a uniform compressive stress,

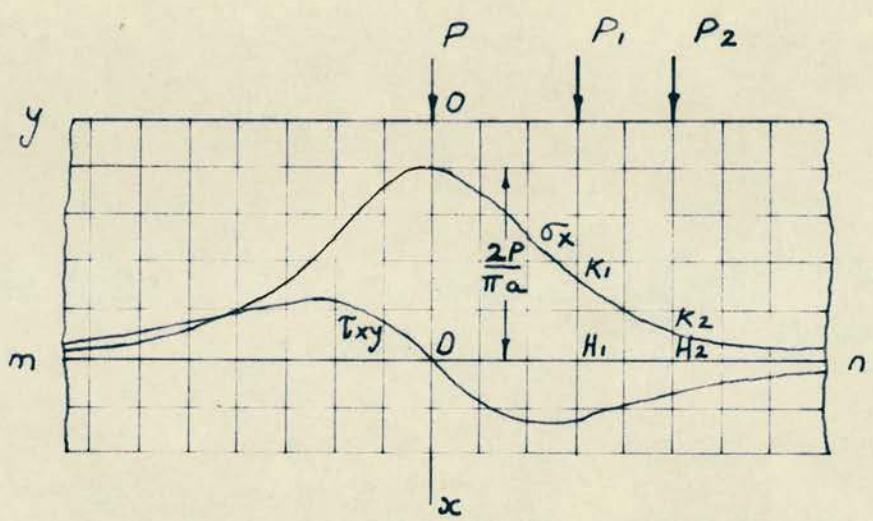
$$p = 2A \theta - 2A \theta_1 = 2A (\theta - \theta_1) = -2A \alpha$$

where α is the angle between the radii R_1 and R_2 .

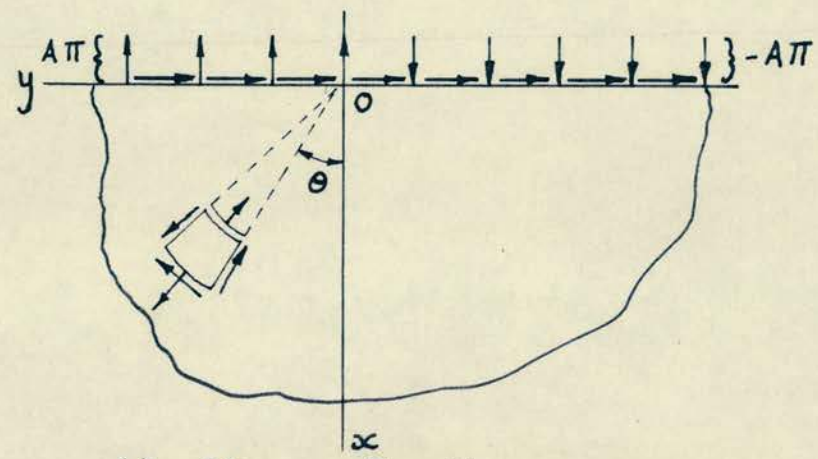
The pure shears may be superposed by means of Mohr's circle, and we obtain a pure shear.



(a) Radial Stress

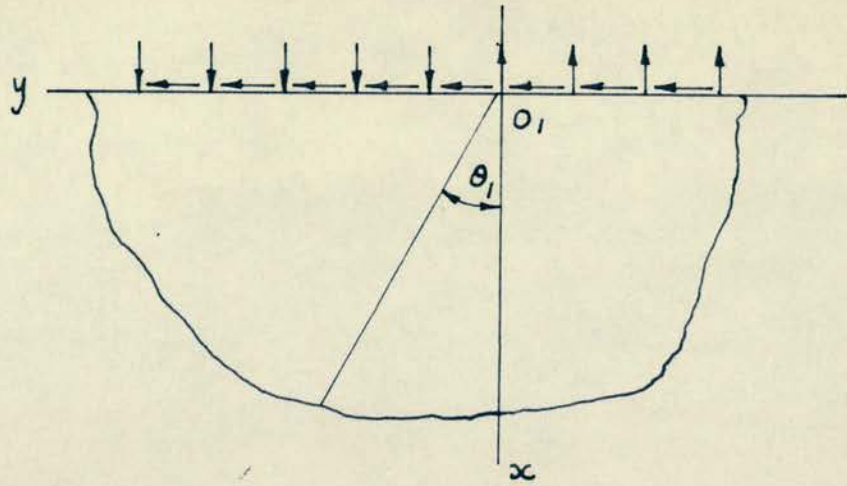


(b) Distribution of Stress

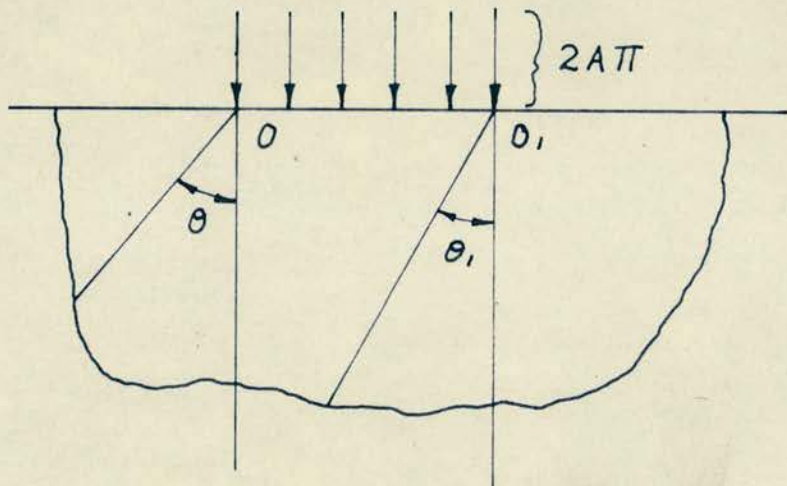


(c) Stress Function

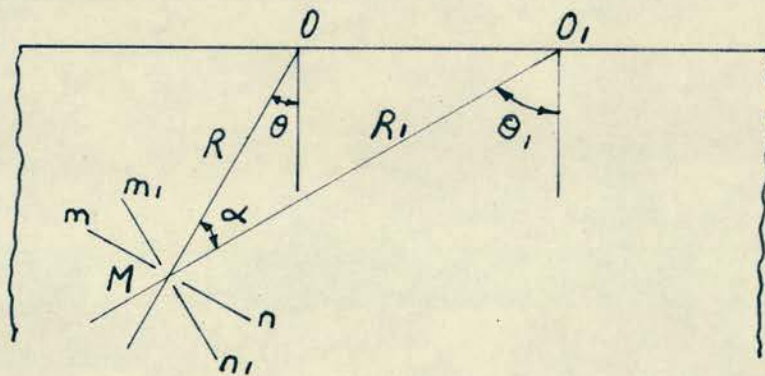
Concentrated Force on a Boundary



(d) Stress Function



(e) Combined Functions



(f) Combined Functions

Concentrated Force on a Boundary

Fig. 2-2 ii

The principal stresses at any point M, are

$$-2A (\alpha + \sin \alpha), \quad -2A (\alpha - \sin \alpha)$$

Along any circle through O and O1, the angle α remains constant, and so the principal stresses are also constant. At the boundary, between the points O and O1, the angle α is equal to π , and both principal stresses are equal to $-2\pi A = -q$. For the remaining portions of the boundary $\alpha = 0$, and both principal stresses are zero.

As a uniform compressive stress exists at any point, then for no point can a horizontal tensile stress exist.

From the expressions for the principal stresses, they have been calculated, and are shown in Fig. 2-3.

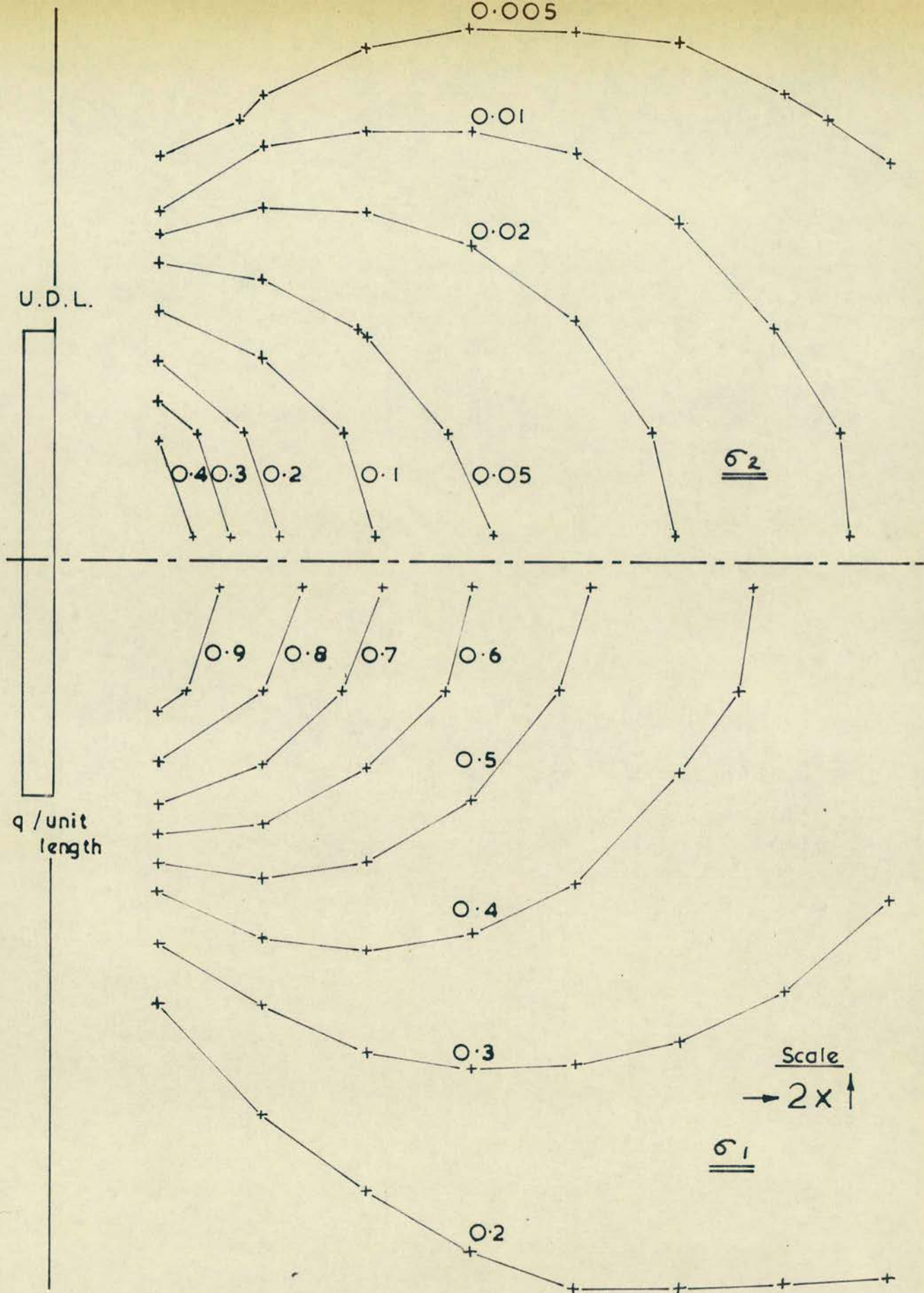
The principal stresses are shown in the form of stress contours, for σ_1 and σ_2 , the principal stresses. The variation in the principal stresses at different horizontal levels is also shown in Fig. 2-4.

From the principal stresses, the principal strain has been calculated, corresponding to

$$\frac{1}{E} (\sigma_2 - \mu \sigma_1)$$

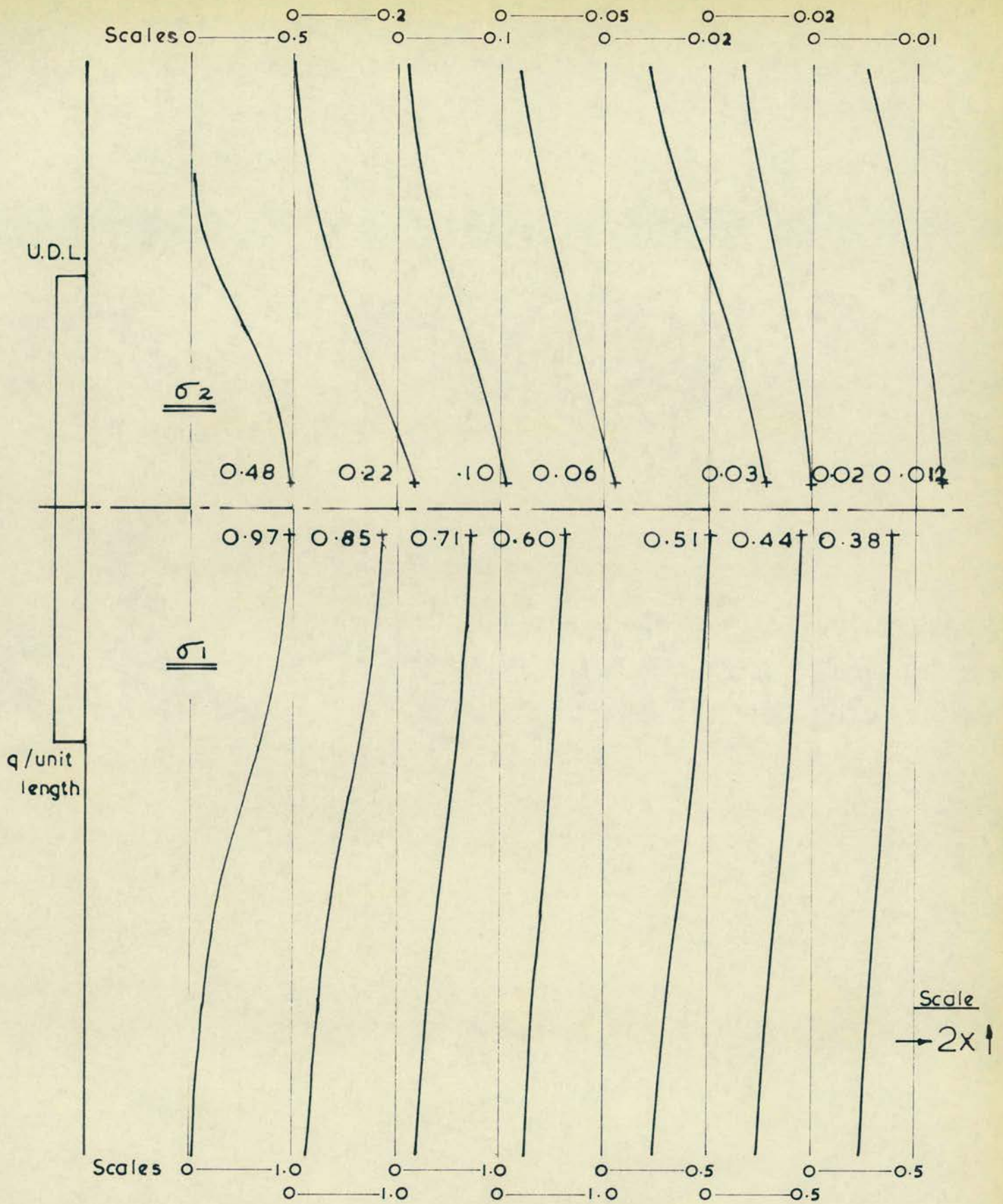
The values plotted are factors of $\frac{q}{E}$, and have been plotted for two values of μ , Poisson's ratio, of 0.1 and 0.15. Fig. 2-5 shows the principal strain contours for $\mu = 0.1$ and 0.15, and it can be observed, that for the larger value of μ , the tensile zone is larger, with a maximum value on the bearing plate centre line, at some level below the bearing plate, the level depending on the μ value chosen.

The above assumes E, the elastic modulus to be constant in all directions.



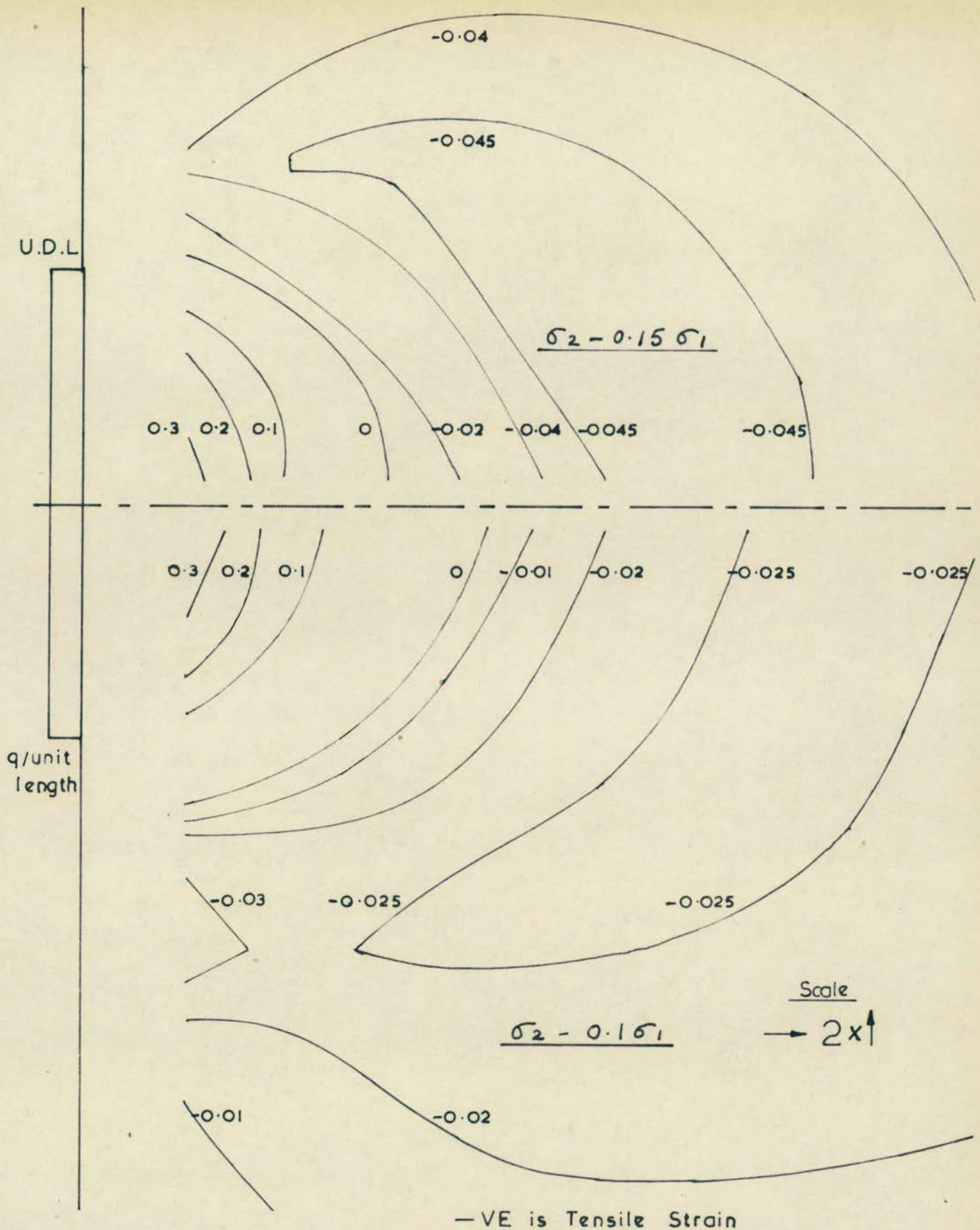
Principal Stress Contours - σ_1 and σ_2 - as Factors of q .

Fig. 2-3



Principal Stresses on Horizontal Sections

Fig. 2-4



Principal Strain Contours for Poisson's Ratios of 0.1 and 0.15.

Fig. 2-5

An investigation of the other principal strain, $\frac{1}{E} (\sigma_1 - \mu \sigma_2)$ reveals that the ratio of σ_1 / σ_2 is such that the term $\mu \sigma_2$ is relatively small compared with σ_1 , and hence the strain is only slightly affected by the minor principal stress, and results have not been plotted.

5. A FORCE ACTING ON THE END OF A WEDGE.

5.1 THE GENERALISED CASE.

The simple radial stress distribution

$$\sigma_R = - \frac{k P \cos \theta}{R}$$

can be utilised to investigate the stresses in a wedge due to concentrated force at its apex (19). Consider a symmetrically loaded wedge, Fig. 2-6(a), whose thickness is unity, and angle is 2α .

The conditions along the faces $\theta = \pm \alpha$, of the wedge are satisfied by taking for the stress components the values

$$\sigma_R = - \frac{k P \cos \theta}{R}, \quad \sigma_\theta = 0, \quad \tau_{r\theta} = 0.$$

The constant k is adjusted to satisfy the condition of equilibrium at the apex.

Equating the internal pressures on a cylindrical surface, to the applied load, we obtain

$$- 2 \int_0^\alpha \frac{k P \cos^2 \theta}{R} \cdot R d\theta = - k P (\alpha + \frac{1}{2} \sin 2\alpha)$$

$$= \underline{- P}$$

$$k = \frac{1}{\alpha + \frac{1}{2} \sin 2\alpha}$$

Then
$$\sigma_R = - \frac{P \cos \theta}{R (\alpha + \frac{1}{2} \sin 2\alpha)}$$

The distribution of normal stresses over any cross-section

perpendicular to the wedge axis is not uniform.

Considering the case of the force P applied perpendicular to the axis of the wedge, the above solution can be utilised if the angle θ , is measured from the direction of the force Fig.2-6(b).

The constant factor k, is found from the equation of equilibrium.

$$\int_{\frac{\pi}{2} - \alpha}^{\frac{\pi}{2} + \alpha} \sigma_R \cos \theta \cdot R \cdot d\theta = -P$$

from which $k = \frac{1}{\alpha - \frac{1}{2} \sin 2\alpha}$

and the radial stress is

$$\sigma_R = \frac{-P \cos \theta}{R (\alpha - \frac{1}{2} \sin 2\alpha)}$$

The normal and shearing stresses over any cross-section parallel to the direction of the force are,

$$\sigma_y = - \frac{P y x \sin^4 \theta}{y^3 (\alpha - \frac{1}{2} \sin 2\alpha)}$$

$$\tau_{xy} = \frac{-P x^2 \sin^4 \theta}{y^3 (\alpha - \frac{1}{2} \sin 2\alpha)}$$

5.2 FORCE ACTING ON A 90° WEDGE.

Considering the two cases above; a wedge loaded along its axis, and one loaded perpendicular to its axis, then if α is replaced by $\pi/4$ the wedge becomes a quarter plane.

The respective values for the radial stresses are then

$$\sigma_R = \frac{-P \cos \theta}{R (\pi/4 + \frac{1}{2} \sin \pi/2)} = \frac{-P \cos \theta}{R (\pi/4 + \frac{1}{2})}$$

and $\sigma_R = \frac{-P \cos \theta_1}{R (\pi/4 - \frac{1}{2})}$

$$\theta_1 = 90^\circ + \theta$$

A combination of these two loading cases leads to a quarter plane,

loaded by a force of magnitude $2P/\sqrt{2}$ along one edge.

The radial stress component may then be represented by

$$\begin{aligned} \sigma_R &= \frac{-P \cos \theta}{R (\pi/4 + 1/2)} - \frac{P \cos \theta_1}{R (\pi/4 - 1/2)} \\ &= \frac{-P}{R} \left[\frac{\cos \theta (\pi/4 - 1/2) + \cos \theta_1 (\pi/4 + 1/2)}{\pi^2/16 - 1/4} \right] \end{aligned}$$

This is for a corner force of $\sqrt{2} P$, and for a corner force of P ,

$$\sigma_R = \frac{-1.93P}{R} \left[0.286 \cos \theta + 1.286 \cos \theta_1 \right]$$

This enables the radial stress to be plotted for the wedge,

$$\sigma_R = \frac{-1.93 k P}{R}$$

Values of σ_R have been calculated, for values of θ and θ_1 , taken at 5° intervals, and values of R , from 1-10 units.

From these values the radial stress distribution may be plotted, and is shown in Fig. 2-7, the stress being expressed as a factor of P .

From the radial stress σ_R , the vertical and horizontal stresses, σ_x and σ_y may be calculated.

For the axially applied force, Fig. 2-6(a)

$$\sigma_x = \sigma_R \cos^2 (45 \pm \theta); \quad \sigma_y = \sigma_R \sin^2 (45 \pm \theta)$$

($\pm \theta$ dependent upon whether θ is measured anti-clockwise or clockwise from the centreline of the wedge.)

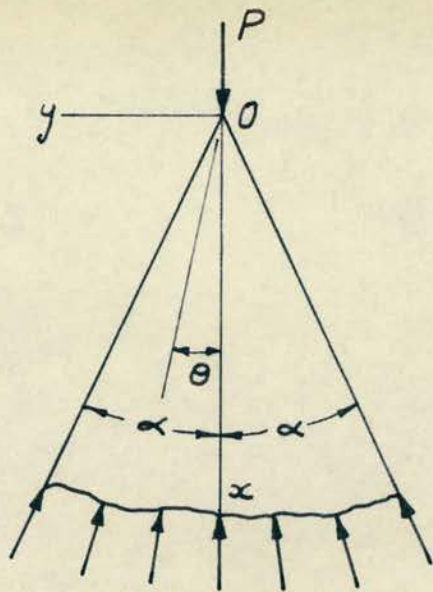
For the force applied at rightangles to the axis of the wedge, Fig. 2-6(b)

$$\sigma_x = \sigma_R \cos^2 (45 \mp \theta); \quad \sigma_y = \sigma_R \cos^2 (45 \pm \theta)$$

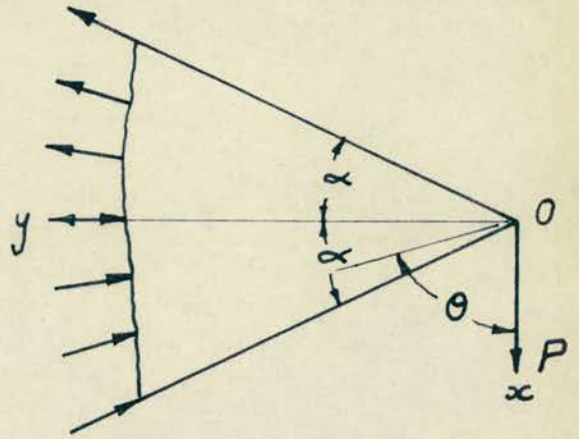
For the two cases, σ_R is different, being given by

$$\frac{-P \cos \theta}{R} \cdot \frac{1}{(\alpha + 1/2 \sin 2\alpha)} \quad \text{and} \quad \frac{-P \cos \theta_1}{R} \cdot \frac{1}{(\alpha - 1/2 \sin 2\alpha)}$$

respectively.



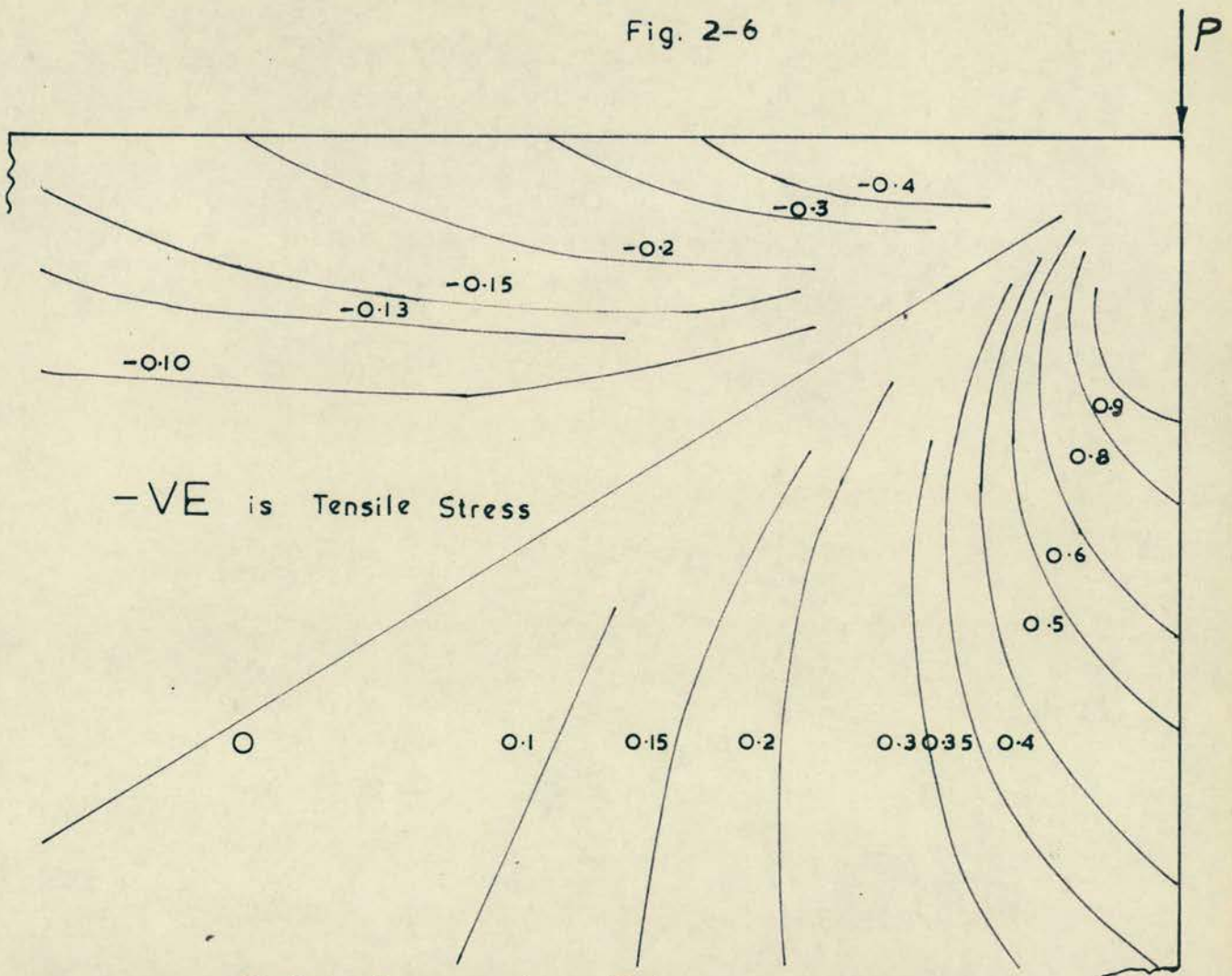
(a)



(b)

Forces Acting on a Wedge

Fig. 2-6



Radial Stresses in a Wedge

Fig. 2-7

σ_x has been taken as the stress in the same direction as the line of action of the force.

Values of σ_x and σ_y have been tabulated for the two cases, for various values of θ and θ_1 , at 10° intervals, and have then been summed. The effect of the variation of R has been investigated, and a correction made for the effective applied force being $\sqrt{2} P$. The final stresses being expressed as fractions of an applied force P.

The results are expressed graphically in Figs. 2-8 and 2-9.

The stress distribution in the immediate vicinity of the wedge apex is ignored, assuming the material will exhibit a degree of plasticity which will not affect the stress distribution further down the section (St. Venant's Principle).

From Figs. 2-6, 2-7, and 2-8, the compressive zone of the wedge can be seen to extend from the loaded edge over a sector whose angle is approx. 58° . This angle is the same for radial, vertical and horizontal stresses.

6. COKER AND FILON'S CONTRIBUTION.

6.1 THE THEORETICAL SOLUTION OF STRESS CONCENTRATIONS.

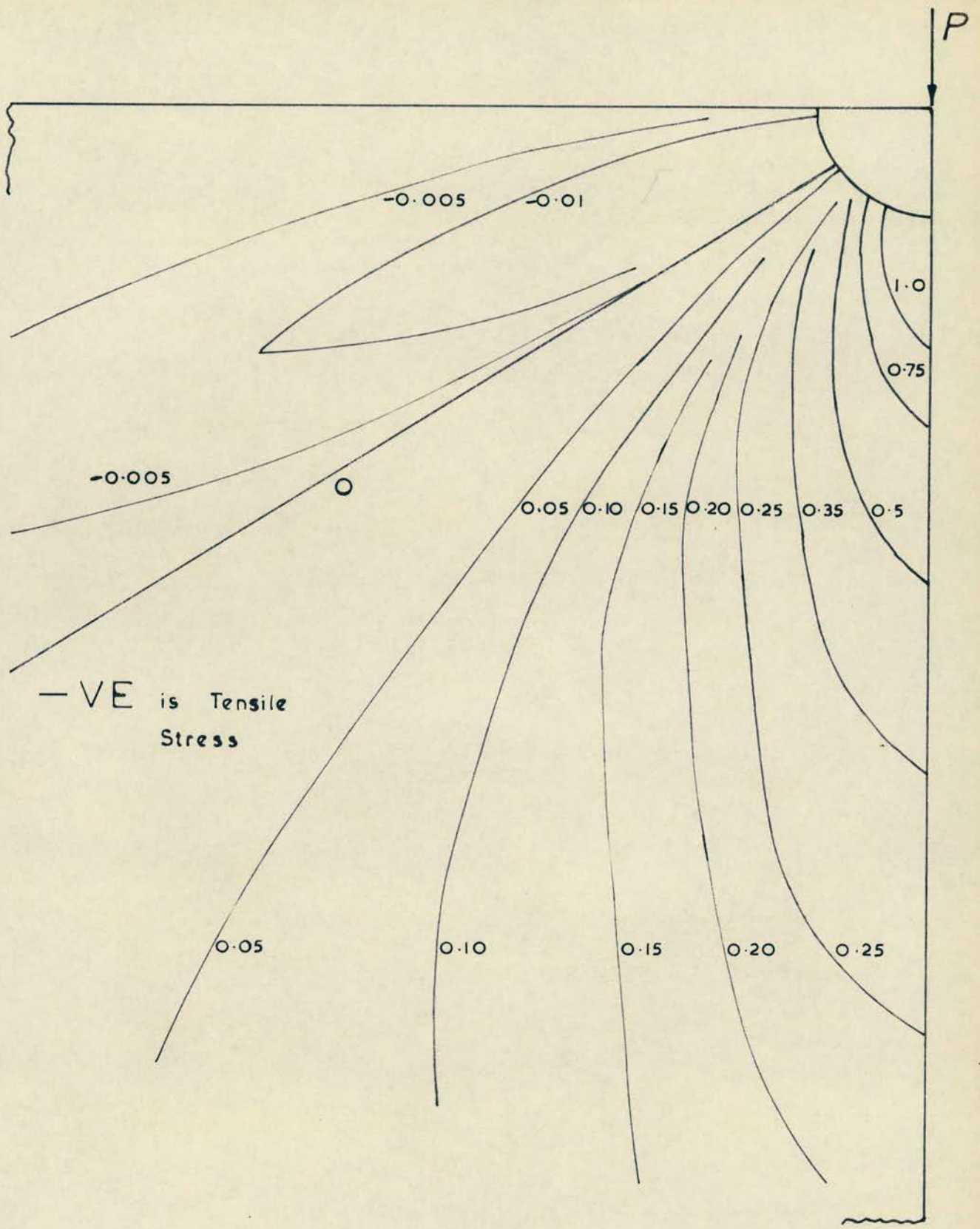
Coker and Filon ⁽²⁰⁾ have presented a solution for a wedge loaded at the apex, by a force acting in any chosen direction.

The stress function chosen leads to a radial stress distribution, where the stress

$$\sigma_R = \frac{-2 P}{R} \left\{ \frac{\cos \theta \cos \beta}{2\alpha + \sin 2\alpha} + \frac{\sin \theta \sin \beta}{2\alpha - \sin 2\alpha} \right\}$$

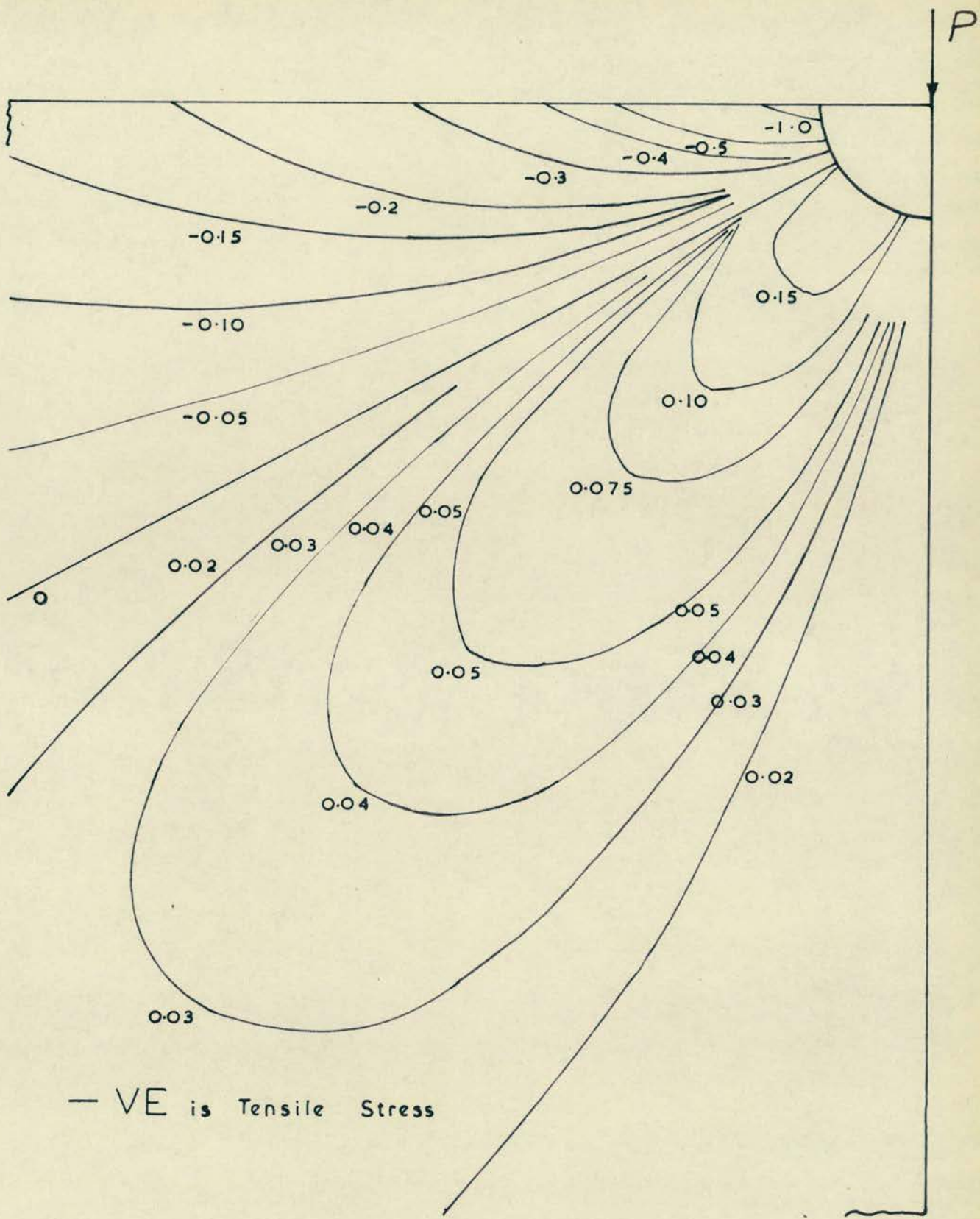
all other stresses being zero. Fig. 2-10.

If $\alpha = \beta = 45^\circ$, then this leads to a wedge with a compressive zone of $57^\circ 30'$, measured from the loaded face, agreeing with the solution



Vertical Stress Distribution for a Wedge

Fig. 2-8



Horizontal Stress Distribution for a Wedge

Fig. 2-9

obtained above. This stress function is in fact a modified form of the functions used to derive the stress distributions above.

A solution for a uniformly loaded portion of a semi-infinite plate is also presented, and is the same as the solution already outlined.

6.2 THE STRESS DISTRIBUTION IN A LONG RECTANGULAR PLATE SUBJECTED TO A CONCENTRATED LOADING.

Optical tests conducted using plastics sensitive to polarised light have shown that the assumptions of the theory are impossible to realise. When the isochromatic bands are examined, it is seen that the extreme edges of the loading show brilliant colour banding in addition to circles passing through the edges. The circles accord with theory, but in addition there are lobe shaped curves starting from the edges, and penetrating into the plate, and these indicate a variation from the uniform stress distribution.

Part of the explanation of this phenomena is that when a bearing plate applies a load, the edges inherently lift, giving an uneven stress distribution.

Further investigations of the stress distribution along the base of the rectangular plate indicate that the vertical stress is greatest along the centre-line of the load. It should be noted, however, that the dimensions of the plate tested were 2.5" deep by 5.14" long, and that the base was supported on a flat steel plate, where restraint to longitudinal movement was provided by friction alone.

Along the vertical centre-line of the plate the stress distribution shows greater values than are given by the theoretical stress function.

6.3 THE STRESS DISTRIBUTION IN SHORT RECTANGULAR BLOCKS
SUBJECTED TO A CONCENTRATED LOAD.

This type of loading is particularly relevant to the practical cases encountered in engineering work. As indicated above the pressure distribution is uniform over neither surface, for the infinitely long plate (relatively), and there is no reason to suppose a decrease in the plate length/bearing plate length ratio will alter the essential nature of the phenomenon.

A photo-elastic test on a 1" x 1" x 1/8" thick plate, loaded over a width of 1/4" by a pressure plate of the same material showed that stress concentrations occur at the edges of bearing plates. The isochromatic bands pass through the ends of the bearing plate, but are not arcs of circles. These factors indicate that the load is neither being applied uniformly, nor distributed in accordance with the assumptions of the stress function.

As these difficulties are encountered in a controlled test it seems extremely likely that in practice similar, if not worse, conditions apply.

7. SHEPHERD'S CONTRIBUTION.

W. M. Shepherd (20) has obtained the solution for the case where the force acts not at the apex, but at a point on one of the straight edges of a wedge with an apex angle of any size.

Utilising stress functions, and considering the wedge as acted on by two forces, one on each face, symmetrically positioned, the stress distribution for the wedge was determined.

Two separate conditions of loading were considered for the analysis. Either both forces, were inwardly normal or one force was inwardly

normal, and the other outwardly normal. A combination of the two loading conditions indicated above leads to a wedge acted on by a single normal force.

Values of the stresses, expressed as factors of the applied loading, have been tabulated, for a wedge with an apex angle of 90° . The stresses are expressed in terms of polar co-ordinates, with the wedge centre line as a reference axis, but may be modified to give the horizontal and vertical stresses, if required.

The method adopted may be utilised for the solution of any sector under the action of forces in its plane, but the evaluation of the stresses involves much tedious calculation.

8. THEORETICAL SOLUTIONS FOR CONCENTRATED FORCES APPLIED TO MEMBERS OF FINITE SIZE.

8.1 INTRODUCTION.

The solutions and modifications outlined above are only applicable when the area over which the load is applied is small in comparison with the total area of the member.

The development of post-tensioned concrete led to considerable interest in the stress distribution in the anchorage zone. The codes of practice which deal with prestressed concrete either made no recommendation for the design of the anchorage zone, or made general comments, or advised the use of some empirical formulae based upon tests on concrete which had little relevance to the problem of a stress concentration.

The first approaches to a theoretical solution of the problem considered only a two dimensional loading condition, where the load

was applied to a portion of the surface of a rectangular block.

8.2. MORSCH'S THEORY.

The theory was based on the following assumptions:-

- (i) the stresses due to a concentrated load are uniformly distributed at a distance equal to the width of the prism,
- (ii) the curvature of the trajectories causes the tensile stresses, the latter being distributed according to a parabolic law.

The distribution of the tensile stresses was based on the measurement of transverse strain, by Krüger, Krüger, however, measured the strain at three positions only, and hence any shape of curve could have been fitted.

The distribution of compressive stress according to Morsch's theory is shown in Fig. 2-11. With reference to this figure, the transverse force $Z = P (a - a_1) / 4h$, and the maximum tensile stress for a rectangular prism of width b is $f_y = 3Z / 2ab$.

No investigation of the stress distribution, or the actual occurring tensile stresses was made.

8.3 BORTSCH'S THEORY.

One of the earlier theoretical approaches to the problem of bearing capacity, as well as stress distribution, in structural units under concentrated loadings was that of Bortsch. He considered the member as a deep beam of infinite length, subjected to a load distributed on the contact area as a cosine function, as shown in Fig. 2-12. The amplitude of the cosine function is $P_1 = \pi P / 2a_1$. The transverse, longitudinal and shear stresses were obtained from a stress function analysis.

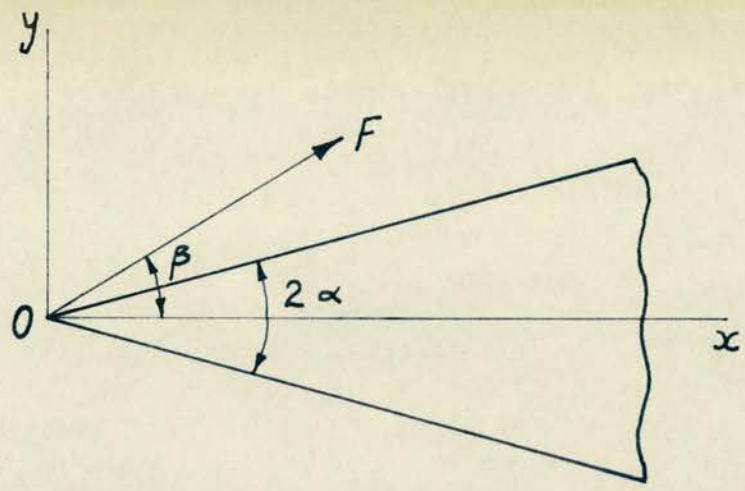


Fig. 2-10

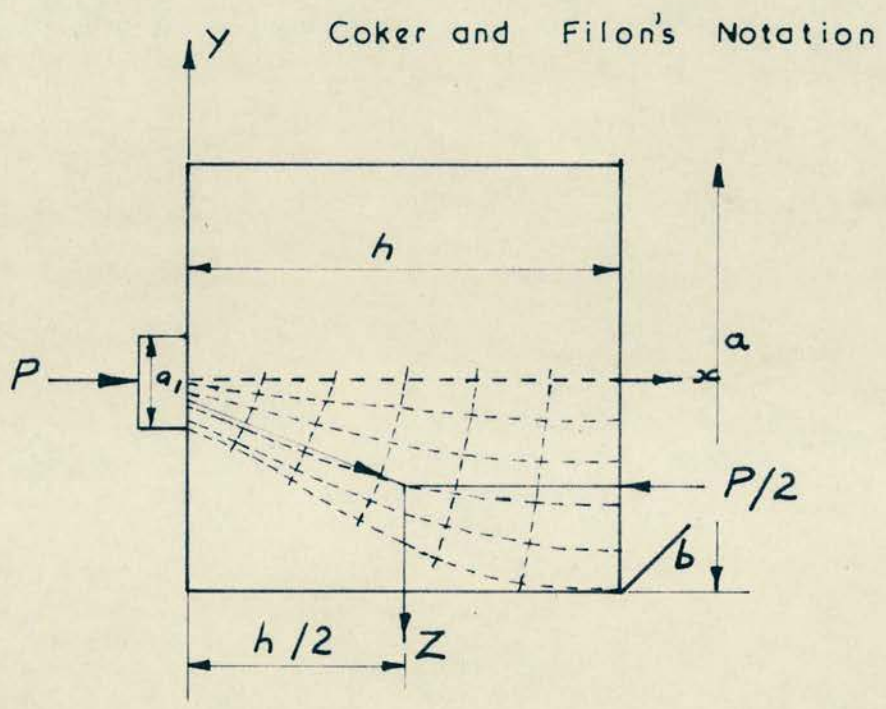


Fig. 2-11

Morsch's Theory - Stress Distribution

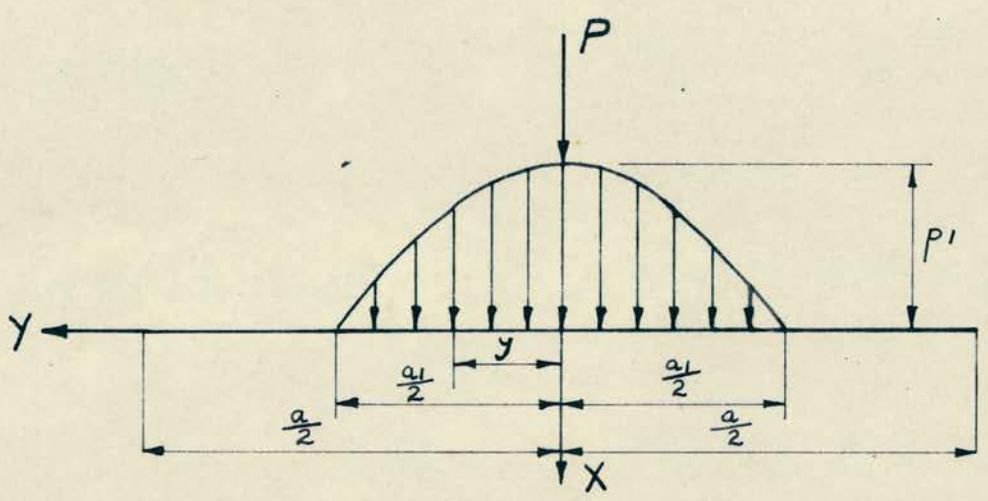


Fig. 2-12

Bortsch's Theory - Load Distribution

The maximum transverse tensile stress occurs on the central axis of the block, and its distance from the end of the block is given by $x / a = 0.2 - 0.3$.

The maximum value of the tensile stress at the above sections ranges from $(0.38 - 0.45) P/a$, for $a_1 / a = (0.2 - 0.1)$.

When $x / a = 1.7$ the tensile stress disappears.

Bortsch dealt with values of a_1/a from 0 - 0.2 and it is not clear if his theory is valid for values approaching unity, which commonly occur in the anchorage zones of post-tensioned members.

8.4 MAGNEL'S THEORY.

Magnel's theory was based on the assumption that the tensile stress diagram due to a bending moment M, at any plane parallel to the central axis of the beam, such as plane AB in Fig. 2-13(a), is that of a cubic parabola, as shown in Fig. 2-13(b). This cubic parabola is given by the equation

$$f_y = A x^3 + B x^2 + Cx + D$$

From the boundary conditions the constants may be derived, and it may be shown that

$$f_y = \frac{5M}{b a^2} \left\{ \frac{16 x^3}{a^3} + \frac{12 x^2}{a^2} - 1 \right\} = K \cdot \frac{M}{b a^2}$$

whence at $x = a/4$, $f_y = 0$.

8.5 CHAIKE'S THEORY.

The work of Chaiké was similar to that of Magnel, but one of the boundary conditions was omitted ($df_y / dz = 0$ at $Z = 2c$) and the polynomial was reduced to one of the second degree.

8.6 GUYON'S THEORY.

Guyon considered the stresses due to point loads applied to the finite edge of a semi-infinite rectangle, and utilised a Fourier series for the solution.

Fig. 2-14 shows the distribution and variation of the transverse stress, f_y , for various a_1/a ratios, where a_1 is half the anchorage plate width, and 'a' is half the width of the corresponding concrete prism.

8.7 BLEICH'S THEORY.

Bleich developed an Airy stress function F, such that

$$f_y = \frac{\partial^2 F}{\partial x^2} ; \quad f_x = \frac{\partial^2 F}{\partial y^2} ; \quad t = \frac{\partial^2 F}{\partial x \cdot \partial y}$$

= shear stress

subject to the governing equation

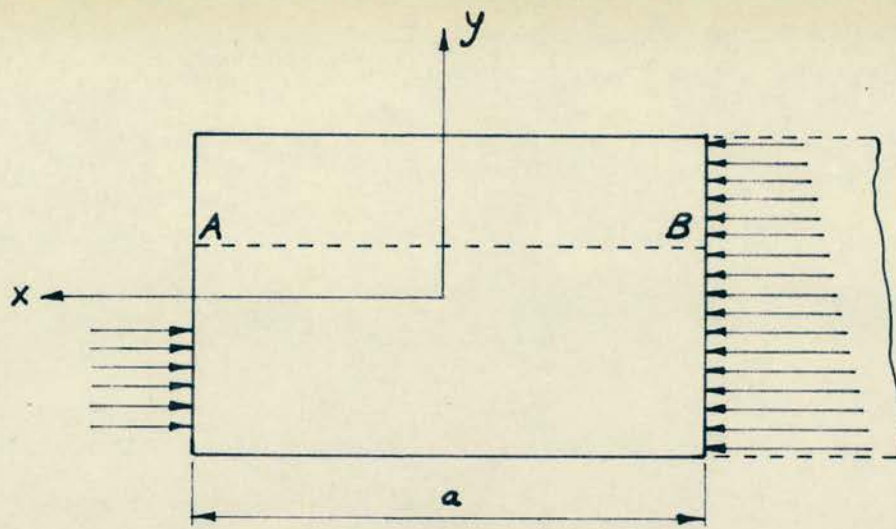
$$\frac{\partial^4 F}{\partial x^4} + \frac{\partial^4 F}{\partial x^2 \partial y^2} + \frac{\partial^4 F}{\partial y^4} = 0$$

The transverse stresses may be calculated, and modified equations are used to satisfy the boundary equations.

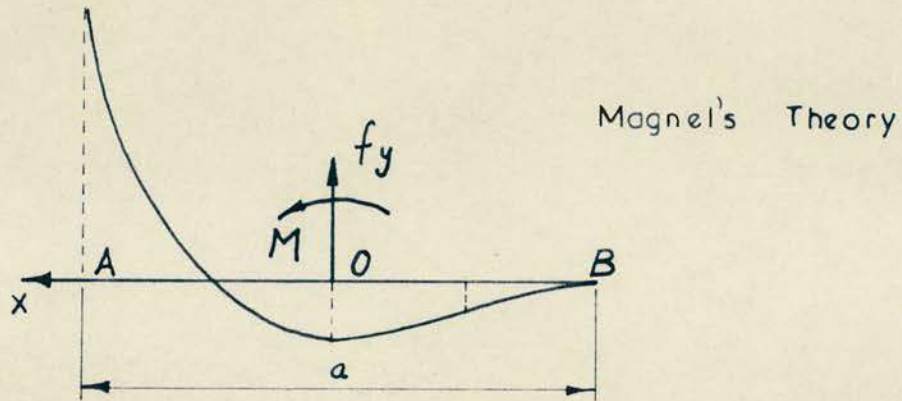
8.8 GERSTNER AND ZIENKIEWICZ'S CONTRIBUTION.

The method of solution, for a stress concentration, adopted by Gerstner and Zienkiewicz⁽²²⁾ may be considered to be the sum of a particular solution and a corrective solution, leading to a satisfaction of all the pertinent boundary conditions. As example of the type of solution is shown in Fig. 2-15.

The particular solution is the elasticity solution by Flamant⁽¹⁸⁾, for the stress distribution in a semi-infinite medium, due to a line

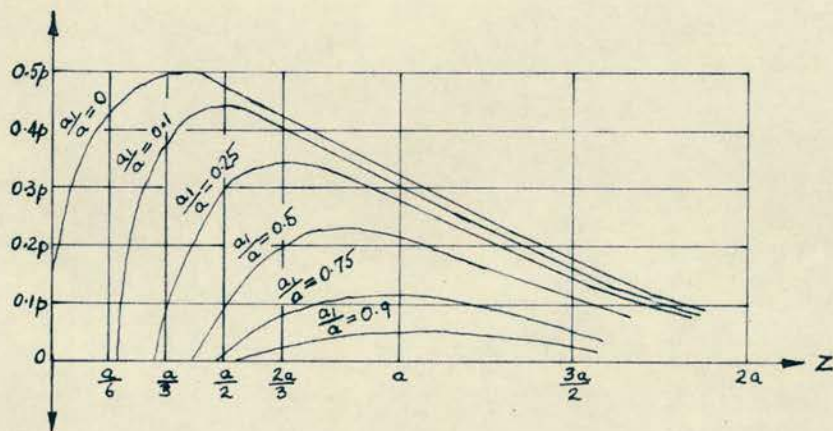


(a) End Block



(b) Transverse Stress Distribution

Fig. 2-13



Guyon's Theory - Stress Distribution

Fig. 2-14

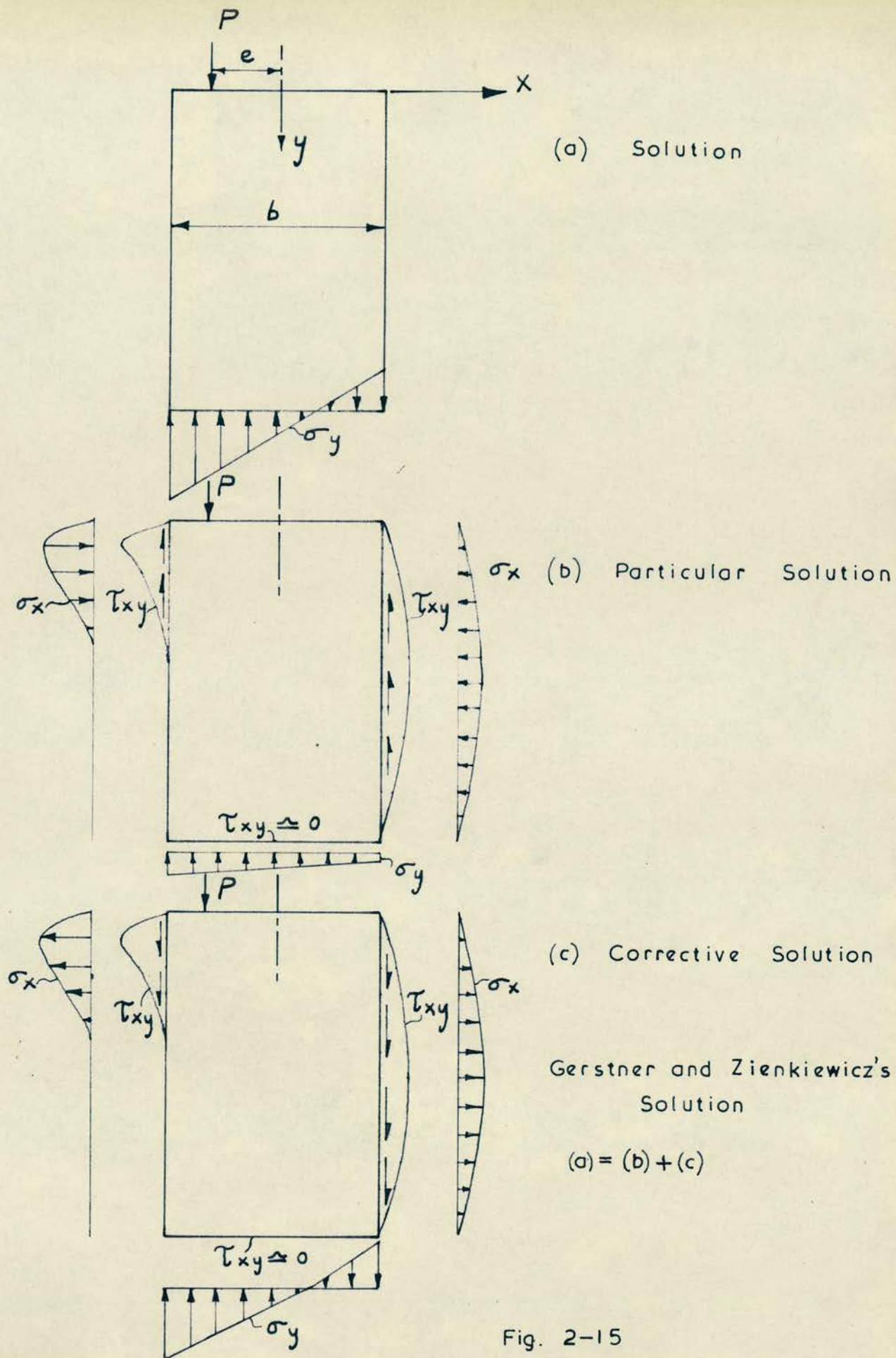


Fig. 2-15

load normal to the surface.

$$f_y = \frac{-2P}{\pi} \cdot \frac{y^3}{(x^2 + y^2)^2} ; \quad f_x = \frac{-2P}{\pi} \cdot \frac{x^2 y}{(x^2 + y^2)^2}$$

$$\tau_{xy} = \frac{-2P}{\pi} \cdot \frac{xy^2}{(x^2 + y^2)^2}$$

The origin of co-ordinates is the point of load application.

The corrective solution may be conveniently obtained by the use of a finite difference technique. In the corrective solution the values of the stress function and its gradient along the boundaries are determined by a standard integration process.

For example, referring to the vertical boundaries of the member, shown in the corrective solution of Fig. 2-15 we have;

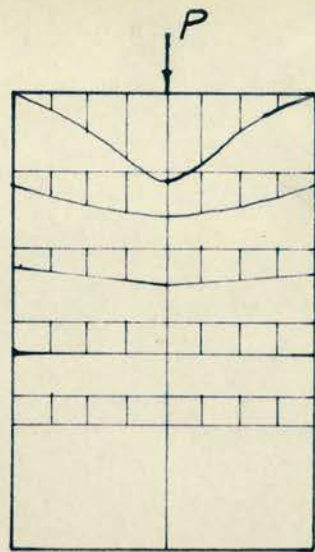
$$-\frac{\partial \phi}{\partial x} = \int \tau_{xy} dy, \quad \phi = \iint f_x dy$$

where ϕ is the Airy stress function and τ_{xy} , and f_x are equal to the stresses from the particular solution, but opposite in sign. Having obtained the stress function, and its gradient along the boundaries the corrective solution is performed in the usual manner. The corrective solution must be carried out to a sufficient depth to assume a linear distribution of the final vertical stresses at some distance from the anchorage.

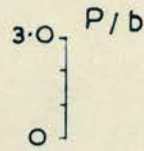
Two cases were investigated, with eccentricities of loading of $e = 0$, and $e = \frac{3b}{8}$, and the stress distributions are shown in Figs. 2-16 and 2-17.

8.9 SUNDARA RAJA IYENGAR'S ELASTIC SOLUTION.

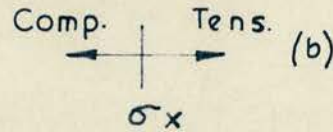
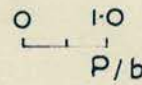
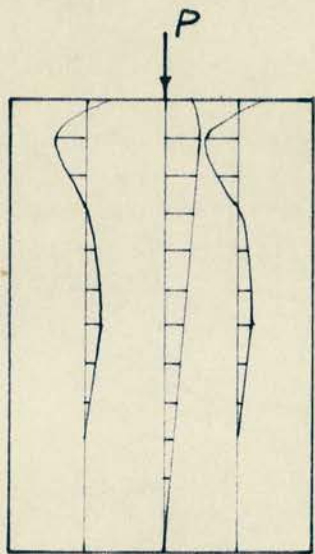
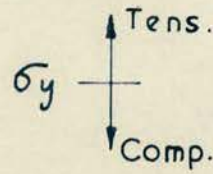
An exact theory for the two dimensional solution, satisfying all



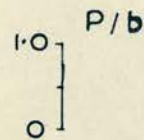
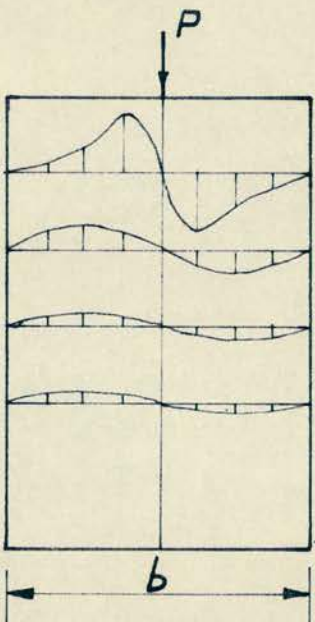
Scales



(a)



Anchorage Zone Stresses
($e \neq 0$)



Gerstner and Zienkiewicz

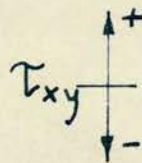
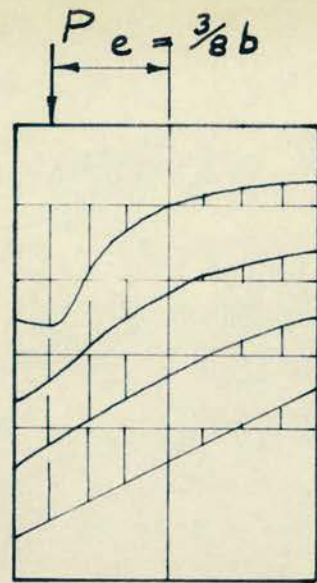
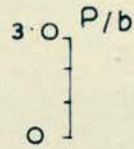


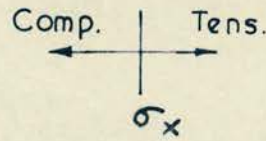
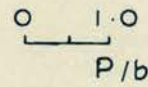
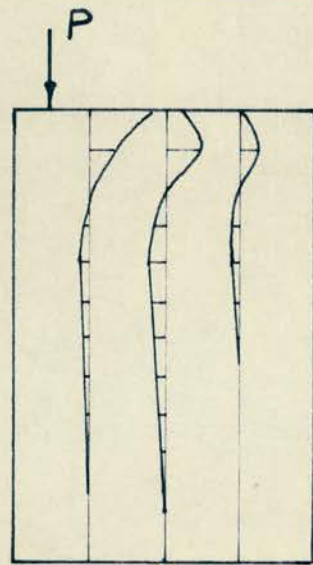
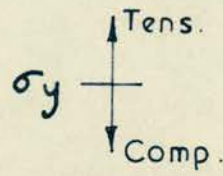
Fig. 2-16



Scales

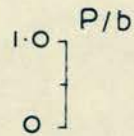
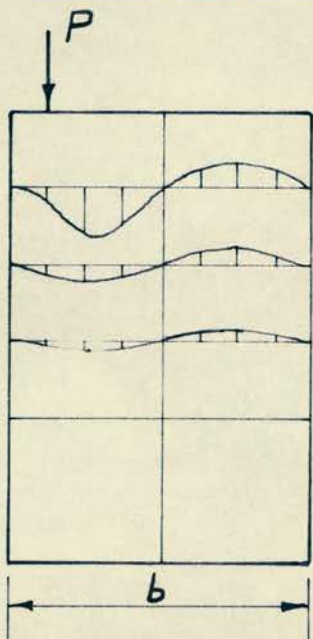


(a)



(b)

Anchorage Zone Stresses
($e = 3/8 b$)



Gerstner and Zienkiewicz

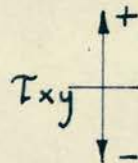


Fig. 2-17

the equations of elasticity and all the boundary conditions has been proposed (23).

8.10 A SOLUTION BY LATTICE ANALOGY.

The solution presented (24) is the stress distribution in a beam, 12" deep, when loaded by a 4" bearing plate, with no eccentricity, and no shearing force. The loading case is shown in Fig. 2-18(a). The stresses were obtained by a relaxation solution by the method of lattice analogy, and are shown in Figs. 2-18(b) and 2-18(c).

Points to note are that the longitudinal stresses become uniform, and the transverse and shearing stresses zero, at a distance from the end equal to $0.8d$. Also, in order to use the lattice analogy, the use of a Poisson's ratio of $1/3$ is obligatory and the transverse strains are susceptible to large change in Poisson's ratio.

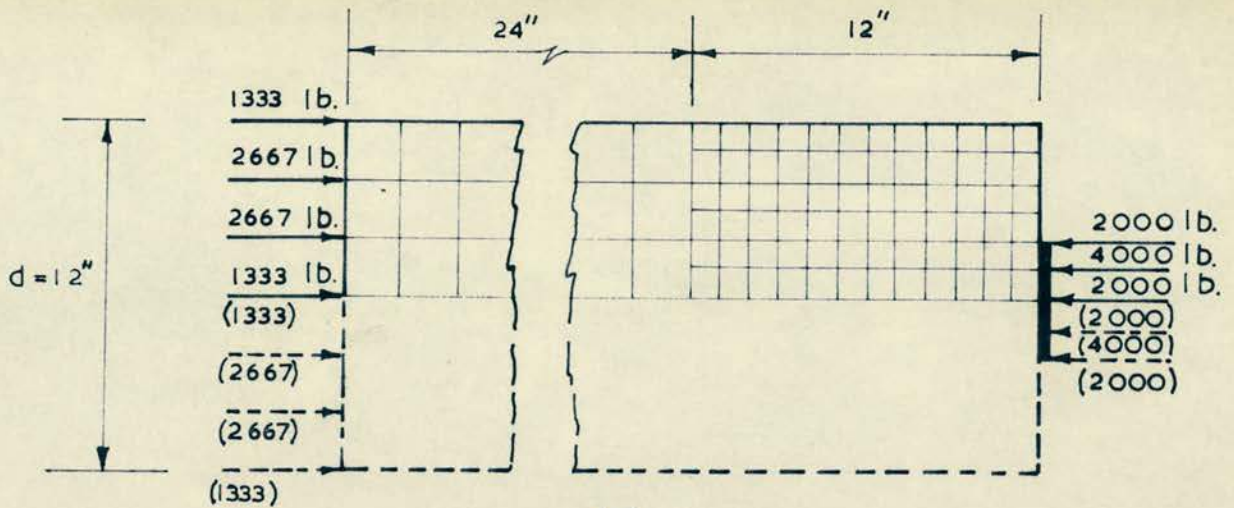
9. A COMPARISON OF THE TWO-DIMENSIONAL THEORIES.

The transverse stresses of Guyon and Gerstner and Zienkiewicz compare well, although the approaches to the problem are different.

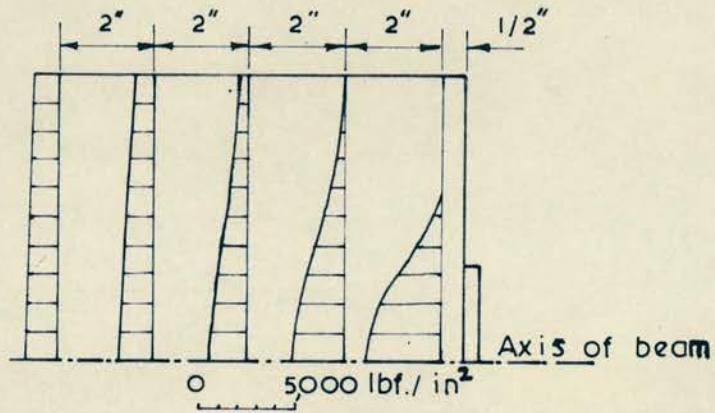
The transverse stresses obtained by Magnel and Chaïke are greater than those of Guyon and their maximum values occur at greater distances from the surface of load application.

Fig. 2-19 gives a comparison of some of the theories, including three-dimensional ones, that are discussed below.

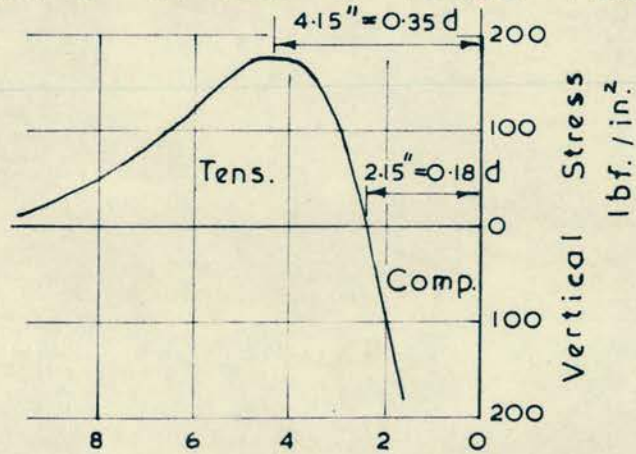
The lattice analogy gave longitudinal compressive stresses which were in good agreement with those obtained from Guyon's theory. The magnitude of the transverse tensile stresses were of the order of half those predicted by Guyon, although the positions of the maximum and minimum values agreed well. The use of a Poisson's ratio of $1/3$ rd.



(a)
Loading Case



Horizontal Stresses on Vertical Planes



Distance Along Horizontal Axis. - in.
(c)

Vertical Stresses on Horizontal Axis

Lattice Analogy

Fig. 2-18

could account for this discrepancy.

10. THREE-DIMENSIONAL THEORIES.

10.1 GUYON'S SOLUTION.

Guyon has formulated an approximate solution, for a square loading, concentric on a square end block. The results of his theory are illustrated in Fig. 2-14.

10.2 SIEVERS' THEORY.

Sievers, following in principle the work of Morsch, used the results of Bleich's analysis of deep beams, and presented an approximate formula for the calculation of the transverse stresses which fulfilled the required boundary conditions.

10.3 DOUGLAS AND TRAHAIR'S CONTRIBUTION.

The approach adopted was to idealise the lead in zone, which will almost certainly be a rectangular block, by replacing the rectangular block by a hollow cylinder. The load is applied uniformly as a pre-stressing force, over a portion of the cylinder, concentric with the duct.

Because of the axial symmetry of the cylindrical zone the variation of θ has no effect upon the stresses which are functions of r and z only. Fig 2-20.

The stress system used is derived from a stress function ϕ and satisfies the equations of equilibrium and compatibility provided that

$\nabla^2 \phi = 0$. The function used is a Purser function, in terms of a Fourier-Bessel series. The boundary conditions that the radial stress should vanish on the inner and outer rims were not satisfied. A method of superposition was then adopted in which the residual radial stresses

on the curved rims were made zero at the expense of other boundary conditions.

The analysis leaves behind residual axial and shear stresses on the plane end, and is therefore not elastically exact.

The computation of stresses in the anchorage zone has been carried out for the values of $c = 3$ ins, $b = 3/8$ ins., i. e. a cylinder of diameter 6 ins., with a central duct of $3/4$ " dia., and with a Poisson's ratio of 0.15.

Complete stress distributions were found for $a = 1.5$ ins. (plunger dia. = 3 ins.) The contours of the three principal stresses are shown in Fig. 2-20. These stress distributions are applicable to any case where the geometric similarity is preserved and show that the maximum tensile stresses are the hoop stresses along the inside boundary.

The distributions of the hoop stress were found for a range of values of "a" (plunger radius), and are shown in Fig. 2-21, the curves being calculated for a constant prestressing force.

10.4 IYENGAR'S AND YOGANANDA'S ELASTIC THEORY.

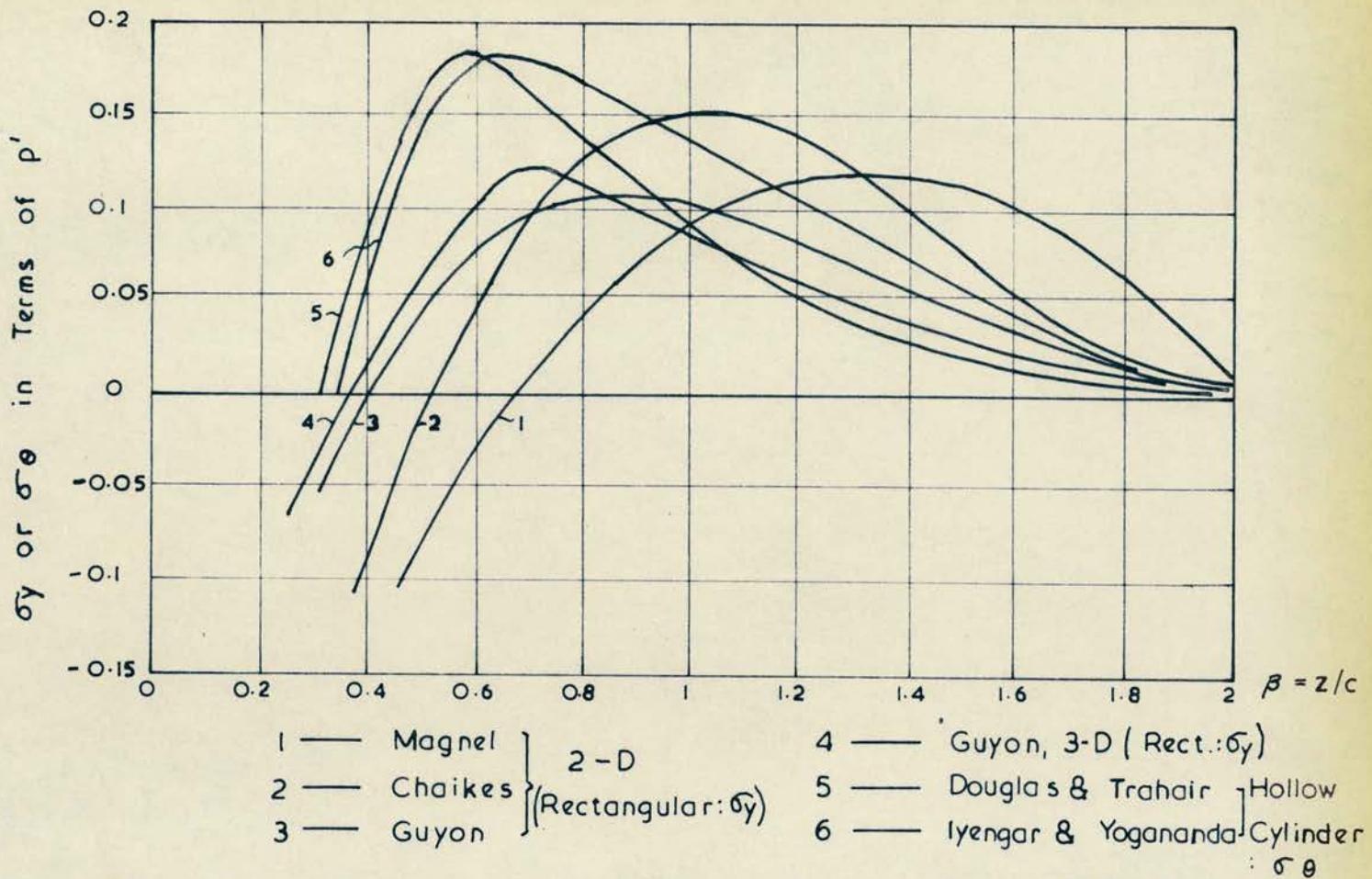
A solution to the end problem of a semi-infinite hollow cylinder has been proposed (16). The solution satisfies the equations of three-dimensional axi-symmetric elasticity and all the boundary conditions.

The theoretical solution is based on a Love function ϕ , satisfying

$\nabla^4 \phi = 0$ where ∇^2 is the Laplacian operator defined as;

$$\nabla^2 = \frac{\partial^2}{\partial r^2} + \frac{1}{r} \frac{\partial}{\partial r} + \frac{\partial^2}{\partial z^2}$$

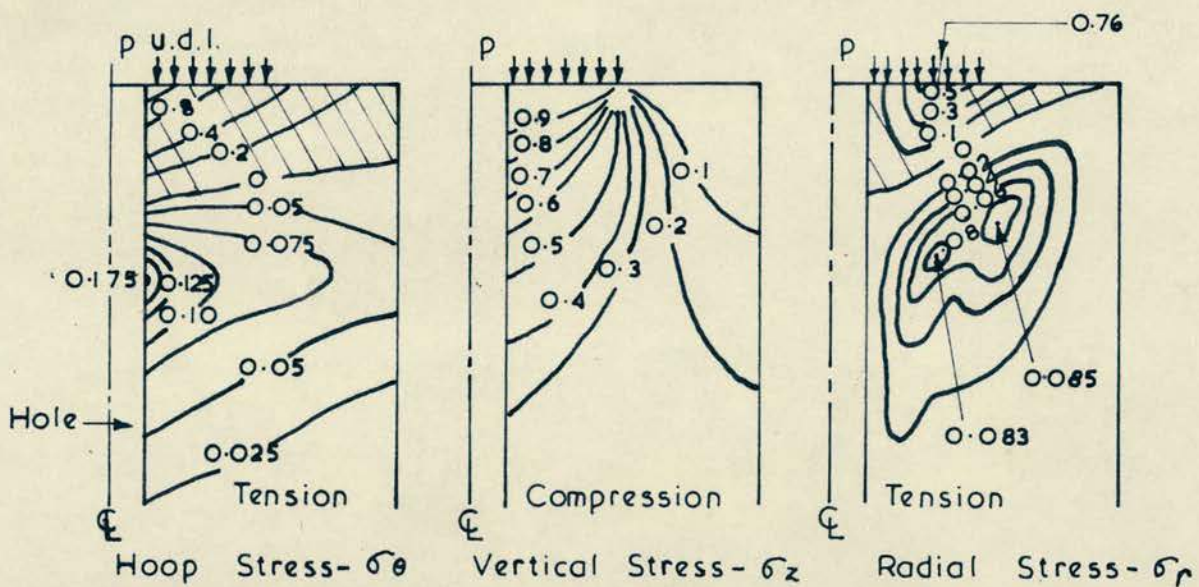
Stresses and displacements can be derived from the function by



Stress Comparisons on the Inner Rim — $r/a = 0.125$. $p = F/\pi(a^2 - b^2)$; $p' = F/\pi(c^2 - b^2)$

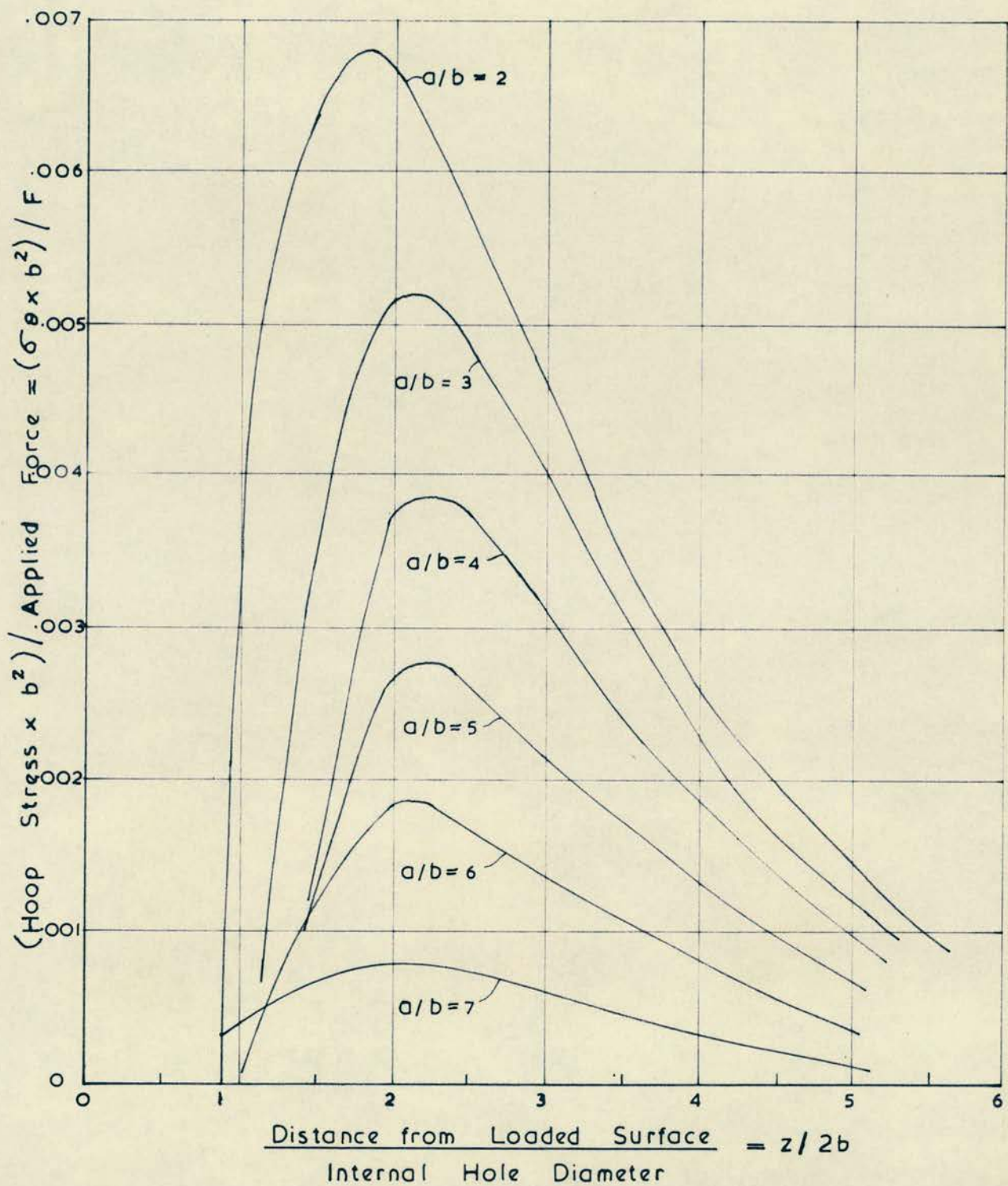
Fig. 2-19

Douglas and Trahair - Theoretical Solution



Stress Contours (Factors of p)

Fig. 2-20



Variation of Internal Hoop Stress Under Constant Applied Prestressing Force - Douglas and Trahair Fig. 2-21

suitable differentiation.

The solution obtained was applied to a hollow concrete cylinder having the following proportions.

Outer diameter/inner diameter = 8, Poisson's ratio = 0.15.

The result for the hoop stress is shown in Fig. 2-19.

11. A COMPARISON OF THE THREE-DIMENSIONAL ANALYSES.

A comparison of the two-dimensional and three-dimensional theories for the transverse and hoop stress distributions are given in Fig. 2-19. The various theories are seen to give widely ranging results, particularly regarding the position of the maximum hoop or transverse stress. The range of the stress values are from $(0.11 - 0.18) p'$, where p' is the average intensity of loading.

In practice, rectangular and other prismatic concrete end blocks with longitudinal cable duct(s) are encountered in post-tensioned concrete beams. An elasticity solution for such a problem is extremely difficult to formulate, but it may well be that experimental work may provide results which enable a rational design of the end blocks to be undertaken.

12. EXPERIMENTAL INVESTIGATIONS OF CONCENTRIC CONCENTRATED LOADINGS.

12.1 THE WORK OF CHRISTODOULIDES.

Christodoulides (26, 27) carried out two-dimensional and three-dimensional photo-elastic investigations, but the particular cases chosen for investigation do not allow a direct comparison with the theoretical analyses.

The trend of results, however, reinforces earlier theories and

the three-dimensional case compares favourably with strain gauge readings on an actual beam.

12.2 THE WORK OF BAN, NUGURAMA AND OGAKI ⁽²⁸⁾

The research carried out was an attempt to verify the earlier two-dimensional solutions suggested by Bleich. Reasonable agreement was obtained between predicted strains and strains measured with electrical resistance gauges. The investigation was restricted to the Lee-McCall method of post-tensioning.

Work carried out on surface strains, measured on the outside of a concrete block, showed agreement with those predicted theoretically along the internal central axis, by the theory of Sievers. The justification of this comparison is not given, and it may be only coincidental.

Ban also concluded that the cracking load remained constant for any area of bearing plate, but may be influenced by the thickness of the bearing plate, the size of the nut used, and the amount of reinforcement in the loaded zone.

12.3 THE EXPERIMENTS OF DOUGLAS AND TRAHAIR.

In conjunction with their theoretical investigation outlined above, Douglas and Trahair ⁽²⁵⁾ conducted a series of experiments to determine the stress distribution on the cylinder which had been theoretically investigated. The hoop strains were measured, using electrical resistance strain gauges, positioned both internally and externally on the inner and outer cylindrical surfaces.

The experiments pointed to several factors of importance. For the same set of loading conditions the ratio p / f_t , (the intensity of

applied prestress/ultimate tensile stress) was much nearer constant than the P/f_c ratio (f_c , the ultimate compressive stress). This result supports the theory that the load at failure depends more on the tensile than the compressive strength of the concrete.

The simple theory of failure, based on failure occurring when the hoop stress at any point reaches the tensile strength of the concrete, as measured by the Brazilian test, gives very low values, compared with the experimentally obtained results. The ultimate loads obtained experimentally are from 3.6 - 4.6 times those predicted by the simple theory. Some explanations of this phenomena assume plasticity, and plastic redistribution of stress over the major portion of the loading range. In this investigation, the strain gauges showed an elastic behaviour up to 75 - 85% of the ultimate load, and the stress distribution is according to the theory. Hence it is probable that the material in the loaded zone behaves elastically up to near failure, with localized stresses far exceeding the simple tensile strength of the concrete.

The conclusion drawn from this investigation was that the theories of failure are inadequate, whereas the theoretical elastic stress distribution was in good agreement with measured strains.

12.4 THE EXPERIMENTS OF ZIELINSKI AND ROWE.

Zielinski and Rowe (29) performed a series of experiments on concrete prisms of four sizes. These were 6" x 6" x 16", 6^{11/16}" x 6^{11/16}" x 16", and 8" x 8" x 12^{1/2}" or x 16". Various types of construction were chosen, varying from no embedded anchorages, and no ducts, to embedded anchorages and inflated ductubes.

In order to simulate the loading which occurs in actual post-tensioning systems, the following procedures were employed.

For specimens with embedded Freyssinet Anchorages;

- (i) load was applied directly to the male cone with all the prestressing wires in position.
- (ii) load was applied through steel disks of the same diameter as the female cone.

For specimens with embedded P.S.C. anchorages; load was applied through steel plates over the entire exposed area of the anchorage.

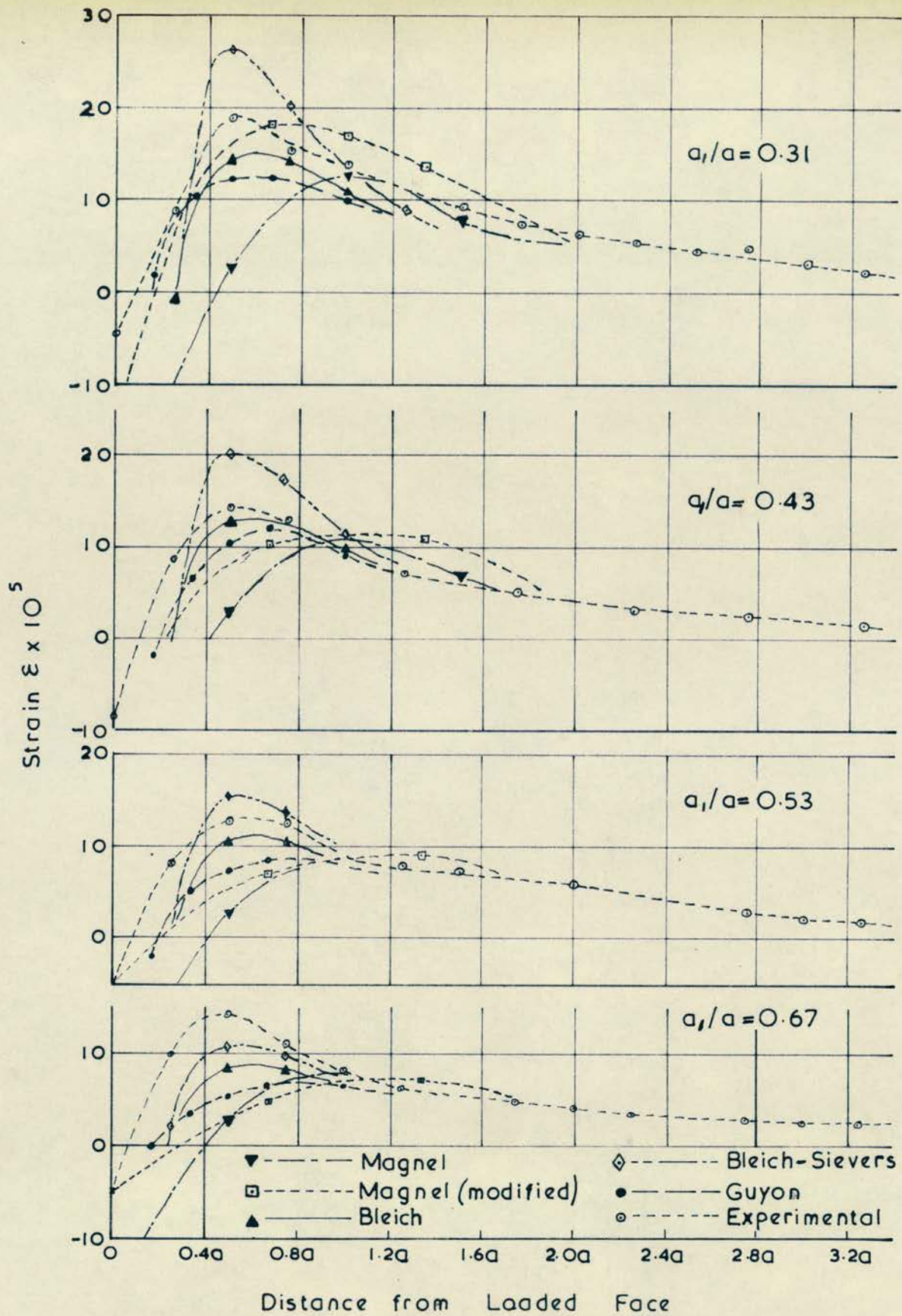
For specimens with external anchorages; load was applied through steel plates, the size of which varied to give the appropriate a' / a ratios.

Load was applied to the specimen, either by a manually operated jack of 50 tons capacity, or by an Avery compression testing machine of 200 T capacity.

Strains were measured, on the surface of the prisms, using a 2" demec gauge. Considerable numbers of strain readings were taken, and strain gauge rosettes were set up.

The maximum tensile strains were found to occur on the centre line of the prism face, and the maximum value was approximately 12% greater, for a cone loading, than for a plate loading.

Fig. 2-22 shows the comparison of the various theories for different values of a' / a , Poisson's ratio being taken as 0.125. The experimental values are included and are shown to be higher than the theoretical values obtained by all but the Bleich-Sievers theory.



Theoretical and Experimental Transverse Strains for Various a_1/a Ratios.

Fig. 2-22

The position of the maximum transverse tensile strain was shown to remain sensibly constant, and was at approximately 0.5a from the loaded end, where 2 a was the prism width.

It was shown that the maximum transverse stress, as a ratio of the uniform compression, (defined as the applied force/the prism area), was greater than the theoretical values for all the a' / a values considered.

From the strain distribution it was possible to calculate the total transverse force. Experimental values ranged from 0.36 - 0.186 of the total compressive force, for varying a' / a ratios. Bleich-Sievers theory gives a range from 0.271 - 0.107.

From the experimental results a formula for the tensile stress (Maximum) was suggested;

$$\frac{f_y \text{ max.}}{f_c \text{ unif.}} = 0.463 \beta^2 - 1.3 \beta + 1.1$$

$$\text{Where } \beta = a' / a .$$

The ratio of the total tensile force to the average compressive force was expressed as

$$\alpha = - 0.403 \beta^3 + 1.528 \beta^2 - 1.574 \beta + 0.714$$

$$\text{for } 0.3 < \beta < 0.7$$

12.5 BAUSCHINGER'S TESTS ON SANDSTONE CUBES.

Bauschinger's tests on sandstone cubes, in 1876, were the first tests to investigate bearing capacity. The range of A_c / A_b (total specimen area/bearing area) ratio investigated, was from 1:1 to 7:1.

The failure pressure was shown to increase as A_c / A_b increased.

The results obtained could be represented by the relationship,

$$q_u = u_w \sqrt[3]{A_c / A_b}$$

where u_w was the crushing strength of the cube.

12.6 MEYERHOF'S TESTS AND THEORY.

Meyerhof (30) conducted three series of tests in which he adjusted the variables concrete block thickness, area of block/area of bearing plate, and amount of reinforcement of the block.

The results obtained indicated increasing bearing capacity with increase of block thickness.

The bearing capacity was shown to increase with increasing A_c/A_b ratio, attaining a limiting value at a high value of A_c/A_b .

The effect of reinforcing the bearing blocks was found to be an increase of strength by up to a factor of three.

Meyerhof proposed a theory of failure, which is illustrated in Fig. 2-23(a). Failure was represented approximately by,

$$S = C + p \tan \phi ,$$

Coulomb-Mohr theory of rupture, the confining action of the surrounding material increasing the resistance in a manner similar to that observed in triaxial compression tests. Failure generally occurs by splitting or shearing along one or several rupture faces in triaxial tests.

Referring to Fig. 2-23(a) it is seen that beneath the bearing plate a wedge or cone of material, corresponding to $\phi = 40^\circ - 50^\circ$, is formed by shearing along a rupture surface, and is forced into the material below.

When the tensile strength of the surrounding material is exceeded the block is split progressively downwards. A simple theory may be suggested for a two-dimensional case.

At the bearing capacity q , of a strip footing, of width B , resting on a block, of thickness H , and width L ($\geq H$) the horizontal splitting pressure can be shown to be

$$P_h = q \tan^2 \alpha - 2 c \tan \alpha$$

where c is the unit cohesion. The resultant of these pressures acts at a depth $B \cot \alpha / 4$, where the semi-wedge angle α , is $(45 - \phi / 2)$.

The maximum bending tensile stress at the point of the wedge of material below the footing is

$$P_t = \left[1 + \frac{6H}{2H - B \cot \alpha} \right] \frac{B \cot \alpha}{2H - B \cot \alpha} \cdot P_h$$

Substituting for P_h from above, and simplifying

$$q = \frac{\left(\frac{2H - \cot \alpha}{B} \right)^2 \cot \alpha P_t}{\frac{8H}{B} - \cot \alpha} + 2 c \cdot \cot \alpha$$

If H/B is large, and substituting the unconfined prism strength $p_u = 2 c \cot \alpha$, then

$$q / p_u = 1 + H P_t / 4 B \cdot c.$$

This relationship indicates that the bearing capacity of the block is proportional to the ratio of block depth to bearing plate width, H/B , for a given ratio of P_t / c , depending on the properties of the material. Compression tests indicate that approximately $c = 0.2 p_u$ for concrete and rock, and approximately $P_t / p_u = 0.2$ for concrete, and 0.1 for sandstone.

Hence P_t / c is approximately 1 for concrete and 0.5 for sandstone.

The theoretical analysis agreed well with the experimental results for rectangular strip bearing plates.

For circular bearing plates the analysis is similar, the bearing

capacity being larger, and depends on the hoop stresses set up.

When splitting is prevented by the use of reinforcement or in the case of blocks which are large in comparison with the size of bearing plate, the bearing capacity is mainly governed by the shearing strength of the material. At failure a wedge or cone is formed, as before, but in this case the material at the side is forced outwards and upwards, by shearing along a curved rupture surface, Fig. 2-23(b). The bearing capacity of the strip loading may then be represented by $q = cN_c$, according to Terzaghi. N_c is a bearing capacity factor, dependent on ϕ , the angle of internal friction, and the L/B ratio (or the inclination β of the equivalent free surface). For the shear failure of a block, with $H = L$, the bearing capacity increases with H/B at approximately twice the rate found for the splitting failure of concrete.

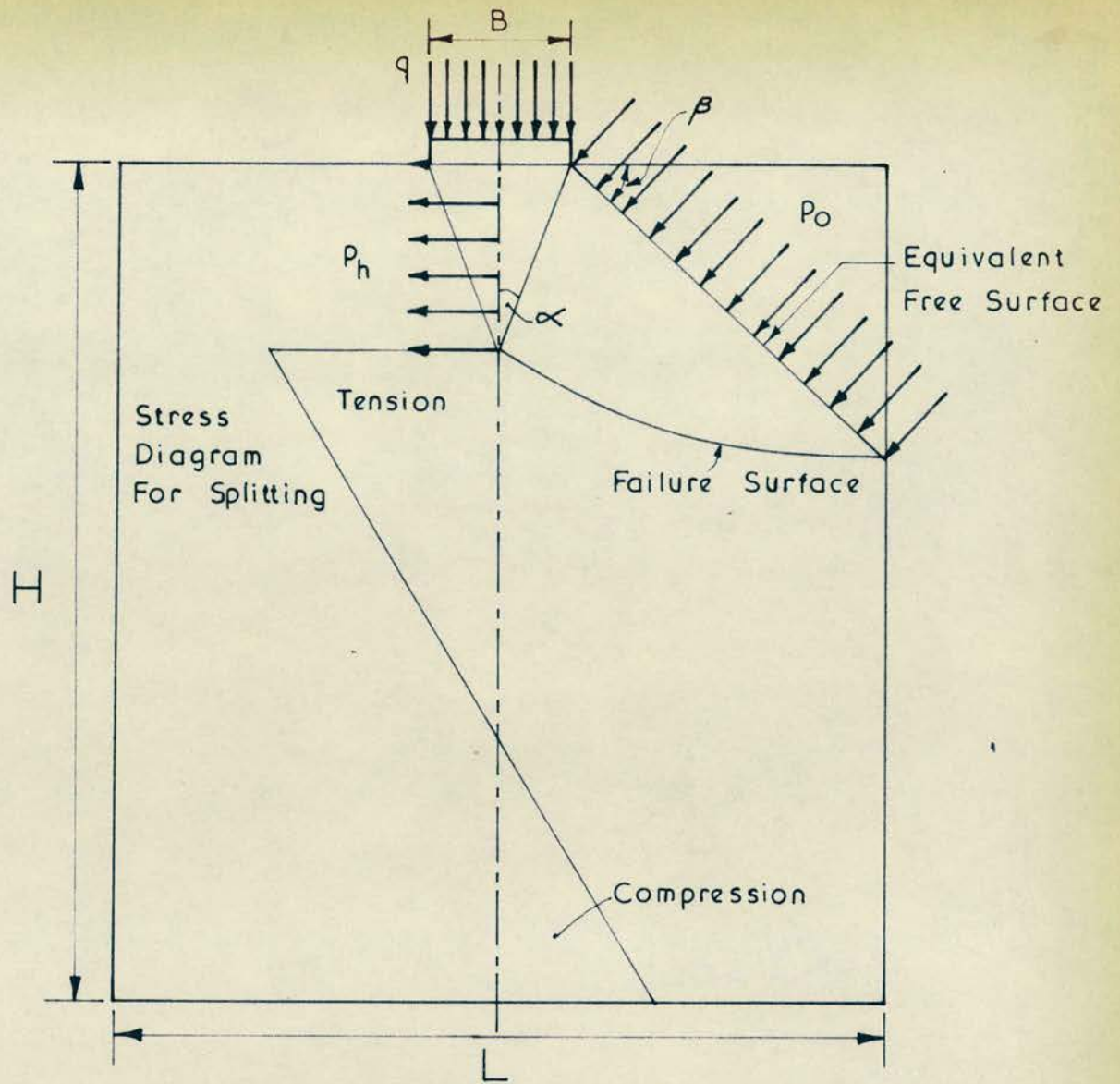
For very large values of L/B the bearing capacity is equal to that of a strip footing on a semi-infinite solid.

12.7 THE WORK OF AU AND BAIRD.

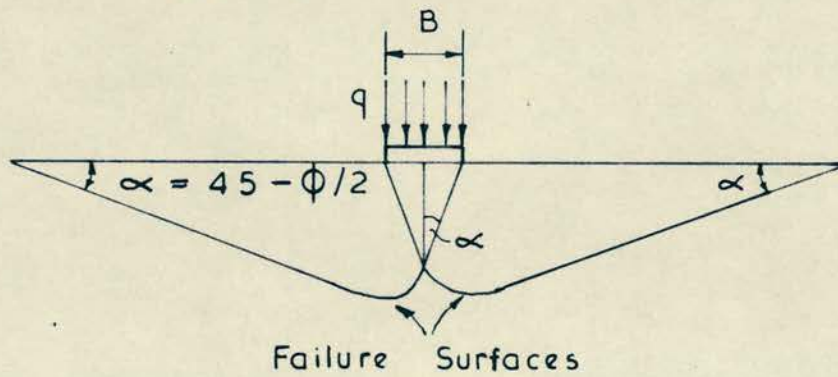
A series of tests was conducted ⁽³¹⁾ to determine the effect of the A_c/A_b ratio, and the "height of the block/width" ratio, for axially loaded blocks. The A_c/A_b ratio was varied from 2-16, and two sizes of concrete block were tested, 8" cubes, and 8" x 8" x 4" blocks. Two different mixes were used, with different maximum aggregate sizes, in order to investigate whether or not the scaling down of the aggregate size gives a better representation of an actual bearing block, Cylinders, 6" x 12" were cast, and tested to obtain f_c^1 , the concrete crushing strength.

The relationship, ultimate bearing stress/crushing strength,





(a) L/B Ratio Low



(b) L/B Ratio High - Shearing Failure

Meyerhof's Failure Theory

plotted against A_c/A_b showed a clear, but not quite linear relationship, the ultimate bearing stress increasing with increasing A_c/A_b ratios.

In the first series of tests, with the 8" cubes, the failure occurred due to vertical splitting of the cubes, accompanied by the formation of a cone below the bearing plate.

In the case of the 8" x 8" x 4" blocks the failure occurred due to radial splitting from the perimeter of the bearing plate.

The failure stresses of the shallow blocks were higher than those of the cubes, indicating that the shallow depth retarded the formation of the cone or pyramid beneath the bearing plate.

The results above indicate that the depth of the bearing block has a pronounced effect on the bearing capacity, when the depth/width ratio is small. No conclusion can be drawn as to the general effect of the depth/width ratio.

12.8 THE WORK OF SHELSON.

Shelson ⁽³²⁾ carried out axial loading tests for the bearing capacity of 8" concrete cubes, varying the A_c/A_b ratio.

The observed failure mode was the formation of a wedge, beneath the bearing plate, which was forced into the concrete, causing a splitting of the block.

Higher failure stresses were obtained with increased A_c/A_b ratios, up to a limit of $A_c/A_b = 30$.

Further tests revealed that when the depth of the bearing block was reduced, a non-wedge type of failure occurred, and higher failure stresses were observed.

A "realistic and reasonable" design formula was proposed,

$$f_c = 0.25 f_c^1 R^{0.3}$$

where

f_c - permissible bearing stress

f_c^1 - cylinder compressive strength at 28 days

R - A_c/A_b

12.9 THE WORK OF CAMPBELL-ALLEN, MIDDENDORF, LIN AND HAWKINS.

The axial load tests carried out were all performed on cylinder specimens of various dimensions.

Campbell-Allen (33) tested both concrete and mortar cylinders, and found that for depth/diameter > 1 , the relationship between q_u / f_c^1 and A_c/A_b was linear for A_c/A_b lying between 1.8:1 and 16:1.

Middendorf (34) tested 8" diameter cylinders, 16" deep, using 3", 4", 5", 6", 7" and 8" diameter bearing plates, and found $q_u \propto$ diameter of plate, i. e. $\sqrt{A_c/A_b}$.

Lin's experiments revealed a similar trend to Middendorf's.

Hawkins (35) concluded that the q_u / f_c^1 ratio attains a limiting value, and that the block depth has no effect on q_u provided the block depth is sufficient to allow the formation of a pyramid.

13. EXPERIMENTAL INVESTIGATIONS OF ECCENTRICALLY APPLIED CONCENTRATED LOADINGS.

13.1 THE TESTS OF KRIZ AND RATHS. (36)

Kriz and Raths conducted a large number of tests on axially and eccentrically loaded plain and reinforced concrete blocks, and observed three types of failure,

- (i) splitting failure,
- (ii) crushing failure,
- (iii) shear failure.

The modes of failure were explained by the following factors,

- (i) high tensile stress in a lateral direction may bring about a splitting failure,
- (ii) compressive stress in the concrete under the plates may result in crushing failure.
- (iii) shear stresses near the corner may lead to a failure along an inclined plane.

The following conclusions were reached.

- (a) The ultimate bearing stress, i. e. q_u is not proportional to fc^1 , the cube strength, but is proportional to $\sqrt{fc^1}$, which is related to the concrete tensile strength.
- (b) q_u is influenced by the bearing plate width, and by the distance of the bearing plate from the edge of the block.
- (c) The type of failure of blocks, without reinforcement depends on the position of the bearing plate on the block. Splitting occurs when the distance "s" from the edge of the block to the centre-line of the bearing plate is $> 1.5"$. When "s" is $< 1.5"$ a shear failure occurs along an inclined plane extending outward from the inner edge of the bearing plate.

Further tests, on reinforced blocks indicated that

- (d) q_u may be increased by lateral reinforcement embedded near the top of the block. The lateral reinforcement arrests the vertical splitting failure, but cannot prevent a shear failure. For $s \leq 1.5"$

a shear failure occurs and the bearing strength is the same as that of a concrete block without lateral reinforcement.

(e) The amount of longitudinal reinforcement does not significantly change the ultimate failure stress.

A formula relating the ultimate bearing stress, and the variables involved was proposed.

13.2 CAMPBELL-ALLEN'S INVESTIGATION.

In 1945 a small number of tests were performed to study the effect of eccentric loading on 4" diameter concrete cylinders. The load was applied through a 1" diameter metal cylinder.

The results indicated that the ultimate bearing stress, q_u , increased with a reduction of the eccentricity of the loading, attaining a maximum value for concentric loading. The ratio q_u / f_c^1 plotted against the eccentricity/diameter of loaded area ratio gave a non-linear relationship. (f_c^1 is the cube strength of the concrete).

13.3 THE WORK OF ADAMS, BARON AND PLEWES.

Concrete blocks were loaded through steel plates, 1" long, extending the full width of the blocks. The block size tested was 10" high, 15" long, and 6" wide. The variables in the test were the distance of the bearing plate from the edge of the block, and the width of the bearing plate.

Failure occurred suddenly, and both vertical cracking, and shearing failure occurred, at the loaded edge, simultaneously.

By a split second removal of the load, as failure occurred, only vertical cracking was observed, when the load was positioned 1" from the edge of the block.

14. A SUMMARY OF THE RESULTS OF TESTS CARRIED OUT ON CONCRETE BLOCKS.

- (i) The failure stress is dependent on the A_c/A_b ratio, but reaches a limiting value as A_c/A_b increases. The relationship between q_u and A_c/A_b has in some cases been found to be linear, and in others q_u was found to be proportional to $\sqrt{A_c/A_b}$.
- (ii) The failure stress is dependent on the edge distance of the bearing plate, increasing with increase of edge distance, i.e. with decrease of eccentricity, to a maximum value on the block centre-line.
- (iii) The failure stress decreases with increasing block depth, but this effect is only important in the region $H < L$, i.e. height of block $<$ length. (Meyerhof disagreed with this result).
- (iv) The mode of failure of the block depends on the positioning of the bearing plate, in relation to the edge of the block.
- (v) Where the block is reinforced laterally, to resist transverse tensile stresses, the ultimate bearing stress is increased, but increasing the amount of reinforcement does not have a significant effect. Also if the failure is due to shear, the reinforcement is ineffective.

15. GHOSH'S INVESTIGATION OF BEAMS SUPPORTED ON BEARING BLOCKS.

15.1 OBJECT AND TYPES OF TEST CONDUCTED.

Ghosh's tests (37) were conducted to investigate the precast concrete beam-column joint, utilising bearing and bond.

In the tests conducted the load was applied to the reinforced concrete bearing block (6" x 6" x 6") through either a reinforced concrete beam, or a steel joist. In the case of load application by

an R.C. beam, the beam was centrally loaded, and subject to flexure, and hence rotation could occur at the bearing block.

Six different types of R.C. beam were cast, to give different end conditions. These conditions are summarised below:

- (i) Load carried fully by bearing.
- (ii) Load carried partly by bearing and partly by dowel action of the projecting reinforcement.
- (iii) Fully by dowel action of the projecting reinforcement, and the shearing resistance at the interface.

The length of bearing was either $\frac{1}{2}$ " or 1" when bearing alone was relied on.

15.2 TEST RESULTS.

The bearing capacity of the block was found to be dependent on the bearing area, whilst that of the beam seemed independent, in the experimental range considered.

For short bearing lengths there is a possibility of failure either in the beam, or in the bearing block, whereas for longer bearing lengths the failure occurs in the beam.

The results from the tests performed using the R.S.J. varied only slightly from the beam tests, and all the results indicated that the bearing failure stress increased as the A_c/A_b ratio decreased, although the failure load decreased.

The observed failure mode of the block was due to the simultaneous formation of vertical and slightly inclined cracks, and the shearing failure of the edge of the block.

The ultimate bearing capacity of the beams was shown to be

increased by increasing the amount of shear reinforcement, and by giving less end cover. Also the provision of projecting reinforcement was advantageous, eliminating all cover.

The best type of joint was that which incorporated some bearing, and had in filled projecting reinforcement.

The effect of the end rotation of the beam was considered for a bearing length of 6", and it was concluded that the maximum effect was a 10% reduction in the failure load of the block.

16. DESIGN SPECIFICATIONS IN CURRENT CODES OF PRACTICE.

16.1 INTRODUCTION.

The exact mechanism of failure where concentrated loadings act is not known, or the theories put forward have not yet gained sufficient approval to be included in the current codes of practice.

The various codes comment generally on the case of concentric and geometrically similar loadings applied to bearing blocks, concrete members, masonry and steel structures. The case of eccentric loading or dissimilar shaped bearing plates is usually ignored.

16.2 INFORMATION GIVEN BY CODES OF PRACTICE, ETC.

(i) BRITISH CODES.

C.P. 114 specifies minimum lengths of bearing, which are 4" on masonry and 3" on steel, concrete and precast units.

C.P. 111 - 1964 ⁽¹⁾ allows an increase of 50% to be made to the normal permissible stress in a brickwork member, when a stress concentration of a purely local nature occurs. Where indeterminate but high stresses occur, the load should be distributed by a spreader beam.

C.P.116 - as C.P. 114. The allowable bearing pressure at a column and footing interface is allowed to exceed by 40% the permissible axial compressive stress in the concrete of the footing. This gives an allowable permissible bearing stress of $0.42 U_w$, U_w being the cube crushing strength.

(ii) FRENCH CODE. (plain or reinforced concrete).

For centrally loaded bearing plates;

$$q_u = U_w \left(4 - 5 \sqrt{\frac{A_b}{A_c}} + 2 A_b/A_c \right)$$

for $A_b/A_c = 1$, $q_u = U_w$; for $A_b/A_c = 0$, $q_u = 4 U_w$.

$$q_w = 0.4 q_u. \quad (q_w - \text{the allowable stress} \\ q_u - \text{the ultimate stress})$$

For an eccentric loading, the area considered is that round the bearing plate which would leave the bearing plate concentrically positioned.

(iii) AMERICAN CODE. (American Concrete Institute).

For bearing on the full area, the allowed stress is $0.25 f_c^1$. (f_c^1 being the crushing strength of cylinders).

For bearing on 1/3rd. of the area or less, the stress allowed is $0.375 f_c^1$.

For intermediate values of A_b/A_c interpolation is allowed.

The increase in permissible stress is only allowed when the minimum edge distance is greater than 1/4 of the greatest dimension of the total area.

(iv) GERMAN CODE - DIN 4227.

$$\text{Allows } q_w = K. U_w \sqrt[3]{A_c/A_b}$$

K varies from 0.47 - 0.35, depending on U_w . This

expression is valid for concentrically loaded concrete members. The dimensions for load distribution must not exceed 5 times the dimension of the loaded area.

(v) DUTCH CODE.

For centrally loaded bearings,

$$q_w = K. U_w \sqrt[3]{A_c/A_b}$$

$$A_c/A_b \geq 27.$$

An increase in the permissible bearing stress, q_w , may be made if the bearing area is adequately reinforced, and the increase is related to the percentage of steel.

(vi) AUSTRIAN CODE.

The permissible bearing stress on concrete, caused by embedded tendons, is allowed to be

$$q_w = \frac{U_w}{\beta (1 + 1.5 U_w/1000)}$$

The value of β depends on and decreases with increasing concrete cover.

(vii) SWISS CODE.

The permissible stress q_w may be taken as $U_w/2$ if the supporting area is adequately reinforced against splitting.

16.3 RECOMMENDED DESIGN SPECIFICATIONS.

(i) Institution of Civil Engineers.

In its "First Report on Prestressed Concrete" the Institution has recommended that the permissible bearing stress q_w , should be taken as

$$q_w = u_t / 2 \cdot \sqrt[3]{A_c/A_b},$$

where,

u_t is the cube strength at transfer.

(ii) A.C.I. - A.S.C.E. Committee 512.

Recommended that the ultimate bearing stress on corbels should not exceed $fc^1 / 2$, and on column heads $6.9 \sqrt{fc^1} (S/W)^{1/3}$, where S is the edge distance to the bearing plate centre-line, and W is the bearing plate dimension.

Recommended that reinforcement should be provided to resist tensile stresses accompanying bearing. If the bearing stress is $> 0.1 fc^1$, then the reinforcement should be provided parallel to the bearing surface, in both directions. A maximum cover of 1" is recommended.

Both the supporting and supported member should be reinforced, and the area of steel required is

$$A_{st} = \frac{V \text{ in }^2}{100000},$$

where

V is the design load in pounds.

(iii) Report by Precast Concrete Sub-Committee of the Research Committee of the Structural Engineers Association of Southern California - 1958.

The allowable bearing stress, in precast concrete must not exceed

$$0.4 \cdot fc^1 \cdot \sqrt[3]{A_c/A_b}$$

This is valid for central bearings.

(iv) Criteria for Prestressed Concrete Bridges - Bureau of Public Roads - U.S.A.

The allowable bearing stress,

$$q_w = 0.6 f_{ci}^1 \sqrt[3]{A_c/A_b} \leq f_{ci}^1$$

where

f_{ci}^1 is the crushing strength of cylinders at the time of tensioning.

16.3 COMMENTS ON SPECIFICATIONS AND RECOMMENDATIONS.

The existing specifications clearly do not make a rational approach to the problem of eccentrically loaded bearings. For axially loaded bearings several codes recognise the importance of the A_c/A_b ratio.

The British codes approaches are based on conservative practice and empirical methods, and have not yet taken account of recent experimental work.

The recommended design specifications of the I.C.E., if adopted into the code, would allow a rational basis for the design of axially loaded bearings.

It is hoped that the test programme carried out on axially and eccentrically loaded bearings of various dimensions, detailed in the later chapters of this thesis will provide a guide to suitable design procedures for brick masonry structures subjected to concentrated loading.

17. A DISCUSSION OF THE THEORETICAL AND EXPERIMENTAL INVESTIGATIONS OUTLINED ABOVE.

Many of the earlier theoretical solutions have been shown to be unsatisfactory for the case of a concentrated loading applied to a three-dimensional structural member. The most serious fault being that the theories underestimate the maximum tensile stresses that do in fact occur. The work of Zielinski and Rowe (28) has shown the nature of the strain distribution, and the magnitude of the strains occurring, for various a^1/a ratios, for concentric loadings on hollow square end blocks, the hollow being cylindrical.

An exact elastic solution has been put forward by Iyengar and

Yogananda (16) but unfortunately has not been applied to square bearing blocks, and hence a direct comparison cannot be made with the tests of Zielinski and Rowe.

The work of Douglas and Trahair (25) indicated that the theoretical approaches postulated gave a good agreement with experimental work, as far as the strain distribution was concerned, but failed to predict the ultimate loads.

Much experimental work has indicated the effect of the A_c/A_b ratio, on the ultimate stress, but the nature of the relationship remains in doubt. The depth of the bearing block has been shown to affect the failure stress, but not for practical cases where $H/L > 1$.

For eccentric bearing experimental work has indicated a reduction in bearing stress as the edge distance is reduced, and has shown that the edge distance affects the mode of failure of the bearing block.

Further work is required to determine design specifications, for eccentrically loaded bearings, which take account of the variables involved.

18. A PHOTO-ELASTIC INVESTIGATION OF THE STRESS DISTRIBUTION DUE TO ARBITRARILY PLACED CONCENTRATED LOADINGS ON RECTANGULAR PLATES.

Hiltscher and Florin (38) have conducted a thorough investigation of the stress distribution, with particular regard to the tensile stresses, when a rectangular plate is loaded at varying distances from the plate corner. The various factors affecting the stress distribution have been fully investigated by adopting different height/length and length/bearing plate length ratios.

The particular interest of Hiltscher and Florin was the stress

distribution produced in precast concrete panels, subjected to concentrated loadings. To simulate the panels they utilised araldite sheets, and determined the difference of the principal stresses using a polariscope, and the sum using a lateral extensometer. Thus the stresses in the panel were determined, and in particular the horizontal stresses. The horizontal stresses were plotted, to indicate the zones requiring tensile reinforcement.

Experimental Results.

A series of preliminary tests were carried out on an araldite sheet 200 x 200 x 10 m.m. thick, and the results are presented in Figs. 2-24, 2-25 and 2-26.

All the plates (araldite sheets) were tested in such a way that the base could be considered as fixed and rigid.

Two types of tensile stress were observed to exist. One type, a "splitting" stress was noted, beneath the load, and the other, a "tearing" stress, was found adjacent to the load, on the free surface of the plate.

The magnitude of these tensile strains varied with the position of the bearing plate. The larger tensile stress, for any load position, was the tear stress, and this reached a maximum when the bearing plate was positioned at the plate corner.

The splitting tensile stress had a maximum value when the bearing plate was in an intermediate position, between corner loading and central loading.

For a b/a value of 10, (the plate width/bearing plate width), the approximate position of the load to give the maximum tensile stress

was $d = b/7.5$ (where d was the distance from the corner to the centre-line of the load). For a b/a value of 30 the approximate position was $d = b/22$.

These results indicate that as the size of the bearing plate decreases the position of the maximum tensile splitting stress moves nearer the vertical free edge of the plate. Figs. 2-27 and 2-28, indicate the variation of the tensile stresses with the d/a ratio, for load concentration factors b/a , of 10 and 30.

Both tensile stresses were found to be independent of h/b ratio (where h was the plate height) if this ratio is not very small.

The extent of the tensile stress zones are shown in Figs. 2-24, 2-25 and 2-26 and indicate that the splitting tensile zone has a maximum area when the load is applied centrally to the plate.

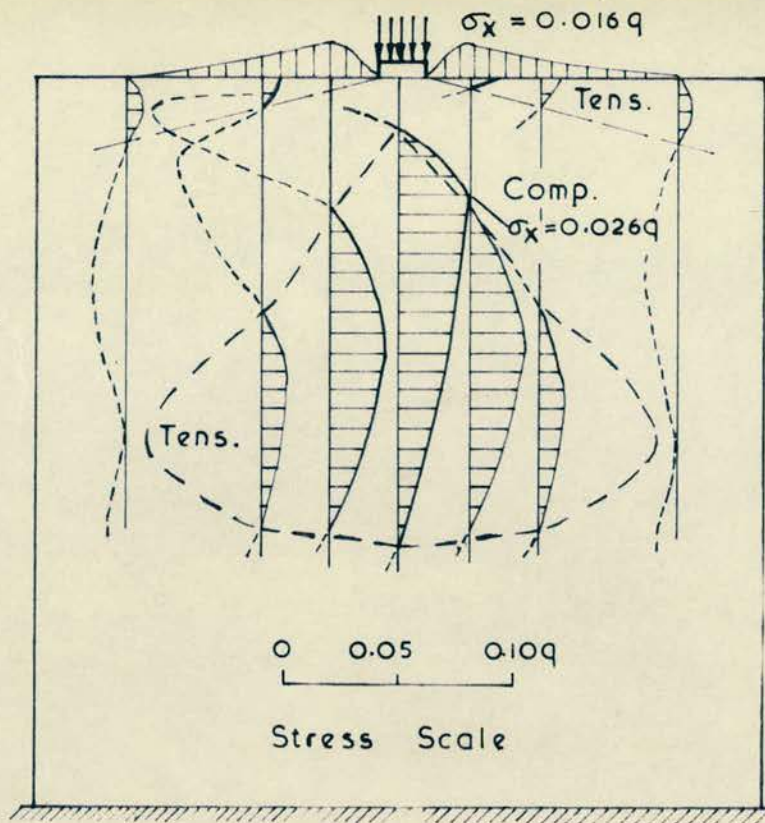
From the tensile stress distributions it was possible to calculate both the magnitude and the position of the corresponding tensile forces. With increasing load concentration factors, b/a , the tear tensile forces increased for the various load positions, whereas the splitting tensile forces decreased.

From the tensile forces the tensile reinforcement required may be calculated, and its positioning may be determined from the nature of the stress distribution.

Diagrams were given, allowing the tensile forces to be calculated, for any b/a , $2d/a$, and h/b ratios. The forces were plotted as functions of the total applied force P .

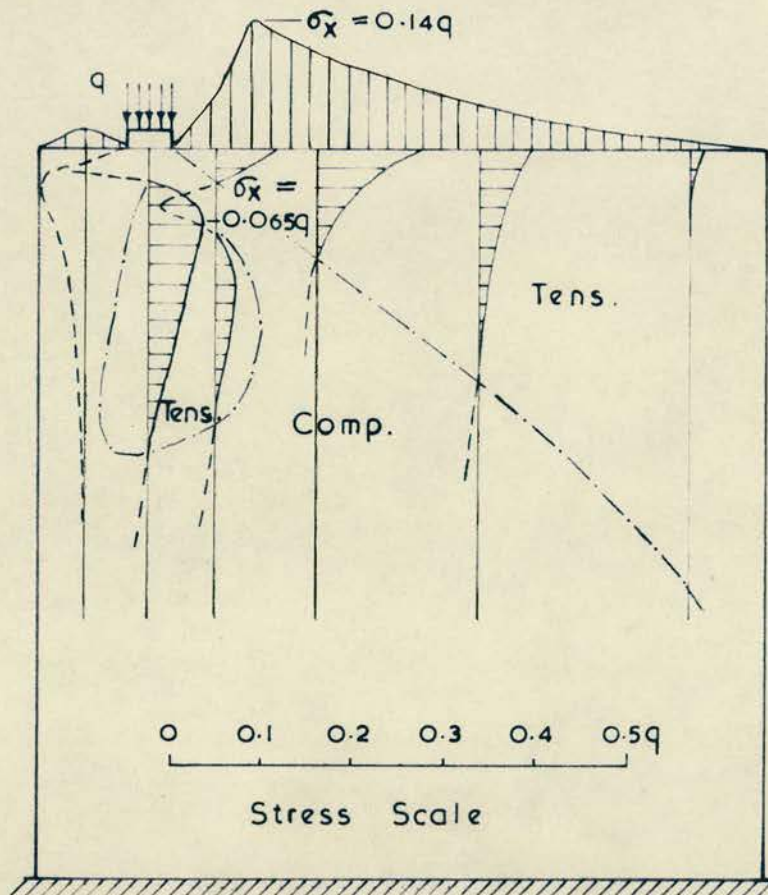
19. A PHOTO-ELASTIC INVESTIGATION OF THE STRESSES IN BRICKWORK SUBJECTED TO A UNIFORMLY DISTRIBUTED LOAD.

q-Intensity of Applied Stress



Tensile Zones and Horizontal Stresses σ_x (Tensile) in a Centrally Loaded Plate

Fig. 2-24



Tensile Zones and Horizontal Stresses σ_x (Tensile) in a Plate Loaded Near the Edge

Fig. 2-25

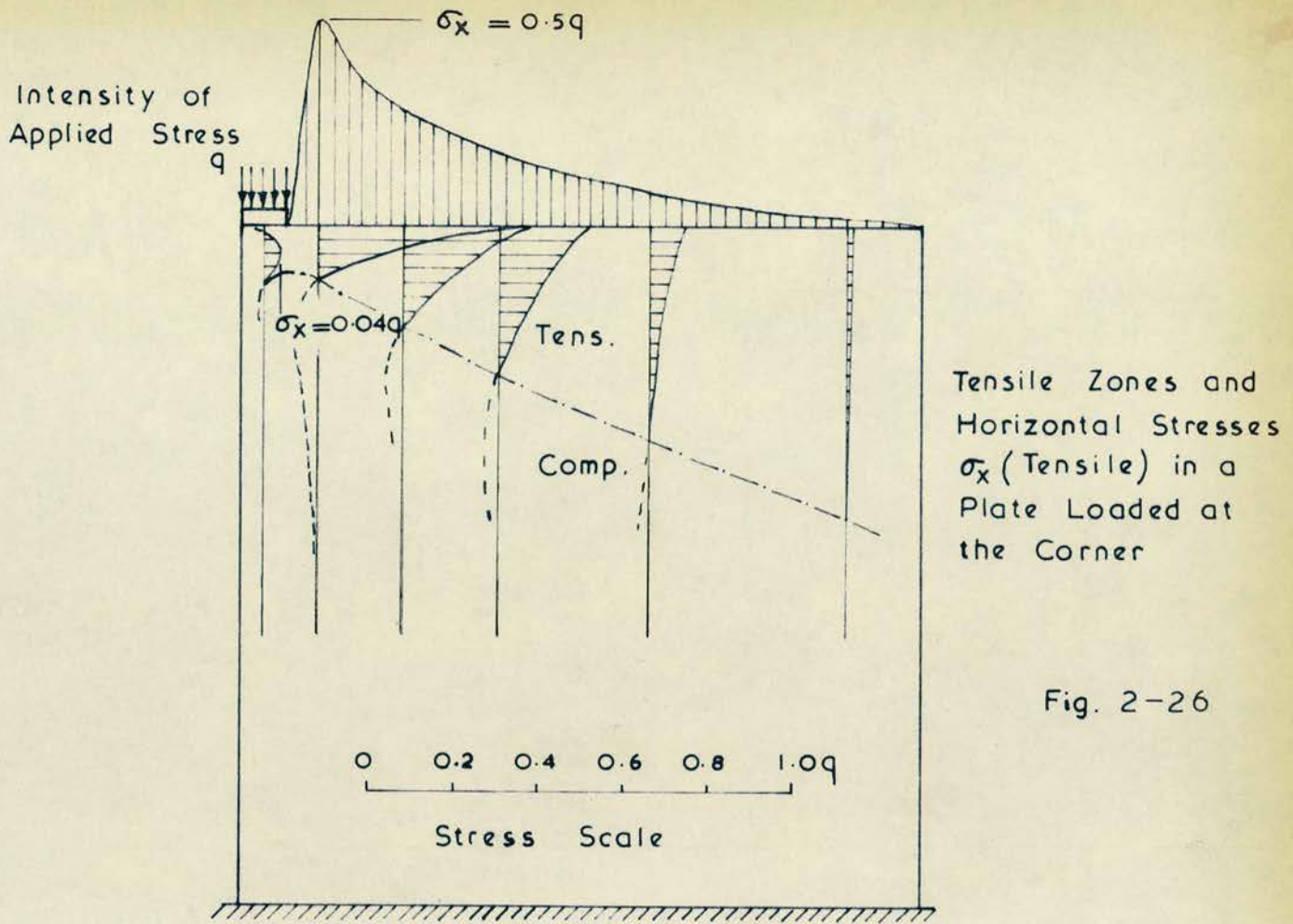
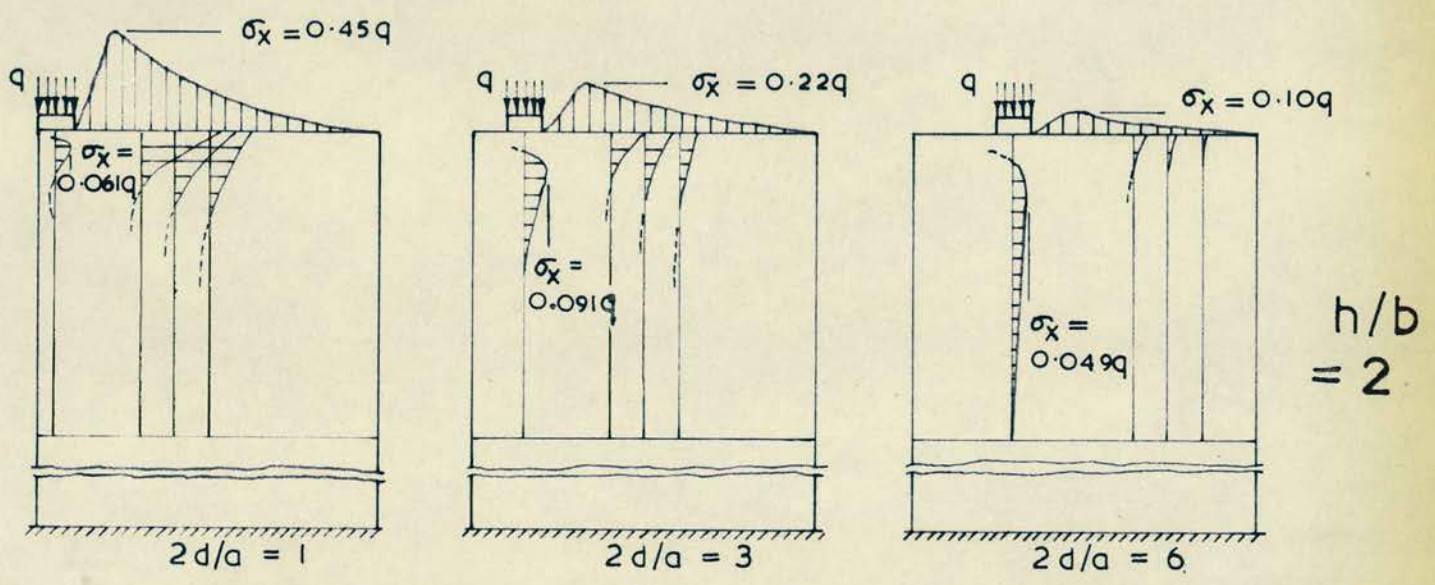


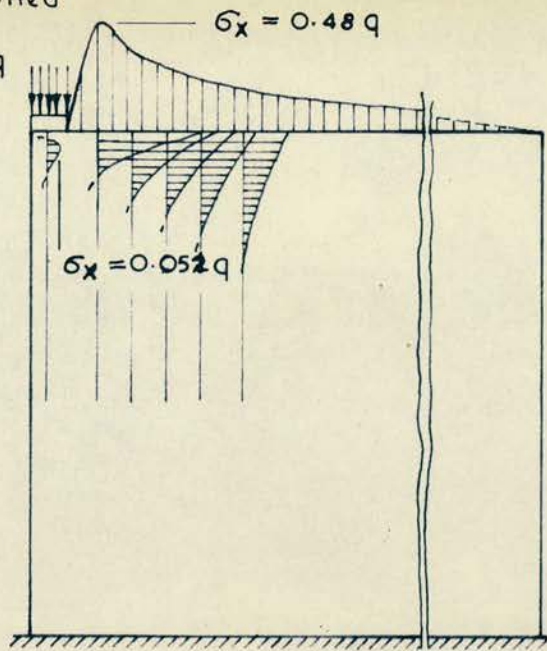
Fig. 2-26



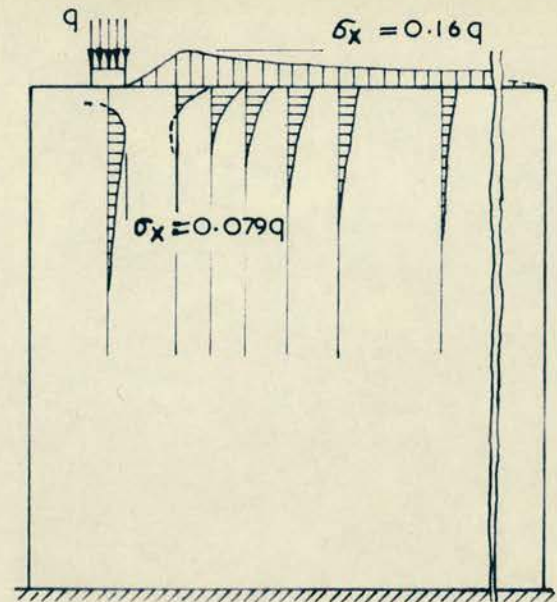
Splitting and Tear Tensile Stresses σ_x in a Plate Loaded by a Strip Load With a Load Concentration Factor $b/a = 10$, at Various Distances $2d/a$ from the Corner. Photo-Elastic Tests - Hiltcher and Florin.

Fig. 2-27

Intensity
of applied
stress

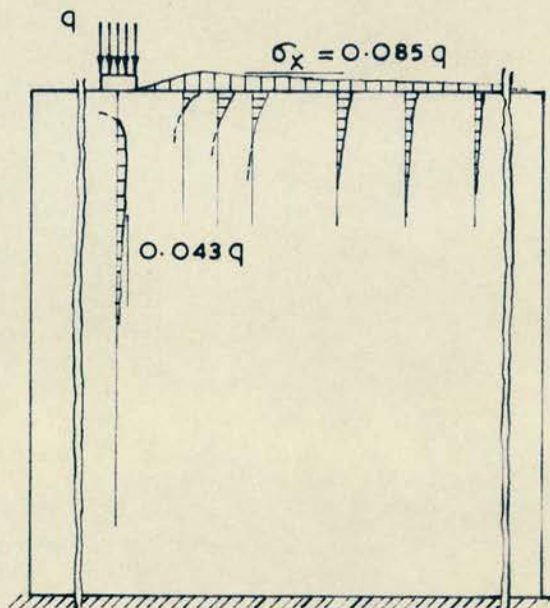


$$2d/a = 1$$

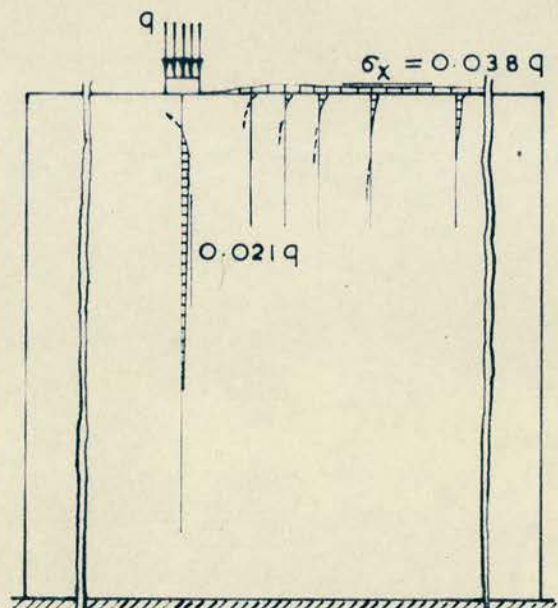


$$2d/a = 4.5$$

$$h/b = 0.5$$



$$2d/a = 9$$



$$2d/a = 18$$

Splitting and Tear Tensile Stresses σ_x in a Plate Loaded by a Strip Load with a Load Concentration Factor $b/a = 30$ at Various Distances $2d/a$ from the Corner.

Photo-Elastic Tests - Hiltcher and Florin

Fig. 2-28.

S. Speer (39) conducted a series of photo-elastic tests, applying a uniformly distributed load to walls, constructed from model bricks made of Eilenberg synthetic resin. The bricks were given either an elastic or a solid bedding. The elastic bedding consisted of using strips of linoleum for the mortar joints. For the solid bedding the bricks were set in a cement made of a fine sand and glue, (Duosan).

These tests showed the existence of horizontal tensile stresses in the brickwork, when the "brickwork" was subjected to compression in the vertical direction. The tensile strains reached a maximum at the centre of the bricks, and decreased to zero at the edges.

When bricks of slightly different heights were used in the same course, with elastic bedding, bending stresses were set up in the individual bricks.

The tests conducted showed that optical methods may be used to elucidate the qualitative distribution of stresses in "brickwork". However, the analysis of the stresses, from the stress fringes obtained is very complex in a jointed structure.

Care must be taken that the materials used for the construction of the model have elastic properties which correspond with those of the actual bricks and mortar under investigation. Difficulty arises, as relatively little is known about the elastic constants of different types of brick and mortar, particularly the Poisson's ratios.

20. THE APPLICATION OF THEORETICAL AND EXPERIMENTAL RESULTS TO BRICKWORK.

The theoretical solutions proposed above are all based on the supposition that the loaded material behaves in a homogeneous,

isotropic, and elastic manner. The comparison of the theoretical and experimental strain distributions has shown that concrete satisfies the criteria, the form of the experimental strain distributions being similar to those of the advanced theoretical analyses.

Concrete is, however, a relatively homogeneous material compared with brickwork, and any loading on a concrete structure may be considered to be distributed in such a way that it is not affected by any one aggregate particle. With brickwork it is likely that a concentrated loading will only be applied to a relatively small number of bricks, and hence the individual brick properties will have a considerable effect.

The effect of the mortar beds on the strain distribution is very difficult to determine. If the elastic properties of the brick and mortar are similar it is doubtful if the vertical strain distribution will be greatly affected by the mortar layers. The horizontal strain distribution is, however, more dependent on the difference in the elastic properties of the two materials, and the vertical jointing of the structure will come into play.

The validity of the theoretical solutions proposed can only be established by comparing the strain distributions found in the brickwork with those indicated by the theoretical approaches, and with those found in concrete structures.

The effect of varying the A_c/A_b ratio, and the edge distance of the bearing plate, must be investigated for brickwork, and compared with the concrete experiments, and the strain distributions found in the photo-elastic tests.

CHAPTER 3.

FULL-SCALE BRICKWORK TESTS.

1. SCOPE OF THE INVESTIGATIONS.

The full-scale tests carried out have investigated various factors affecting the failure stresses of, and the strain distributions in, brick walls, subject to load concentrations.

The tests were conducted in two distinct series.

The first was concerned with the bearing capacity of brick walls, when subjected to concentrated loadings of varying lengths, applied at the wall end.

The distribution of horizontal and vertical strains, in the walls, was determined, using a Demec gauge with an eight inch gauge length. The measurement of strain was performed for both centrally and end loaded walls.

In all twelve walls were tested, and four contained brick fabric reinforcement in varying quantities.

The second test series investigated the effect of the variation of the position of a bearing plate, of a fixed dimension, on the horizontal strain distribution in the wall.

The strains were measured using a Demec gauge, with a two inch gauge length, and having a strain sensitivity of 2.48×10^{-5} per division.

The two investigations are described fully in the following two sections, which have been kept distinct.

2. THE FAILURE STRESSES OF, AND STRAIN DISTRIBUTIONS IN BRICK WALLS SUBJECT TO STRESS CONCENTRATIONS.

2.1 INTRODUCTION.

The purpose of the tests conducted was to determine the failure stresses of and the strain distribution in brickwork details subjected to a concentrated load, such as would in practice be applied by a lintel or a cross-beam.

No reference has been found to previously conducted work of this nature, in which an investigation of the strain distribution has been carried out.

2.2 MATERIALS USED.

i. Bricks.

The bricks used for the construction of the wall specimens were a pressed doubled frogged type.

Samples were taken from the brick stockpile in accordance with B.S. 1257:1945 ⁽⁴⁰⁾ (Now amended to B.S. 3921:1965), and tested according to the same specification. The average compressive strength obtained was 6,675 pf. s.i. Table 3-1.

The bricks used were relatively dense, and had a low water absorption. When bricks were cut longitudinally for construction internal cracks were found, running across the width of the bricks.

ii. Sand.

A local sand was used. It was thoroughly dried to eliminate all moisture and give controlled test conditions. The grading of the sand is shown in Table 3-2 and Fig. 3-1, and the sand was found to conform to the limits of B.S. 1200 ⁽⁴¹⁾.

iii. Cement.

"Ferrocete" rapid hardening cement was used throughout.

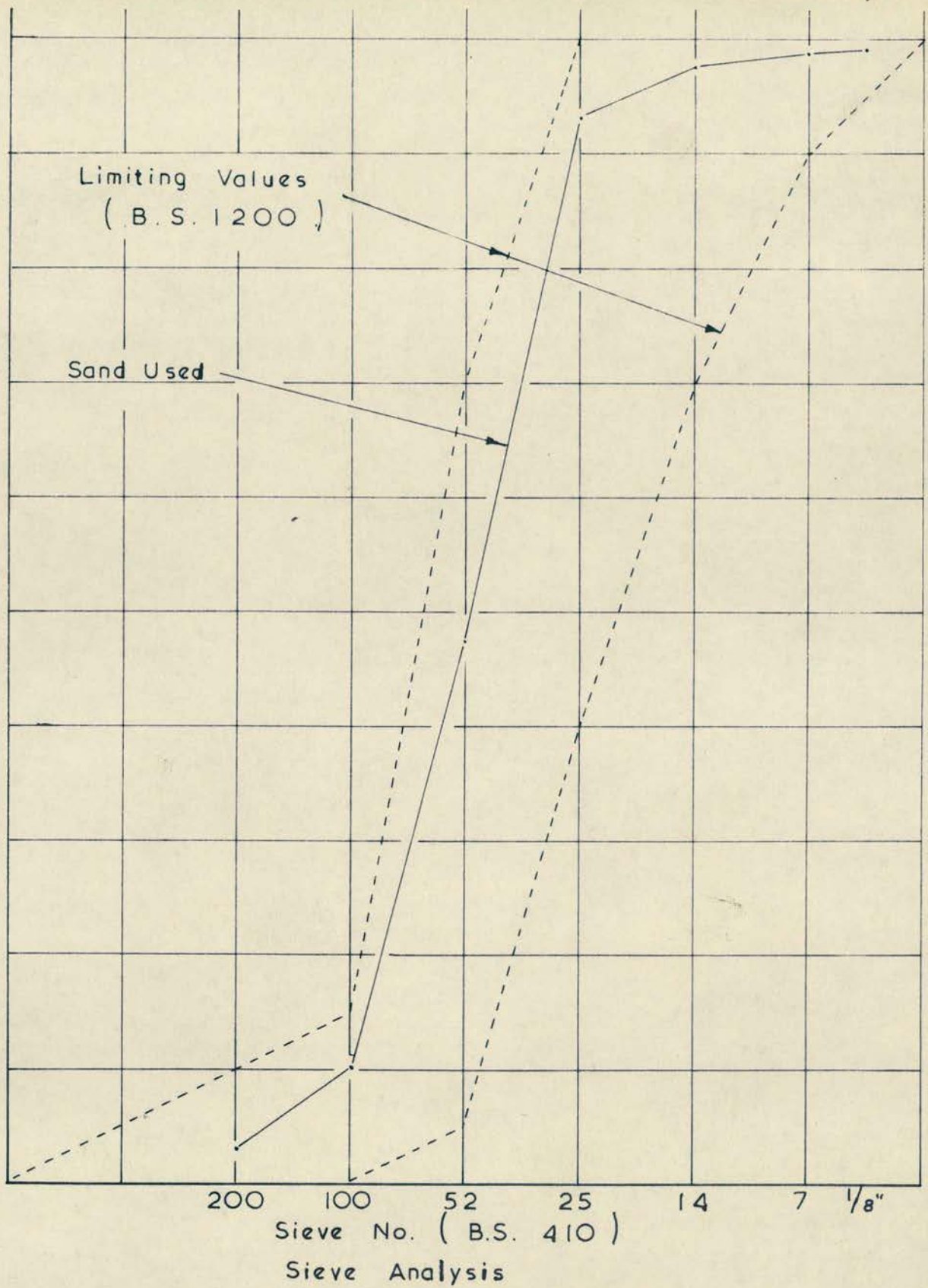


Fig. 3-1

2.78" mortar cubes were made, as stipulated in B.S.12 (1958)⁽⁴²⁾ and the average crushing strength at 7 days exceeded the recommended 4,000 pf. s. i.

iv. Mortar.

A 1:3 cement:sand mortar was used throughout, the mix being by volume. In addition each batch was weighed to check that a consistent mix was obtained. The water:cement ratio was left unspecified, but sufficient water was allowed to give a reasonable consistency for bricklaying. The amount of water used in each mix was checked by weighing. 4" mortar cubes were made from each mortar mix, and after curing they were stored under water until required for crushing with the piers.

v. Curing.

The mortar cubes were placed under damp sacks for 24 hours after which the moulds were removed and the cubes stored under water until required.

2.3 PREPARATION OF SPECIMENS.

i. Method of Pier Construction.

As time had to be allowed, after construction, for the curing of the piers, they could not be constructed in the testing machine, which was in daily use. For this reason piers were constructed on 1" M.S. plates, which had four side attachments to facilitate handling.

The piers were constructed by an experienced bricklayer, who checked mortar bed thicknesses using a graduated batten, and who plumbed and levelled the piers.

The piers were constructed in Old English bond and had the nominal size of 27" x 9" x 24". Mortar beds were $\frac{3}{8}$ " thick and all vertical and bed joints were completely filled with mortar.

Four piers were constructed containing reinforcement in various quantities, and variously placed. The reinforcement used was B. R. C. fabric brick reinforcement, consisting of two $\frac{1}{8}$ " rods, 6" apart, linked every 6" by an $\frac{1}{8}$ " rod.

ii. Auxiliary Specimens Constructed.

In addition to the 4" mortar cubes cast, brickwork cubes were also constructed both 9" x 9" x 9" high and 9" x 9" x 12" high.

Brickwork cubes have been suggested as a possible way of ascertaining the strength of brickwork constructional units, and some work has already been carried out experimentally.

The use of the brickwork cube as a control specimen is discussed in Chapter 5.

Particular care must be taken to obtain the desired thickness of mortar beds and joints, as it has been shown by a considerable range of tests that the brick cube strength is inversely proportional to the mortar joint thickness.

The method of cube crushing has been the subject of considerable testing and discussion⁽⁴⁴⁾, e.g. as to how cubes should be crushed, to give consistent results, and to most closely resemble conditions in the brickwork unit.

Cubes constructed were crushed between $\frac{1}{8}$ " plywood sheets in a 200 T capacity Denison testing machine, which had a ball seating for the upper platen. Results are given in Table 3-3.

2.4 TESTING EQUIPMENT.

i. Load Application.

Loads were applied to the piers in a 100^T capacity Avery Universal testing machine. Load was transmitted through the head of the machine, by way of a rigid M.S. bearing plate of the required dimensions.

Bearing plates were 9", 7", 6" and 4½" long, and of the same width as the piers. Where the top of the pier was not absolutely level, and there might have been a tendency for non-uniform load application, a sheet of ½" plywood was used, and if this proved insufficient the pier was levelled with sand, and an ⅛" plywood sheet used.

ii. Strain Measurement.

As an overall pattern of the strain distribution on the face of the pier was required a Demec gauge of 8" nominal length was used. This enabled a large number of readings to be taken in the vicinity of the point of load application. With an 8" gauge length readings could either be taken on one brick in a horizontal direction, or over several mortar joints in both horizontal and vertical directions. Such strain measurements were thought to be of more value than those that could be obtained from point strain measurements using other methods.

Plate 3-l shows a typical pier before testing.

2.5 PIER TESTS.

When the required stainless steel Demec points had been attached to the pier, using Durofix, it was placed in position in the Avery testing machine. The mild steel bearing plate was levelled, to be horizontal with the head of the machine, and zero load Demec readings were taken.

Load was applied in increments of ten tons and Demec readings were taken after each increment. Several load cycles were carried out on each pier, with various bearing plates, and care was taken not to exceed the cracking load of the pier, which was estimated at approximately 2,000 pf. s. i.

Tests conducted were mainly concerned with end loading conditions, but some tests investigated centrally applied loads.

After several cycles of loading the piers were tested to destruction, taking Demec readings at every load increment. After failure, the piers were reversed, and load was applied, at a constant rate, to the other end, until failure occurred.

2.6 RESULTS.

A summary of the end bearing test results is given in Table 3-4. Plates 3-2 & 3-3 show typical failure patterns of the piers.

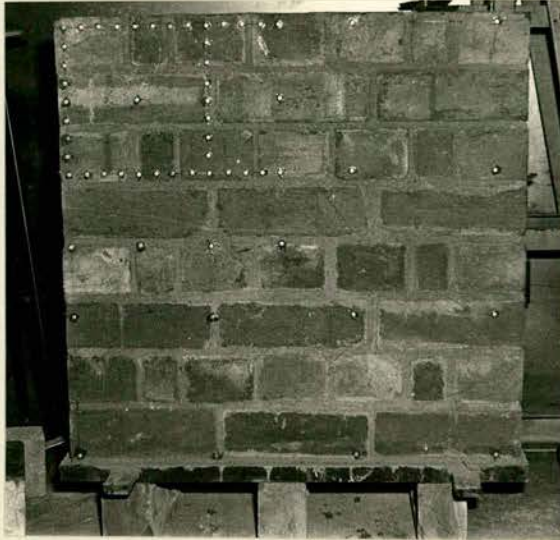
From the strain readings taken several groups of graphs were plotted, and are discussed below.

i. End Bearing Plates.

From Table 3-4 giving the failure loads, failure stresses, and size of the bearing plates, Figs. 3-2, and 3-3 were plotted.

In Fig. 3-2 a statistical line of best fit has been calculated for the experimental results. This line approximately passes through the origin, as might be expected, and appears to fit the results obtained. This would indicate that within the range of bearing plate size tested the failure stress is independent of the bearing plate size.

Fig. 3-3 indicates however that the failure stress does in fact increase, as the bearing plate size decreases, within the range tested.



A Typical Pier Before Testing
Plate 3-1



A Typical Failure - 6" End Bearing Plate
Plate 3-2

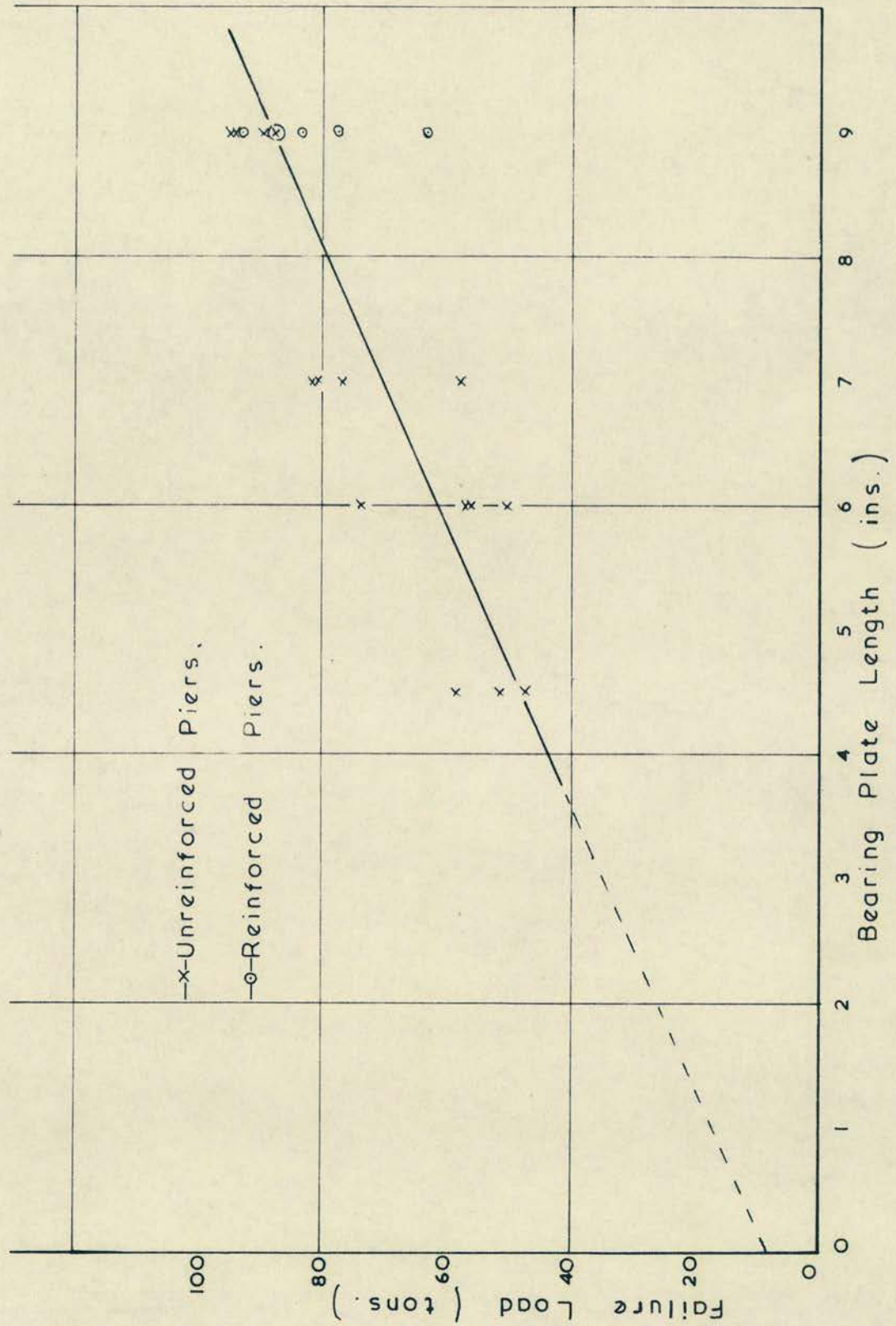
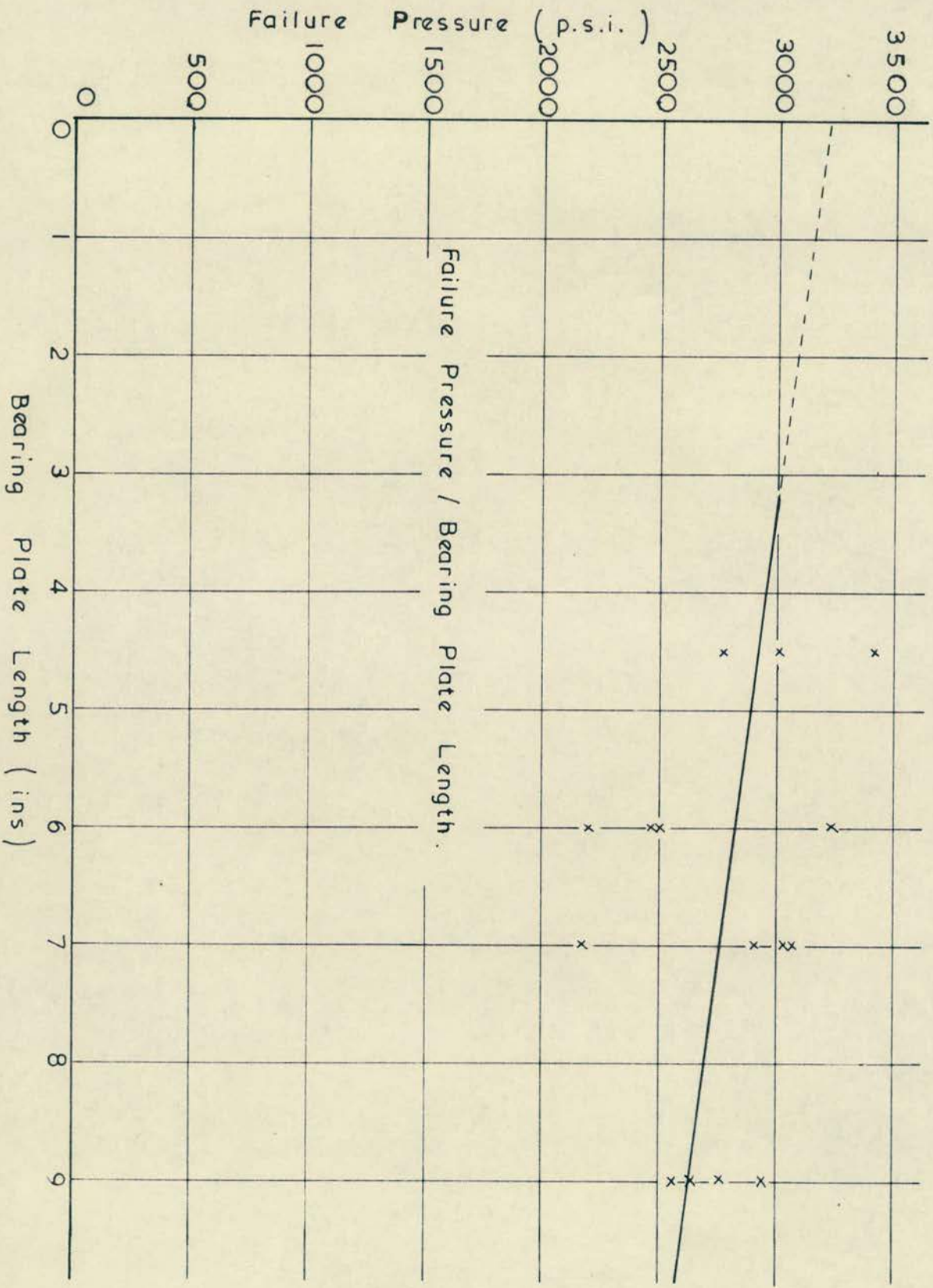


Fig. 3-2

Fig. 3-3



The linearity of the relationship cannot be established from the range of results obtained.

The failure loads of the second ends of the piers tested were similar to those of the first ends.

The failure stresses for the reinforced piers (Nos. 9-12) are given in Table 3-5, but have been omitted in the calculation of the lines of best fit.

2.7 DISCUSSION OF RESULTS.

i. Permissible Stresses.

The permissible bearing stresses for a brickwork unit, constructed with bricks of a 6,675 pf.s.i. crushing strength, and a 1:3 cement: sand mortar, are given in Table 3-4. The basic stress has been determined from C.P. 111:1964, and increased by 50%, as allowed by para. 315e. for a concentrated loading. A reduction factor has been applied, as detailed in para.315b., to allow for the cross-sectional area of the pier being less than 500 in². The reduction factor is given by $(0.75 + A/2,000)$, where A is the area (in²) of the horizontal cross-section of the wall or column. The code is at this point considering a uniformly loaded cross-section, and does not specify if A is considered as being the total area, where a concentrated loading occurs.

For the above reason permissible stresses are given in Table 3-4 based on both the total pier area and the bearing plate area. Considering A as the whole area the reduction factor is 0.88, whereas taking A as the area of the 4½ ins. wide bearing plate the reduction factor is 0.77. These two factors lead to allowable stresses of 607 pf.s.i. and 531 pf.s.i. respectively, representing a reduction of 12.5%.

Recent work ⁽³⁷⁾ on concrete bearing blocks has shown that the ultimate bearing stress depends on the A_c/A_b ratio, i.e. the ratio of the area of the bearing block to the area of the bearing. As A_c/A_b increases, i.e. as the bearing area becomes smaller, the ultimate stress has been shown to increase, eventually tending to an upper limit.

If similar results are anticipated in brickwork, and Fig. 3-3 indicates that the failure stress does in fact decrease with increasing bearing plate length, then it would seem logical to take the whole pier area into account when computing the reduction factor, removing the anomaly of decreasing allowable bearing stress with increasing A_c/A_b ratios.

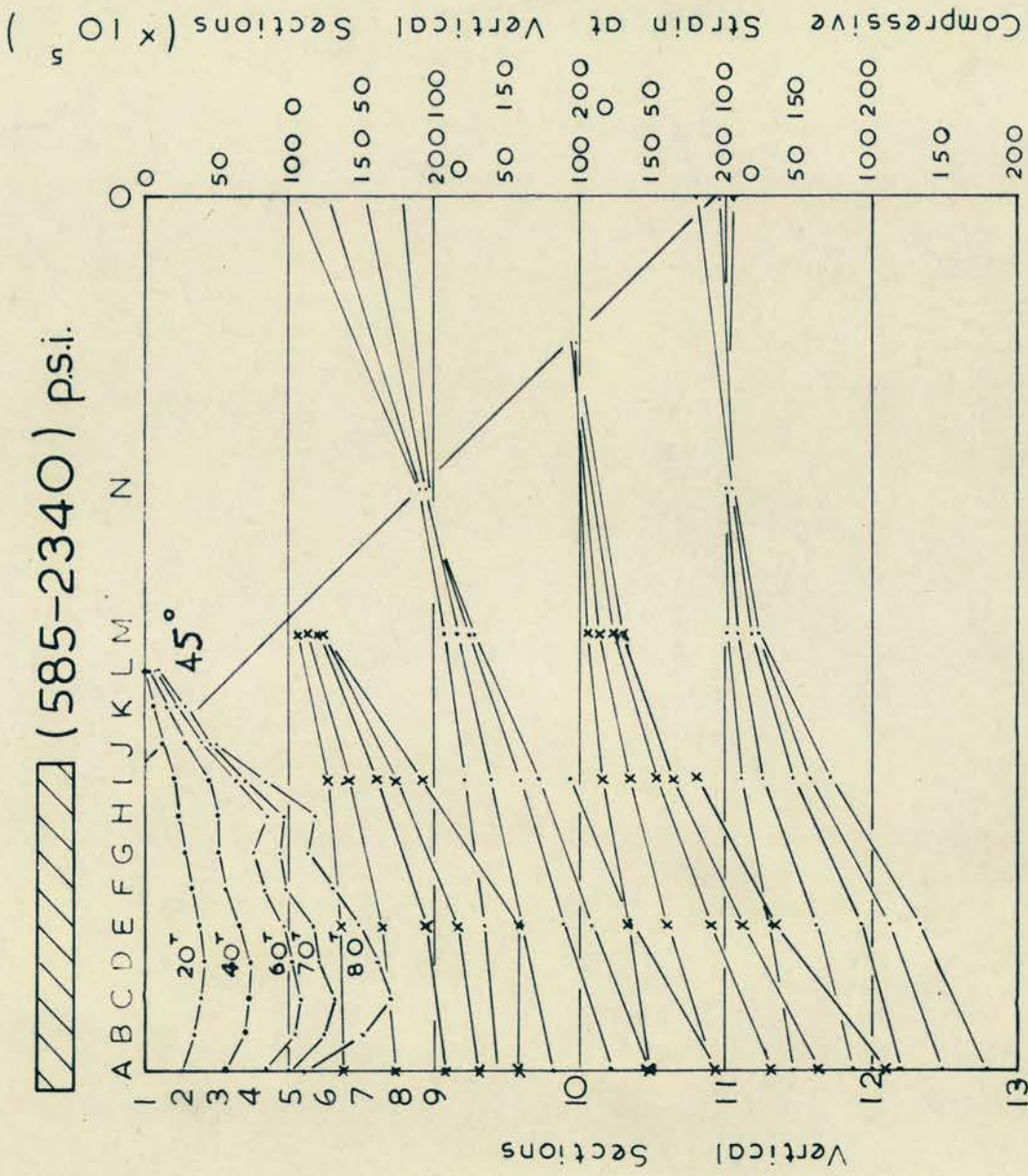
Ratios of the failure stresses to the code permissible stress are given in Table 3-4, and these range from 3.6 to 5.6 if the whole area is considered, as suggested above. If only the area of bearing is considered the range is 4.0 to 6.4.

A safety factor of 3.6 may be considered rather low, although no consideration of the eccentricity of the load has been taken.

The failure load, used for the calculation of the safety factors outlined above, has been taken as the ultimate load of the piers. In the tests initial cracking occurred at loads ranging from 54 - 95% of the ultimate load. The safety factor against initial cracking may thus be lower than 2.

ii. Vertical Strain Distribution.

Figs. 3-4, 3-5, 3-6 and 3-7, show the strain distributions for pier 4 loaded through end bearing plates, 9", 7", 6", and $4\frac{1}{2}$ " long.



9" End Bearing Plate. Pier 4.
Vertical Strain Distribution

Fig. 3-4

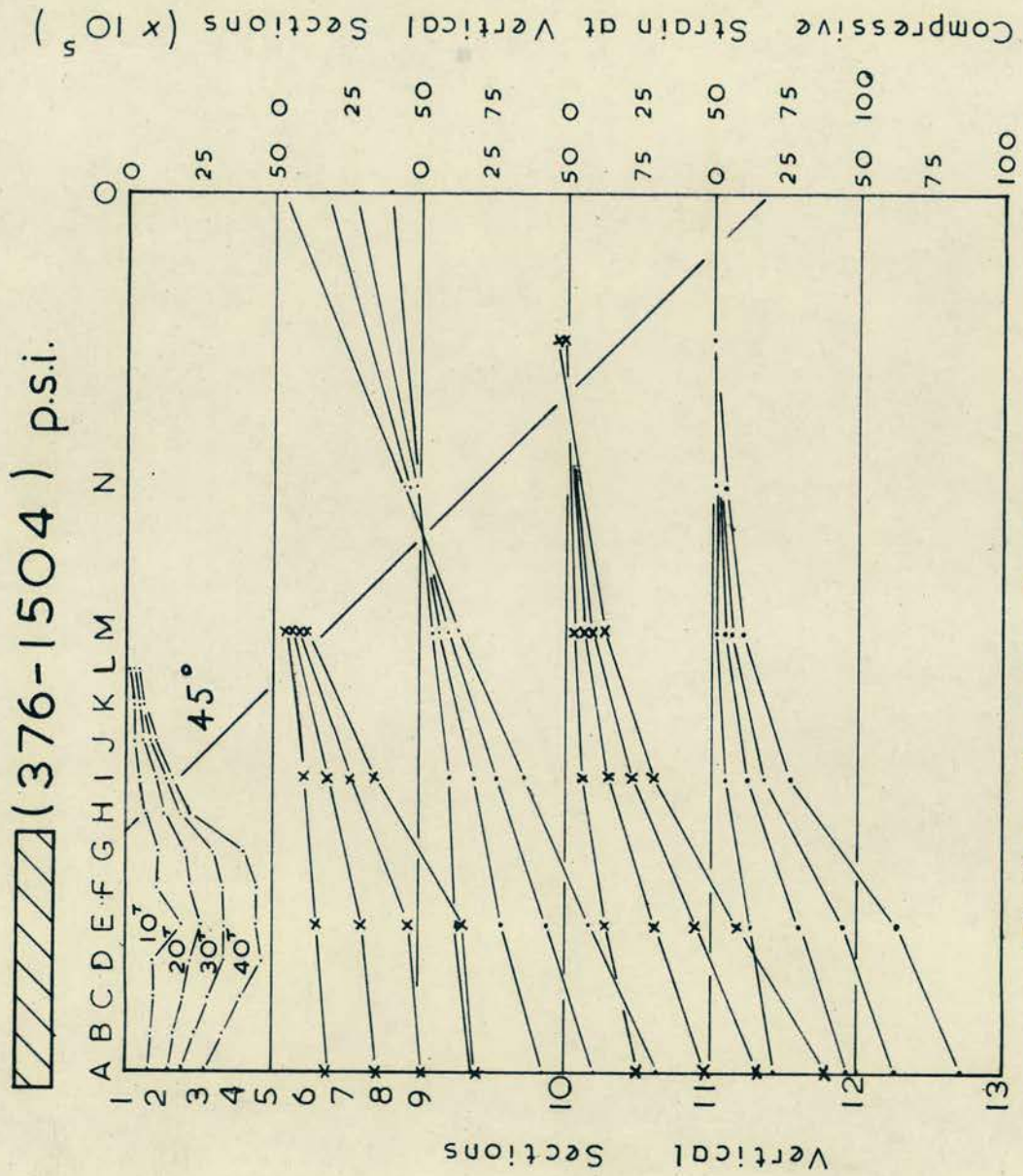


Fig. 3-5

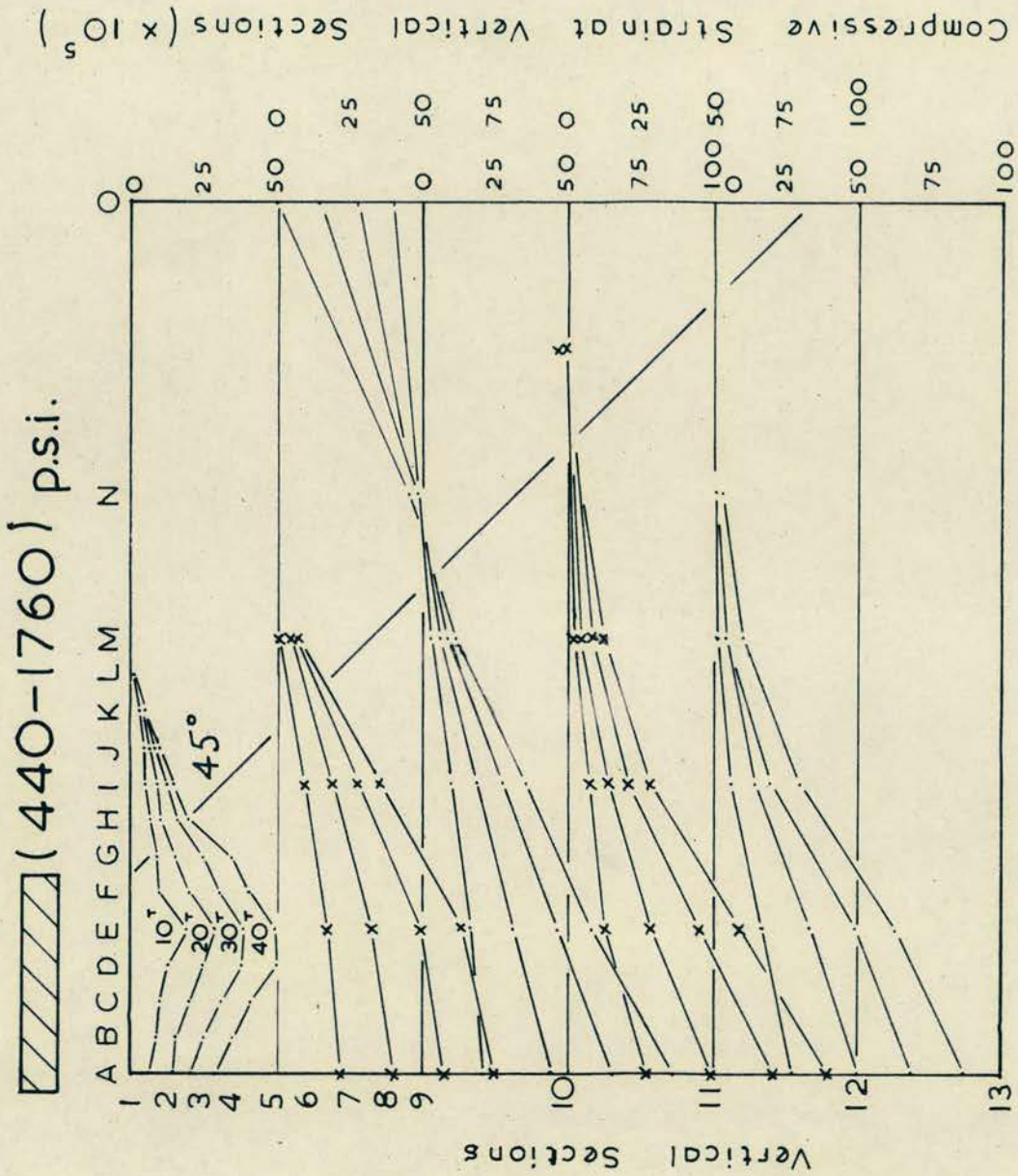

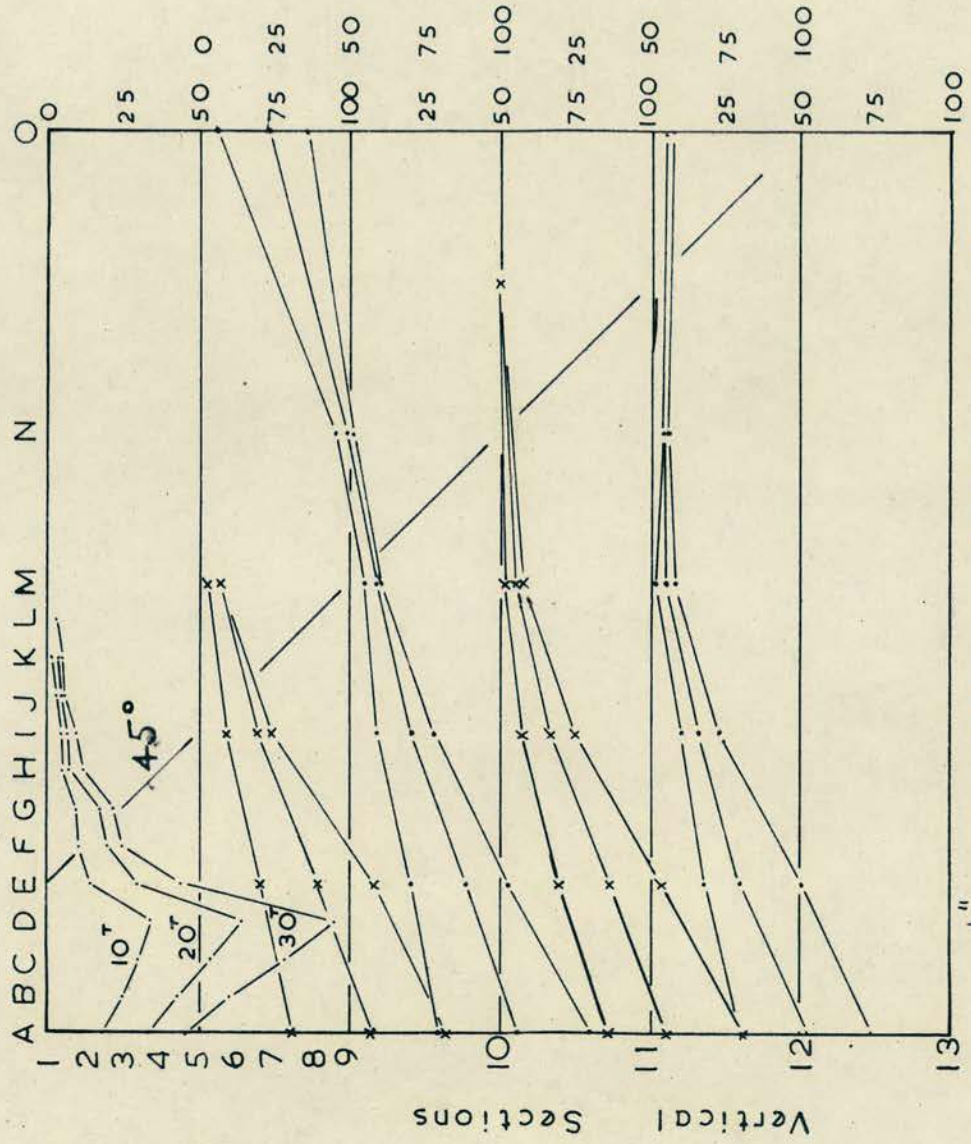


Fig. 3-6

 (585-1755) p.s.i.

Compressive Strain at Vertical Sections ($\times 10^5$)



4 1/2" End Bearing Plate, Pier 4.
Vertical Strain Distribution

Fig. 3-7

In all the loading cases it can be seen that the concentrated loading produces a "bulb of pressure" directly beneath the bearing plate; with the highest strains occurring approximately under the centre of the bearing plate.

Bulbs of pressure are known to occur when a homogeneous isotropic material is loaded, perpendicular to a flat surface, by a concentrated force.

The analysis of concentrated loadings has been investigated by Boussinesq⁽¹⁷⁾, Westergaard and many others, and their solutions have been applied in the field of soil mechanics and for the solution of the stress distribution in anchorage blocks of prestressed concrete components. Expressions are developed for the stress conditions at any point, and stress contours plotted from the theoretical expressions show the bulb of pressure stress distribution. The theoretical approaches may be developed for either a 2-D or a 3-D loading case, and are discussed in Chapter 2.

Using photo-elastic techniques it is possible to show the bulb of pressure phenomenon quite simply, using plastics having birefringent properties and polarised light. Examples of photo-elastic investigations of stress concentrations are given in Photo-elasticity⁽²⁰⁾ by Coker and Filon, and they clearly illustrate the phenomenon in an isotropic material.

An article⁽⁴⁵⁾ in Die Bautechnik described work carried out on the investigation of stresses in wall panels with openings, employing photo-elastic methods. Plate 3-4 illustrates the load distribution under



A Typical Failure - $4\frac{1}{2}$ " Central Bearing Plate.
Plate 3-3



Stress Distribution - Photo-Elastic Investigation.
Plate 3-4

a concentrated load at the end of one such panel. The distribution of the load, to a considerable depth in the section, can be seen clearly.

The extent of the load distribution across the pier is of interest. C.P.111:1964 suggests a maximum distribution at 45° , but the American codes commonly accept 30° as the desirable maximum. Figs.3-4, 3-5, 3-6 and 3-7 show that although load is partially distributed up to a 45° sector, the largest proportion of the load is carried in a more confined area directly below the bearing plate. Thus, the measured compressive strain, at the edge of the pier, and towards its base, is considerably in excess of that indicated by the code.

iii. Design Implications.

a) Theoretical Considerations.

If we consider a design that might be applied to a brickwork detail, subjected to a concentrated eccentric load, the reaction would be taken as distributed triangularly along the base, in such a way that its resultant coincided with the line of action of the applied load. Thus, when the load is applied at the end of the wall the distribution would be over a length equal to 1.5 times the bearing plate length.

If this principle is applied to Fig.3-4 the strain distribution corresponds quite closely to the design criteria at level 11-13.

From Figs. 3-5, 3-6 and 3-7, however, it is seen that the reaction is distributed considerably more than expected from the design criteria. In fact, for all four loading cases the strain is distributed to approximately the same extent across the section. Thus, from the triangular reaction and reaction-load concurrence criteria, the

calculated stress will be higher than that actually occurring.

Considering two experimental distributions.

Firstly Fig. 3-4, with a 9" bearing plate, and a surface stress of 100 pf. s. i. Then by a triangular reaction distribution, the maximum design stress is approximately 130 pf. s. i. From the experimentally obtained strains the maximum stress is 125 pf. s. i.

Secondly Fig. 3-7 with a $4\frac{1}{2}$ " bearing plate, and a surface stress of 100 pf. s. i. By a triangular reaction distribution, the design stress will be 130 pf. s. i.

The experimentally plotted strain results give a maximum stress of 72.5 pf. s. i.

Thus while applying for a 9" bearing plate, for a $4\frac{1}{2}$ " plate the triangular distribution with concurring load and reaction is conservative.

Both computations carried out above depend on the strain distribution representing the stress distribution. If the strain measured represents the stress, then the areas under the strain diagrams will at any particular level be in the ratio of the applied loads.

Also, if the load is fully distributed down the section then the areas should be the same, for given loads, at different sections.

Using a planimeter, the areas were measured. From Fig. 3-4 at levels 1-9 and 12-13, the following results were obtained. At level 1-9, the loads were in the ratio $20 T : 40 T : 60 T : 70 T : 80 T$, i. e. $1 : 2 : 3 : 3.5 : 4$, and the areas under the strain diagrams $1 : 2.02 : 2.93 : 3.5 : 4.38$. At level 12-13, the load ratios were as above and the area ratios $0.92 : 1.90 : 3.0 : 3.66 : 4.36$.

These both correspond quite closely.

The ratios of the strain areas at the two levels were taken at $20 T$, $40 T$, $60 T$, $70 T$ and $80 T$, and were $1 : 0.98$; $1 : 1$; $1 : 1.09$; $1 : 1.11$ and $1 : 1.06$ respectively, corresponding well.

From the examples given above it should be noted that the experimentally observed stress distributions do not confirm the calculated maximum stresses, based on either a uniform or a triangular load distribution although in a few cases results conform reasonably.

In the above computations the values of the strains were taken from the strain distribution, measured on one face of the pier only. The assumption was made that the strains were of the same magnitude, and were distributed in the same manner on both pier faces. For practical considerations of access, strain readings could not be taken on both faces.

b) A Consideration of the Observed Strain Distribution.

From the experimental results the following remarks can be made about the nature of the stress distribution under the end bearing plate.

1. The stress distribution under the bearing plate takes the form of a pressure bulb, and is particularly well defined at high surface stress.
2. Further away from the area of load application the stress distribution becomes triangular, the highest stress occurring at the edge of the pier, and towards its base.
3. The extent of the load distribution across the pier varies from pier to pier, but is approximately the same for all bearing plate lengths.
4. Higher vertical compressive stresses occur under the 9" bearing

plate than under the $4\frac{1}{2}$ " bearing plate for the same applied surface stress.

5. For the same bearing plate, and the same applied vertical stress, the actual experimentally measured strain varied considerably. In some cases the actual form of the strain distribution also varied, and this must be attributed to certain non-uniformities of the surface loading, perhaps caused by dimensional faults in the pier construction, or individual variations in brick dimensions.

The design basis of C.P.111 : 1964 is one of allowable compressive stress, based on a uniform surface distribution of load. Also the basic stress given in the code is related to the compressive strength of the brick unit, tested in uniform direct compression.

From the experimental results it can be seen that the stress is not uniform under a concentrated loading, and a maximum value occurs towards the base of the pier, where the stress distribution is triangular.

From strain distribution diagrams plotted from several tests the load can be seen to distribute itself approximately 9" - 12" across the pier sections. Assuming a nine inch distribution, giving the highest stresses, then the maximum stress occurring may be calculated.

Considering a $4\frac{1}{2}$ " bearing plate, then with a triangular distribution over 9", the maximum calculated stress is the same as the surface stress.

However, for a 9" bearing plate, with a 9" distribution the maximum stress will be twice the applied surface stress. The magnitude of the observed strains have borne this out in some, though not all cases.

Thus, if the total load bearing capacity criteria was to be based

on a maximum compressive stress/strain criteria, the $4\frac{1}{2}$ " bearing plate could be expected to have the same total load capacity as the 9" bearing plate. Experimental results have not confirmed this, although the failure stress appears to increase with decreasing bearing plate length.

Comparing the maximum compressive strains observed, and taking the average, for $4\frac{1}{2}$ " bearing plates (six tests) and 9" bearing plates (7 tests) the ratio was 1 : 1.53 for the same surface stresses.

From the above observations it can be seen that the ratios of the failure stresses are not the same as those of the maximum compressive strains measured. This phenomenon leads to a consideration of whether the failure is purely a compressive one, or one due to combined stresses.

iv Mode of Failure.

With end bearing plates the initial failure usually took the form of a vertical crack initiated on the pier faces, in the second brick course below the bearing plate.

With increasing load, this crack spread down the pier section, and spalling occurred below the bearing plate.

The final failure took the form of crushing of the loaded section, followed by a shearing away of a considerable brick section.

When such a shear failure occurs, initiated at the inside of the bearing plate the failure load will depend on the length of the slip surface.

The resistance to failure along any surface will depend upon many of the physical and mechanical properties of the brickwork. Amongst

these will be the coefficient of friction μ , sometimes considered as an angle of internal friction ϕ , and defined as $\mu = \tan \phi$. The cohesion of the brickwork is a factor of some importance, and will depend on many variables, including the mortar strength, and the bond of mortar and brick. The determination of ϕ , the angle of internal friction, is possible, and μ or $\tan \phi$ has been shown to be approximately 0.7 for certain types of brickwork ⁽⁴⁶⁾. The determination of the cohesion, C, is however a more difficult proposition, and no data is readily available for brickwork.

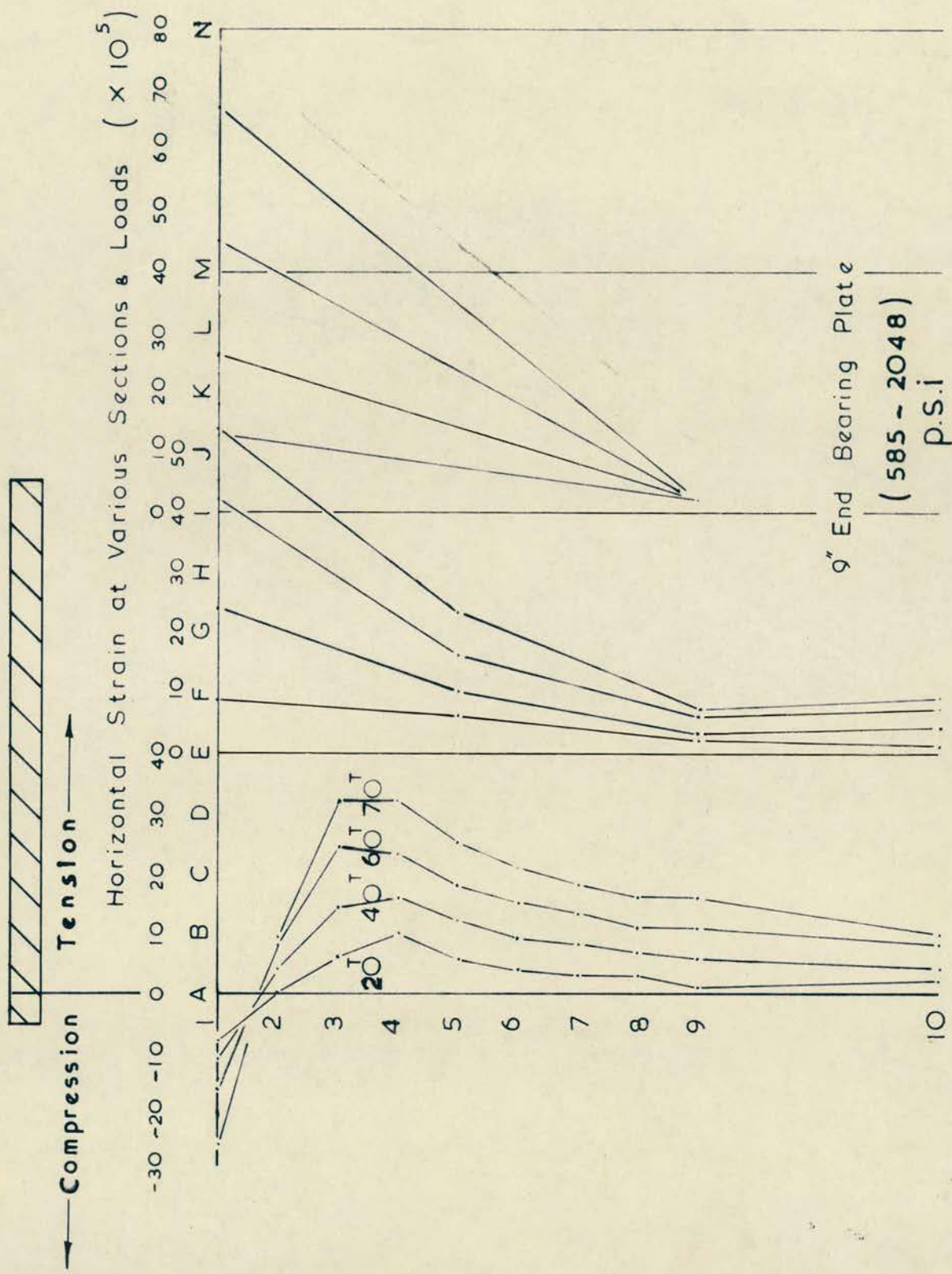
v. Horizontal Strain Distribution.

Fig. 3-8 shows the typical horizontal strain distribution under a 9" end bearing plate. Similar strain distributions were obtained with all the end bearing plates, with horizontal compressive strains occurring immediately beneath the bearing plate. A few inches down the section a position of zero strain occurs, and below this horizontal tensile strains exist. The horizontal tensile strains occurring have a bulb of pressure distribution, on a vertical section through the centre line of the bearing plate.

Significant horizontal strains were only measured in the vicinity of the bearing plate towards the top of the pier. At the inner edge of the bearing plate the tensile strains are high, indicating the tendency of a section of the pier to tear away. This type of tensile strain is discussed in Chapter 2, and in the third section of this chapter.

vi. Stress/Strain Relationships.

Figs. 3-9 and 3-10 illustrate the variation of strain, with



Horizontal Strain Distribution Pier 4

Fig. 3-8

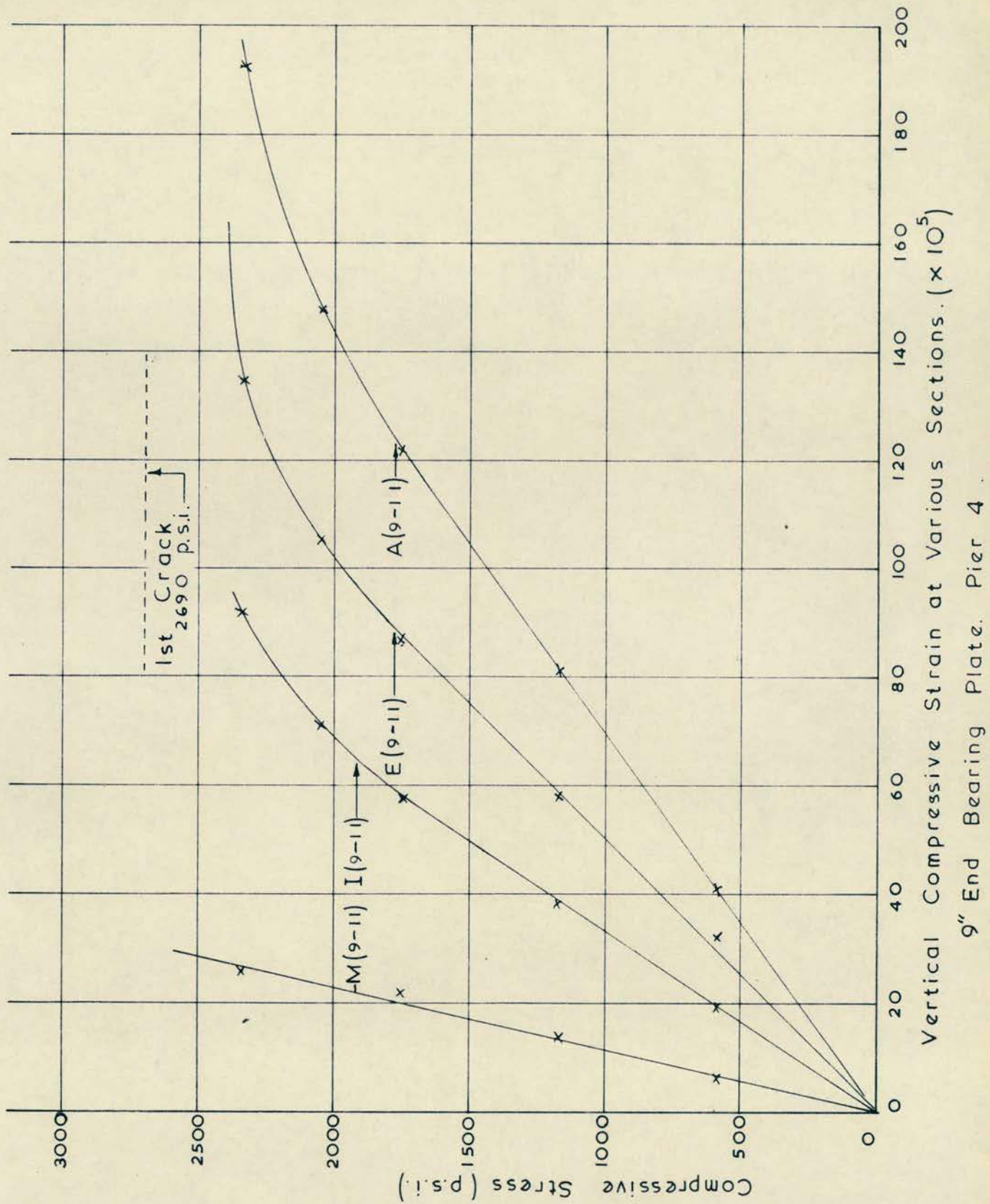
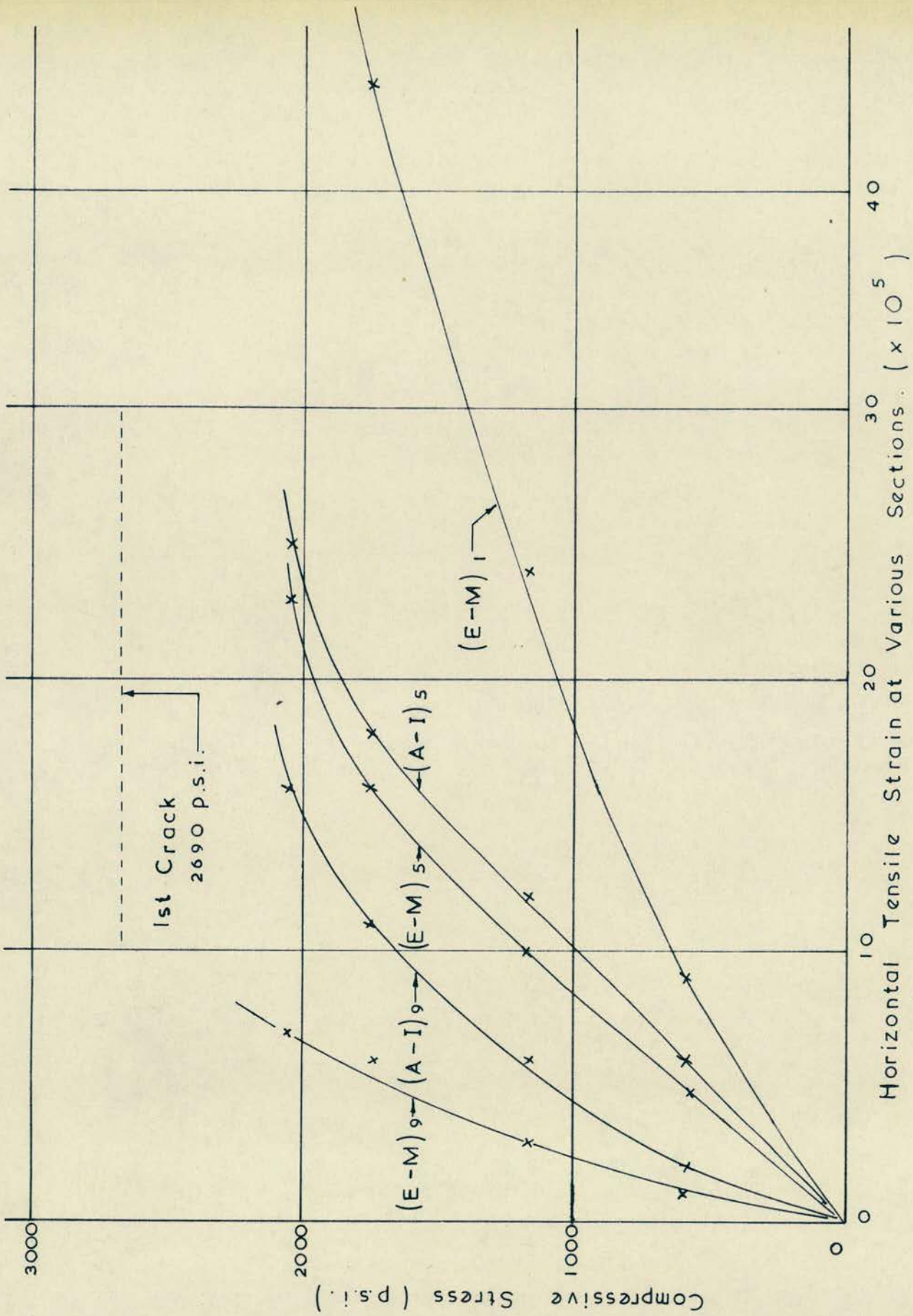


Fig. 3-9



9" End Bearing Plate. Pier 4.

Fig. 3-10

average applied compressive stress, in both a vertical and a horizontal direction.

The linearity of the stress/strain relationship is demonstrated in the case of measured compressive strain up to an average applied compressive stress of 2,000 pf. s. i. Above 2,000 pf. s. i. linearity is not maintained, and Young's Modulus decreases, until the first crack occurs at approximately 2,700 pf. s. i.

The average applied compressive stress is obtained by dividing the applied load by the area of the bearing plate.

The maximum compressive strain measured before cracking occurred was greater than 2×10^{-3} .

The average applied compressive stress/tensile strain relationship does not appear to be linear, and exhibits a slightly curved characteristic, particularly at higher stresses. The maximum tensile strain measured before cracking, for a test on pier 4 with a 9" end bearing plate, was 5.4×10^{-4} .

A non-linear stress/strain relationship is not surprising for the horizontal strain, as the strain is produced by a number of complex factors. These are thought to include the poisson's ratio effect, the action of a wedge of brickwork below the bearing plate being forced into the pier, the shear forces acting at the brick to mortar interface, the tendency for the mortar to fail at a stress well below the brickwork strength and the bending of individual bricks due to uneven bedding.

The summation of the effects mentioned above may well not be linear when compared with the average applied compressive stress,

and the further complications of vertical mortar joints, and their capacity to transmit horizontal tensile stress, must be considered.

vii. Strain Distribution and Compressive Stress.

a) Extent of Distribution.

Figs. 3-11 and 3-12 show the vertical strain distributions under a 9" bearing plate for loads of 20 and 60 tons. The increase in load did not lead to an increase in area over which it was distributed. The total area of distribution adhered to the 45° concept of the code. With the increase in the load the measurable strain rose from 3×10^{-4} to 10×10^{-4} . Taking a horizontal section across the pier the strain can be seen to have increased linearly towards the edge of the pier.

The transmission of stress has occurred to the base of the pier, and the greatest compressive strain occurs towards the edge and base of the pier.

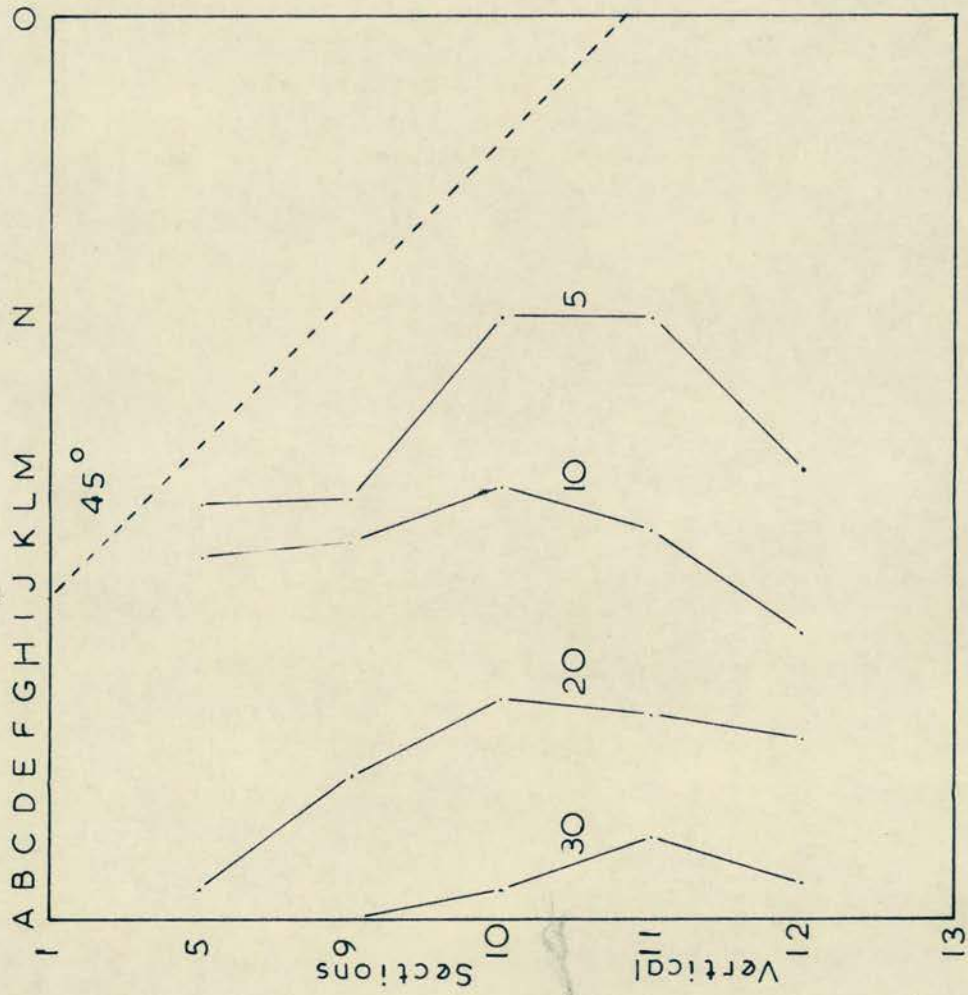
b) Extent of Strain.

Figs. 3-13 and 3-14 show the variation of the positions of certain strains with a variation of stress. As the compressive stress is increased higher strains are observed at positions distant from the bearing plate, although above 20 tons there is little increase in the total area over which the load is distributed.

viii. Uniformity of Loading.

Fig. 3-15 shows the results of readings taken to check the uniformity of load distribution across the width of the pier. Readings were taken between 8 points on the end face, and in Fig. 3-15 a fairly uniform distribution of compressive stress is shown.

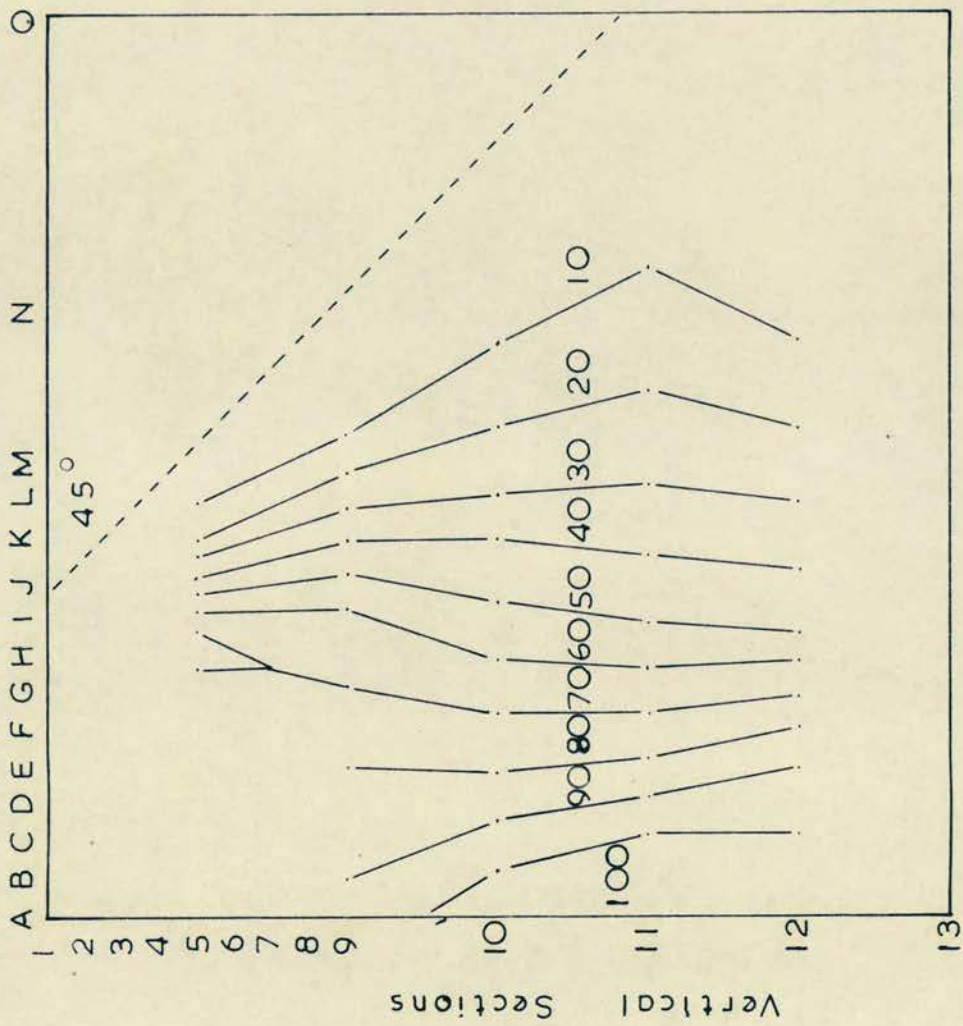
 585 p.s.i.



Vertical Strain Contours (x 10⁵) at 20 Tons
 9" End Bearing Plate. Pier 4.

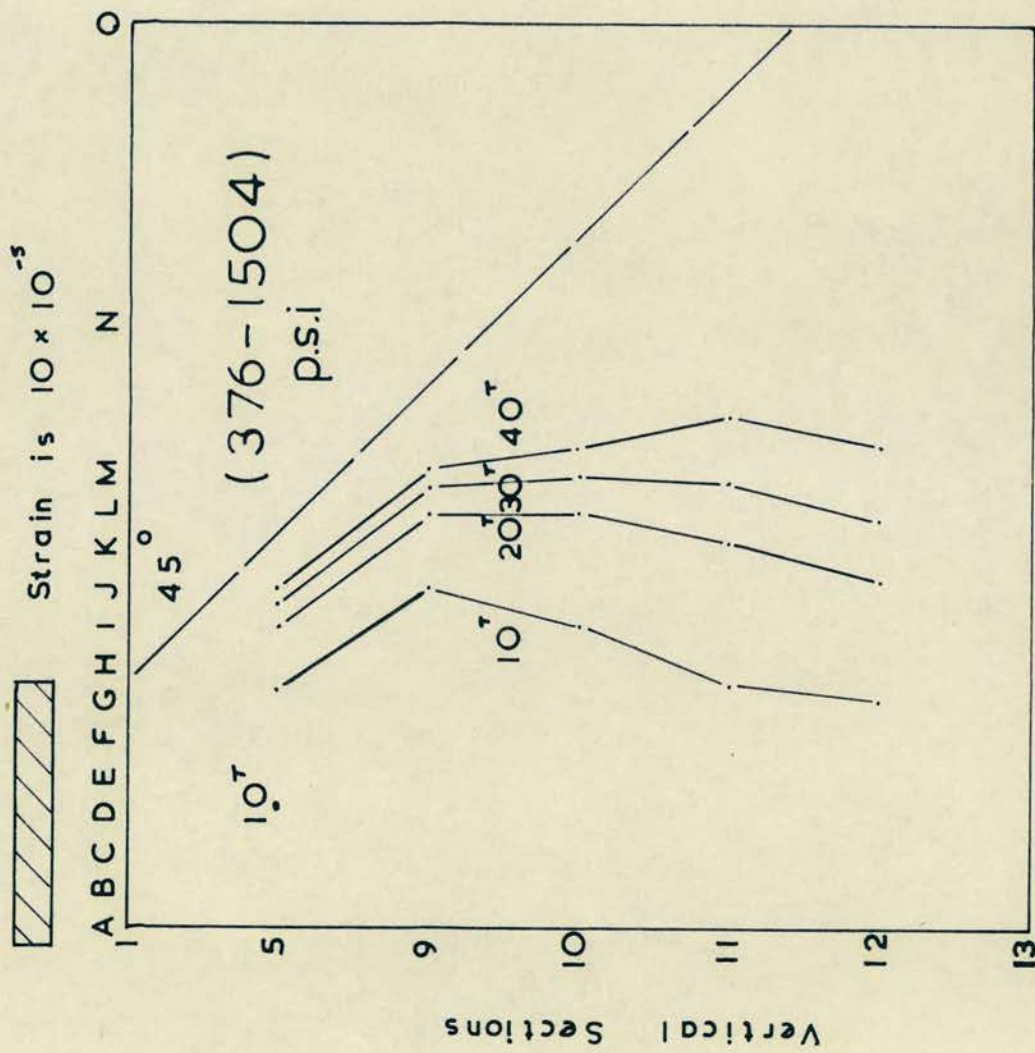
Fig. 3-11

 1755 p.s.i.



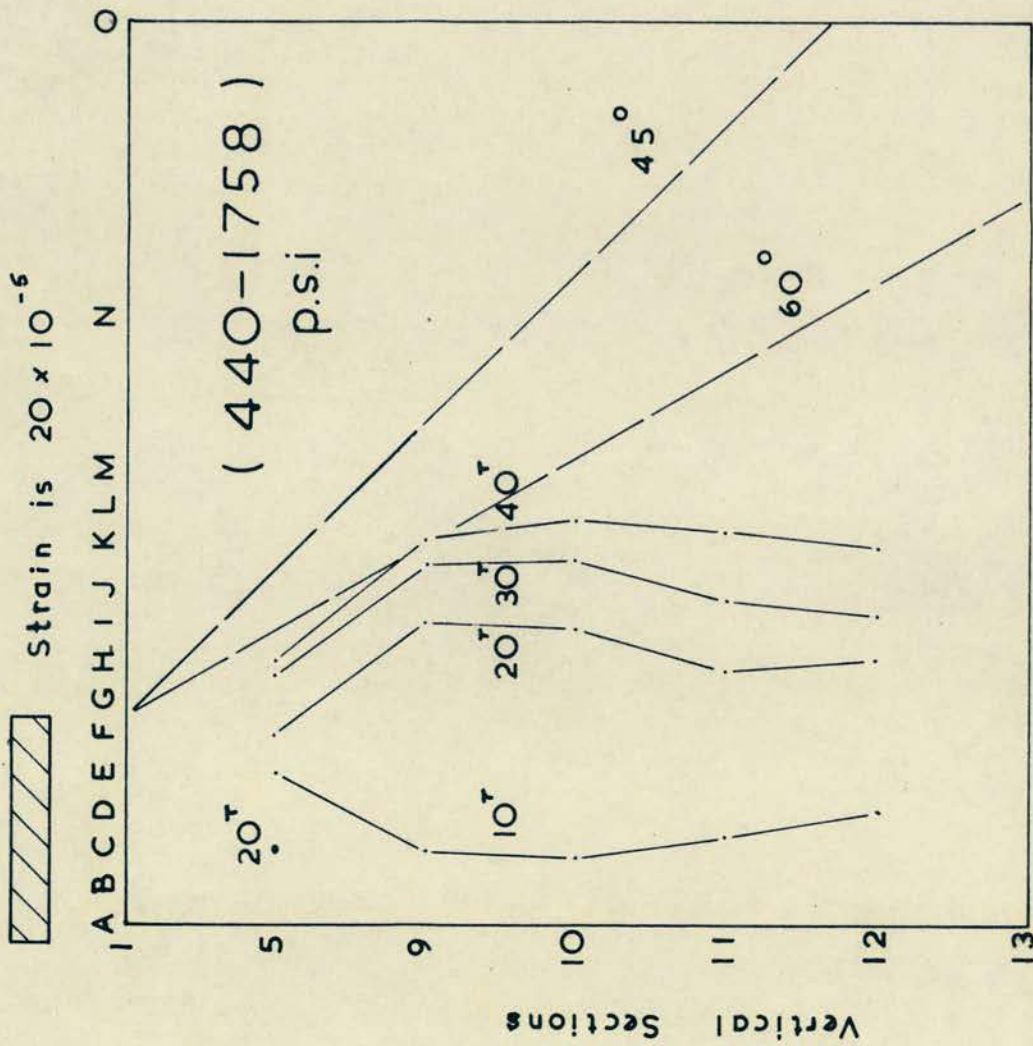
Vertical Strain Contours ($\times 10^5$) at 60 Tons
9" End Bearing Plate . Pier 4.

Fig. 3-12



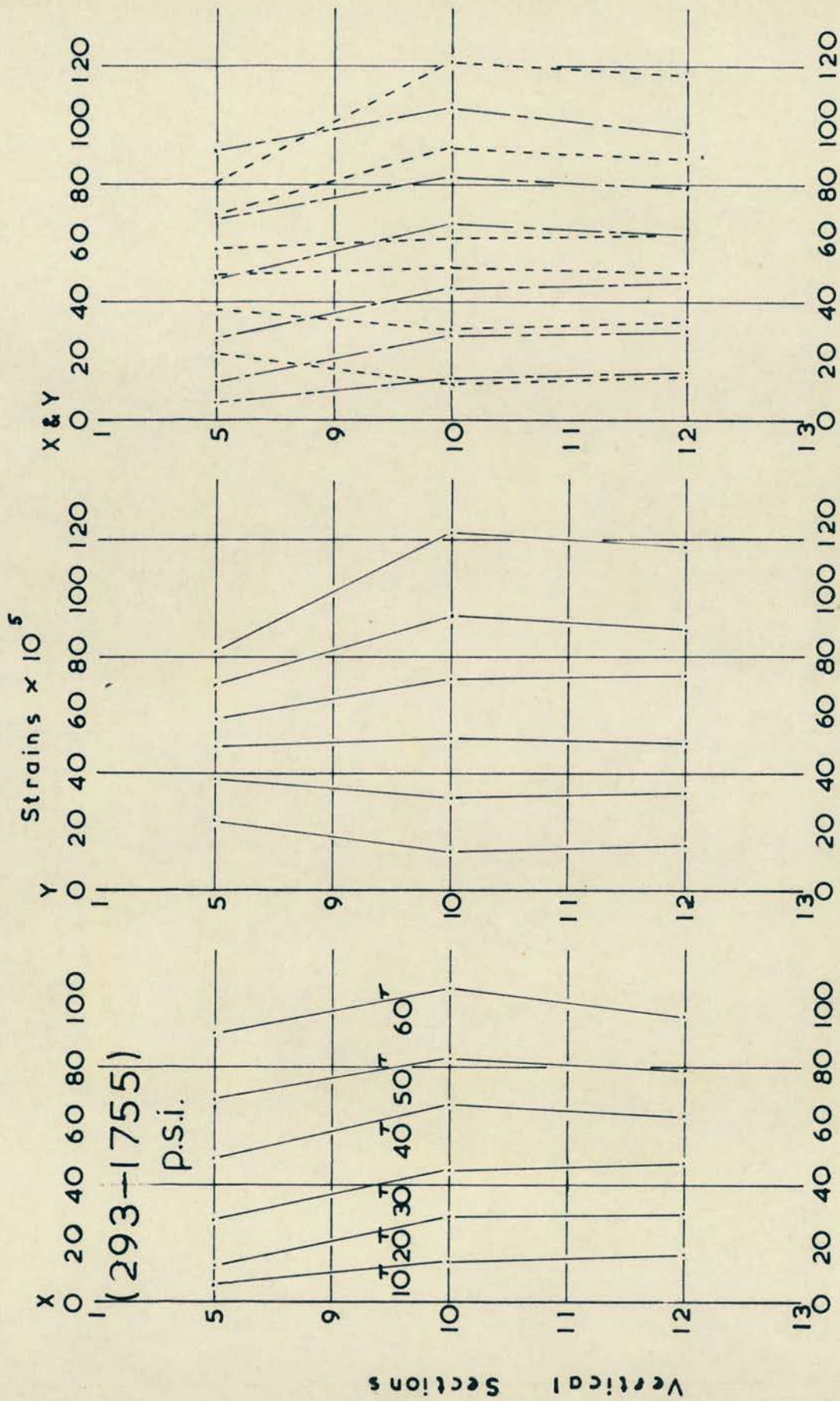
Compressive Vertical Strain Contours at Various Loads.
7" End Bearing Plate. Pier 4.

Fig. 3-13



Compressive Vertical Strain Contours at Various Loads
6" End Bearing Plate. Pier 4.

Fig. 3-14



Vertical Strain Contours
9" End Bearing Plate. Pler 4.

Vertical Sections
Fig. 3-15

ix Reinforced Piers.

The failure stresses shown in Table 3-5 for the reinforced piers are inconclusive and the load bearing capacities were lower than anticipated, not exceeding those obtained for unreinforced piers. No explanation can be offered for the results, as the mortar cubes were of adequate strength.

However, the maximum amount of reinforcement used, as a % of the vertical cross-section was low, being only 0.08%, and it may well be that larger amounts of reinforcement would affect the strength to a greater extent.

For a conclusion to be reached as to the effect of reinforcement on the strength of brickwork, a further extensive series of tests is required.

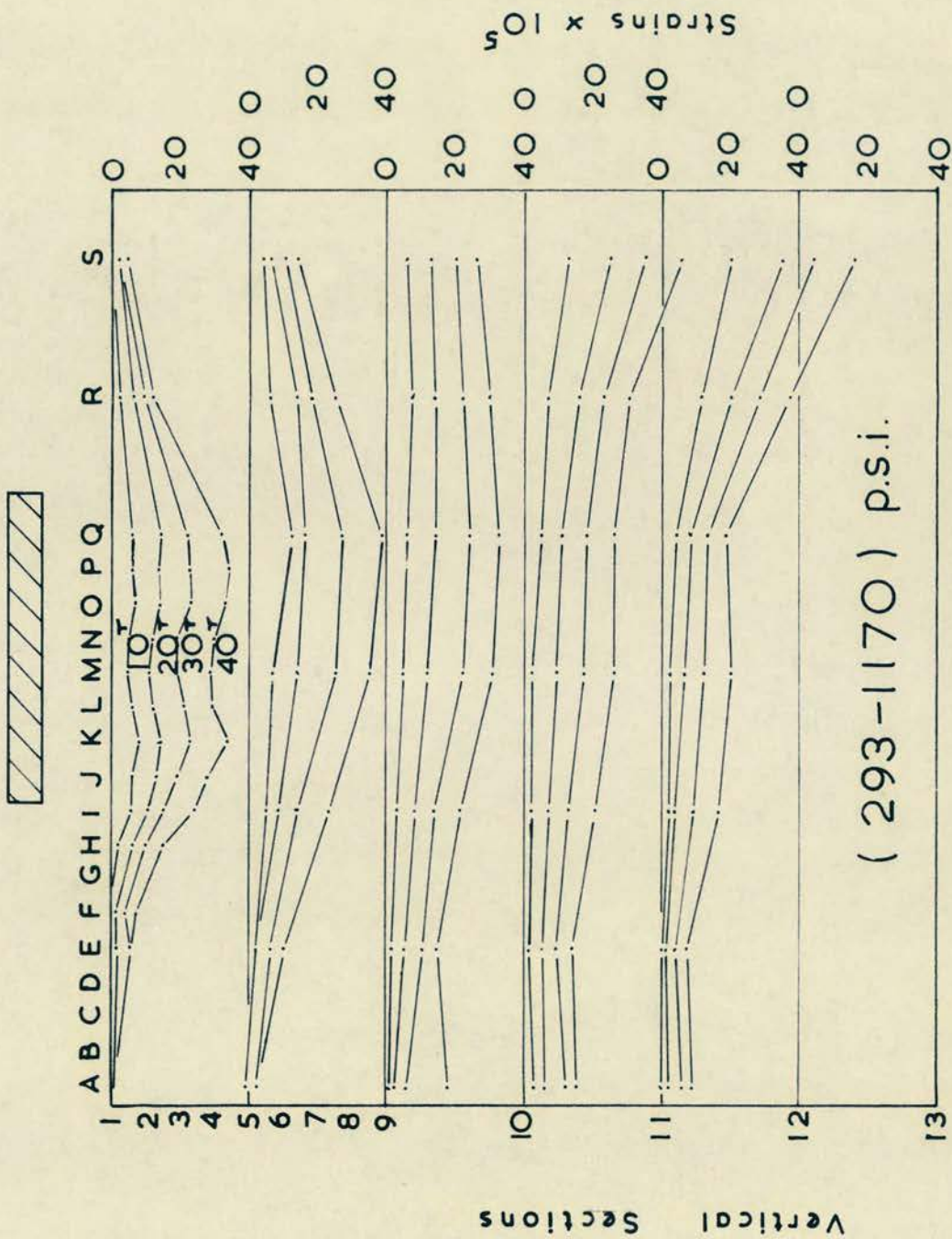
2.8 CENTRAL BEARING PLATES.

i. Vertical Strain Distribution.

Figs. 3-16, 3-17, 3-18 and 3-19, show the vertical strain distributions for pier 12 (reinforcement in top 3 courses) loaded centrally through bearing plates of lengths 9", 7", 6" and $4\frac{1}{2}$ ".

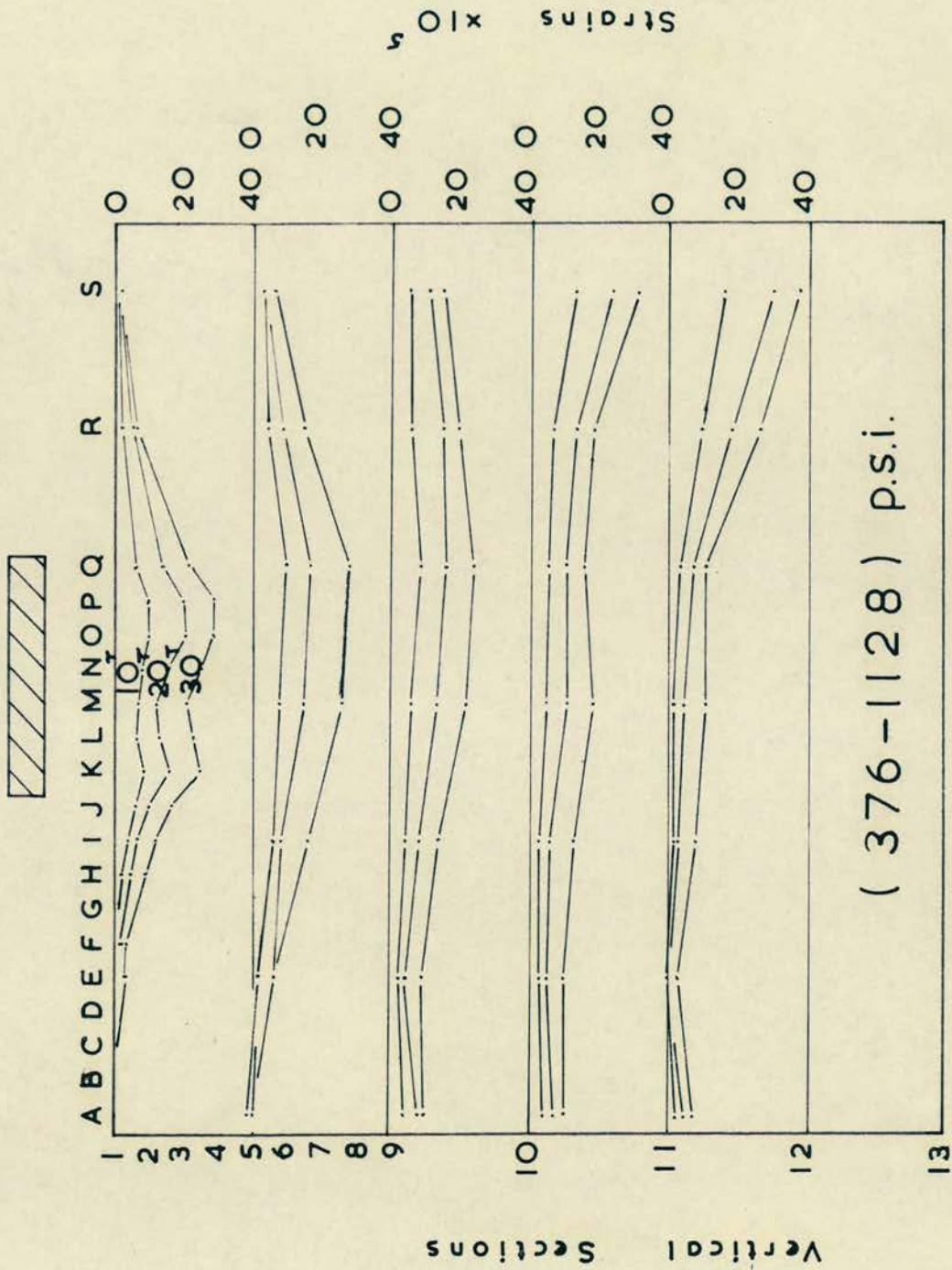
In each case it can be seen that there is a bulb of pressure directly beneath the bearing plate, and that the load is transmitted down the pier section.

The strain concentration shown on the right of the pier is surprising, and occurs with all four loading cycles, suggesting that it is not incorrect positioning of the load, causing eccentricity. With pier 11 (reinforced every 3rd course), the same positioning of loads led to a strain concentration at the same level, but on the left side of



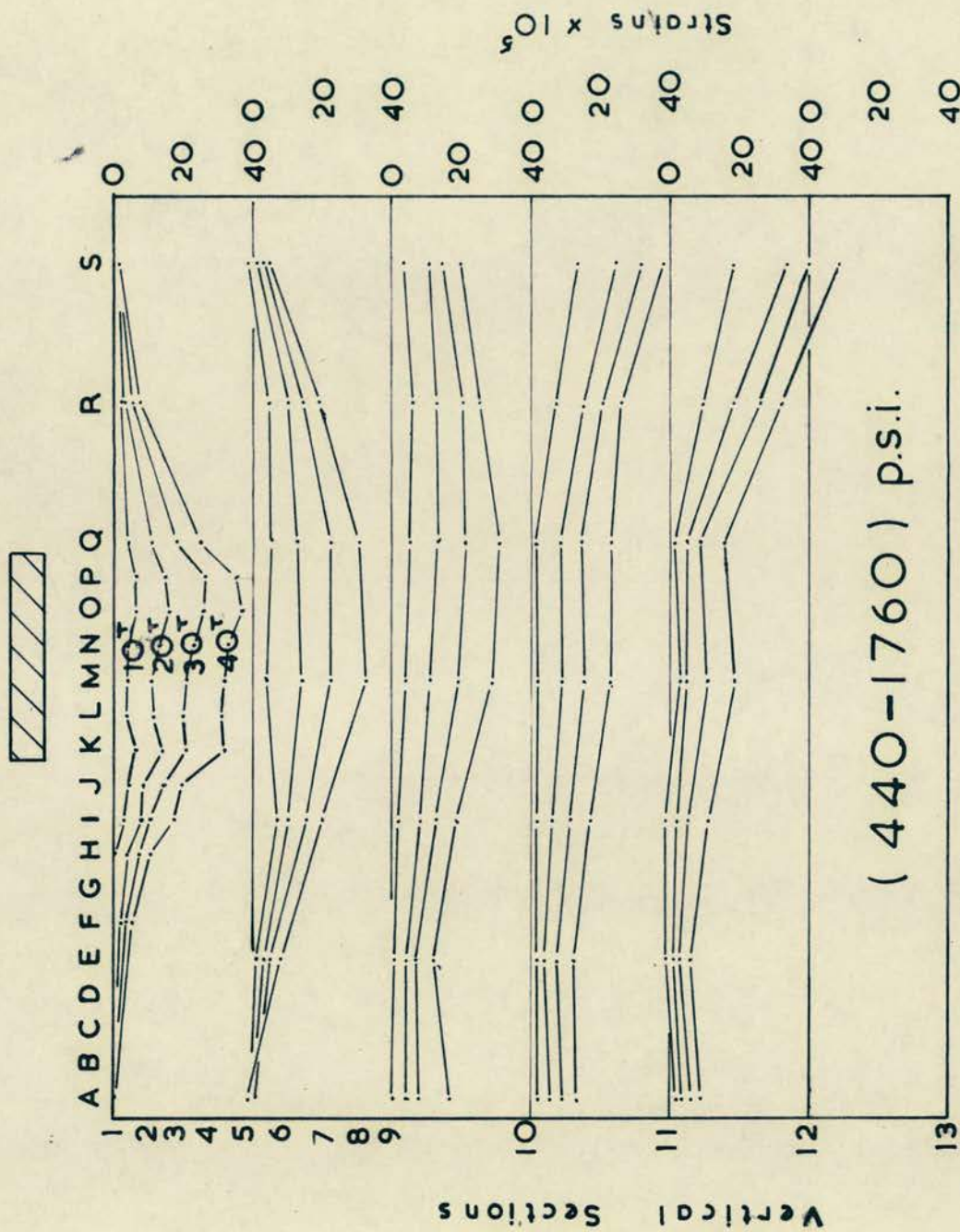
Compressive Vertical Strain Contours at Various Loads
9" Central Bearing Plate. Pier 12.

Fig. 3-16



Compressive Vertical Strain Contours at Various Loads
7" Central Bearing Plate. Pier 12.

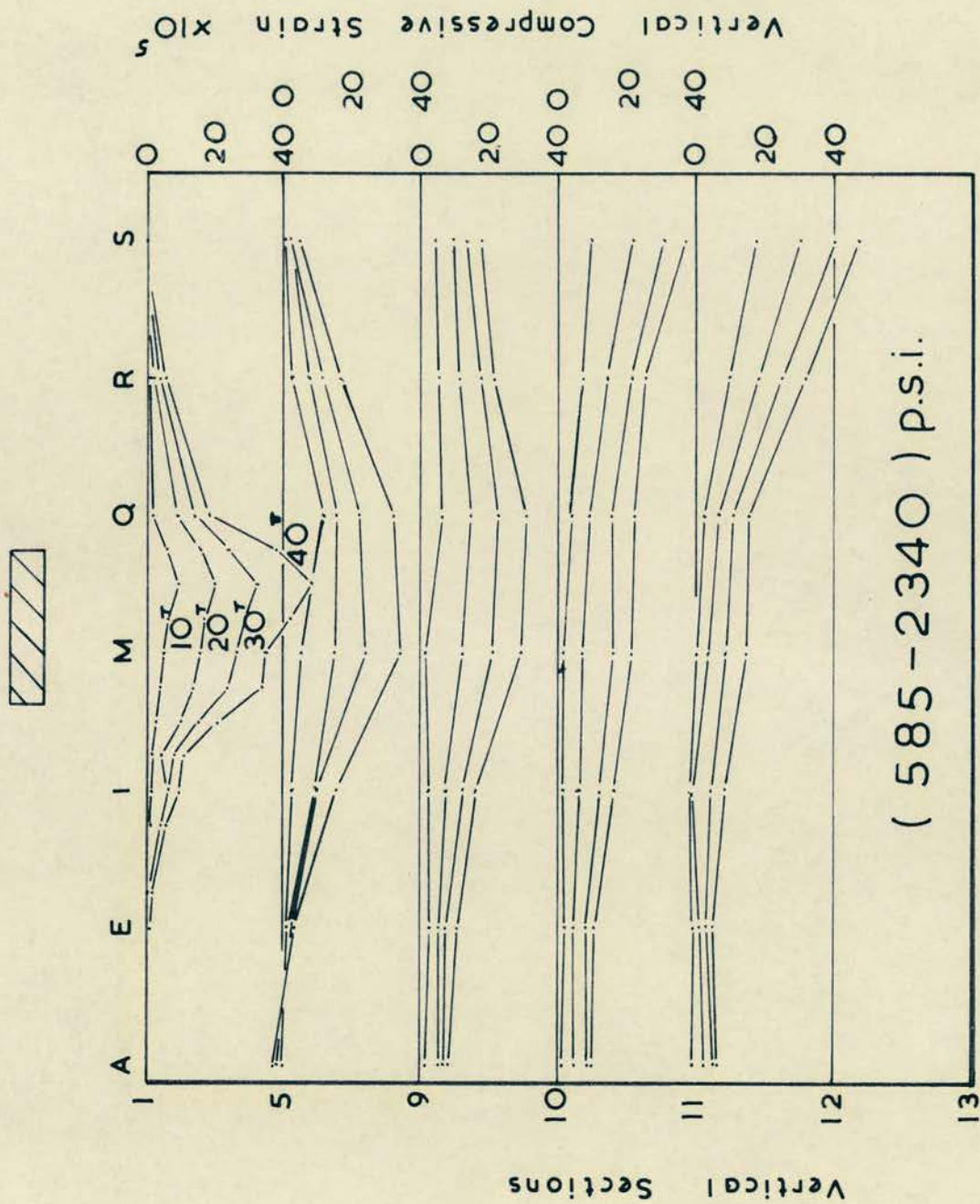
Fig. 3-17



(440-1760) p.s.i.

Compressive Vertical Strain Contours at Various Loads
6" Central Bearing Plate Pier 12

Fig. 3-18



Compressive "Vertical Strain Contours at Various Loads.
 4½" Central Bearing Plate. Pier 12.

Fig. 3-19

the pier. No explanation of this phenomenon can be offered, and it does not occur with piers 9 and 10 (reinforced every course, and every other course respectively), and the strain distributions in piers 9 and 10 are purely of a pressure bulb type.

ii Horizontal Strain Distribution.

Fig. 3-20 shows a typical example of the horizontal strain distribution. The horizontal strains observed are relatively small in comparison with the vertical ones, and do not represent as clear a pattern. Directly under the load there is an area of compressed brickwork, where the strains are high. Further down the pier section the compression changes to tension, and a tensile bulb of pressure exists on a vertical section line through the centre line of the bearing plate.

iii Vertical Strain Contours.

Figs. 3-21 and 3-22 illustrate the vertical strain contours for a $4\frac{1}{2}$ " central bearing plate, at applied loads of 20 and 40 tons.

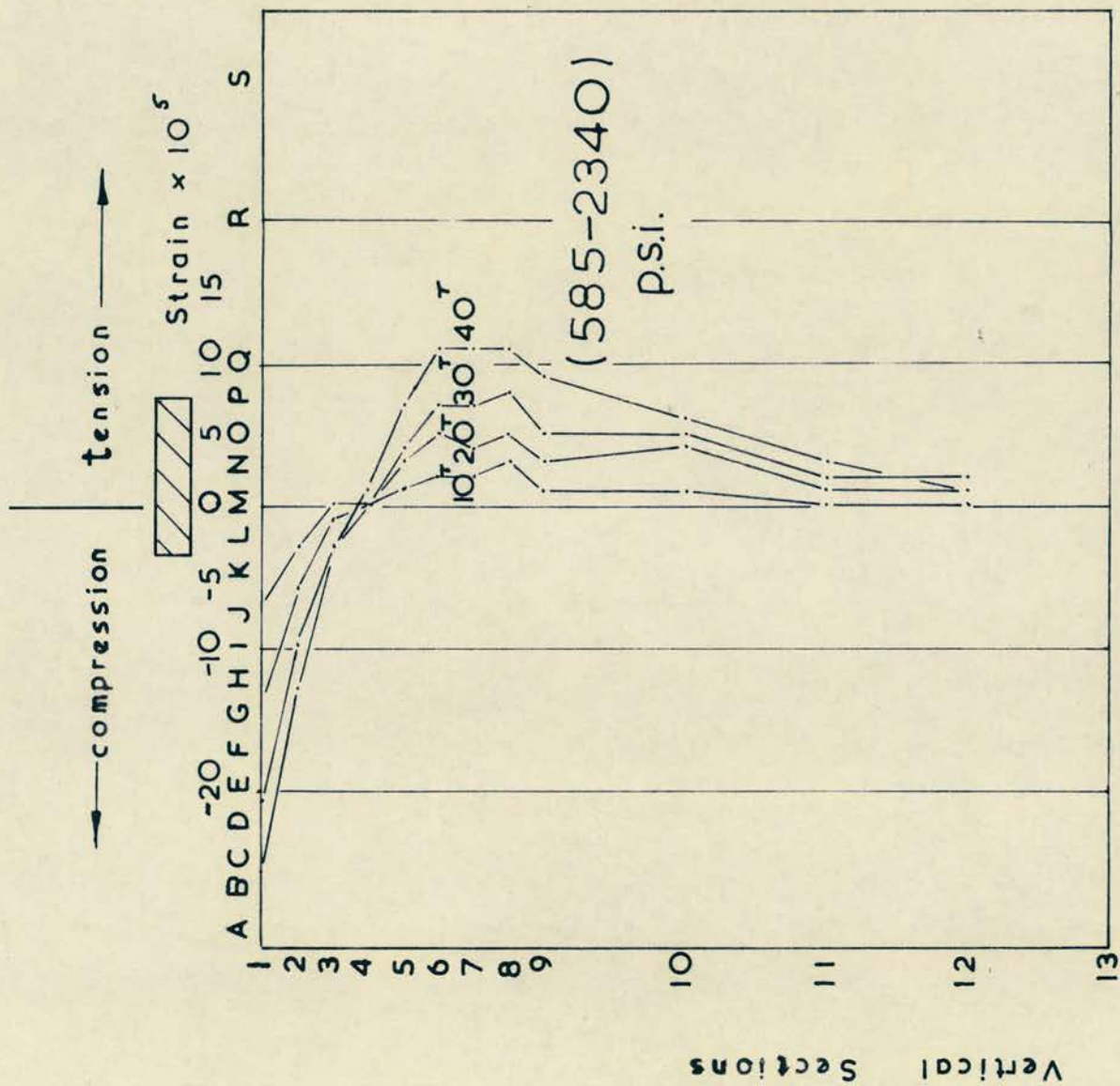
The strain distribution is clearly of a pressure bulb type, with the highest compressive strains occurring directly under the bearing plate, and apart from the high strain contours on the right towards the base, the distribution is as expected.

Fig. 3-23 represents the increased distribution of the load as the bearing pressure increases.

Figs. 3-24 and 3-25 show the compressive strain contours for pier 9, at 20 and 40 tons. In this case there is a pressure bulb stress distribution, with no eccentricity of strain distribution.


2.9 CONCLUSIONS.

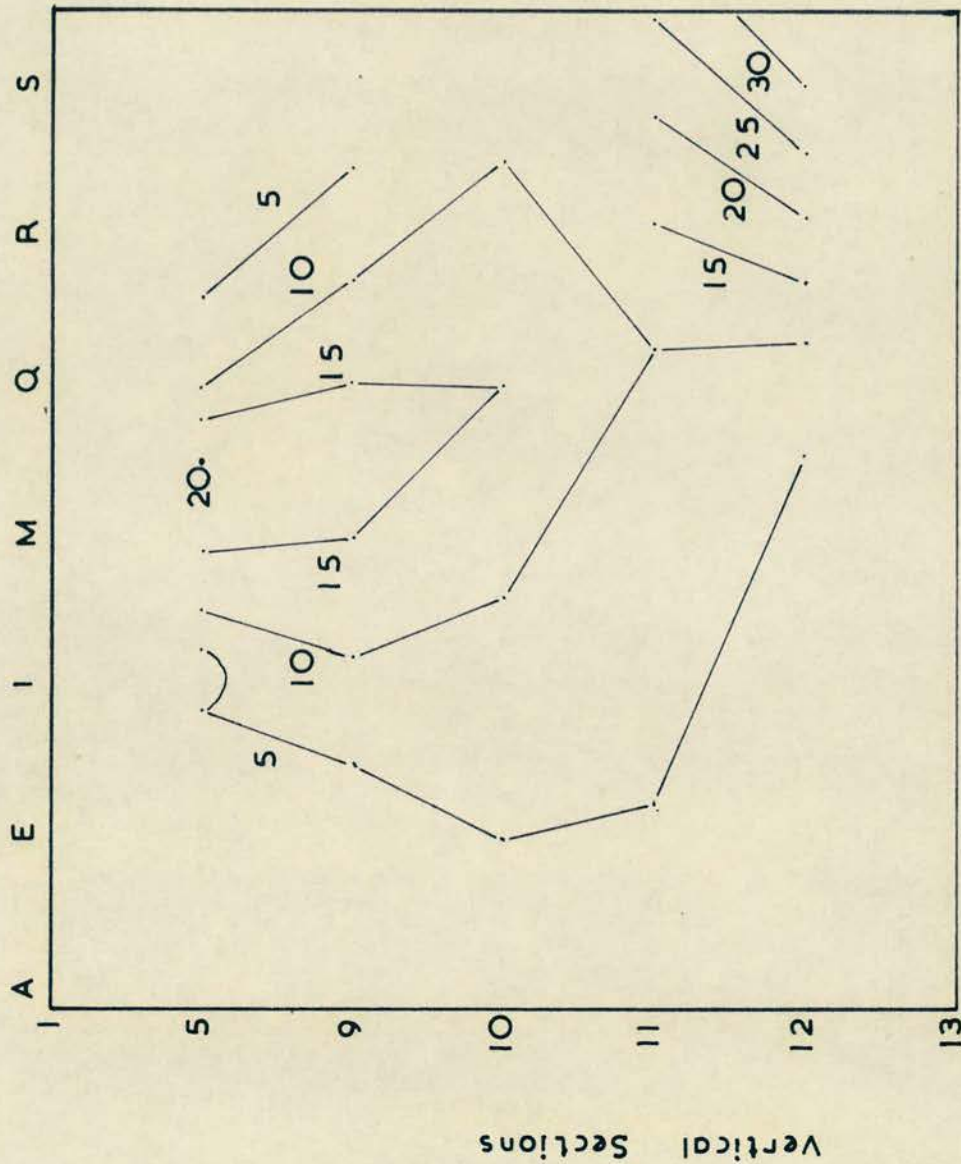
i. For the brick and mortar combination investigated, and in the



Compressive & Tensile Horizontal Strain Contours at Various Loads.
 4 1/2" Central Bearing Plate. Pier 12.


Fig. 3-20

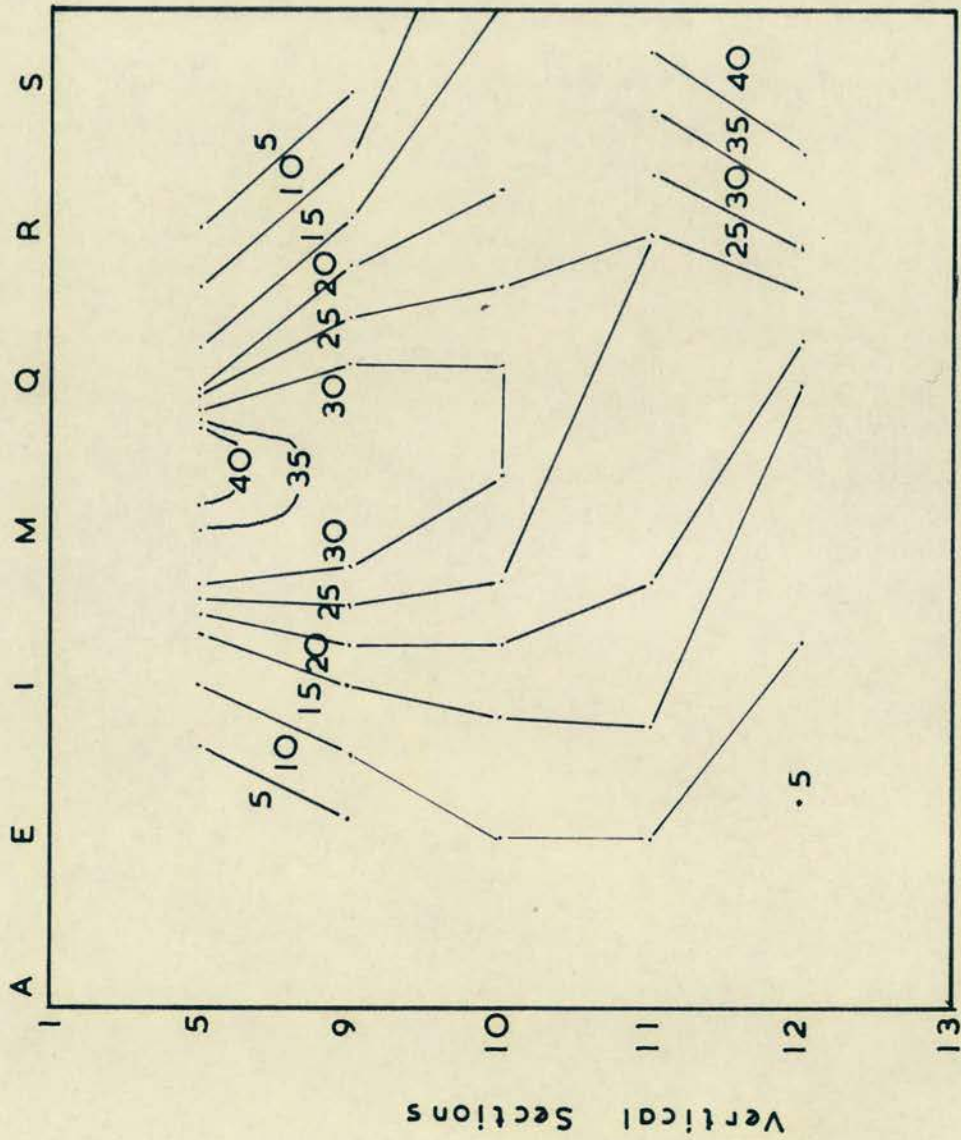
 1170 p.s.i.



Vertical Strain Contours ($\times 10^5$) at 20 Tons
 4 1/2" Central Bearing Plate . Pier 12.

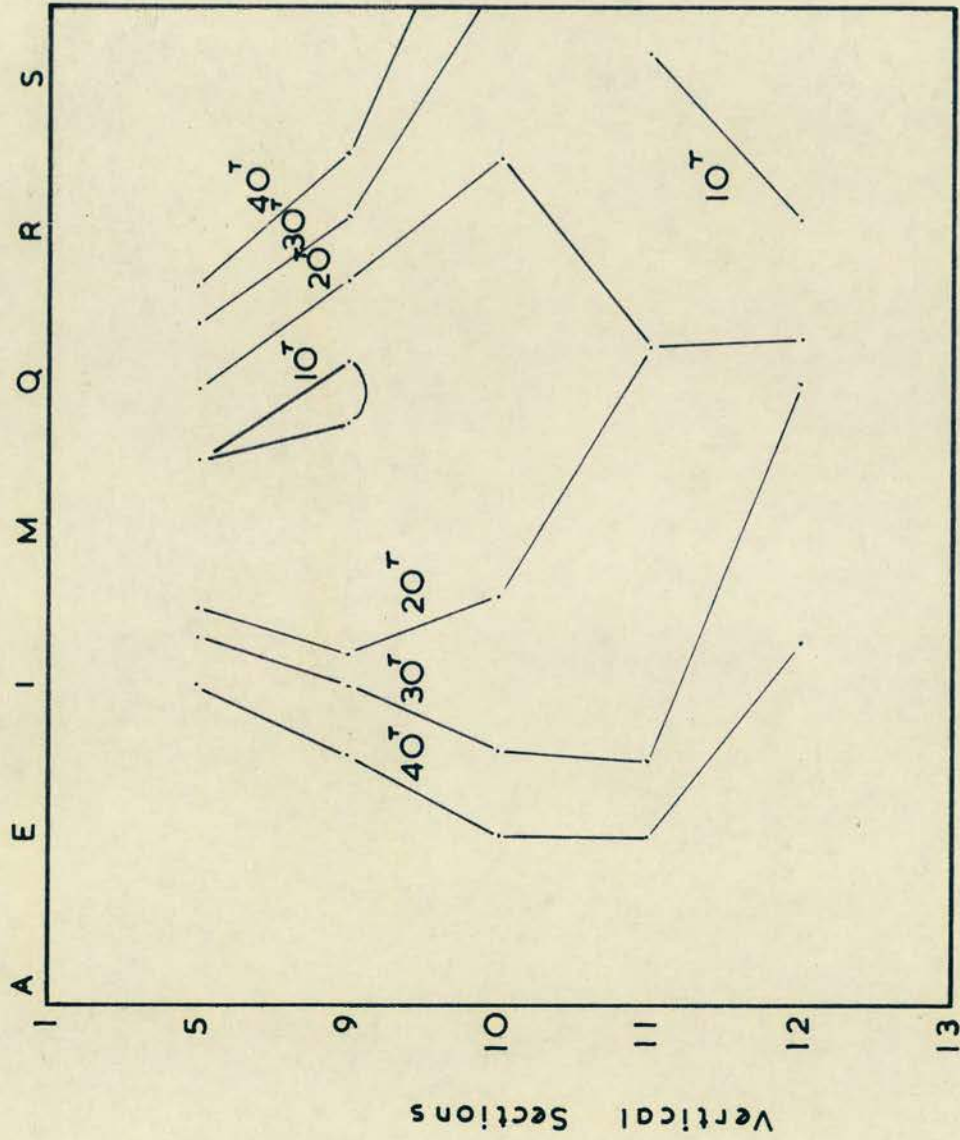
Fig. 3-21

 2340 p.s.i.



Vertical Compressive Strain Contours ($\times 10^5$) at 40 Tons.
 $4\frac{1}{2}$ " Central Bearing Plate. Pier 12.

Strain is 10×10^{-6} (585-2340) p.s.i.



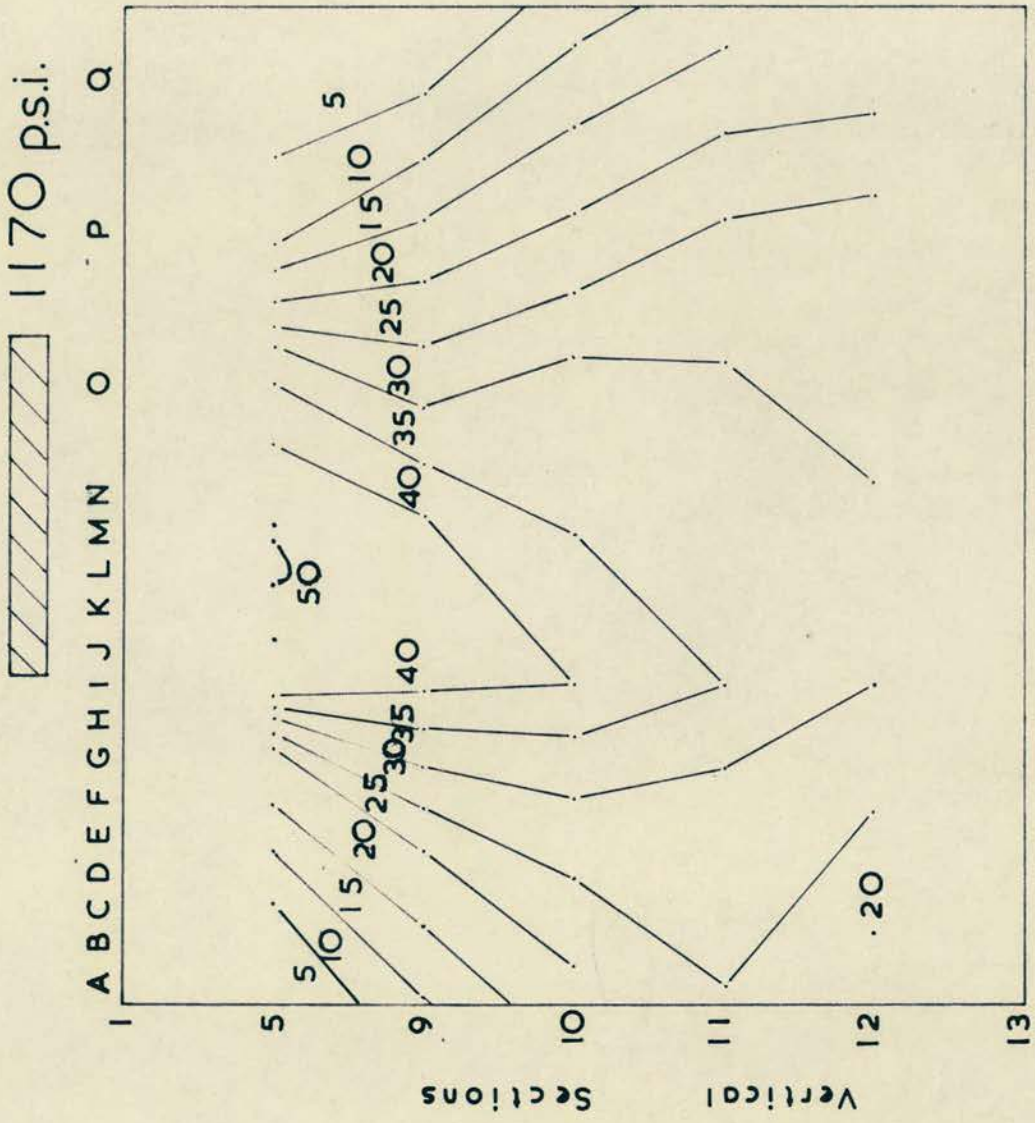
Vertical Compressive Strain Contours at Various Loads
 4½" Central Bearing Plate. Pier 12.

Fig. 3-23



Vertical Compressive Strain Contours ($\times 10^5$) at 20 Tons
9" Central Bearing Plate. Pier 12.

Fig. 3-24



Vertical Compressive Strain Contours ($\times 10^5$) at 40 Tons.
9" Central Bearing Plate. Pier 12.

Fig. 3-25

range of the bearing plate sizes chosen, the failure load, for end bearing plates, increased as the length of the bearing plate increased. The exact nature of the relationship between the failure load and the bearing plate length was not established.

The failure stress was, however, shown to increase, with decreasing bearing plate length, indicating a non-linear relationship between failure load and bearing plate length. In the range of bearing plate sizes investigated the increase in failure stress was linear with a decrease in bearing plate length.

Model tests described in Chapter 6 have indicated that the relationship between failure stress and bearing plate length is non-linear, the failure stress increasing rapidly as the size of the bearing plate approaches a line load condition.

- ii. A definite vertical compressive strain pattern existed, for both end and central loadings, and consisted of a bulb of pressure directly below the bearing plate, and a distribution of the load down and across the piers.
- iii. The distribution of compressive strain under an end bearing plate extended to the 45° sector suggested by C.P. 111 : 1964.
- iv. Although the strain distribution extended to a 45° sector, a large percentage of the load was taken directly beneath the bearing plate, and a uniform 45° distribution did not in fact occur.
- v. For end loadings the maximum compressive strain usually occurred towards the base of the pier, and the strain distribution was triangular at this level. The extent of the significant strain distribution varied from 9" - 12" across the section.

- vi. Higher vertical compressive strains were measured for 9" bearing plates than for $4\frac{1}{2}$ ", for the same average applied compressive stresses. However, the failure stresses were not in the ratio of the measured compressive strains, although they were higher for the $4\frac{1}{2}$ " bearing plates.
- vii. Safety factors from 3.6 - 5.6 were obtained, comparing the allowable stresses with the ultimate stresses. However, if the cracking load is taken as the criterion, the safety factor was as low as 2 in some cases, casting some doubt on C.P. 111 : 1964 which recommends a 50% increase in the basic stress, for concentrated loadings.
- viii. The mode of failure for end bearing plates appeared to be the shearing off of a wall section along a plane or curved surface, originating at the inner edge of the bearing plate. This failure was preceded by vertical cracking, and some local crushing or spalling.
- ix. The relationship between average applied compressive stress and compressive strain was linear, in all but the failure zone. The beginning of the failure zone being the stress at which initial cracking takes place.
- x. The relationship between compressive stress and tensile strain was non-linear.
- xi. The section of the pier over which the load was distributed did not significantly increase with increased bearing pressure.
- xii. An increase in bearing pressure increased the strain at any particular section where strain was already present.
- xiii. Central bearing plates produced a bulb of pressure, in both a vertical and a horizontal direction; the vertical being compressive,

and the horizontal tensile.

xiv. The load distribution in a centrally loaded pier was confined largely to an area directly beneath the bearing plate, although a small proportion of the load was distributed up to a 45° sector.

xv. The addition of horizontal reinforcement of the type and quantity described in this report appeared to have no effect on the failure stress of the piers.

3. THE EFFECT OF THE VARIATION OF THE BEARING PLATE POSITION ON THE STRAIN DISTRIBUTION IN A BRICKWORK PIER.

3.1 INTRODUCTION.

Recent work by Hiltcher and Florin ⁽³⁸⁾ described in Chapter 2 has shown that the tensile strain distribution in a rectangular plate loaded along a portion of its horizontal boundary, by a vertically applied force, varies considerably with the position of the load and with the ratio total plate area/ area of loading.

Their work was concerned with the provision of reinforcement in the tensile zones of precast concrete members, when such members are subject to concentrated loadings. A photo-elastic investigation was carried out and the effect of varying the height/width, width/bearing length and edge distance/bearing length ratios was investigated.

From the test results it was assumed that the positions where tensile reinforcement was required, in the concrete panels, corresponded to the tensile zones determined from the photo-elastic tests. It was also assumed that the amount of reinforcement could be calculated from the magnitude of the strains observed, and the zones over which they were present.

If photo-elastic tests can be relied upon to give a good representation of the behaviour of a precast concrete unit, then it is possible that the strain distribution in brickwork is also similar, and similarly affected by a variation of the parameters concerned.

The photo-elastic tests of Speer (39) detailed in Chapter 2 showed that tensile strains can also exist which are caused by the different elastic properties of the brick and mortar layers, and by elastic bedding conditions. These strains are of a local nature, with maximum values at the centre of the bricks.

Unfortunately the loadings applied were uniformly distributed across the whole section, and hence the qualitative results are not directly applicable to the investigation described in this section.

In order to investigate the correlation between photo-elastic tests on a homogeneous plastic material, and tests on non-homogeneous brickwork, a series of loading tests was carried out.

3.2 SCOPE OF THE TEST PROGRAMME.

For practical reasons the extent of the test programme was somewhat limited. Only one size of pier was tested, 27" x 24" x 9", constructed as described in section 2.3 of this chapter.

The bearing plate length chosen was the smallest used in the previous test series, a $4\frac{1}{2}$ " x 9" x 1" thick M.S. plate.

The positions of loading investigated were end bearing, 5.25", 8.25", and 11.25" from the end, and central bearing. The distances given above were measured from the vertical end face of the wall to the centre-line of the bearing plate.

In all four walls were tested, Nos. 13, 14, 15 and 16, and the amount of reinforcement in the walls was varied.

Wall 13 had no reinforcement.

Wall 14 had B. R. C. fabric brick reinforcement consisting of two $\frac{1}{8}$ " rods, 6" apart, linked every six inches by an $\frac{1}{8}$ " rod, in the top, 3rd, 5th and 7th horizontal mortar joints. Joints were numbered from the top of the pier downwards.

Wall 15 contained the same type of reinforcement in every horizontal mortar joint.

Wall 16 had the same type of reinforcement in the top three mortar joints only.

The dimensions of the walls tested, the bearing plate size, and the edge distances of the bearing plates gave properties corresponding to those investigated in the photo-elastic tests as follows.

Height of wall/width of wall, $H/B = 0.89$. Width of wall/width of load, $b/a = 6$. $2x$ the edge distance/width of load, $2d/a = 1, 2.55, 3.66, 5$ and 6 .

The strains on one face of the wall (27", long x 24" high) were measured, using a 2" Demec gauge, which had a sensitivity of strain of 2.48×10^{-5} per division.

Vertical strain readings were taken below the position of load application in each test, in order to check the uniformity of the load application.

Horizontal strain readings were taken along the top of the wall face, and in the area below the bearing plate, and were the main

factor of interest in the tests.

3.3 TEST PROCEDURE.

The walls were tested in a 100^T Avery testing machine as in the previous series, and the load was applied through the rigid platen. The top of the wall was levelled with sand, where necessary, and an $\frac{1}{8}$ " plywood sheet was used, to ensure an even distribution of load.

After taking the zero load Demec gauge readings the load was applied in 10^T increments, up to a maximum of 30^T, corresponding to an average applied stress of 1,700 pf. s. i., Demec readings being taken at each load increment.

After the wall had been tested with the required bearing plate positions the final test to destruction was conducted, with the bearing plate central.

The same positions of loading were applied to each wall, to allow the comparison of the effect of the reinforcement in varying quantities, both on the strain distribution and on the failure stress.

3.4 TEST RESULTS.

i. Failure Stresses.

The failure stresses obtained were as follows.

Wall 13 - 4,450 pf. s. i. (No reinforcement).

Wall 14 - 4,100 pf. s. i. (Reinforcement in every second horizontal joint).

Wall 15 - 5,400 pf. s. i. (Reinforcement in every mortar joint).

Wall 16 - 4,400 pf. s. i. (Reinforcement in the top three mortar joints).

ii. Strain Distribution.

The vertical compressive strains were plotted, and were found to be similar in their mode of distribution to those obtained in the previous tests. The distribution was found to be reasonably uniform beneath the bearing plate, indicating that the load was applied in the required manner. When a uniform distribution is referred to, it means that no unusual stress concentrations were noted. The expected pressure bulb type of strain distribution occurred in all cases.

The vertical strain distribution for a typical wall, number 15, (reinforced in every joint) is given in Figs. 3-26 and 3-27. The strain distribution has been plotted, for $2d/a$ ratios of 1, 2.55, 3.66 and 6. The strain distribution has been plotted for different horizontal sections.

The horizontal strain distribution for wall 15, is shown in Figs. 3-28 and 3-29. The strain distributions have been plotted for $2d/a$ ratios of 1, 2.55, 3.66 and 6, and show the splitting tensile strains beneath the bearing plate, and the tear tensile strains, along the top of the wall.

It should be noted that the tear tensile strains measured in the tests on walls 13, 14, and 16, vary considerably from those shown, both in magnitude and position. In all cases the horizontal strains measured in the region of the load indicated a compressive strain.

The splitting tensile strain distribution was found to be essentially the same in form, if not magnitude, in all the tests conducted.

iii. Modes of Failure.

a) Wall 13.

Initial cracking occurred at approximately 2,400 p.f.s.i., and

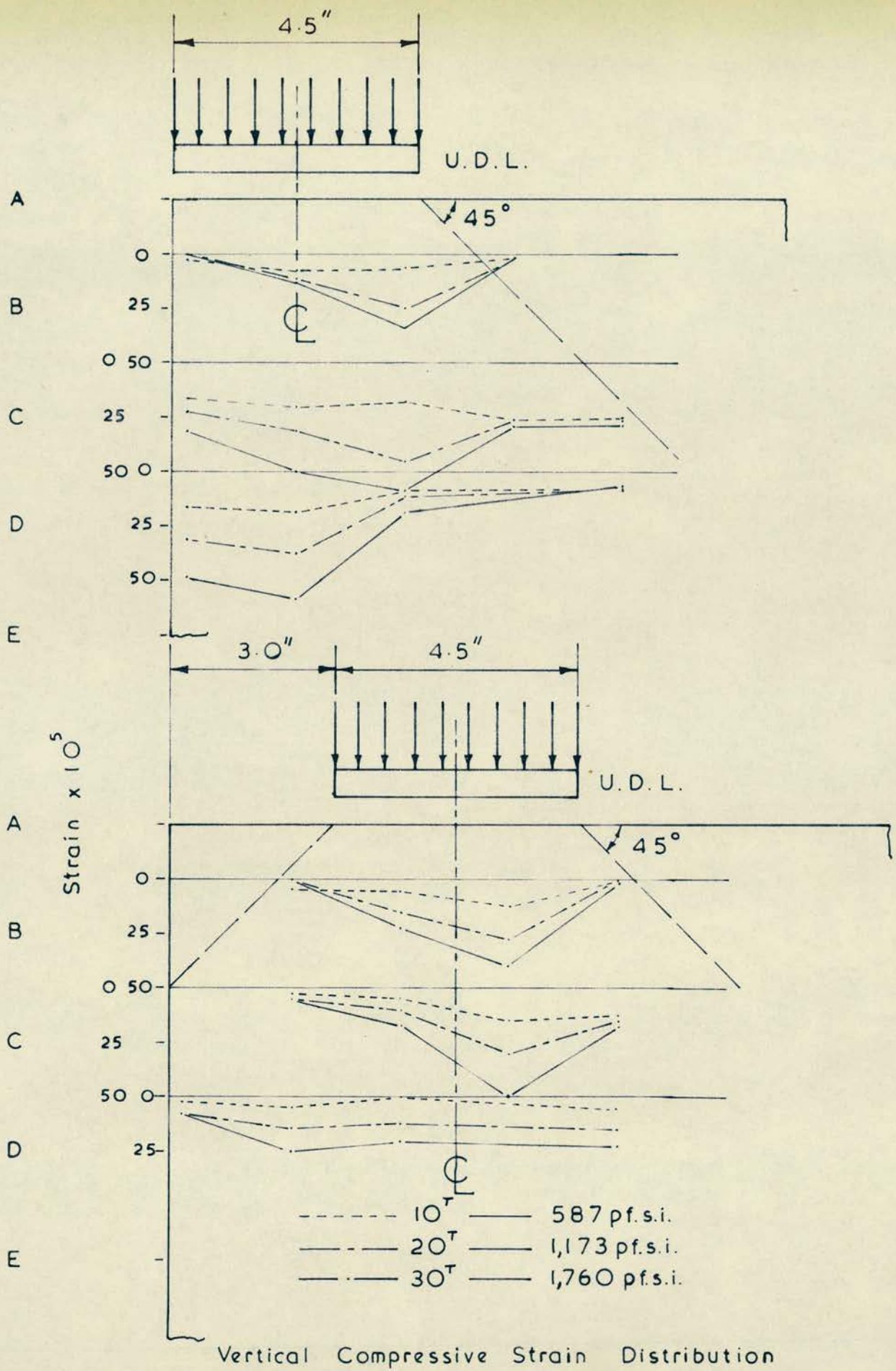


Fig. 3-26

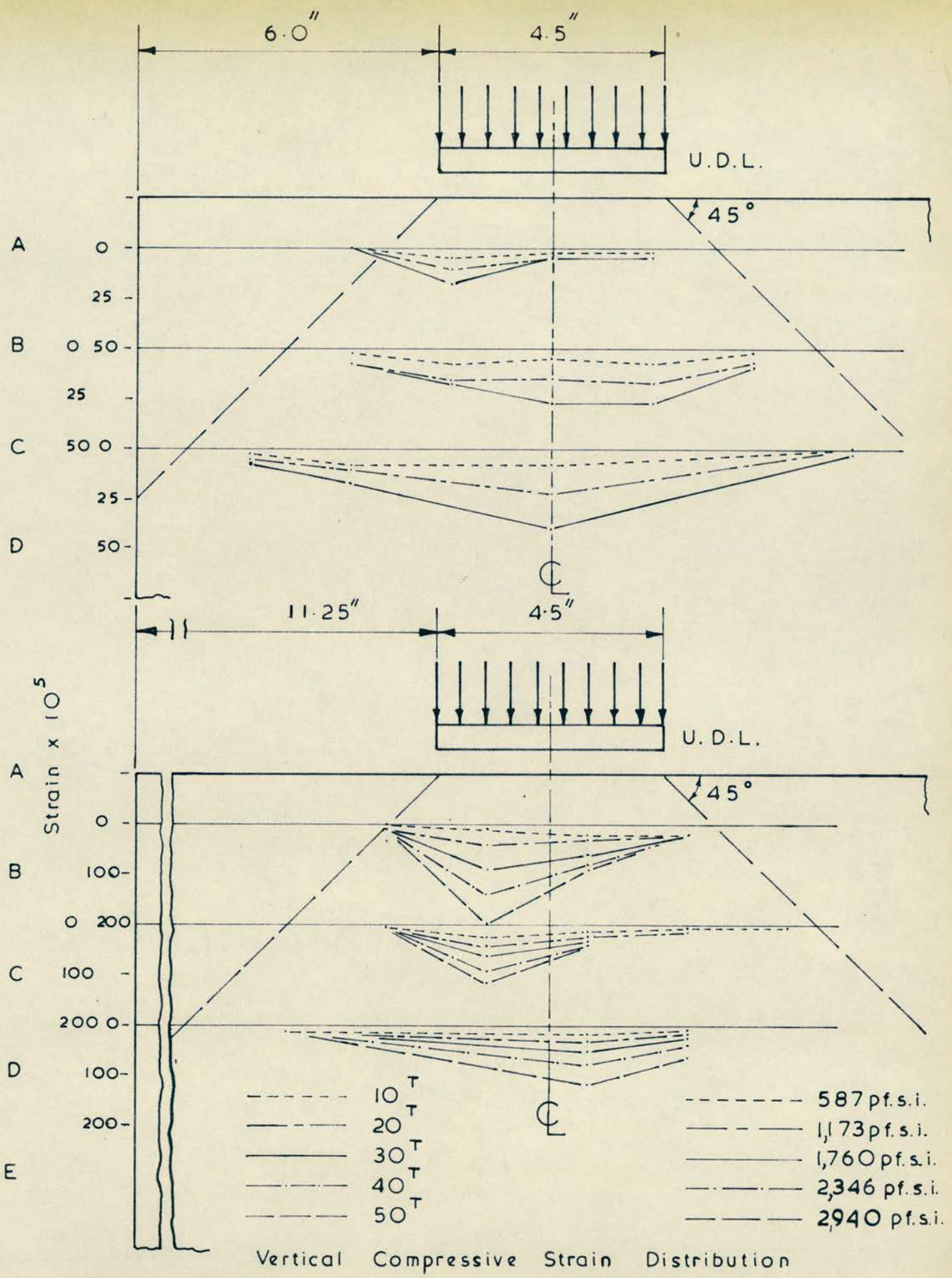
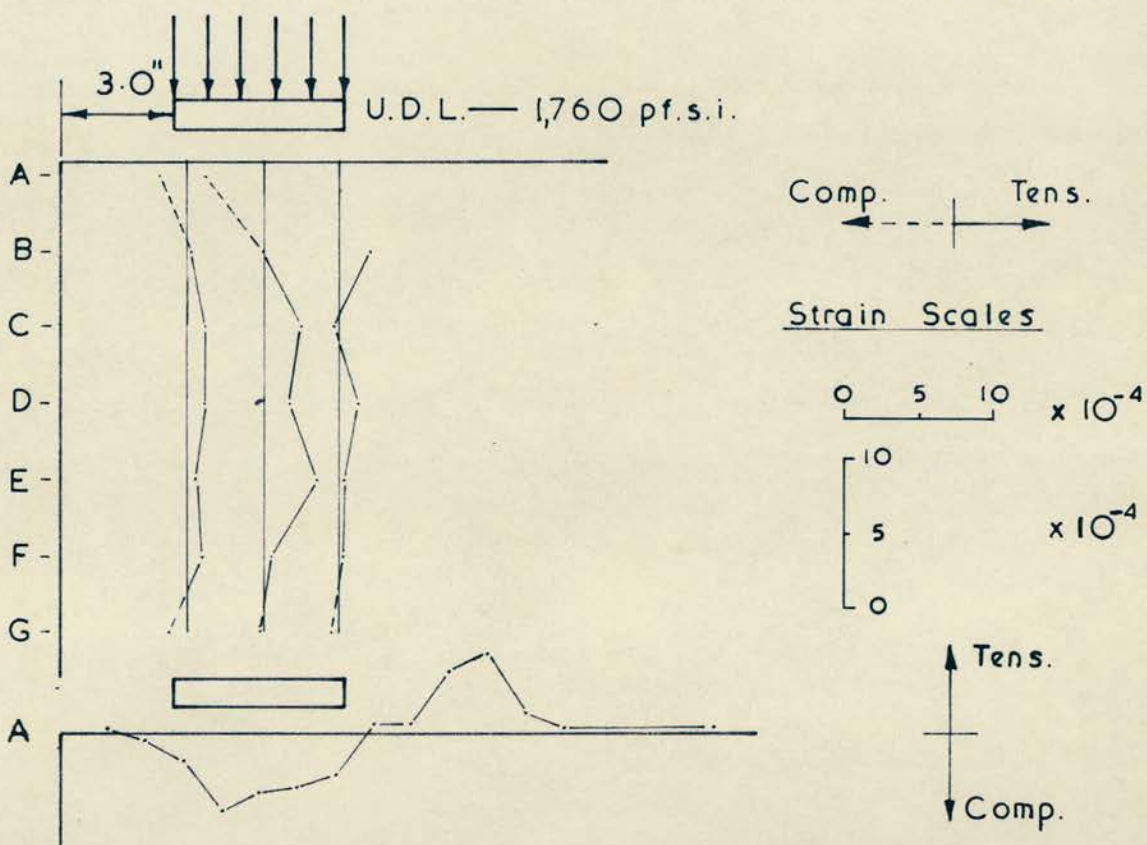
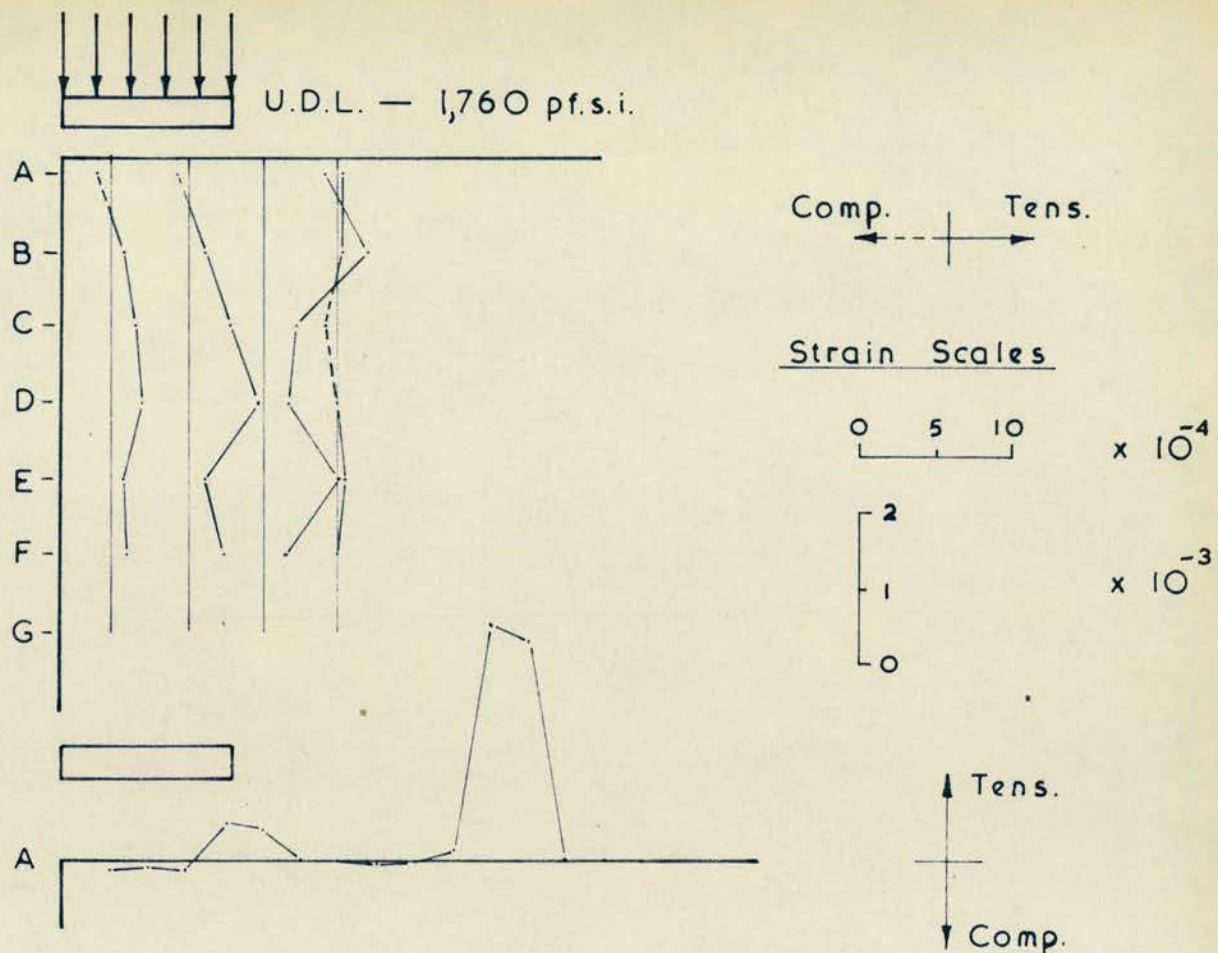
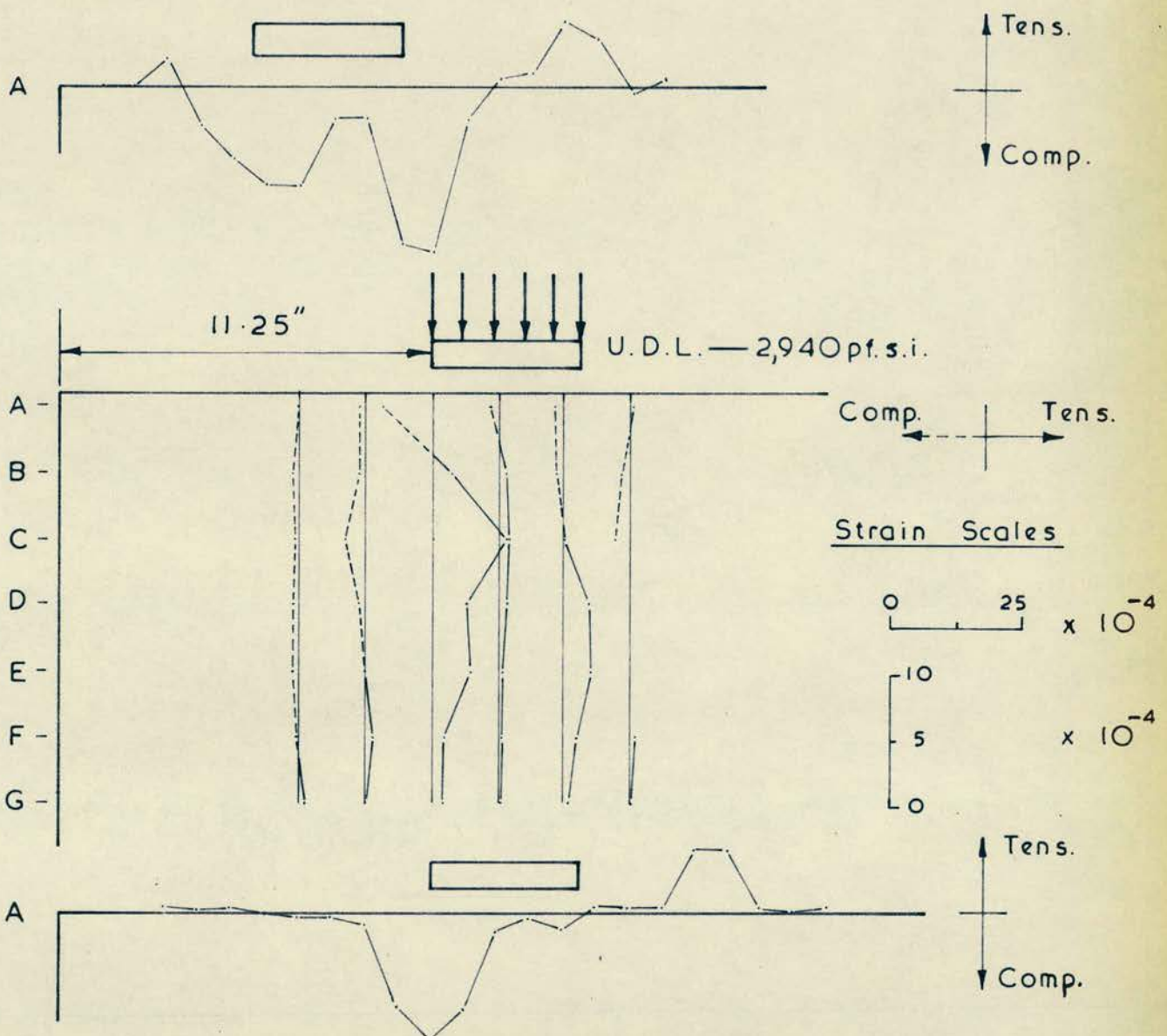
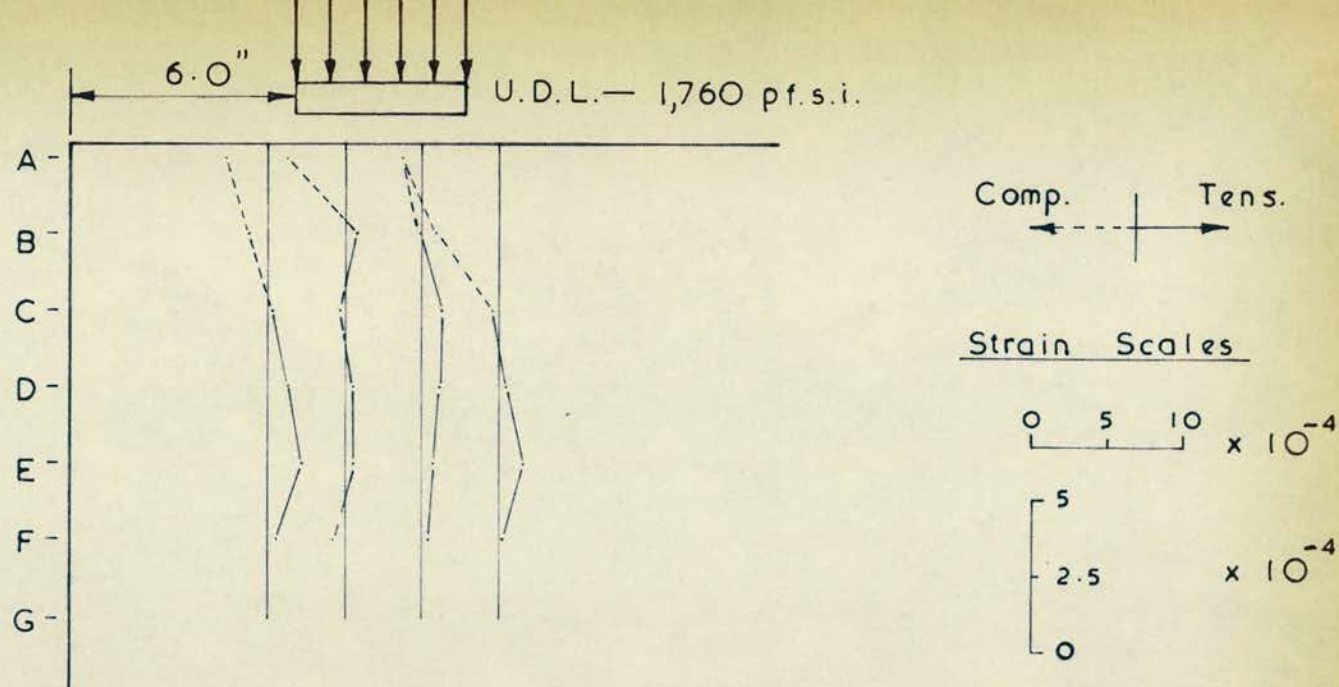


Fig. 3-27



The Horizontal Strain Distribution on Vertical and Horizontal Section(s) — 4.5" Bearing Plate.



The Horizontal Strain Distribution on Vertical and Horizontal Section(s) — 4.5" Bearing Plate

Fig. 3-29

took the form of a vertical split below the bearing plate.

At 3,500 pf.s.i. spalling occurred on one face, in the header brick below the bearing plate, and may have been caused by an initial unevenness of the top surface of the wall. Further cracking then occurred in the zone of load application, and complete failure occurred due to crushing and spalling on both faces, beneath the load.

At failure the vertical splitting was accentuated, and the wall broke away along a horizontal line at the base, as the bearing plate was driven into the wall.

b) Wall 14.

Initial cracking occurred at 3,700 pf.s.i., and took the form of a vertical split below the centre-line of the bearing plate. Diagonal cracking followed, the cracks originating below and towards the edge of the bearing plate. Spalling then occurred, followed by a complete failure of the wall directly under the bearing plate. Plate 3-5 shows Wall 14 after failure.

c) Wall 15.

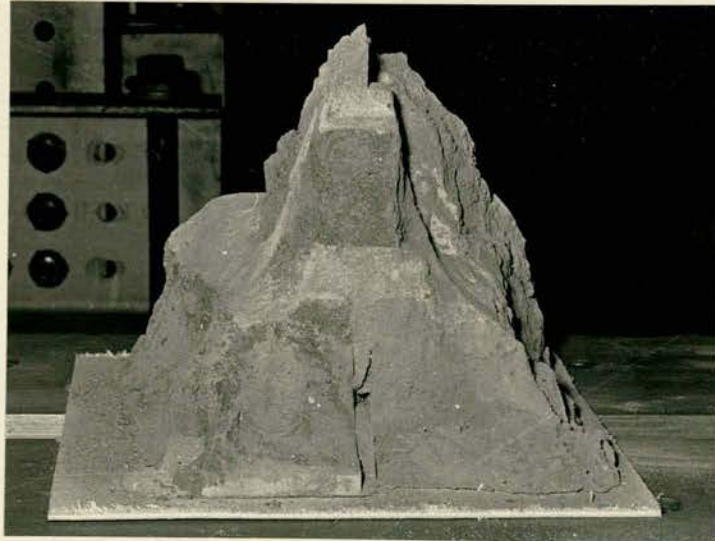
Initial cracking occurred at 3,400 pf.s.i., and took the form of a slightly diagonal crack initiating from below the bearing plate. Spalling followed, on one face below the load, and slight spalling then occurred on the other face at a higher load.

At 5,200 pf.s.i. severe spalling occurred on both faces, and a noise, indicative of the snapping of the reinforcement wires, was heard, and the complete failure of the wall followed.

The bearing plate was driven into the wall, and the load capacity of the wall was still quite high.



A Typical Wall, No. 14 - Showing Demec Studs
for Strain Measurements, and Failure Mode.
Plate 3-5



A Typical Brickwork Cube Failure Mode.
Plate 5-1

d) Wall 16.

Initial cracking occurred at approximately 2,800 pf. s. i. and took the form of a vertical crack, below the bearing plate, but slightly off the centre-line of the wall.

Spalling then occurred on both wall faces, below the load, and was followed by the sudden failure of some of the reinforcement. The complete failure of the wall then occurred, due to crushing below the bearing plate. The failure of the reinforcement was observed to be of a tensile type.

3.5 DISCUSSION OF RESULTS.

i. Failure Stresses.

The failure stresses of the walls indicate that the failure stress was only increased when reinforcement was incorporated in every mortar joint. As this was a single test no definite conclusion can be drawn from the result as to the effect of horizontal reinforcement on the strength of a brickwork detail subject to a concentrated load.

The failure stresses of walls 13, 14 and 16 were very similar, and indicate that the amounts of reinforcement used in these tests had little effect on the strength of the walls.

The area of reinforcement incorporated per mortar joint was only 0.05 in.² which would allow a horizontal force of only 1,790 lbs. f. per mortar joint to be developed, based on a steel yield stress of 16^T/in². This horizontal force compares with an average applied compressive load of 177,000 lb f. at failure.

ii. Strain Distribution.

The vertical strain distributions plotted in Figs. 3-26 and 3-27 indicate that the strain measured on the vertical end face of the wall is only high when the load is applied at the edge of the section. When the load is applied at a distance of 5.25" from the edge the strain distribution is similar to that obtained from the centrally applied loading case.

The form of the strain distribution variation with edge distance would indicate that a shear failure, indicated by the breaking away of an end portion of the wall along a diagonal plane, will only occur when the load is applied at or in close proximity to the edge. These conclusions are borne out by the $1/3$ rd. scale tests conducted to investigate the effect of the edge distance and described in Chapter 6.

The horizontal strain distributions plotted in Figs. 3-28 and 3-29 indicate that two types of tensile strains exist in a brickwork structure subject to a concentrated load.

One type may be described as a splitting tensile strain which occurs in the zone below the bearing plate, and attains a maximum value at some depth beneath the load.

The other type is a tear type of tensile strain, and occurs along the free surface of the brick wall, in the vicinity of the concentrated load, although not necessarily immediately adjacent to it.

The strain distribution for the wall with the largest amount of reinforcement, wall 15, was comparable with that of wall 13, (no reinforcement) indicating that the provision of tensile reinforcement of the type and quantity used does not affect the strain distribution.

Directly beneath the load the horizontal strains are compressive, and relatively large in magnitude compared with the tear strains along the free surface, except in the case of an edge loading, when high tear strains are noted. These compressive strains are however of relatively little importance in the consideration of the design of the brickwork element.

iii. Conclusions from the Strain Distributions.

A comparison of the splitting and tear tensile strains leads to the following conclusions.

a) When the bearing plate is positioned at the section edge then the tear tensile strain is greater than the corresponding splitting strain by a factor which may be as large as 10 : 1 (Wall 13). The results presented in Figs. 3-28 and 3-29 for Wall 15 indicate a ratio of 5 : 1.

b) As the $2d/a$ ratio is increased then the ratio tear tensile strain/splitting strain decreases, and may be as low as $1/3$ for central bearing plates.

c) Below the load there is a zone of horizontal compressive strain, which is consistent with the concept of a wedge of material, below the bearing plate, being driven into the brickwork. Meyerhof⁽³⁰⁾ proposed this concept, and carried out work on the bearing capacity of rock. As expected from his work splitting strains exist beneath the zone of local compression, and also tear tensile strains on the free horizontal edge, outside the zone of compression. Meyerhof indicated that the maximum horizontal splitting strain occurred at the base of the wedge, and recorded splitting strains have a maximum value in

this region.

d) The provision of reinforcement to increase the resistance of the brickwork to the horizontal forces set up would depend on the area of application of the concentrated force. Reinforcement would be most useful for loading cases where the load is applied at the edge of the section. The reinforcement should be placed to resist the tear tensile force, near the inner edge of the bearing plate.

All the tests carried out, on full-scale, 1/6th scale and 1/3rd. scale walls have indicated that the end bearing condition always leads to failure at stresses which are lower than for any other loading condition.

e) When the load is centrally applied the splitting and tear tensile strains are comparable, and general reinforcement in the area of the load concentration and for some distance on either side of it should increase the strength of the unit if the amount provided is greater than that used in the tests described above.

The maximum amount of reinforcement provided in the tests was only 0.08% of the vertical cross-sectional area of the wall, and was positioned in such a way that it was not necessarily 100% effective. Reinforcement of say 3% of the area should produce increases in strength.

f) The horizontal strains measured gave a good indication of when and where the initial cracking was going to occur. When the initial cracking stress is approached the strain starts to increase rapidly, as cracks start to form, and the vertical joints open as the brick to

mortar bond deteriorates.

3.6 A COMPARISON OF THE RESULTS WITH PHOTO-ELASTIC TESTS.

The tests of Hiltcher and Florin⁽³⁸⁾ on an ideal isotropic, homogeneous medium gave results which qualitatively agree with the results obtained from the strain readings on the brick walls. Their results are shown in Figs. 2-24 to 2-28.

The form of strain distribution is similar as is its variation with the bearing plate position.

Quantitatively the results are at variance, and indeed the results for the brick walls vary considerably.

Table 3-6 gives the ratio of the tear tensile strain/splitting tensile strain for both the photo-elastic tests and the brick wall tests, for various bearing plate positions.

Table 3-6

Ratio of Tear Tensile Strain/Splitting Tensile Strain.

Position of Load	Photo-Elastic ($h/b = 1 ; b/a = 10$)	Brickwork ($h/b = 0.89 ; b/a = 6$)
End Bearing	8 : 1	(10 - 5) : 1
Intermediate	2.24 : 1 ; $\left\{ \frac{2d}{a} = 3 \right\}$	(4 - 1.5) : 1 ; $\left(\frac{2d}{a} = 2.55 \right)$
Central	1.67 : 1	(.65 - .2) : 1

The discrepancy between the tests conducted is particularly noticeable when the load is centrally applied. The strain ratios measured are less than those expected from the photo-elastic tests.

The strain measurements indicate that the splitting tensile strains vary only slightly for the different load positions considered,

and the photo-elastic tests confirm this result. The ratio between the maximum and minimum splitting tensile strains was 3.0 for the brickwork compared with 2.5 for the photo-elastic tests.

The tear tensile strains were found to vary considerably for different load positions, the maximum to minimum ratio being (12-20) : 1 for the brickwork tests, compared with 11: 1 for the photo-elastic tests.

3.7 CONCLUSIONS.

- i. The effect of reinforcement has not been determined. A series of tests with larger percentages of reinforcement is required.
- ii. The vertical strain distribution varies only when the bearing plate approaches the edge of the wall.
- iii. The form of the horizontal strain distribution may be predicted by photo-elastic tests. Two main types of tensile strains exist, splitting and tearing strains.
- iv. The variation in the magnitude of the strains, when the load position is varied is similar for brickwork and photo-elastic tests, although the strains for different walls varied considerably.
- v. The magnitude of the horizontal stresses in the brickwork have not been calculated, as the nature of the behaviour of brickwork subject to tensile stress is not known. Hence although it seems likely that the photo-elastic tests predict the stresses in brickwork further investigation is required if reinforcement is to be designed for the tensile stresses in brickwork.

Table 3-1

Physical Properties of Bricks

Crushing strength lbf/ins ²	6675
Range	5,270 - 8,040
Standard Deviation	393
Coefficient of Variation	13.4%

Table 3-2

Sieve Analysis (B.S. 1200: 1955) of Local Sand

B.S. Sieve No.	Sieve Size (mm)	% on Sieve	% Passing Sieve
$\frac{1}{8}$ "	3.180	0.85	99.2
7	2.411	0.43	98.7
14	1.204	1.25	97.5
25	0.599	4.33	93.2
52	0.295	45.6	47.5
100	0.152	37.2	10.3
200	0.076	0.48	3.1

Table 3-3

Brickwork Cube Tests

Brick Cube No.	Cube Description	pf. si. Failure Stress
1	4 courses	2,580
2	"	3,140
3	"	2,990
4	3 courses	3,710
5	"	3,720
6	"	2,510
7	"	3,570
8	"	2,760

Table 3-5

Reinforced Pier Tests

Pier No.	Description	Load Position	Failure Stress pf. s. i.
9	Reinf. every course	Central 9" B.P.	2,720
10	" " 2nd "	9" End B.P. End 1	1,850
10	" " " "	9" " " " 2	2,080
11	" " 3rd "	9" " " " 1	2,270
11	" " " "	9" " " " 2	2,570
12	" top 3 courses	9" " " " 1	2,440
12	" " " "	9" " " " 2	2,780

PIER TESTS

Tests on Walls No. 1 - 8								
Wall No.	Size of Bearing Plate (ins.)	Load at failure (ton f.)	Failure stress (pf. s. i.)	End Tested (1st or 2nd)	Wall strength/ Brick strength	Permissible Bearing Stress C.P. 111 1964		Safety Factors
						Reduced for full area	Reduced for Bearing Plate Area	
4	9" x 8.5"	94.8	2930	1st	.439	607 pf. si.	545 pf. s. i.	4.8 - 5.4
7	9" x 8.5"	89.8	2630	1st	.394	" "	" "	4.3 - 4.8
6	9" x 8.5"	94.2	2760	2nd	.414	" "	545 "	4.5 - 5.1
3	9" x 8.5"	87.3	2560	2nd	.398	" "	" "	4.2 - 4.7
2	7" x 8.5"	80.4	3027	1st	.453	" "	538 "	5.0 - 5.6
8	7" x 8.5"	81.3	3060	1st	.458	" "	" "	5.1 - 5.7
8	7" x 8.5"	76.8	2900	2nd	.434	" "	" "	4.8 - 5.4
2	7" x 8.5"	57.8	2165	2nd	.325	" "	" "	3.6 - 4.0
1	6" x 8.5"	56.8	2490	1st	.373	" "	535 "	4.1 - 4.6
5	6" x 8.5"	73.7	3240	1st	.485	" "	" "	5.3 - 6.0
1	6" x 8.5"	50	2195	2nd	.329	" "	" "	3.6 - 4.1
5	6" x 8.5"	56.2	2470	2nd	.370	" "	" "	4.1 - 4.6
3	4.5" x 8.5"	47.2	2764	1st	.414	" "	531 "	4.5 - 5.2
6	4.5" x 8.5"	58.4	3420	1st	.512	" "	" "	5.6 - 6.4
7	4.5" x 8.5"	51.2	3000	2nd	.450	" "	" "	4.9 - 5.6

TABLE 3-4

CHAPTER 4.

MODEL WORK

1. A REVIEW OF PREVIOUS INVESTIGATIONS OF THE MODEL
TECHNIQUE APPLIED TO LOAD BEARING BRICK STRUCTURES.

1.1 INTRODUCTION.

The use of a model technique for brickwork has several advantages, which may be summarised under one heading, economic. It is possible to envisage testing full-scale brickwork units and structures of any size, and indeed it may be desirable in many cases to do so, to enable the validity of the model technique to be established. However the cost of the construction of the full-scale elements, and more important that of the equipment to test them, is often prohibitive.

The model technique enables a large number of specimens to be constructed at the same time, under controlled conditions, and stored, until required for testing. Alternatively a large structure may be built up from smaller units. Such a structure may be tested, using test rigs of a simple construction, together with jacks, load cells and dead weight. The load capacity required is greatly reduced from that required for the full-scale tests.

Before the model technique for brickwork was established a considerable amount of testing was required to ensure that the model materials and methods of construction evolved gave results which correlated with the same tests carried out on full-scale brickwork.

1.2 BENJAMIN AND WILLIAMS.

Benjamin and Williams (47) investigated the scale effect

involved when using model brickwork. The bricks used for the construction of the models tested were however merely full-scale bricks orientated to give different wall thicknesses.

The joints used were the same thickness, regardless of the scale of the model.

Results showed a wide scatter, but it was concluded that scale factors had little effect on the results.

Further tests were conducted cutting the full-scale bricks to obtain different scale factors. Results obtained were similar to those from the tests with uncut bricks.

The tests outlined above were conducted to investigate scale effects for infilled brick panels in reinforced concrete frames and hence for other conditions of loading scale effects might be more important.

1.3 VOGT.

Vogt ⁽⁹⁾ carried out a series of test (1957-58) to investigate the use of model bricks for the construction of specimens for basic brickwork tests.

Bricks of 1/10th scale were used to construct piers 6 cms. x 6 cms. x 30 cms. high. The joints were made of mortars of different strengths, and in one group of tests strips of cardboard were used. This latter group gave high ultimate strengths, and demonstrated the importance of the tensile strength of the joint material.

Vogt had difficulty in obtaining model bricks with a high standard of dimensional accuracy, and experimental results produced a wide scatter. The possibility of using a model technique for brickwork

testing was however clearly demonstrated.

1.4 MURTHY.

Murthy ⁽⁴⁸⁾ investigated several of the variables of brickwork construction, using $1/6$ th and $1/3$ rd scale model bricks which were specially manufactured by the British Ceramic Research Association (B.C.R.A.), and were dimensionally uniform to a high degree.

The tests were conducted to reproduce work carried out at the Building Research Station, (B.R.S.).

The mortar strengths, slenderness ratios and eccentricities of loading of brickwork piers were varied, the models being constructed with scaled down mortar joints. One inch and 2.78" mortar cubes were cast as control specimens for the batches of mortar used.

A further test series, using models constructed from $1/6$ th scale bricks, repeated the tests of Prasan ⁽⁴⁹⁾ on $4\frac{1}{2}$ " thick storey height walls.

The tests led to certain conclusions about the brickwork properties and the scale effects, and these are summarised below.

- i. The results for $1/6$ th, $1/3$ rd and full-scale tests were similar when the non-dimensional factors Brickwork Strength/Brick Strength and Mortar Strength/Brick Strength were plotted against each other. The brickwork strength increased with increasing mortar strength. The useful limit of mortar strength was not clearly indicated, but probably occurred at a Mortar/Brick strength ratio of approximately 0.5. The practical limit of Brickwork/Brick strength was found to be 0.4 - 0.5.

ii. Although the results followed the same general trend indicated in i. above it was found that the failure stresses of model brickwork were higher than those of full-scale brickwork. The joint size had been scaled down, and all other factors were the same.

It is possible that a higher degree of joint filling was achieved in the models constructed than in the full-scale structures, and this could account for the higher failure stresses. Workmanship factors have been shown to affect the failure stresses by up to 40%.

iii. The failure stresses of 1" mortar cubes were found to be higher than those of 2.78" cubes, and the difference increased as the mortar strength increased, being a maximum of 25% for a 1 : 3 cement : sand mix, by volume.

Ideally to reproduce the strength of full-scale brickwork satisfactorily it is necessary to use a mortar in the model, the 1" cubes of which have the same mortar strength as the 2.78" cubes made from the mortar used in the full-scale structure.

iv. Using the relationship established by Davey and Thomas ⁽³⁾ for the effect of brick strength on brickwork pier strength, the results of Prasan's tests have been compared with those of Murthy. The predicted results for Murthy's tests were found to be in good agreement with those obtained experimentally.

The strength of full-scale brickwork may therefore be predicted by testing models constructed from bricks of the same compressive strength.

v. The effect of slenderness ratio and eccentricity of loading on

the failure stresses of the piers was found to be the same for full-scale, 1/3rd scale and 1/6th scale brickwork.

vi. From strain measurements, obtained using an 8" Demec gauge, and from deflection readings taken using dial gauges, Murthy concluded that it would be difficult to assess the deformations and deflections of full-scale structures from model tests. The main reasons behind this conclusion were the wide variation in the elastic modulus, and the type of deflection profile obtained, when the same materials and type of construction were used.

Theoretically if the elastic properties of the model brick and mortar used are the same as those of the full-scale brick and mortar then the elastic properties of the brickwork constructed (model and full-scale) should be identical.

The elastic properties of brick, mortar and brickwork have not yet been fully investigated, although Hast (6) has conducted several experiments to determine certain elastic properties. (Chapter 1)

vii. The modes of failure of the full-scale and model piers and walls were the same, and generally took the form of vertical splitting. However, in some cases splitting was accompanied by crushing, and higher failure stresses were noted.

The general conclusion reached was that the use of model brickwork provided a satisfactory method of assessing the strength of full-scale brickwork.

Further tests were conducted on bond shear, bond tension, the effect of precompression, and the strength of single and multi-storey

(3) structures subject to shear forces. The results, whilst providing useful information as to the mode of behaviour of brickwork structures, were not compared with any full-scale tests.

1.5 SINHA.

Sinha (46) carried out several series of experimental tests, using 1/6th scale bricks of the same type used by Murthy.

The influence of the moisture content of the brick before laying, and the compression placed on a brick couplet during curing, were investigated, from the point of view of bond tension and shear.

The effect of different types of wall bond on the compression strength of wall elements was checked, and found to be negligible.

The main investigation was concerned with the effect of horizontal and vertical forces acting on brick cross-wall structures. In these structures systems of walls are used to resist the wind forces, by virtue of their shear strength. This system requires two sets of walls, built at approximately rightangles, to resist any direction of wind loading, the horizontal loads being transmitted from one wall to the next by the action of the reinforced concrete floor slab.

Sinha realised that although the testing of isolated wall panels provided useful information concerning their shear strength, the only way to find out how an actual structure behaved, when made up of a series of walls, with openings simulating doors etc., and interconnected by reinforced concrete slabs, was by testing such a structure. In this type of structure the floors, shear walls, cross-walls, and the roof slab act compositely, giving a very complex form of behaviour.

Several single storey structures, subject to precompression, were investigated, and also one five storey structure.

From the tests conducted Sinha concluded that for brickwork structures subject to horizontal and vertical forces the failures occurring could be divided into two distinct types.

- i. A shear failure at the brick mortar face, governed by the initial bond strength and the frictional resistance due to precompressive force.
- ii. Cracking through the brick and mortar, governed by the maximum tensile stress occurring.

A formula for the failure stress was proposed which gave results similar to those obtained by experiment.

The shear strength of the structures tested was found to increase when the precompression was increased, due to increased frictional resistance, and the suppression of diagonal tensile stresses.

The test results agreed with full-scale tests on brick couplets and individual walls, and hence it was judged to be suitable to use model tests for this type of structure.

1.6 GENERAL CONCLUSIONS.

The model technique has been shown to be valid for brickwork units of various types, including two brick couplets, small brickwork piers, and walls of a single leaf, or double leaf bonded type.

Work is at present in hand to extend the range of full scale tests to multi-storey shear wall structures, which have been tested in model brickwork.

From the results already obtained it is reasonable to assume that model brickwork may be utilised to investigate stress concentrations. Full-scale tests will also be performed to validate this assumption.

2. THE SCOPE OF THE MODEL INVESTIGATION UNDERTAKEN.

2.1 THE BASIC AIMS.

A section of the model investigations carried out has repeated the full-scale tests (Chapter 3), increasing the number of the specimens tested and extending the range of bearing plate sizes investigated. The aim of the tests was as before, to investigate the effect of the bearing plate length on the failure stress.

The model tests outlined above were also extended to cover the case of centrally loaded piers, loaded through bearing plates of various lengths, and piers loaded through bearing plates positioned at various distances from their edges.

The elastic properties of the materials used and the brickwork constructed have been investigated.

The distribution of strain under a load concentration was investigated for central and end bearing load conditions.

A series of tests was conducted to investigate the strength and elastic properties of brickwork cubes.

Two series of tests were carried out on model cavity walls. The aim of the tests was to determine the load distribution in a cavity wall subject to a load concentration. The walls were subject to either concentric loadings, of different types, or loadings which were eccentric about either one or both axes of the walls. In the second

series of tests special attention was paid to ascertaining the distribution of load between the two leaves of the cavity wall, and the stress conditions in each leaf.

The model investigations may be divided into two distinct sections. One is concerned with the strength properties of brickwork subject to a stress concentration, the size of the loaded area, and its position being of considerable importance. The other is concerned with the distribution of strains in the loaded sections, and the mode of transfer of load from the point of application to other parts of the structure.

A summary of the test programme conducted is given below.

2.2 MATERIALS USED.

The investigation has been carried out using $1/6$ th and $1/3$ rd scale model bricks, of a high dimensional accuracy and of the same type as those used by Murthy⁽⁴⁸⁾ and Sinha⁽⁴⁶⁾.

The mortar used throughout was a 1 : 3 by volume, cement:sand mix, and the mortar joints were scaled down $3/8$ " joints. 1" mortar cubes were cast as control specimens throughout.

The sand used was Leighton Buzzard No.21.

2.3 THE PHYSICAL AND STRUCTURAL PROPERTIES OF THE BRICKS AND MORTAR.

The compressive strength and water absorption of the brick were determined.

The 1" mortar cubes were tested for compressive strength.

2.4 THE ELASTIC PROPERTIES OF THE BRICKS AND MORTAR.

The elastic moduli of the bricks and mortar used were

determined.

2.5 THE ELASTIC PROPERTIES OF THE BRICKWORK.

The elastic moduli of the types of brickwork constructed were determined from wall tests.

2.6 THE STRENGTH AND ELASTIC PROPERTIES OF BRICKWORK CUBES.

Brickwork cubes of three and four courses were constructed from $1/3$ rd scale bricks and were tested for compressive strength. Strain measurements were also taken both vertically and horizontally on the cube faces.

2.7 FAILURE STRESSES UNDER CONCENTRATED LOAD.

The effect of the variation of the bearing plate length, on the failure stress, was investigated, for end and centrally loaded piers. $1/6$ th and $1/3$ rd scale models were tested.

2.8 THE STRAIN DISTRIBUTION UNDER CONCENTRATED LOAD.

In two $1/3$ rd scale walls the strain distribution was investigated, for end and centrally applied load.

2.9 THE EFFECT OF EDGE DISTANCE.

The effect of the variation of the edge distance of the bearing plate on the failure stress of $1/3$ rd scale piers was investigated.

2.10 CAVITY WALL TESTS.

Two series of loading tests were carried out on $1/3$ rd scale cavity walls of storey height.

i. The strain distribution was measured, when the load was applied with varying eccentricity in a number of ways. Strain readings were taken on the external faces of both leaves.

ii. The investigation was carried out as indicated in **i.** above, but particular attention was paid to the strain distribution across the two leaves.

Lateral deflection measurements were taken in several tests.

CHAPTER 5.

THE PHYSICAL, STRUCTURAL AND ELASTIC PROPERTIES
OF THE MATERIALS USED FOR MODEL TESTS.

1. THE PHYSICAL AND STRUCTURAL PROPERTIES OF THE BRICKS,
SAND AND MORTAR.

1.1 BRICKS.

The three types of model bricks used, one $1/6$ th scale and two $1/3$ rd scale, were extruded wire cut types. The $1/6$ th scale bricks were extruded in a direction perpendicular to their length, whilst the $1/3$ rd scale bricks were extruded along their length.

Two types of $1/3$ rd. scale bricks were used. Type I, used for the construction of models for concentrated loading tests, and Type II, used to construct brickwork cubes, and for the construction of cavity wall models.

The two types of $1/3$ rd scale bricks differed in several ways, apart from their different compressive strengths. Type I was extruded, with rounded corners, making the measurement of the exact brick dimensions awkward. Type II extruded through a second die had well defined sharp corners.

Type I bricks were difficult to cut in half, and frequently broke in a manner other than intended. It was noticed, on cutting, that the interior of the bricks seemed to contain an elliptical harder core, and commonly the small outside portions surrounding the brick core spalled away on cutting.

Type II bricks were easy to cut, and seemed homogeneous throughout.

On examination of the cut surfaces of bricks of Type I and Type II, many small stones were seen to be incorporated into the clay matrix of both bricks.

Standard tests on the $1/6$ th and $1/3$ rd scale bricks were performed in the manner specified in B.S. 1257 : 1945 (40) - now amended to B.S. 3921 : 1965.

Two basic tests were conducted, water absorption and compressive strength and the results are presented in Table 5-1. The absorption test chosen was a 24 hour immersion test.

For the tests 12 random samples of the brick were chosen, as suggested in the specification, and the average results are presented, together with the coefficients of variation, and the standard deviations.

Average dimensions have also been given to the nearest 0.05".

Compressive tests were also carried out on bricks which had a moisture content determined by the conditions prevailing in the laboratory. Basically these bricks were dry, having a low moisture content.

At this point it is relevant to say that having conducted the standard compressive strength test in the manner specified by B.S. 1257 : 1945, rather unexpected results were obtained when the brickwork cubes were crushed. The results indicated that the average brickwork cube strength was approximately the same as the brick strength. This result was immediately suspect, and tests were conducted on the bricks to determine if the brick compressive strength was radically affected by the moisture content.

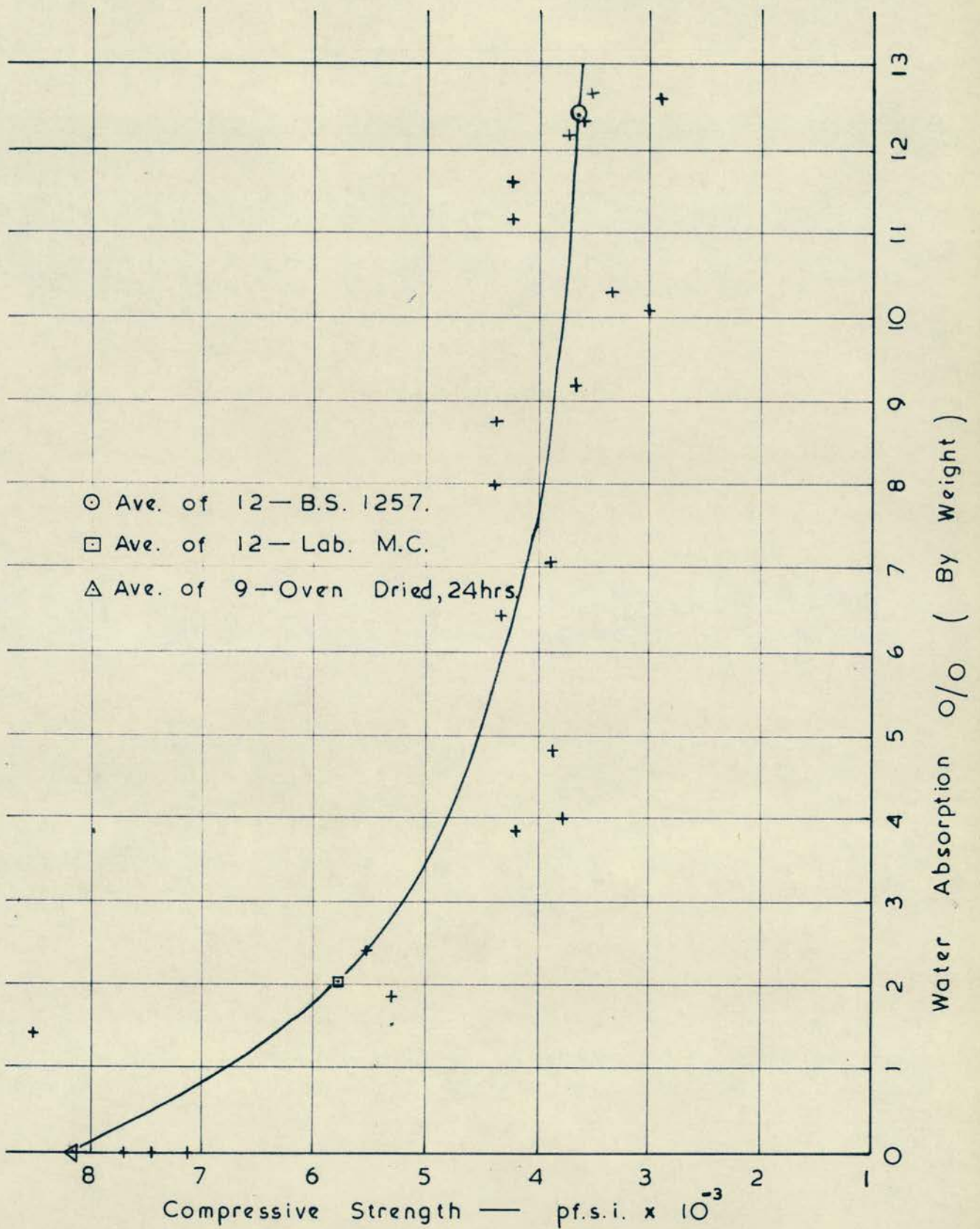
The dry compressive strength was found to be greater than the standard saturated compressive strength. For the $1/6$ th scale brick an increase of 16.5% was noted. For the $1/3$ rd scale Type I brick an increase of 2.3% was noted, and an increase of 60% for Type II.

An extensive series of tests revealed that there was a definite relation between the % water absorption of the $1/3$ rd scale Type II brick and the compressive strength. Fig. 5-1 shows the nature of the relationship. The compressive strength was found to be relatively constant in between a saturated condition and a water absorption of 4%. Below this figure the compressive strength increased rapidly, and approximately linearly, reaching a maximum value at a zero water absorption.

Therefore, where the model structures tested were in a dry condition it would seem relevant to take the dry compressive strength where there is a large difference between the dry and saturated results. Thus for the Type II $1/3$ rd scale bricks the brickwork cube strengths have been related to the dry brick strength. Similarly for the cavity wall tested.

No definite explanation can be offered for the discrepancy between the compressive strengths obtained from the two types of test. It is known that internal pore pressure in concrete cubes can lead to a reduction in the compressive strength of the cubes if moisture is prevented from leaving the sample. Such a condition resembles the undrained triaxial test.

The tests conducted as per B.S. 1257 were at the standard rate



The Relation Between Compressive Strength and Water Absorption

Fig. 5-1

of 2,000 pf. s. i. /minute which would allow some reduction in pore pressure as the test proceeds.

For the $1/6$ th scale bricks the increase in the compressive strength on drying could be explained by the undrained, or partially drained nature of the standard test. For the Type I $1/3$ rd scale bricks, the 2.3% increase, on drying could be explained on a purely statistical basis.

1.2 SAND.

The sand chosen was Leighton Buzzard No.21. The result of a sieve analysis is given in Table 5-2 and illustrated in Fig. 5-2. This sand has been previously used for model work ⁽⁴⁶⁾ and is known to be suitable.

1.3 MORTAR.

A 1:3 by volume, cement: sand mortar was used, corresponding to a 1:4 by weight mix. Rapid hardening Portland cement conforming to B.S. 12 ⁽⁴²⁾ was used.

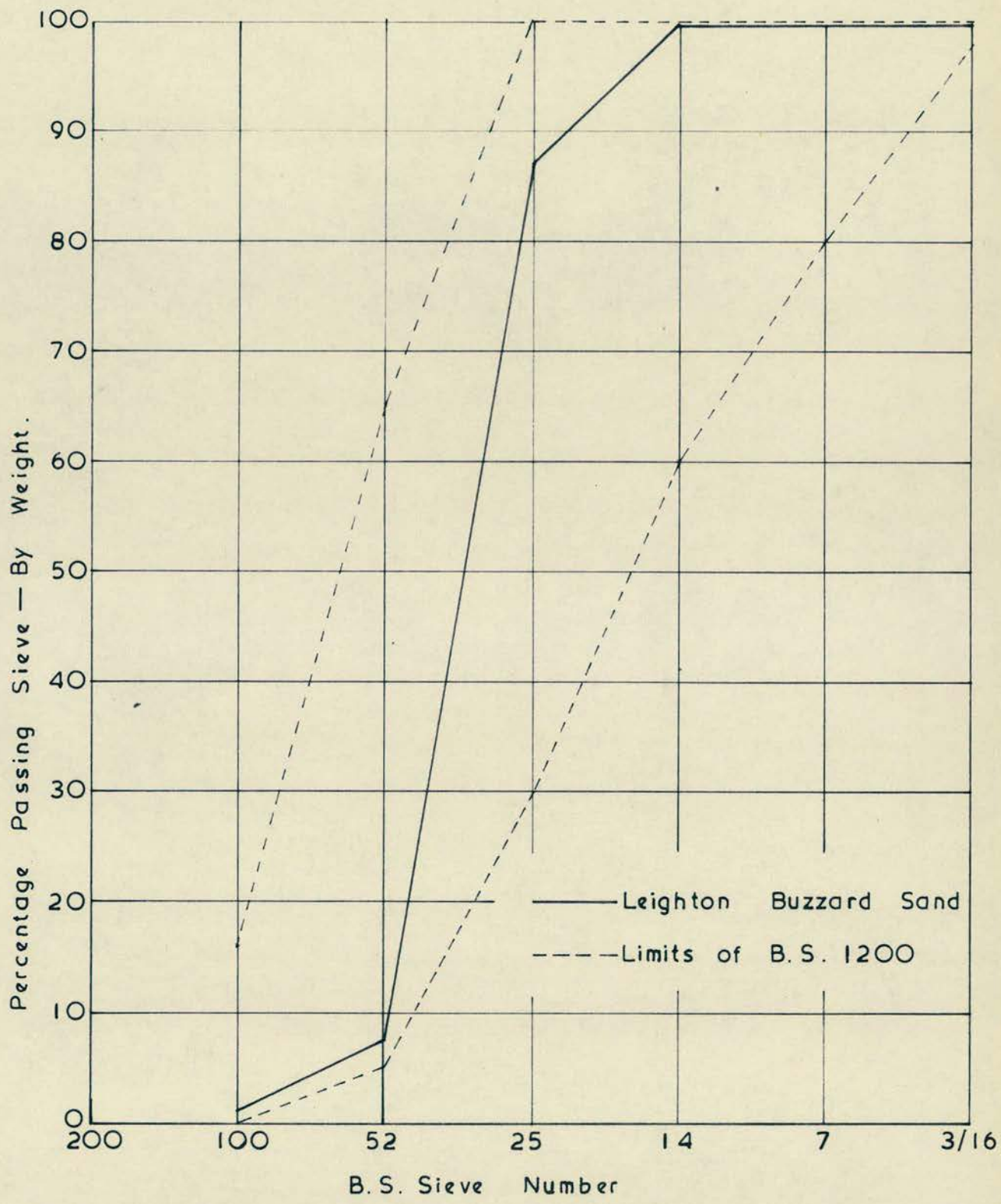
1" mortar cubes were cast from the mortar mixes, and stored under water, after initial curing under damp sacks, until required for testing with the corresponding models.

2. THE ELASTIC PROPERTIES OF THE BRICKS AND MORTAR.

2.1 BRICKS.

i. $1/6$ th Scale.

The elastic modulus of the $1/6$ th scale bricks was determined by Morsey, using an Instron testing machine, and was found to be 1.4×10^6 pf. s. i.



Grading Curve for Leighton Buzzard Sand

Fig. 5-2

ii. $\frac{1}{3}$ rd Scale.

The modulus of elasticity of the $\frac{1}{3}$ rd scale bricks was determined using a 2" Deme c gauge, and taking one reading on the centre line of each face.

Type I - The average modulus of elasticity was found to be approximately 0.8×10^6 pf.s.i.

Five bricks were tested, between $\frac{1}{8}$ " plywood sheets, and Fig. 5-3 shows the average stress/average strain relationships for bricks 2, 3 and 4. Fig. 5-4 shows the results for brick No.1, plotted in greater detail. This illustrates the non-uniform load distribution on the four faces, at low applied load.

Type II - The average modulus of elasticity was found to be 0.7×10^6 pf.s.i. Five bricks were tested, between $\frac{1}{8}$ " plywood sheets, and the results are given in Fig. 5-5, which gives the average strains on the four faces.

Types I and II - For both types the modulus of elasticity was found to increase with increasing stress in the region 0 - 500 pf.s.i. (approximately). The modulus then stabilises, and remains fairly constant, with a slight tendency to decrease, over a large stress region, decreasing rapidly as failure is approached.

2.2 MORTAR.

The elastic properties of the 1 : 3 (by volume) mortar mix used were investigated by Sinha (46) by testing 1" mortar cubes in a Hounsfield tensometer, and an elastic modulus of 2.2×10^6 pf.s.i. was found.

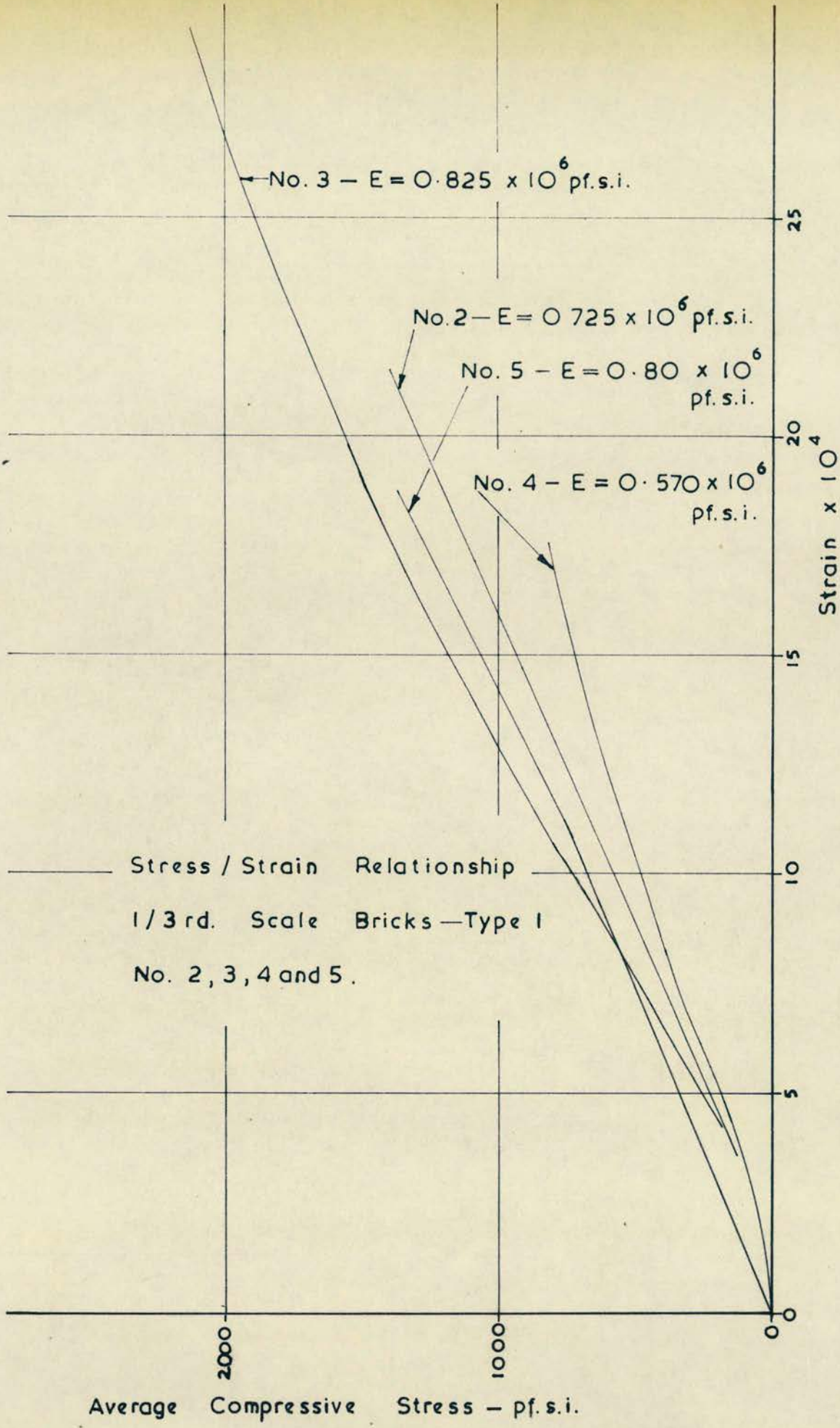


Fig. 5-3

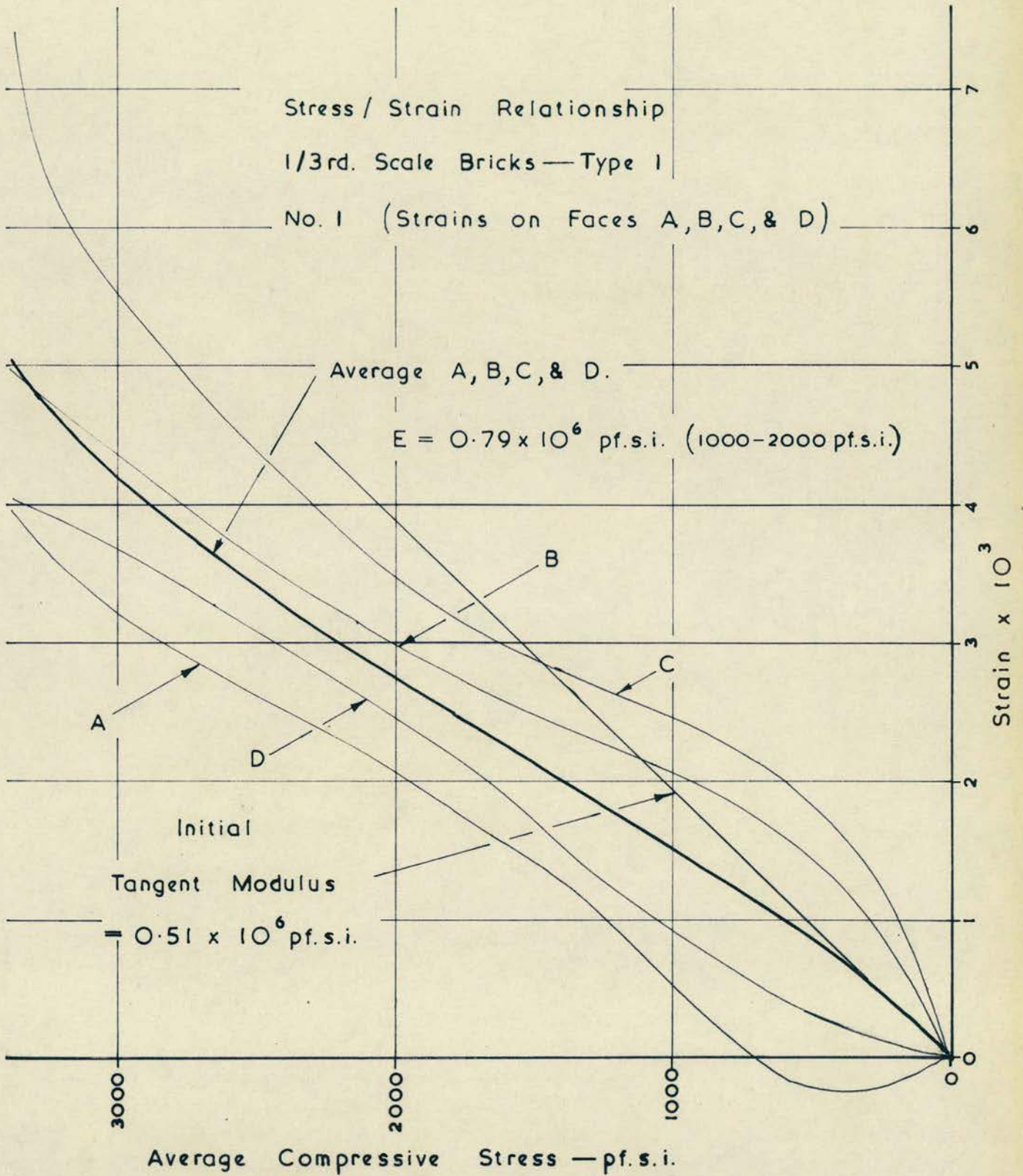


Fig. 5-4

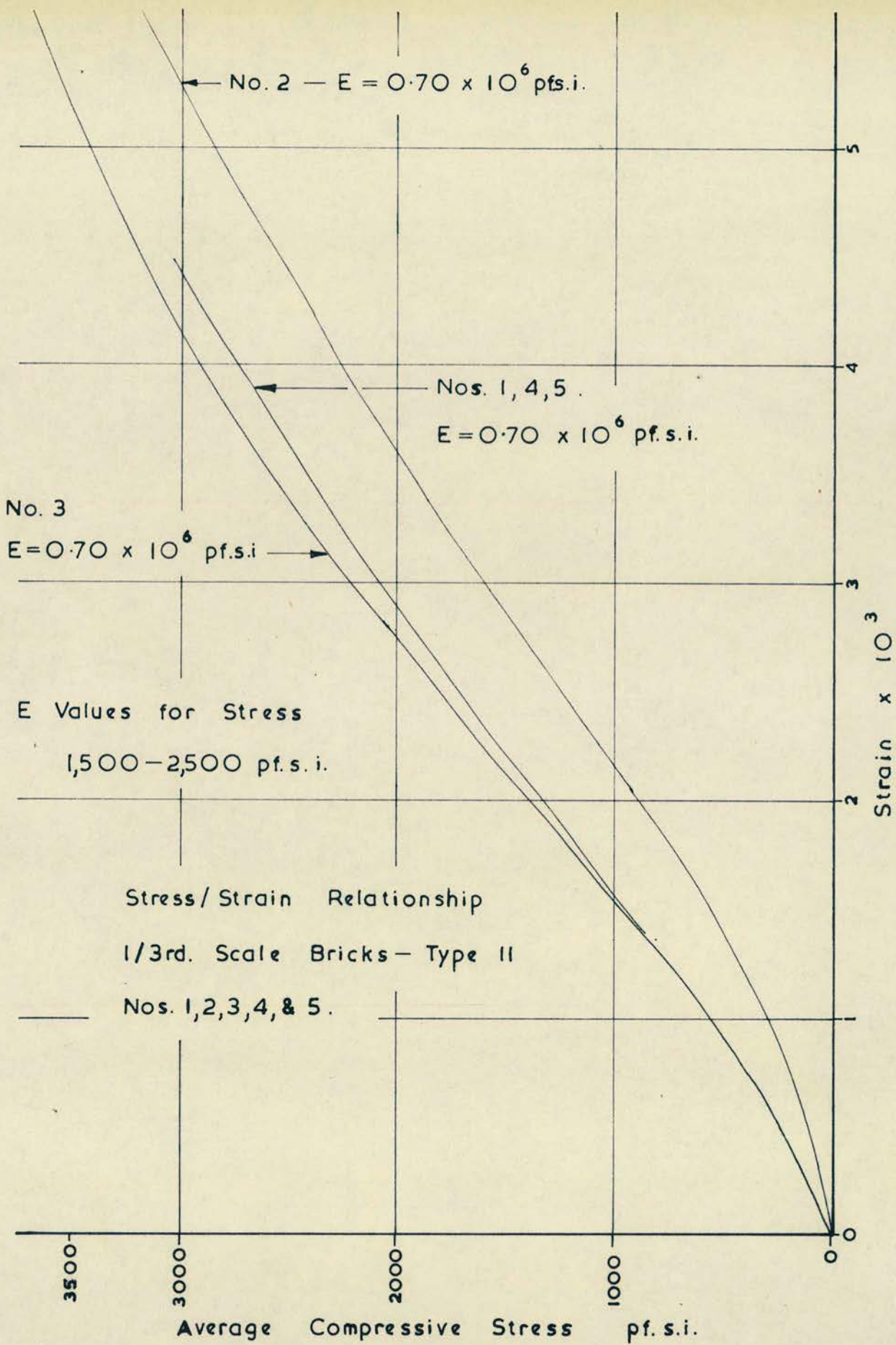


Fig. 5-5

3. THE ELASTIC PROPERTIES OF THE BRICKWORK.

3.1 1/6TH SCALE.

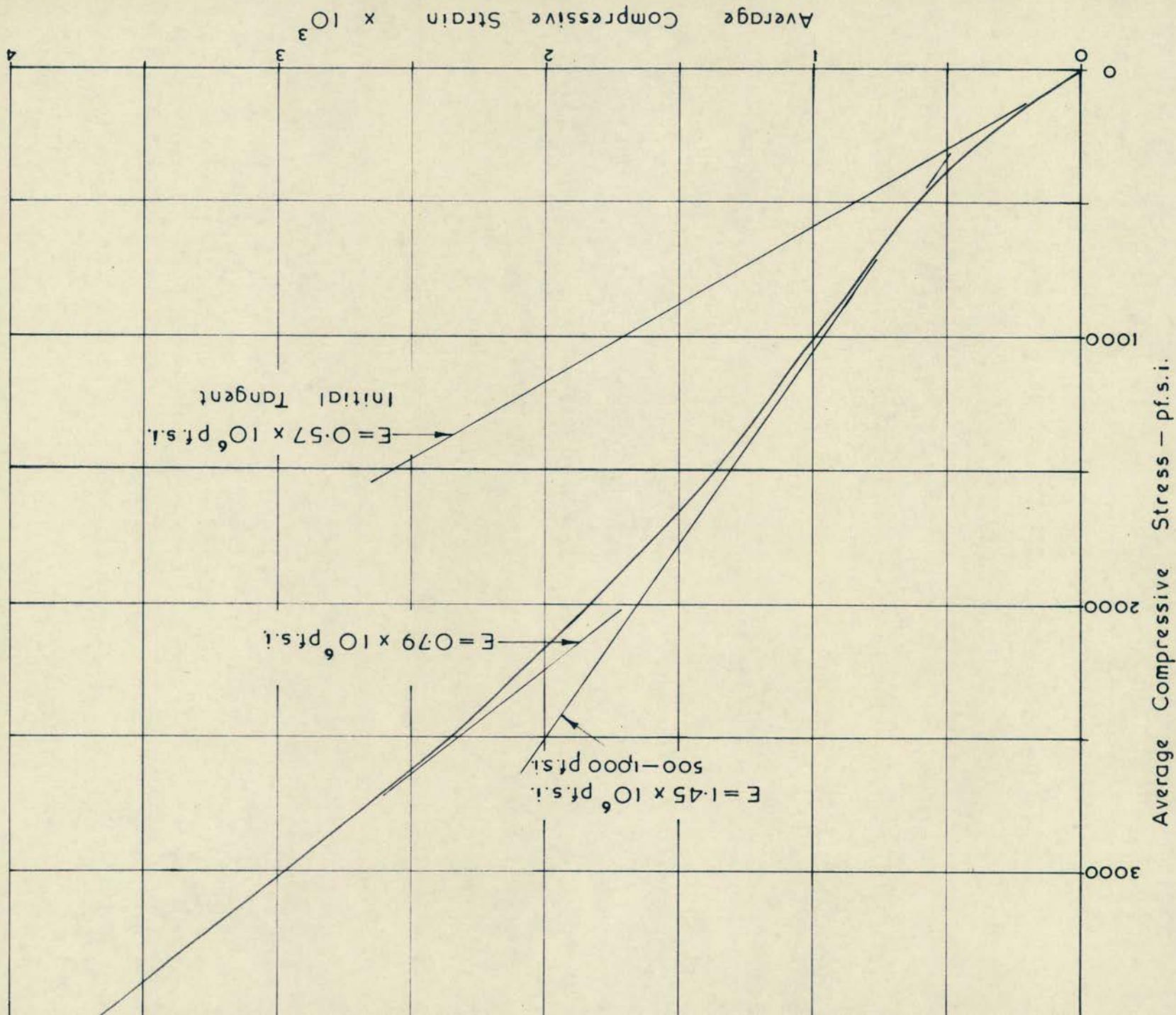
The modulus of elasticity of the 1/6th scale brickwork constructed was obtained from a direct compression test on a model wall, 4.6" long x 2.57" high x 0.69" thick, Strain readings were taken at 1" intervals across both faces, using a 2" Demec gauge, and the average stress/average strain relationship is shown in Fig. 5-6.

The modulus of elasticity varied considerably with the applied stress. The initial tangent modulus was approximately 0.6×10^6 pf. s. i. The secant modulus increased from zero applied load, up to an applied stress of 1,800 pf. s. i., and then decreased until failure occurred at 5,095 pf. s. i. Values of the secant modulus have not been calculated, but the tangent modulus reached a maximum value of approximately 1.45×10^6 pf. s. i. at 500 pf. s. i. Above 1,100 pf. s. i. the tangent modulus decreased, reaching a value of 0.8×10^6 pf. s. i. in the zone of failure.

3.2 1/3RD SCALE - TYPE I BRICKS.

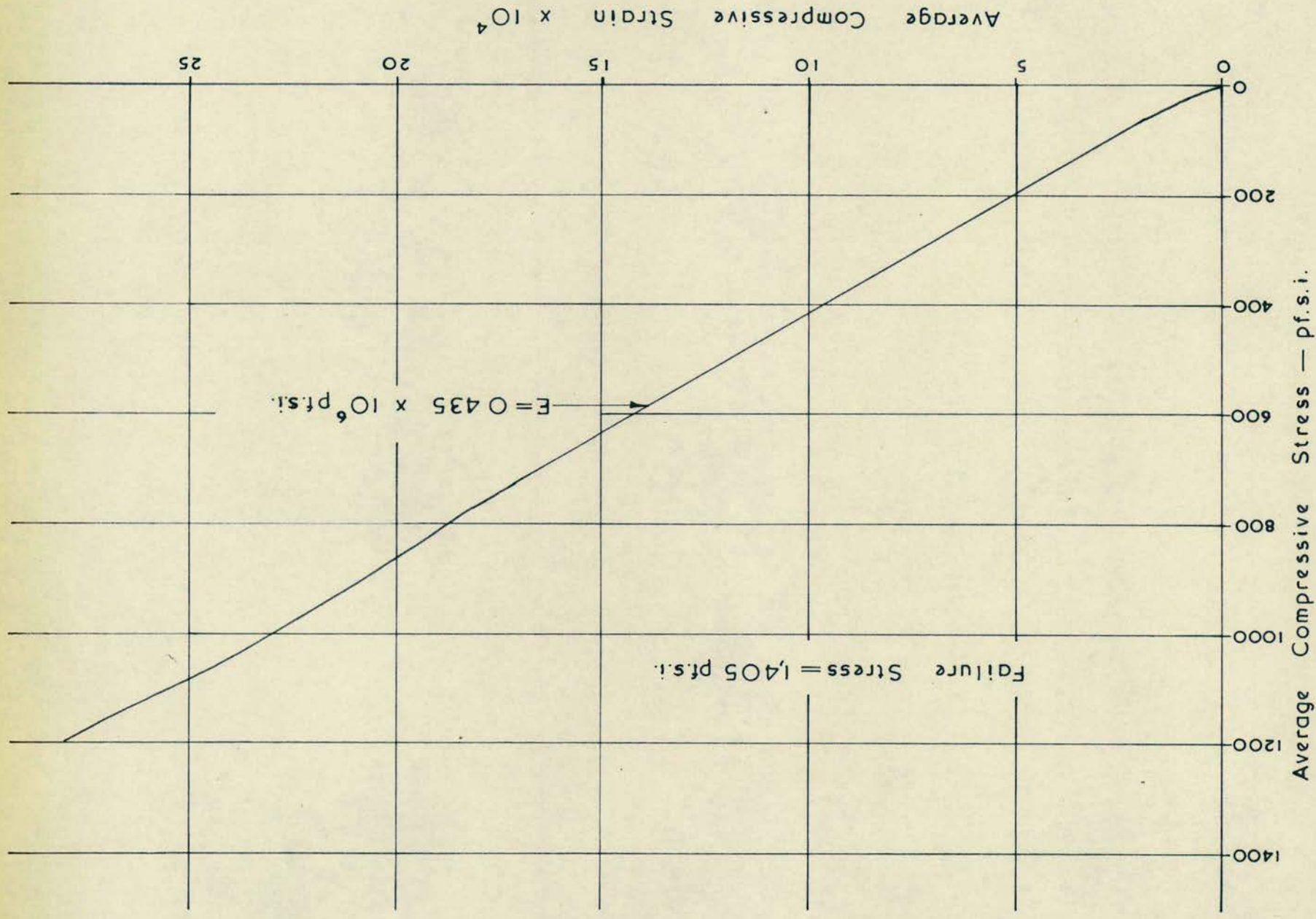
The modulus of elasticity of the brickwork was obtained from a direct compression test on a wall 11.4" long x 10" high x 1.47" thick. Demec readings were taken at 1" intervals across both faces, using an 8" Demec gauge, and the average stress/average strain relationship is presented in Fig. 5-7.

The "E" value obtained was 0.435×10^6 pf. s. i., and the stress/strain relationship was approximately linear, in a region from low stress to the failure zone.



Stress / Strain Relationship — 1/6 th. Scale Wall

Fig. 5-6



Stress / Strain Relationship — 1/3rd. Scale Wall — Type I Brick

Fig. 5-7

The wall failure stress was 1,405 pf.s.i., giving a brickwork/brick strength ratio of 0.482.

3.3 1/3RD SCALE - TYPE II BRICKS.

The modulus of elasticity has been obtained from the tests on the 1/3rd scale cavity walls constructed. Two tests on wall No.1, and one on wall No.2 have been considered.

The "E" value was found to be approximately 0.6×10^6 pf.s.i. at 270 pf.s.i.

4. MODEL BRICKWORK CUBES.

4.1 DISCUSSION OF THE BRICKWORK CUBE TEST.

If load bearing brickwork is to play an increasing role in the construction industry, then the necessity for control specimens is evident. These specimens must be easily constructed on site, by the bricklayer, and readily transported to the testing station.

For brickwork, the testing of samples of the brick chosen, to find if it satisfied the requirements of C.P.111 : 1964, is a definite prerequisite to construction. However, once construction has commenced, the checking of mortar samples is of little value, it being established that, above certain rather low values, the mortar strength does not greatly influence the brickwork strength. Factors such as the moisture content of the bricks, and the quality of workmanship of the bricklayer are of greater importance than the compressive strength of the mortar.

A more valuable type of test is one in which the bricks and mortar are combined in a similar way to which they are being used

in the construction, and the unit produced is then tested.

A suitable sort of unit to produce for testing is the brickwork cube, consisting of six bricks, built into a unit in alternate stretcher and header bond, to give three courses. Alternatively a four course assemblage of eight bricks has been proposed as suitable.

Recently considerable research has been carried out into the properties of brickwork cubes, (50, 51, 52, 53, 54, 55) and the conclusion was that they provided suitable control specimens for brickwork quality control.

A point of particular interest is the effect of the mortar joint-thickness on the brickwork cube compressive strength. Research has shown (43, 53) that the cube strength is inversely proportional to the mortar joint thickness, and hence the joint thickness in the control specimen should be the same as that being used for the brickwork on site. Results suggested that the joint thickness should be limited to $3/8$ ".

Results obtained for tests on different joint thickness are presented in Table 5-3.

Work has been carried out to determine the type of capping required for the brickwork cubes, in order to obtain consistent and representative results, for the strength of the complete structure.

Stedham (50, 51) has suggested constructing the three course cube with three mortar courses, whereas West (55) recommended only two mortar courses, with no capping.

Tests conducted indicated that crushing the cubes between either

$1/8$ " thick plywood sheets, or between $3/16$ " strawboard sheets give similar results. As plywood was thought to be rather variable in manufacture, strawboard was recommended.

Tests by Bradshaw correlated the brickwork cube strengths with the associated wall strengths. The walls constructed were 3' wide, 8' - 2" high, and nominally $4\frac{1}{2}$ " thick, and were tested in between reinforced concrete slabs. Three and four course brickwork cubes were constructed, generally making three of each for each wall. Results indicated that the four course cube gives lower crushing strengths, and is more representative of the brickwork strength. The ratio Wall strength/Three course cube strength ranged from 0.60 to 1.03, and the ratio Wall strength/Four course cube strength ranged from 0.68 to 1.15. The range of Wall strength/Brick strength exhibited a greater variation from 0.17 - 0.43, which is explained by fact that the brick strength does not depend in any way upon the mortar strength.

The conclusion of the research outlined above was that the brickwork cube could be suitably used as a control specimen for site brickwork.

4.2 ELASTIC PROPERTIES OF THE 9" BRICKWORK CUBE.

Lenczner (52) recently investigated the vertical and horizontal strain distributions in brickwork cubes, using an 8" Demec gauge.

Modulus of elasticity values were calculated for the cubes, and compared with those of the bricks and mortar used.

The Stress/Strain relationship was found to be non-linear. Large horizontal strains were measured on the stretcher bricks themselves,

and across vertical mortar joints.

4.3 THE SCOPE OF THE TEST PROGRAMME.

i. Specimens Constructed.

Twenty six brickwork cubes were constructed from Type II $1/3$ rd scale model bricks. Thirteen cubes were three courses high, and thirteen were four courses high.

Mortar joints were constructed $1/8$ " thick, and the mortar used was a 1:3 (by volume), cement : sand mix, using Portland rapid hardening cement, and Leighton Buzzard No.21 sand.

All the cubes had a plywood base, $1/8$ " thick, and an $1/8$ " base mortar course.

The cubes were constructed using timber jigs to maintain dimensional accuracy.

1 " mortar cubes were made from the mortar batches, and after curing for 24 hours under damp sacks, were stored under water until required.

ii. Compression Tests.

All the brickwork cubes constructed were tested in a rigid head Avery testing machine. The load was applied slowly, to allow complete observation of the cube behaviour. Thus the rate of loading was considerably slower than the suggested standard speed of 2,000 pf.s.i./min., each test taking up to 45 minutes.

An $1/8$ " plywood sheet was used to evenly distribute the load on the top faces of the cubes.

Where strain readings were being taken the load was held at the

level required while the strain readings were taken.

iii. Strain Measurements.

Vertical and horizontal strain measurements were made on the faces of five cubes. Three were of three courses, and two of four courses. These measurements were made using a 2" Demec gauge with a strain sensitivity of 2.48×10^{-5} per division. Vertical and horizontal readings were taken on all four faces of the cubes.

Readings were taken on the three course cubes from top to bottom, near the left and right hand corners, and in one case in a central position. Horizontal readings were taken on each course.

In the case of the four course cubes two Demec studs were placed on each course of bricks, and the corresponding readings were taken, giving two sets of vertical readings, first to third course, and second to fourth course. Four horizontal strains were measured.

4.4 TEST RESULTS AND OBSERVATIONS.

i. Compression Test Results.

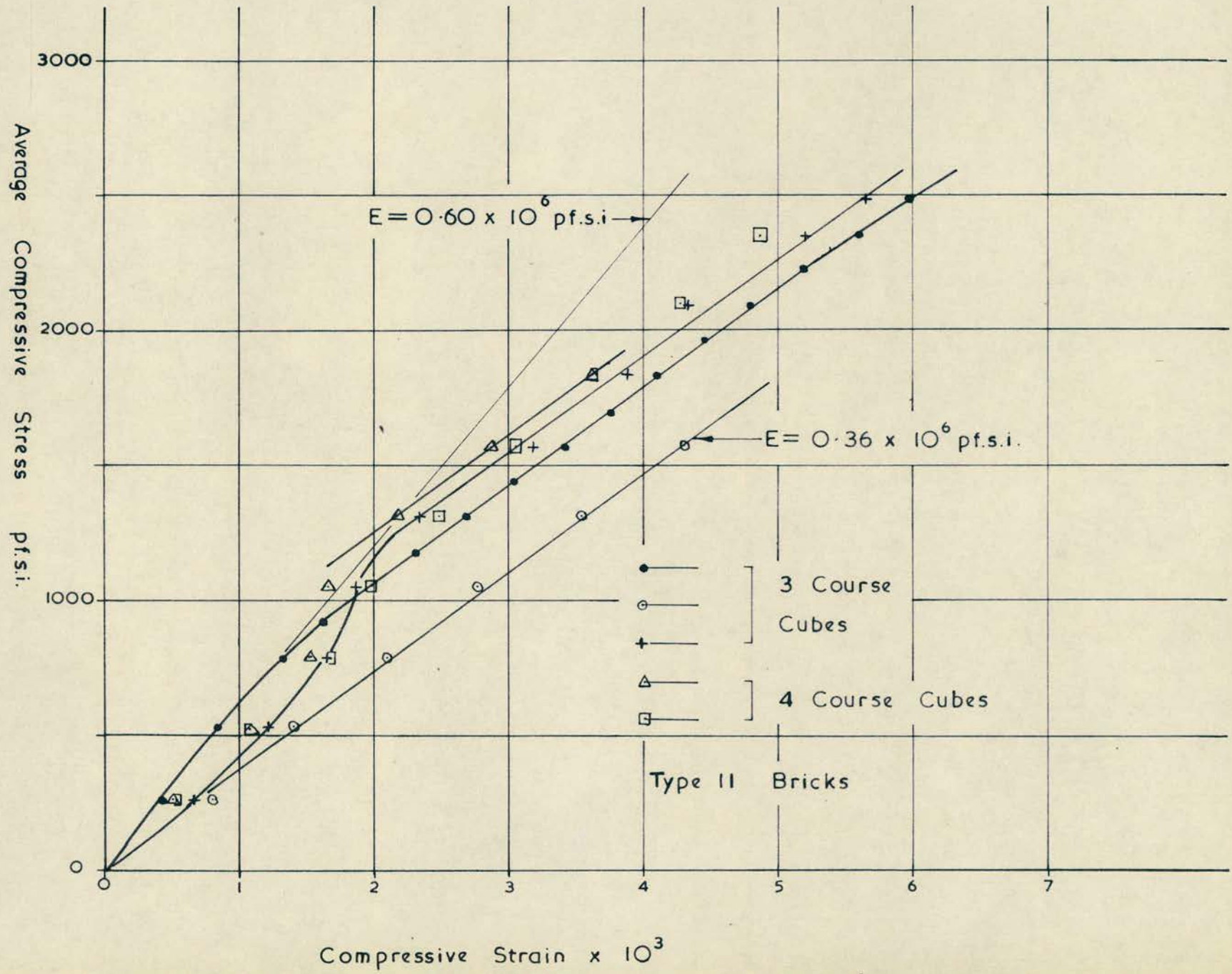
The results of the compression tests and other relevant information are given in Table 5-4.

ii. Strain Measurements.

The vertical Stress/Strain relationships for the five cubes tested with measurement are presented in Fig. 5-8. The strain values presented are the average of the readings taken on the four faces.

To illustrate the variation in the strain from one position to another on the cube, due to uneven load application or distribution Fig. 5-9 is presented, giving the individual strain readings taken on

Stress / Strain Relationship — 1 / 3rd. Scale Brickwork Cubes.
 Fig. 5-8



Compressive Strain—1/3rd. Scale Brickwork Cube Faces.

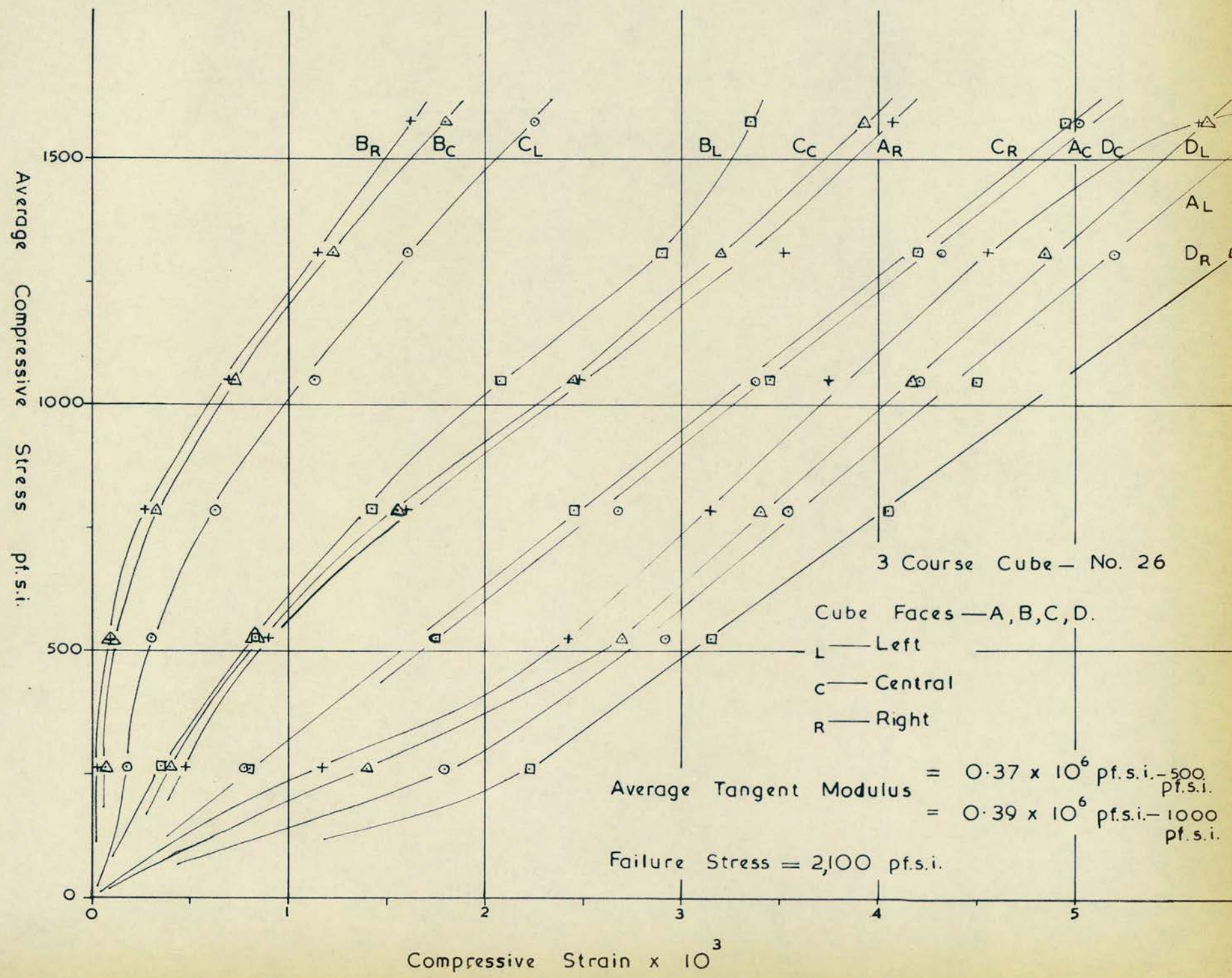


Fig. 5-9

one cube.

The results obtained for the five cubes are similar and the moduli of elasticity are also similar for all cubes, in the stress interval 1,000 - 2,500 pf.s.i., and a value of 0.35×10^6 pf.s.i. (approximately) was calculated, on a tangent basis. At the stress level 1,000 pf.s.i. vertical cracks have almost certainly occurred, and these cracks may explain the rather low moduli obtained.

The initial tangent moduli were the same or greater and ranged from 0.35 to 0.60×10^6 pf.s.i.

After initial cracking of the cubes had occurred the Stress/Strain relationship was reasonably linear, until the zone of failure was reached.

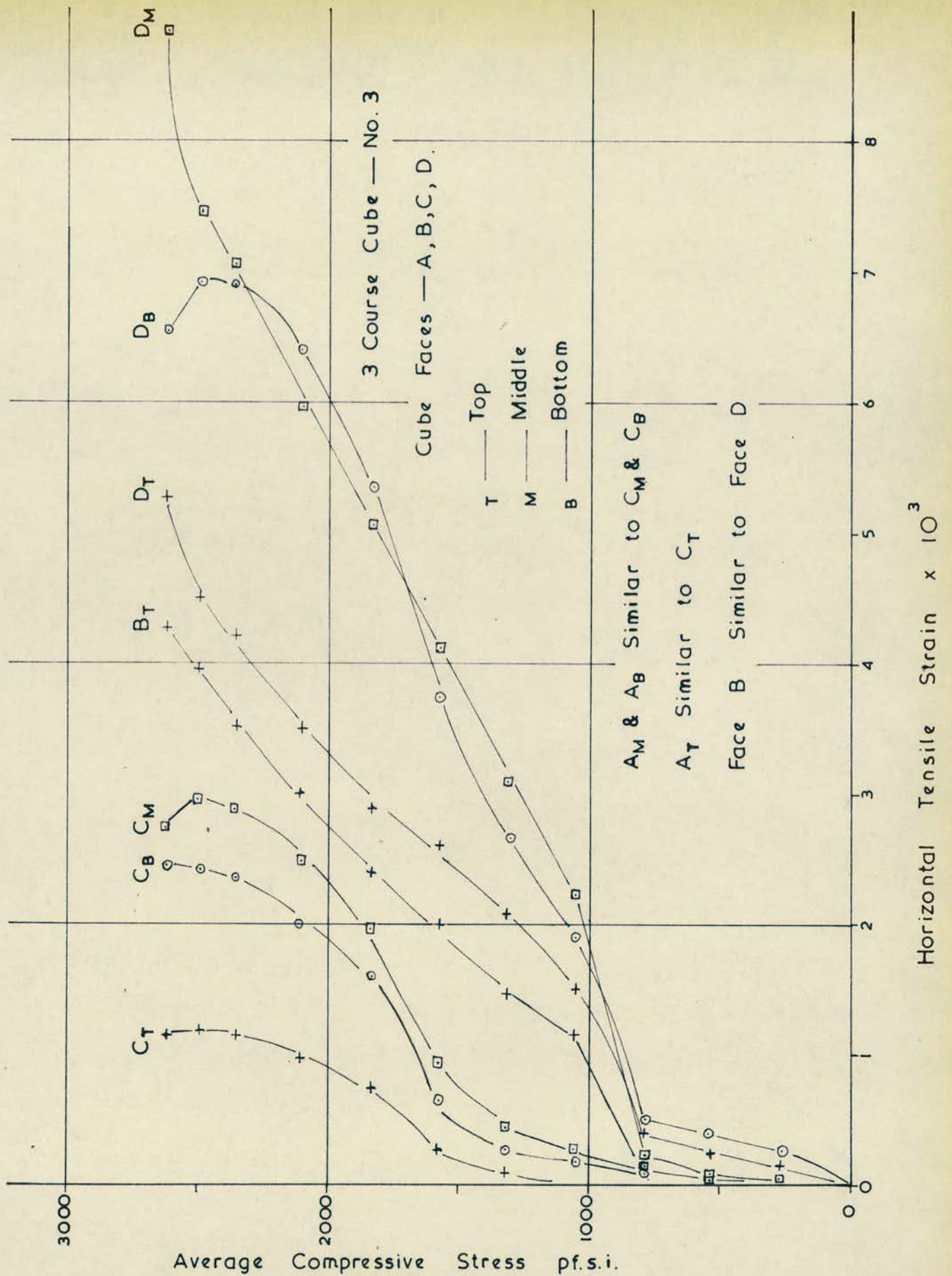
The Vertical stress (average)/Horizontal strain relationship for one cube is illustrated in Fig. 5-10. The relationships were initially linear in the low strain range, but the stress at which vertical splitting cracks occur was clearly denoted by a sharp increase in the strain, and the end of the linearity of the Stress/Strain relationship.

Opposite faces of the cubes show similar results, and it was observed that cracks generally occur simultaneously on opposite faces.

Similar results were obtained from the tests on the other four cubes, and in no case was the horizontal strain of any appreciable magnitude before vertical cracking occurred. This applied to strains measured on individual stretcher bricks, or across vertical joints.

iii. Mode of Failure.

The initial failure of the cubes was due to the formation of



Stress / Horizontal Strain Relationship — 1/3 rd. Scale Brickwork Cube

Fig. 5-10

vertical cracks, at fairly low stresses, (500 pf. s. i.), although in a few cases cracks were not visible until a high stress was reached. Where a high stress was reached without visible vertical cracking, the initial failure was apparent as spalling on the faces, and at the corners.

It appeared likely that the unevenness of initial loading caused the formation of vertical cracks at a low stress in some cases.

The final failure mode was the familiar shear failure which occurs with concrete cubes (Plate 5-1). For some loadings, where the load was unevenly distributed the failure was only partially of a shear type, the pyramid being formed on two or three sides only.

Plate 5-1 appears after page 95.

4.5

DISCUSSION OF RESULTS.

i. Compression Tests.

The average compressive strengths of the three and four course cubes were 2,640 pf. s. i. and 2,365 pf. s. i. respectively, having a ratio of 1.1 : 1.0.

The Brickwork/Brick strength ratios were 0.45 and 0.41 respectively, taking the dry compressive strength of the brick. The cubes were stored in the laboratory before testing, and were dry.

The range of cube compressive strength was 2,100 - 3,120 pf. s. i. for the three course cubes, and 1,975 - 2,640 pf. s. i. for the four course cubes. These ranges of values indicate that the brickwork cube is as suitable for brickwork as the concrete cube is for concrete strength, or the mortar cube for mortar strength, in so far as the variability of the results is concerned.

The coefficients of variation of the compressive strengths of the three and four course cubes are 10.3% and 11.5% respectively.

A further series of tests would be required to determine the suitability of the brickwork cube as a measure of the strength of piers or walls constructed of the same materials. However, it is likely that the range of wall strength is from 0.6 to 1.2 times that of the brickwork cube strength ⁽⁵³⁾, and hence a reasonable estimate of the minimum wall strength can be obtained.

ii. Strain Measurement.

The results obtained indicate that the elastic behaviour of a brickwork cube is somewhat different from that of a wall constructed as a complete unit.

The difficulty encountered in constructing a dimensionally exact cube may account for the variation in the behaviour, and it seems unlikely that the elastic properties need to be counted against the usefulness of the brickwork cube as a control specimen.

From the results obtained there is no evidence that bricks are capable of sustaining tensile strains of any magnitude, during the tensile straining of brickwork.

Table 5 - 1

Physical Properties of the Bricks Used.

Type of Brick	Dimensions ins.			Crushing Strength B.S. 1257 pf. s. i.	Dry Crushing Strength pf. s. i.	Standard Deviation (s)	Coefficient of Variation (%)	Standard Deviation (s)	Coeff. of Variation (%)	Water Absorption 24 hr. by Weight.
	L	B	D							
1/6th	1.45	0.69	0.47	6,520	7,595	766	11.76	763	10.05	11.9
1/6th	1.45	0.70	0.46	6,057	-	764	12.6	-	-	-
1/3rd Type I	2.77	1.45	1.0	2,912	2,980	309	10.6	315	10.6	-
1/3rd Type II	2.9	1.4	0.94	3,603	5,795	313	8.7	382	6.6	12.4
						B.S. 1257 Test.		Dry Test.		

Table 5 - 2

Sieve Analysis - Leighton Buzzard Sand.

B.S. Sieve Designation	3/16"	No. 7	No. 14	No. 25	No. 52	No. 100
Percentage Passing by Weight - Average of 3 Samples.	100	100	100	86.66	7.58	1.33

Table 5 - 3

The Effect of Mortar Joint Thickness on Brickwork Strength.

Joint Thickness (ins.)	Strength	Ratio
	Brickwork Cubes and Piers.	American Tests.
1/4	1.15	1.12
* 3/8	1.00	1.00
1/2	0.99	0.84
5/8	0.95	0.69
3/4	0.88	0.54
7/8	0.79	-
1	0.77	-

* Strength of brickwork with 3/8" joints taken as unity.

American tests - six brick high wallettes.

Bradshaw - three and four course cubes.

Table 5 - 4

The Properties of Three Course Brickwork Cubes.
Type II 1/3rd Scale Bricks.

CubeNo.	Age at Test-Days.	Compressive Strength pf. s. i.	Brickwork/ Brick Strength Ratio.	Approximate Initial Cracking Stress. pf. s. i.
1	24	3,120	0.54	1,000 - 1,450
2	23	2,590	0.45	< 1,300
3	27	2,700	0.47	800 - 1,000
4	27	2,400	0.41	1,950
5	27	2,540	0.44	900
6	28	2,520	0.44	525 - 800
7	200	2,404	0.38	> 2,000
8	31	2,700	0.47	1,250
9	29	2,750	0.48	650 - 800
10	29	3,020	0.52	800
11	25	2,880	0.50	> 2,500
12	29	2,630	0.45	> 2,400
13	32	2,100	0.36	1,000 - 1,300
Average		2,643	0.45	

Standard Deviation = 271 pf. s. i. Coefficient of Variation = 10.3%.

Ratio Brickwork/Brick Strength based on Dry compressive strength of 5,795 pf. s. i.

Average mortar strength at test = 2,100 pf. s. i.

Table 5 - 5

The Properties of Four Course Brickwork Cubes.

Type II 1/3rd Scale Bricks.

Cube No.	Age at Test-Days.	Compressive Strength pf. s. i.	Brickwork/ Brick Strength Ratio.	Approximate Initial Cracking Stress. pf. s. i.
1	30	2,070	0.36	800
2	30	1,975	0.34	> 1,300
3	27	2,140	0.37	500
4	30	2,295	0.40	650
5	27	2,640	0.46	400
6	200	2,239	0.39	900
7	26	2,350	0.41	500
8	30	2,240	0.39	980
9	26	2,430	0.42	800 - 1,000
10	33	2,300	0.40	800 - 1,000
11	29	2,530	0.44	1,050
12	200	3,008	0.52	2,600
13	25	2,530	0.44	1,050
Average		2,365	0.41	

Standard Deviation = 271 pf. s. i. Coefficient of Variation = 11.5%.

Ratio Brickwork/Brick Strength based on Dry compressive strength of 5,795 pf. s. i.

Average mortar strength at test = 2,100 pf. s. i.

CHAPTER 6.

CONCENTRATED LOADING ON MODEL BRICK WALLS.

1. THE SCOPE OF THE INVESTIGATION.

1.1 THE VARIATION OF BEARING PLATE LENGTH.

The primary object of the tests carried out was to ascertain the effect of the variation of the bearing plate length on the failure stresses for brick walls, loaded either centrally or at one end.

Walls were constructed of either $1/6$ th scale or $1/3$ rd scale Type I model bricks.

1.2 THE EFFECT OF EDGE DISTANCE.

A secondary aim was to investigate the effect of the variation of the edge distance of the bearing plate on the failure stress of the walls.

1.3 AGE FACTOR.

The tests were carried out in two series, one shortly after construction, and another after approximately one year, to ascertain whether or not specimen age was an important factor.

1.4 STRAIN MEASUREMENT.

Horizontal and vertical strain measurements were made on two $1/3$ rd scale walls to enable a comparison of the strain distributions in full-scale and model brickwork to be made. Central and end loading cases were considered, and the bearing plate length was varied.

2. THE TEST PROGRAMME.

2.1 MODELS CONSTRUCTED.

Approximately 75 $1/6$ th scale, and 60 $1/3$ rd scale, model

walls were constructed, together with mortar cubes.

2.2 SERIES I TESTS.

The first test series was carried out approximately 30 days after construction of the walls.

In this series 38 $1/6$ th scale walls were tested and 45 $1/3$ rd scale walls.

Central and end bearing plate tests were carried out, using bearing plates of various lengths. The effect of the edge distance on the failure stress was investigated, using relatively undamaged portions of $1/3$ rd scale walls that had already been tested. Work was concentrated on bearing plate lengths of two sizes, 0.5" and 1.05", at varying edge distances.

Slight damage of the wall portion was allowed providing it occurred out of the expected failure zone.

In this series two $1/3$ rd scale walls were tested taking strain measurements on both faces, using a 2" Demec gauge. One wall was subjected to central loading and the other to end loading, using bearing plates of various lengths.

2.3 SERIES II TESTS.

The second series was conducted approximately one year after the construction of the models. At this point the mortar cubes showed an increase of approximately 50% over the 30 day strength.

In this series 35 $1/6$ th scale walls and 15 $1/3$ rd scale walls were tested.

The variation in bearing plate length was restricted to $1/6$ th

and 1/3rd scale models of full-scale bearing plates from 4.5 to 9 ins. long. In the 1/3rd scale tests only two sizes of bearing plate were used, 4.5 ins. and 9 ins. scaled down. The reason for this was to obtain statistically more valid results, with the limited numbers of specimens available.

Strain measurements were made on the same two walls tested in series I. The walls were then tested to failure, to enable more significant strains, and in particular tensile strains, to be measured.

3. MATERIALS USED.

3.1 BRICKS.

1/6th scale bricks, and 1/3rd scale bricks of Type I, were used to construct the model walls. Details of the physical properties of the brick are given in Table 5-1.

3.2 SAND.

The sand used was Leighton Buzzard No.21. A sieve analysis is given in Table 5-2, and illustrated in Fig. 5-2.

3.3 MORTAR.

A 1:4, cement: sand, by weight mix was used, the cement being rapid hardening Portland.

4. DIMENSIONS OF MODELS.

The walls constructed were of a single leaf type, and were four stretcher bricks long, and nine courses high for both the 1/6th and 1/3rd scale models constructed.

Mortar joint thicknesses of 1/16" and 1/8" were used for the 1/6th and 1/3rd scale models respectively.

Nominally the model walls were 5.80" long x 4.73" high and 11.46" long x 10.0" high for 1/6th scale and 1/3rd scale respectively, corresponding to approximately 2'-10" long x 2'-6" high in full-scale brickwork.

5. METHOD OF MODEL CONSTRUCTION.

In order to control the dimensional accuracy of the models constructed jigs were made. These consisted of a base board, and a stiffened plywood backing sheet, together with side pieces.

The levels of each course, and the mortar joints were marked on the plywood sheet, and the jig was greased using cube mould oil.

Before construction commenced the bricks were soaked under water for approximately two hours, to reduce the water absorption during laying. Using dry bricks made the mortar difficult to handle, as it quickly lost its work ability on contact with the bricks.

During model construction 1" mortar cubes were cast. These were made filling the mould in three layers and hand tamping.

6. THE CURING OF SPECIMENS.

The walls constructed were cured under damp sacks for 24 hours, before removing them from the jigs. They were then stored under water, until near the time of testing. The 1" mortar cubes were cured in the same way.

7. THE METHOD OF TESTING.

7.1 PREPARATION OF THE SPECIMENS.

In order that the wall could be supported uniformly, and so that the load could be uniformly distributed, any mortar protruding

from the joints was filed down, to give level bedding conditions.

Where strain readings were to be taken Demec studs were fixed in the required positions, using Durofix cement.

7.2 LOADING CONDITIONS.

A course grade of sandpaper was used to provide a frictional base for the walls, and to even out any small discrepancy in bearing conditions.

A layer of damp sand was used to ensure an even bedding for the bearing plates on the top surface of the wall. This was thought to be necessary, as the testing machine was a rigid head type, and stress concentrations would certainly occur if the specimen was not perfectly level.

All specimens were tested in an Avery compression testing machine, which could be adjusted to give a maximum scale reading of as low as 5 tons.

7.3 BEARING PLATES.

As 1" thick mild steel bearing plates had been used for the full-scale wall tests, 1/6" and 1/3" thick mild steel plates were used for the model tests. These thicknesses were such that they might be considered rigid.

The bearing plate sizes chosen were 1/6th and 1/3rd of those used for the full-scale tests together with two smaller sizes, chosen to simulate higher stress concentrations. Details of bearing plate sizes are given in Table 6-1.

7.4 THE RATE OF LOAD APPLICATION.

B.S. 1257:1945 and the new standard B.S. 3921:1965 recommend a rate of loading of 2,000 lbf/in.²/minute for the testing of brick specimens, and this rate has also been recommended as suitable for brickwork cube tests.

For a specimen whose expected failure stress is in the region from 1,000 pf. s.i. to 2,000 pf. s.i. this means a testing time range for specimens from 1/2 - 1 minute. As observations were to be made of the formation of cracks, and the failure modes, a rate of loading of 2,000 lbf/in.²/minute was too high, and it was decided to apply the load slowly, making careful observations. Each test took from 1/4 - 1/2 an hour, depending on the failure stress of the walls.

Where strain measurements were made the duration of the tests was dictated by other factors.

The rate of loading is not regarded as having had a significant effect on the test results. If the rate is increased, above 2,000 lbf/in.²/minute then increased failure stresses may be obtained. Also, if the rate of loading is decreased greatly, reducing the test to a creep type, then lower failure stresses may occur. However, for moderate rates of loading the time effect may be considered as non-critical.

8. THE RESULTS OF TESTS.

8,1 1/6TH SCALE TESTS.

The results of the end and central bearing plate tests for the series I (short term), and series II, (long term) tests are given in detail in Tables 6-2 to 6-17. The average results are shown in

Figs. 6-1 and 6-2, in which the average failure stress is plotted against the bearing plate length (Fig. 6-1) and against the ratio wall length/bearing plate length (Fig. 6-2).

Mortar cube strengths are given in Table 6-18.

8.2 1/3RD SCALE TESTS.

The results of the end and central bearing plate tests for the series I (short term) and series II (long term) tests are given in detail in Tables 6-19 to 6-30. The average results are shown in Figs. 6-3 and 6-4 in which the average failure stress is plotted against the bearing plate length (Fig. 6-3) and against the ratio wall length/bearing plate length (Fig. 6-4).

Mortar cube strengths are given in Table 6-31.

8.3 EDGE DISTANCE EFFECTS.

The results of the series I, 1/3rd scale tests, investigating the effect of edge distance are given in Tables 6-32 and 6-33. The edge distance is taken as being the distance from the corner of the wall to the centre line of the bearing plate. Results are presented graphically in Figs. 6-5 and 6-6, where failure stress is plotted against edge distance, for bearing plates 1.05" long and 0.52" long.

8.4 STRAIN MEASUREMENTS.

Tables of results of the strain measurements are not presented, but a graphical presentation is given in Figs. 6-7, 6-8, 6-9 & 6-10. These illustrate the strain distribution for end and central bearing plate tests.

Only the results of the series II tests are presented, as the

average applied stresses were considerably higher than in the series I tests. The nature of the compressive strain distributions under bearing plates of various sizes were similar in both series however, and the results presented are typical.

8.5 MODES OF FAILURE.

The modes of failure of the walls are noted in the tables of results, and are discussed later.

9. DISCUSSION OF TEST RESULTS.

9.1 END BEARING TESTS.

Figs. 6-1 and 6-3, showing the variation of failure stress with bearing plate length, for 1/6th scale and 1/3rd scale bearing plates, indicate that as the bearing plate length decreases, then the failure stress increases.

The relationship between failure stress and bearing plate length is non-linear, particularly when the bearing plate length is relatively small.

For the 1/6th scale walls the failure stress increases with decreasing bearing plate size, but the highest average stress found, 6,420 pf. s. i., for a bearing plate length of 0.28", is not statistically significant. The results for series I and series II tests are similar.

For the 1/3rd scale walls the curves for the two test series are similar, showing an increase in compressive strength of approximately 12% over the year between the test series.

Fig. 6-11 giving the relationship between the brickwork/brick ratio and the bearing plate length allows the comparison of the 1/6th,

1/3rd and full-scale tests. The smaller slenderness ratio of the full-scale walls cannot be taken into account, and the effect of the header bond is also neglected.

The full-scale results (from fewer tests than the model work) and the 1/6th scale series I results, give similar curves, approximately parallel. The 1/3rd scale tests, series I and II, and the 1/6th scale series II also give similar curves. As the two 1/6th scale test series vary only in age all the results may be taken to conform to the same pattern within the limits of experimental accuracy.

The trend for full-scale, 1/6th scale and 1/3rd scale walls is similar, with increasing brickwork/brick strength ratio as the bearing plate length decreases.

9.2 CENTRAL BEARING TESTS.

Figs. 6-1 and 6-3 show the relationship between the failure stress and the bearing plate lengths for 1/6th and 1/3rd scale brickwork.

The relationship is non-linear, with increasing failure stress with decreasing bearing plate length. The increase in failure stress is particularly noticeable when the bearing plate length becomes relatively small.

For the 1/6th scale models the two series of tests show no significant differences due to age.

The 1/3rd scale tests indicate an increase in failure stress of 15-20% over the year between the test series.

Fig. 6-12 gives the relationship between the brickwork/brick

ratio and the bearing plate length, and allows a comparison of the full-scale, 1/6th scale and 1/3rd scale test results.

The 1/6th and 1/3rd test results follow a similar pattern, and the results for the 9" full-scale bearing plate fits the trend. The 4½" full-scale bearing plate results are higher than might have been expected, but three out of four of the walls contained horizontal reinforcement in varying amounts. The effect of the reinforcement was not, however, apparent from the individual tests, although the wall with the most reinforcement had the highest failure stress. Certainly the inclusion of reinforcement cannot have lowered the failure stress.

Considering the 9" bearing plate result, only one test was conducted, and it may be that this result is below the general average for this bearing plate. The ratio for the single 9" central bearing plate/average 9" end bearing plate strengths is 1.07, compared with 1.25 for the 1/6th scale, and 1.26 for the 1/3rd scale.

Further tests are required to confirm the behaviour of centrally loaded full-scale specimens, but from the results obtained, full-scale, 1/6th scale and 1/3rd scale follow the same trend of increased bearing failure stress with decreased bearing plate length.

9.3 A COMPARISON OF CENTRAL AND END BEARING PLATE RESULTS.

Figs. 6-1 and 6-3 show the failure stress/bearing plate length relationship for the central and end bearing tests for the 1/6th and 1/3rd scale tests.

The curves obtained are similar in the bearing plate range

4.5" - 9" full-scale. The values of failure stress are approximately 1.3 times as great for the central bearing plates as for the end bearing plates for both 1/6th and 1/3rd scale models.

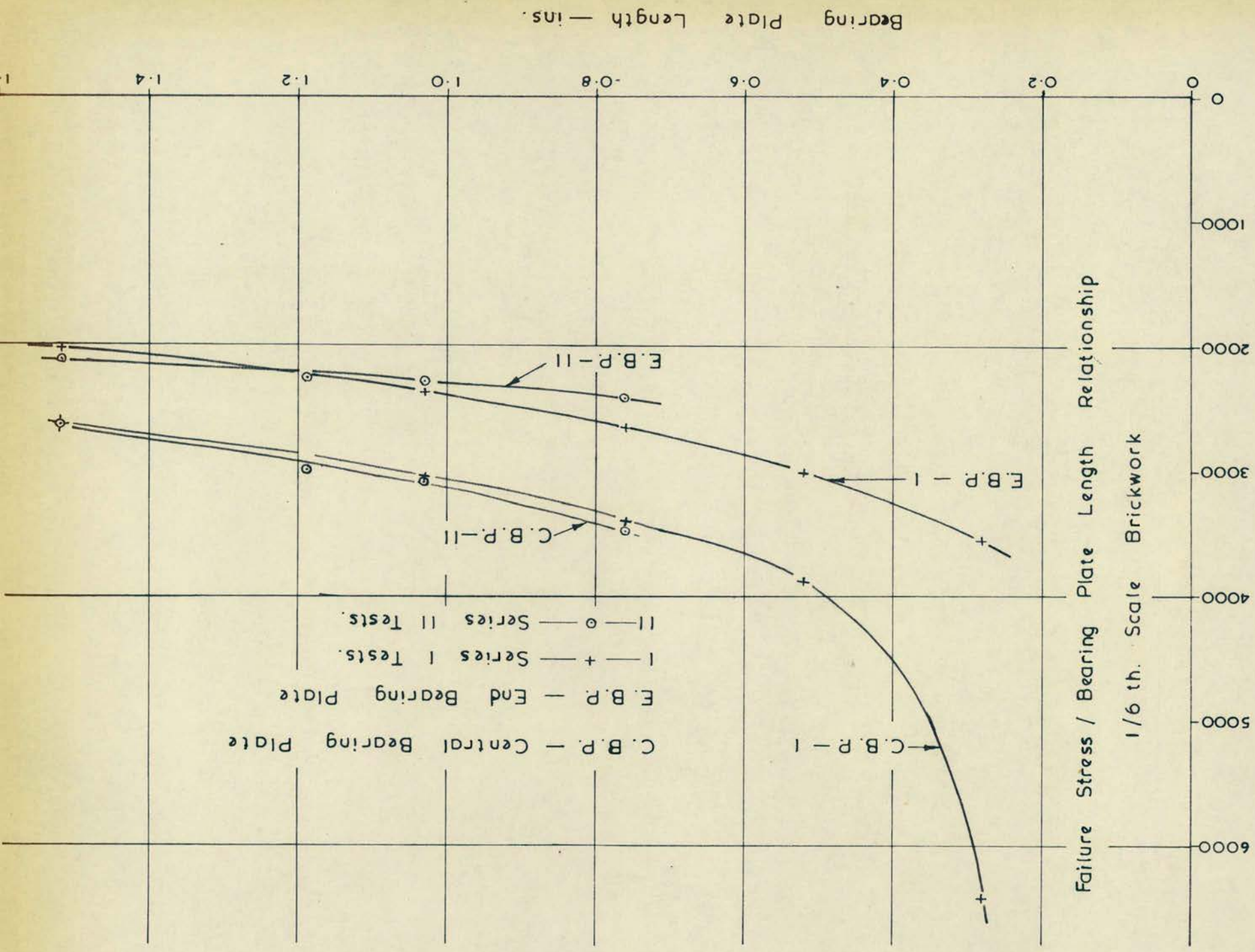
For the smaller bearing plates, the failure stress increases more rapidly for central bearing plates than for end bearing plates, as the bearing plate length decreases. The ultimate strength of the brickwork is thought to be the compressive strength of the brick, which may be attained as the bearing plate size tends to zero.

Figs. 6-2 and 6-4, show the failure stresses plotted against the L/a ratio (the ratio of the wall Length/bearing plate length) for the 1/6th and 1/3rd scale walls.

The relationship between failure stress and L/a appears to be linear for the larger bearing plates, in the region $L/a = 4-10$. Values of $L/a < 4$ have not been investigated and it cannot be assumed that the relationship is linear in this zone. Figs. 6-5 and 6-6, showing the effect of edge distance indicate that the transition zone between end and central bearing, or end and intermediate bearing is well defined, with the failure stresses increasing rapidly as the edge distance increases.

As the L/a ratio decreases then the central and end bearing plate failure stresses should approach each other, coinciding when $L/a = 1$. A further series of tests is required to investigate values of $L/a < 4$, before the complete nature of the relationship between L/a and the failure stress can be established.

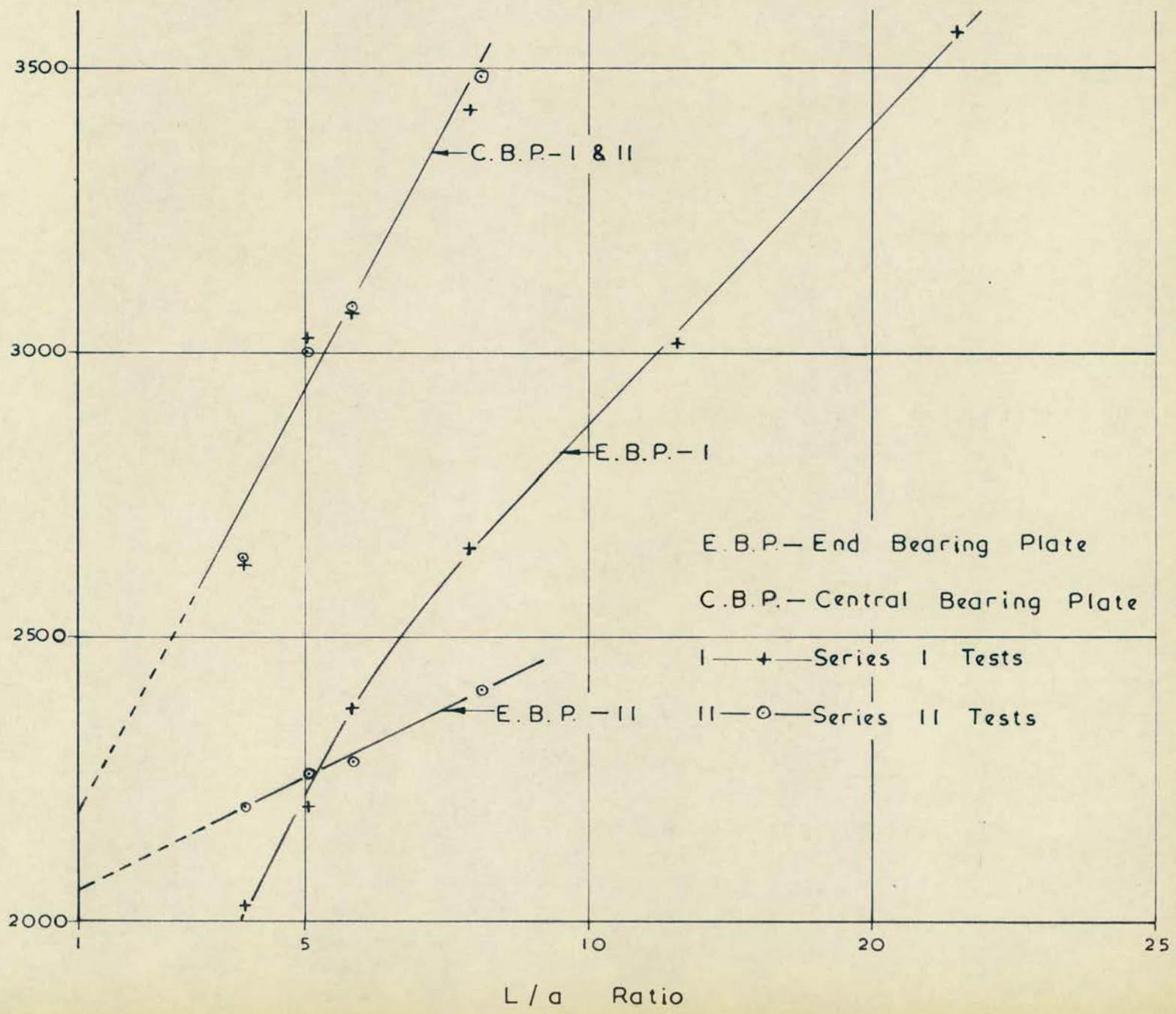
9.4 STATISTICAL ASPECTS OF THE RESULTS OBTAINED.



Failure Stress ps.i.

Fig. 6-1

Failure Stress / (L/a) Relationship
 Fig. 6-2



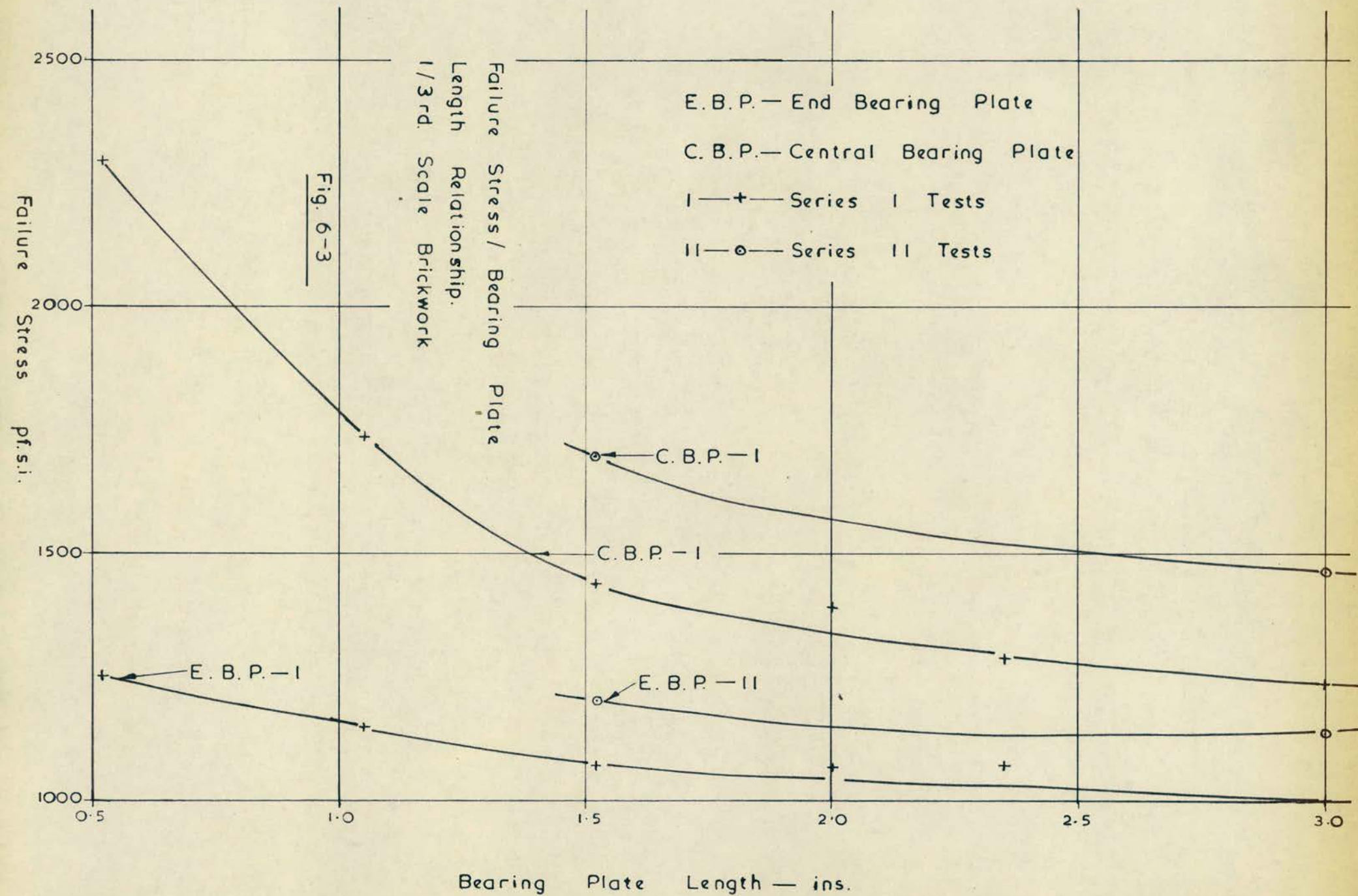
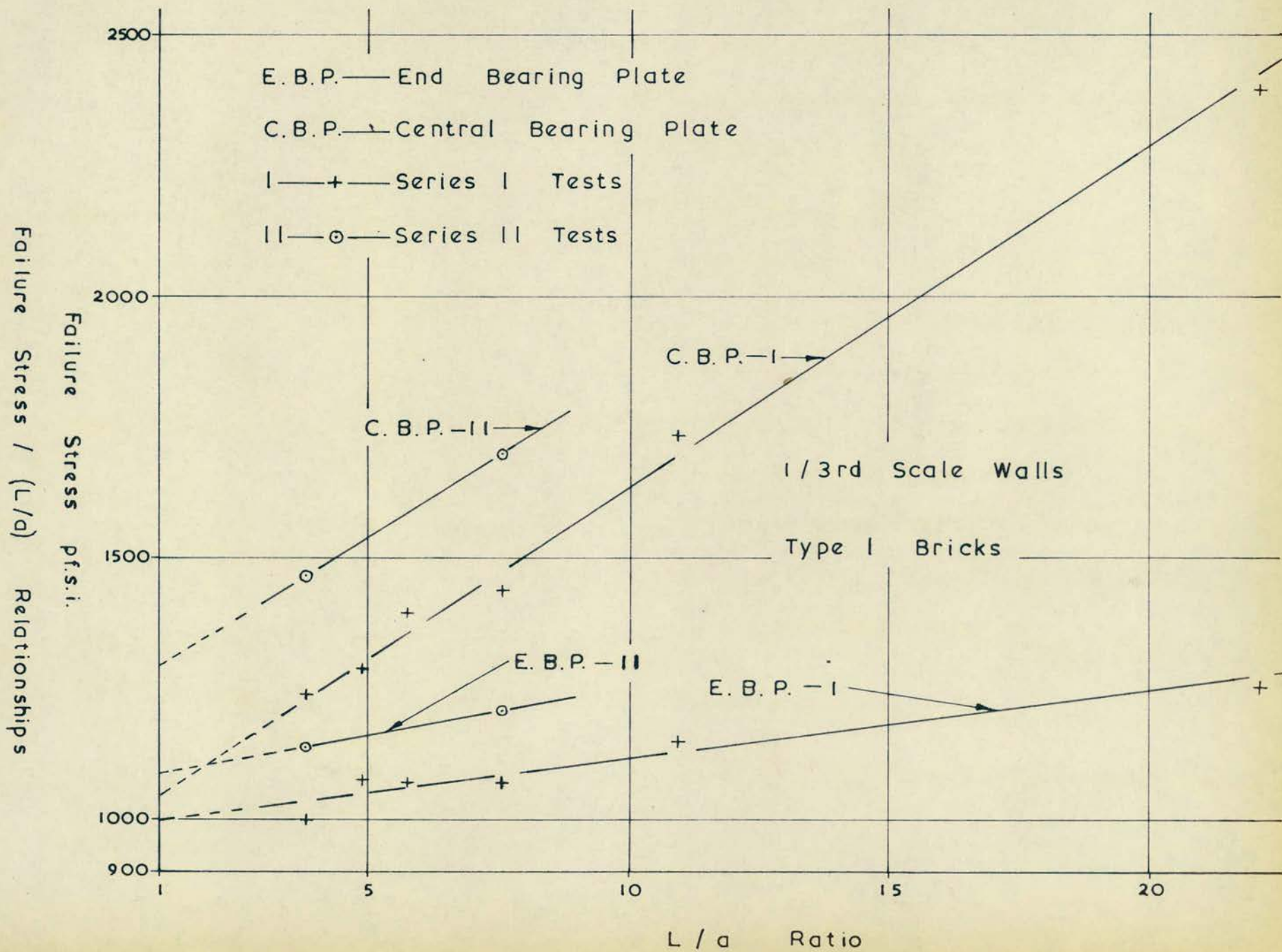


Fig. 6-4



The Effect of Edge Distance on Failure Stress
Fig. 6-5

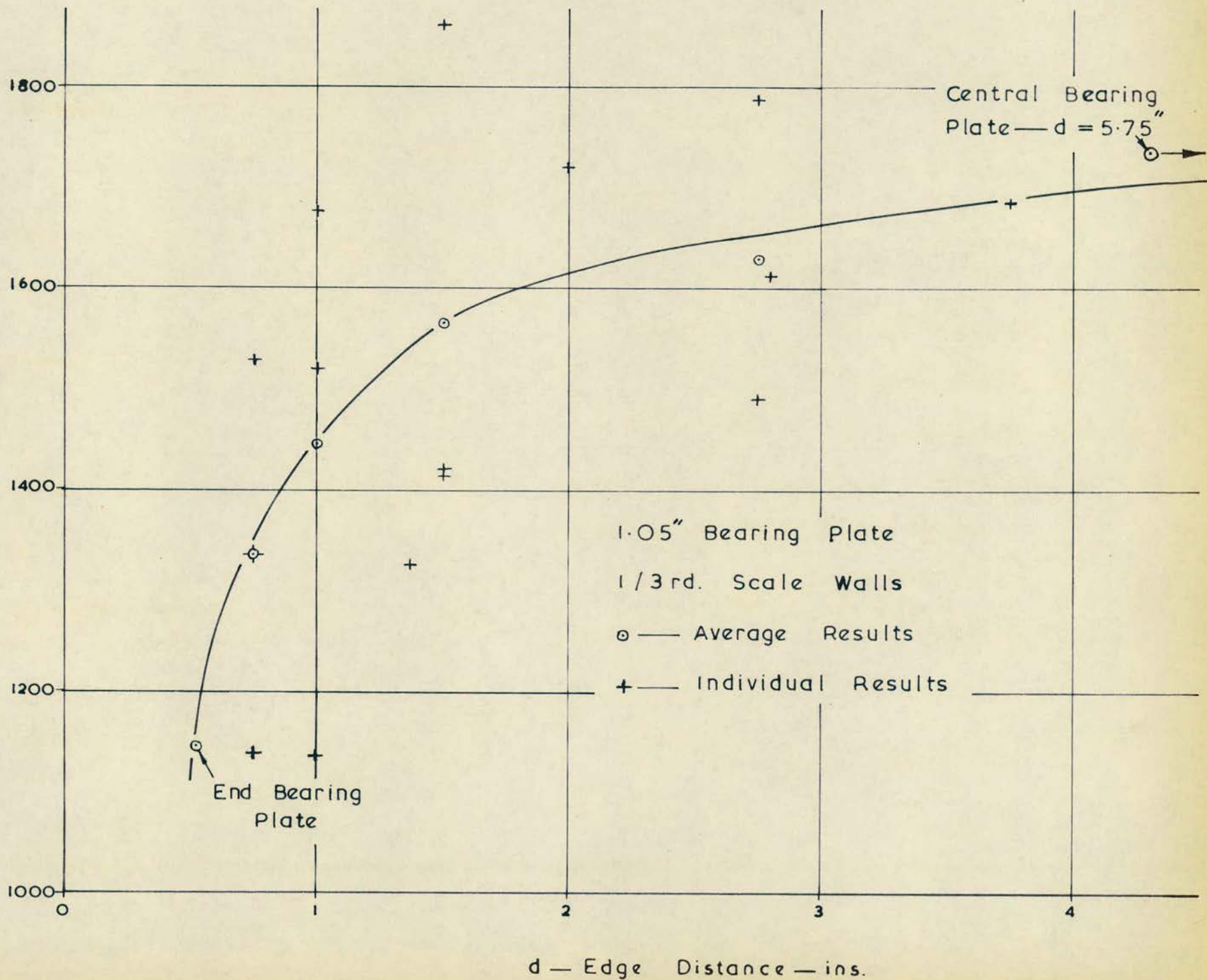
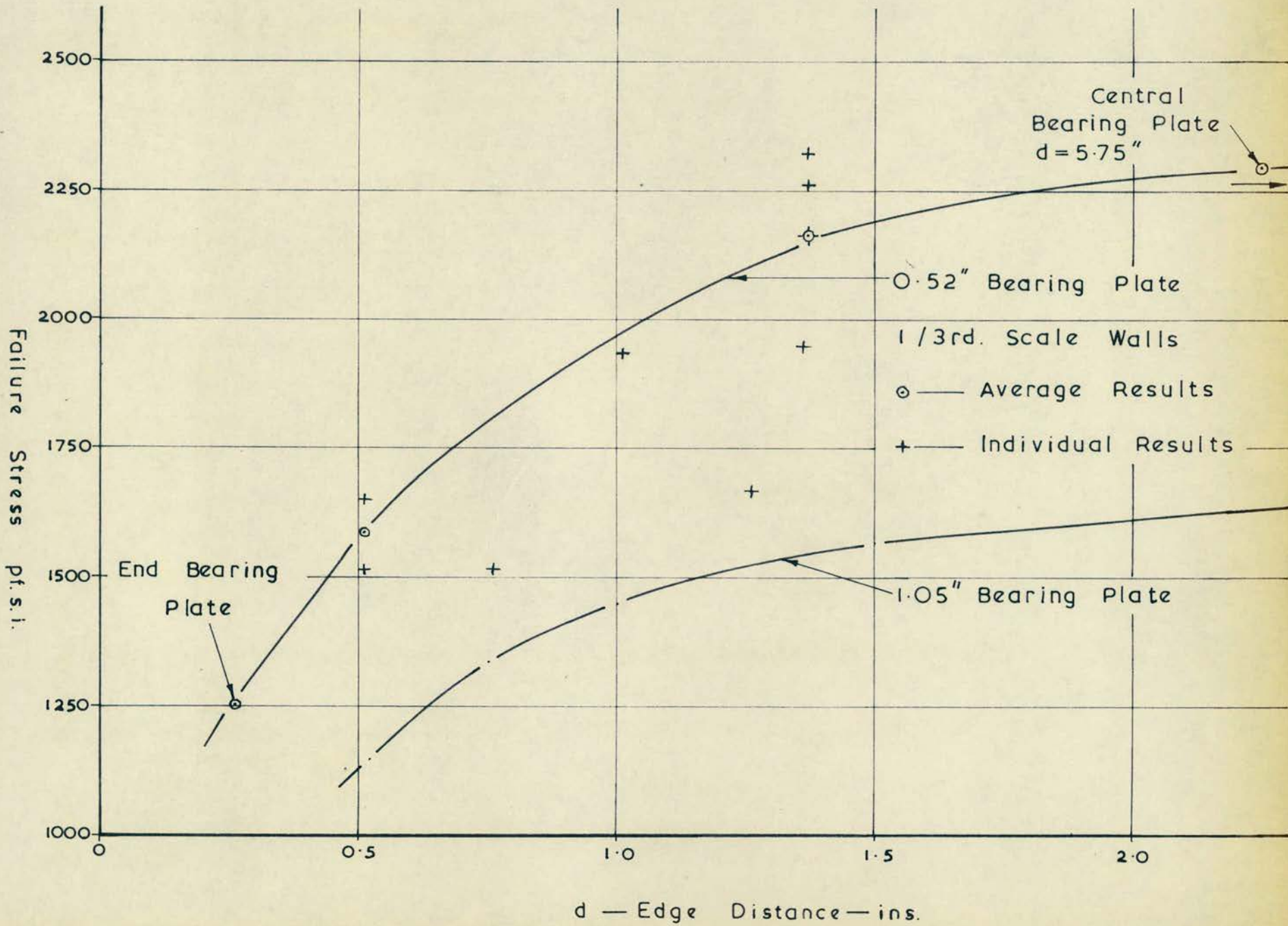
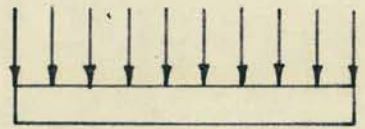


Fig. 6-6
The Effect of Edge Distance on Failure Stress





1/3rd. Scale Wall 3.02" End Bearing Plate

Vertical Strain Distribution

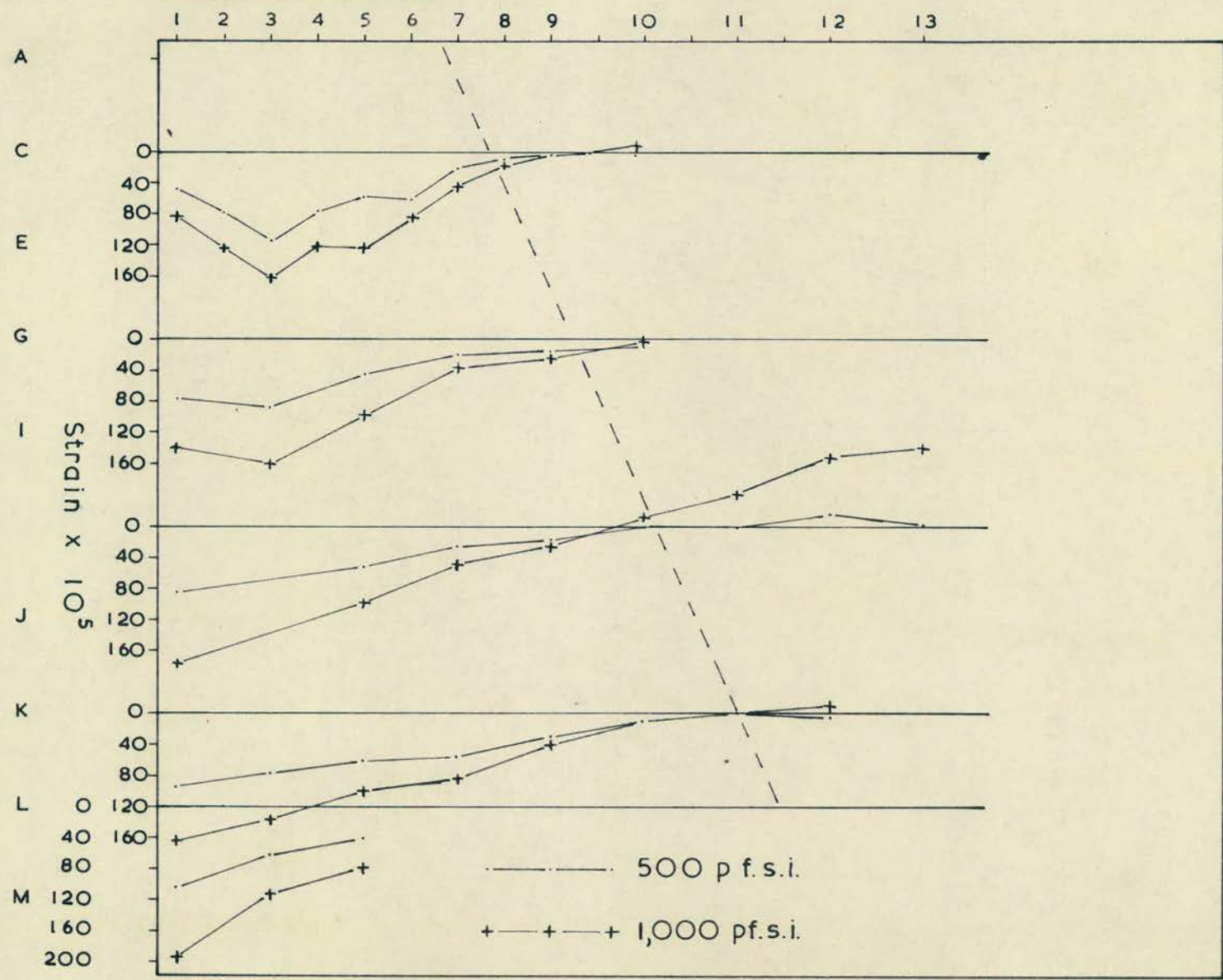


Fig. 6-7

1/3rd Scale Wall — 3.02" End Bearing Plate

Horizontal Strain Distribution

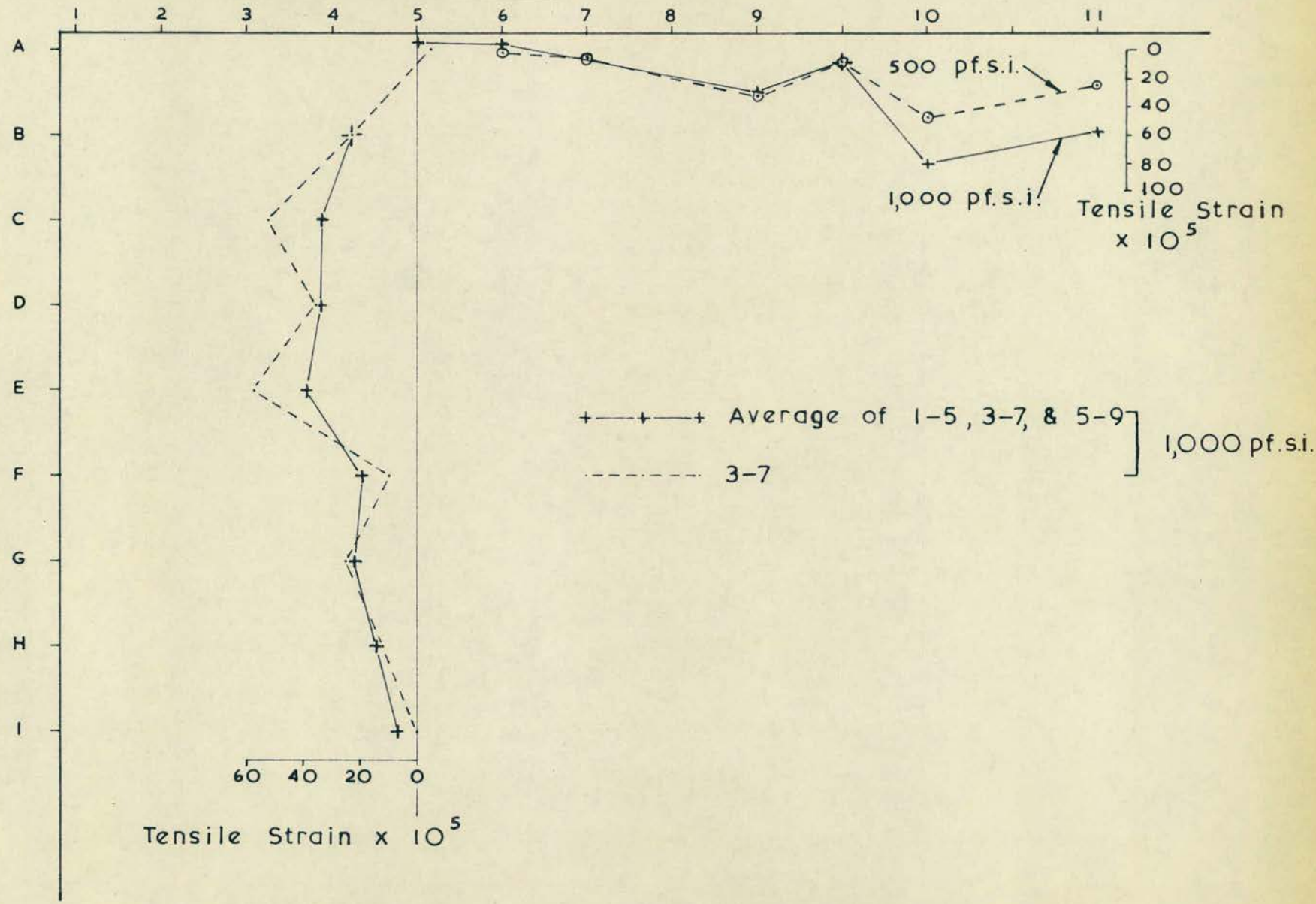
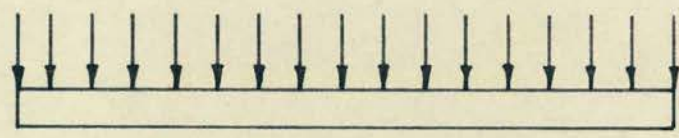
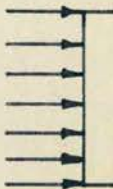
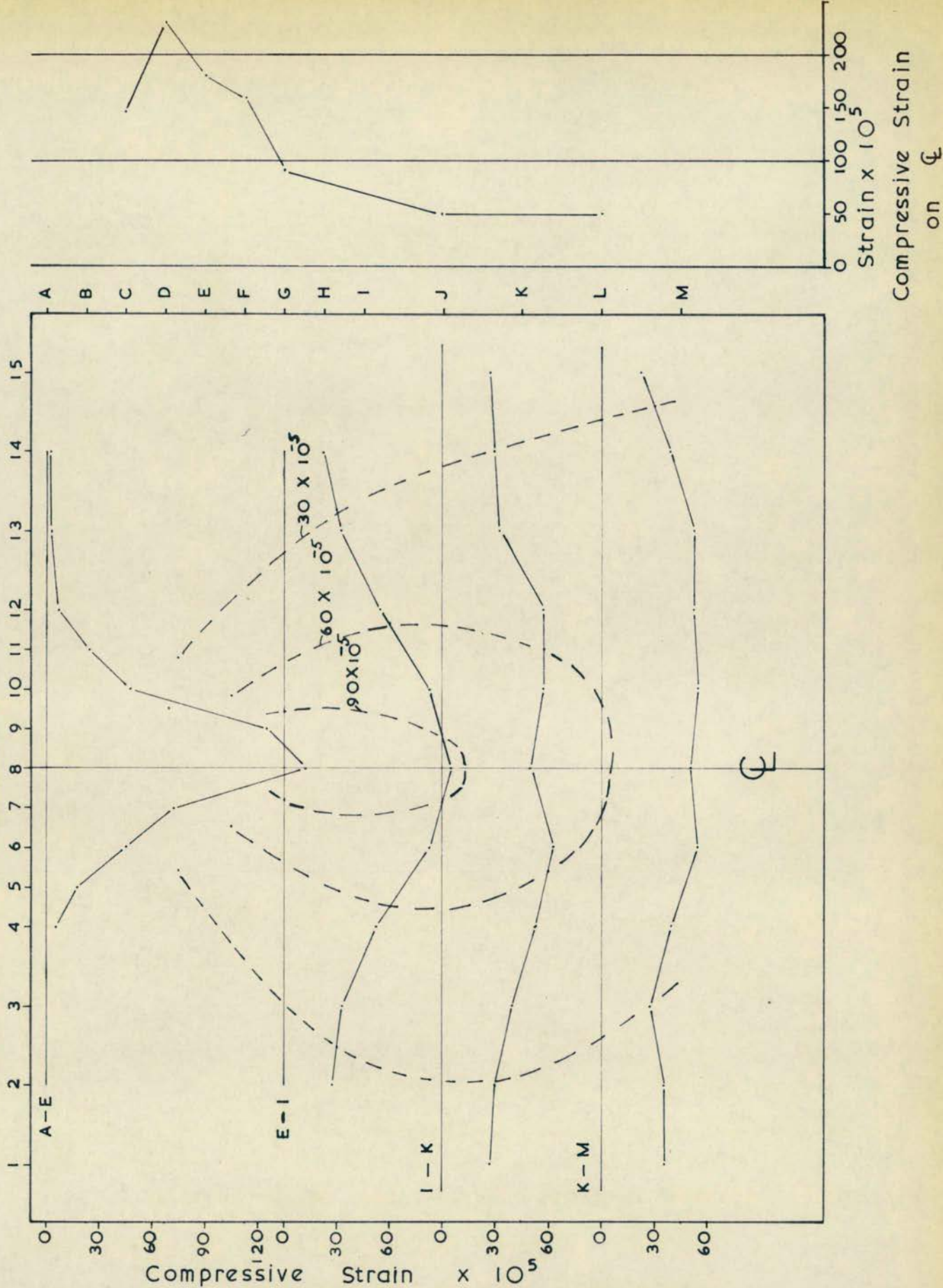


Fig. 6-8

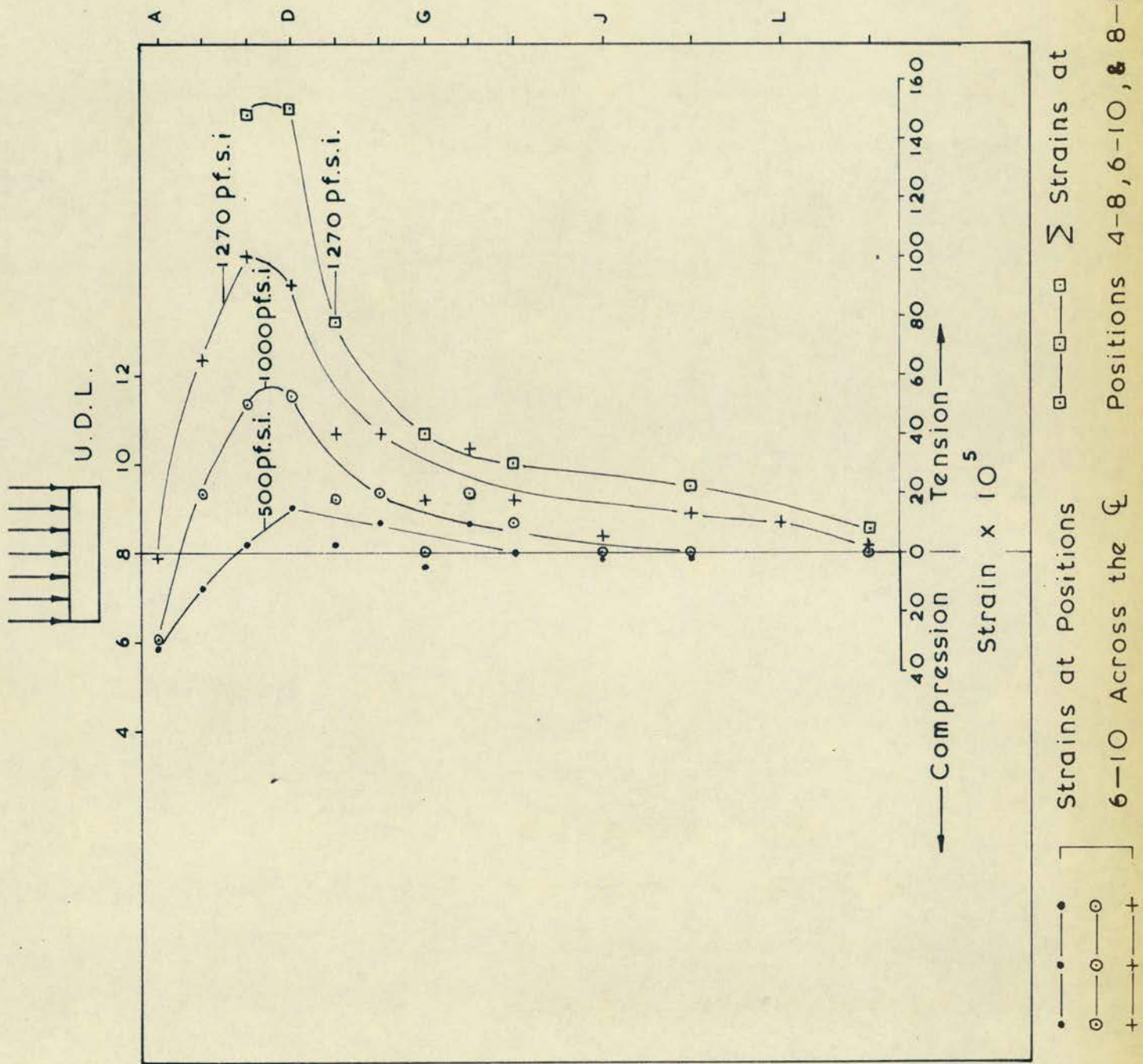
U.D.L.— 1,270 pf.s.i.

1/3rd. Scale Wall—1.52" Central Bearing Plate

Vertical Strain Distribution

Fig. 6-9



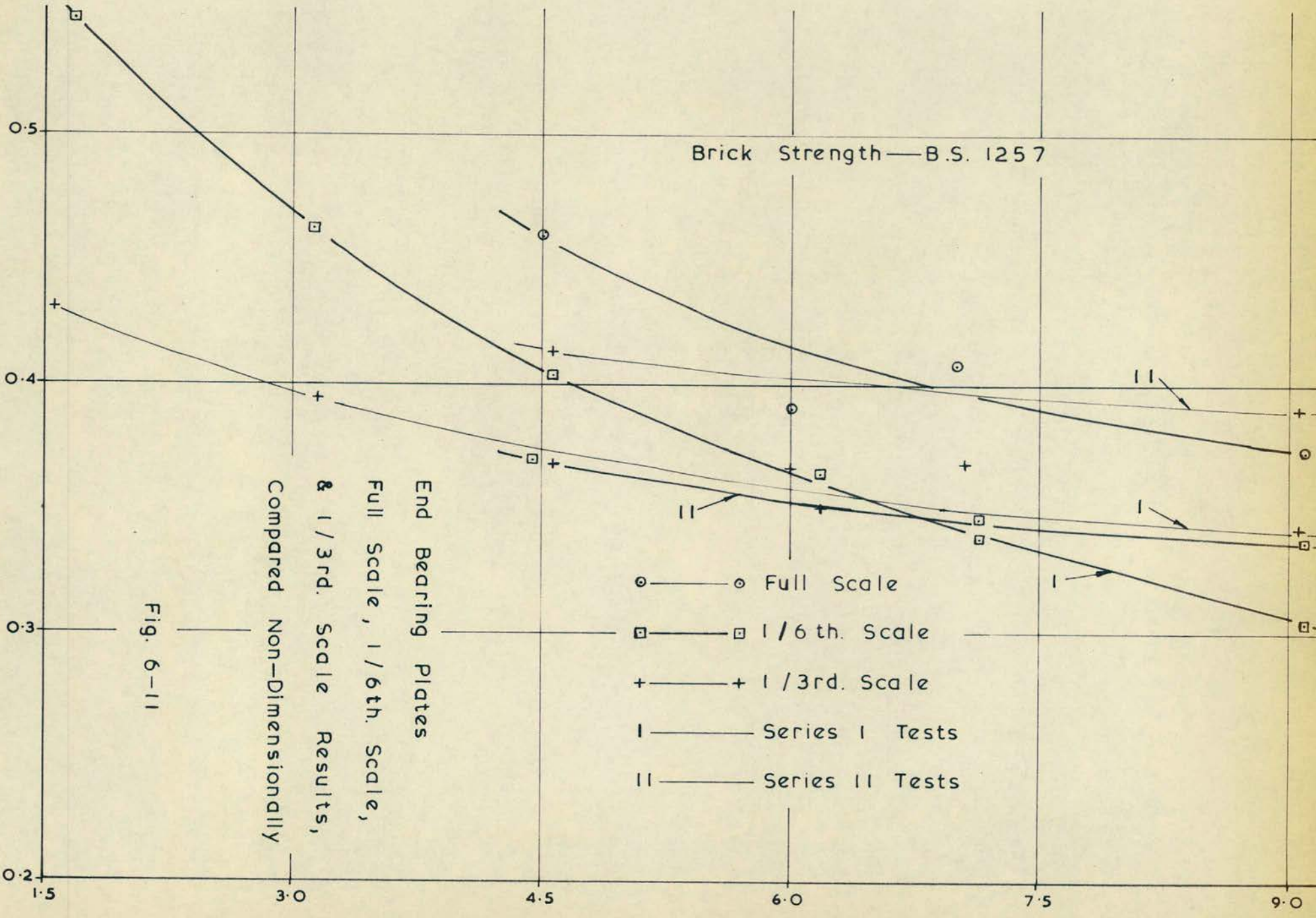
1/3rd. Scale Wall — 1.52" Central Bearing Plate

Horizontal Strain Distribution

Fig. 6-10

Brick Strength—B.S. 1257

Brickwork Strength / Brick Strength Ratio



End Bearing Plates
Full Scale, 1/6th. Scale,
& 1/3rd. Scale Results,
Compared Non-Dimensionally

Fig. 6-11

- — Full Scale
- — 1/6th. Scale
- + — 1/3rd. Scale
- I — Series I Tests
- II — Series II Tests

Corresponding Full Scale End Bearing Plate Length — ins.

Brick Strength — B.S. 1257

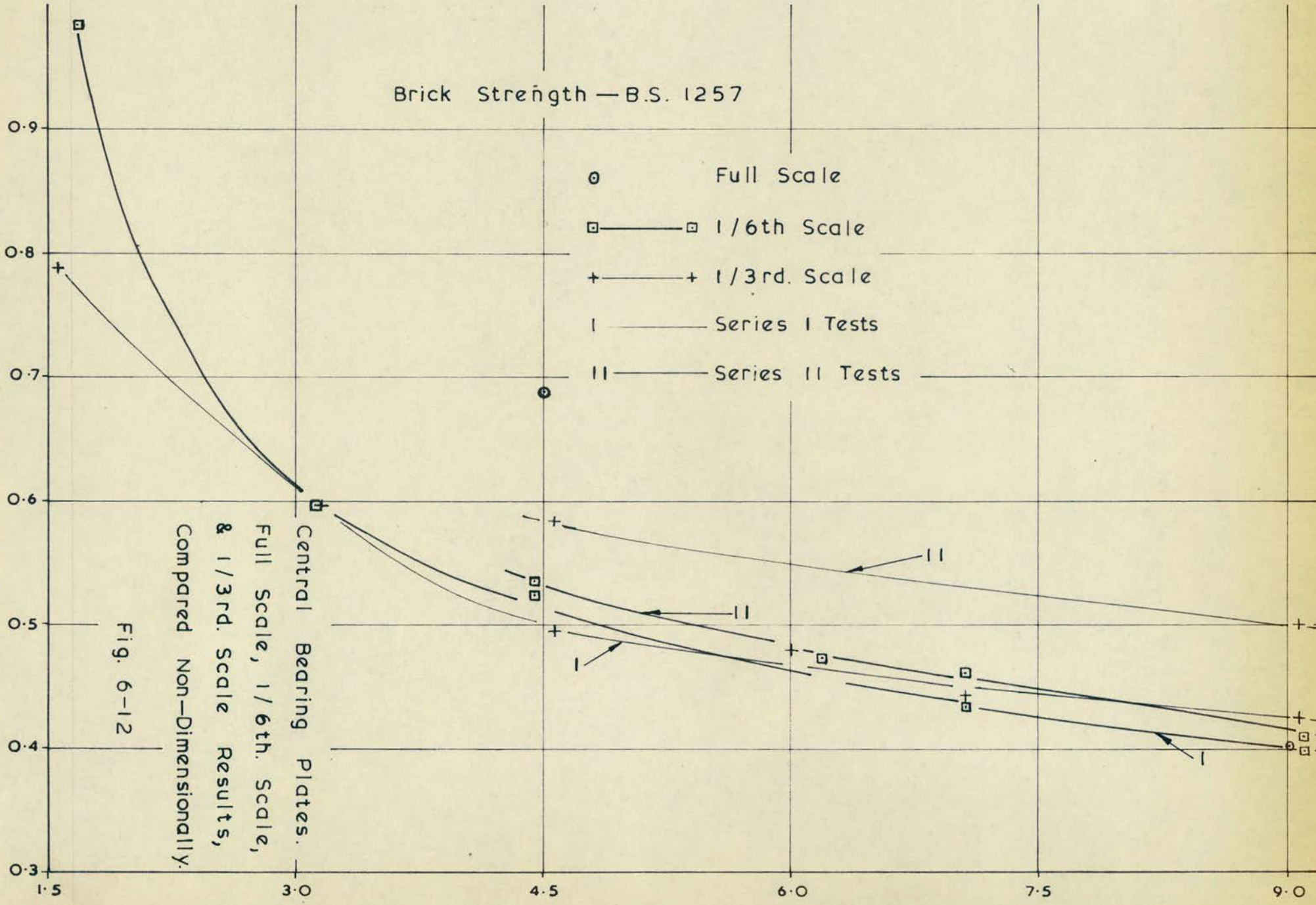
Brickwork Strength / Brick Strength Ratio

- Full Scale
- 1/6th Scale
- + 1/3rd. Scale
- I Series I Tests
- II Series II Tests

Central Bearing Plates.
 Full Scale, 1/6th. Scale,
 & 1/3rd. Scale Results,
 Compared Non-Dimensionally.

Fig. 6-12

Corresponding Full Scale Central Bearing Plate Length — ins.



The range of results, the Standard Deviation and the Coefficient of Variation have been given with the tables of results, where the number of tests has justified a statistical investigation. A suitable minimum number was thought to be six in a series.

The statistical calculations, and in particular the coefficient of variation give a good idea of the value of the results obtained.

The values of the coefficient of variation ranged from 4.9 - 18.9% for particular bearing plate sizes. An overall coefficient of variation has been calculated, for the model brickwork, based on the average of the value of the sum of the coefficient of variation x number of tests in series, i. e. $\frac{\sum (v \cdot n)}{N}$, where N is the total number of tests conducted. The value obtained was 11.8% and this value indicates the acceptability of the results obtained, from the point of view of consistency. The coefficient of variation, of the brick compressive strength, for the bricks from which the models were constructed, was 11.65%. Hence the variation in the test results has practically stayed within the limits of the brick strength variation.

The above suggests that factors such as variability of workmanship and mode of loading have played little part in the tests, as they would have inevitably increased the coefficient of variation.

The average coefficient of variation of the 1" cubes was 16.6%. The fact that this is higher than that of the brickwork is not surprising, as the effect of mortar strength on brickwork strength is known to be only marginal, above a mortar strength of 1,000 pf. s. i.

C.P. 111: 1964 - Structural Recommendations for Loadbearing Walls, recommends certain procedures for determining the allowable basic stress of a brickwork unit.

The basic stress, obtained from Table 3, depends on the standard compressive strength of the unit used, and the grade of mortar.

Where the cross-sectional plan area does not exceed 500 ins.² the basic stress is multiplied by a reduction factor equal to $0.75 + A/2,000$, where A is the area in ins.² of the horizontal cross-section of the wall or column.

A reduction in the basic stress is also made if the slenderness ratio exceeds 6, for an axially loaded member, and the reduction factor is given in Table 4.

When a unit is subjected to a concentrated load, due to a loading of a local nature, as at girder bearings, column bases, lintels etc., the basic allowable stress given after the reductions above may be exceeded by not more than 50%.

The requirements above have been carried out for the three types of brick used, and the final allowable basic stresses obtained, and are shown in Table 6-34. In the final rows of the table the Bwk. / Brick ratios are given which one would expect to obtain from tests for a safety factor of 1, and of 5 compared with the C.P. allowable stresses.

Consultation of Figs. 6-1 and 6-3 leads to the following conclusions.

For the end bearing plates the safety factors are lower than 5 for the full-scale, the 1/6th scale, and the 1/3rd scale brickwork, for a wide range of bearing plate sizes.

For central bearing plates the safety factor is greater than 5 in some cases, and less than 5 in others.

Table 6-35 gives a summary of the average and minimum safety factors, obtained from the tests, based on C.P. 111 allowable stresses. Safety factors are based on the failure stresses, and not the initial cracking stresses. The lowest safety factor found was 2.7, which reasonably justifies the Code specification, as this was the lowest of a large number of tests.

It is interesting to note that the minimum safety factors for the full-scale, the 1/6th scale and the 1/3rd scale walls were 3.2, 2.9 and 2.7 respectively. The average safety factors for the 9" end bearing plate, or its equivalent, were 4.3, 4.1, and 4.1, respectively for the three types above.

The factors provide a justification of the use of the model technique for bearing stresses.

Based on the above the present allowable basic stresses would seem reasonable. Certain factors however remain in need of investigation, before any definite recommendations can be made. These include workmanship factors, which were ignored in the tests carried out. Care was taken, in the construction of the models, to fill all vertical and horizontal mortar joints, ensuring optimum conditions. American (43) tests indicate that a workmanship factor

as high as 60% may be encountered with brickwork.

Another factor of importance is the nature of the bedding material for the bearing plate. Work at present in progress has shown that large differences in the compressive strength of the tested material occur when the packing or levelling materials are varied. Stainless steel plates have given high failure stresses, whereas materials such as rubber sheets have given relatively lower failure stresses.

Materials such as mortar, possessing low tensile strengths, but a relatively high degree of plasticity will behave in an intermediate manner, distributing the load, and restraining the brickwork to a degree dependent on the relative deformation properties of the mortar and brickwork.

The test series described in this thesis were conducted using damp sand as a levelling material. Such a material will distribute the load quite uniformly, if used in a thin layer, and the degree of restraint provided to the specimen will be intermediate between that of steel platens and rubber sheets.

9.6 EDGE DISTANCE EFFECTS.

Results are presented in Tables 6-32 and 6-33 and Figs. 6-5 and 6-6 for two sizes of bearing plate, which were 1/3rd scale models of 3" and 1.5" bearing plates.

These bearing plate sizes represent a high degree of load concentration, but may be taken as representing what might occur when a lintel or cantilevered slab deflects under load, transferring

the load to the edge of the wall section.

The number of tests conducted for each bearing plate was limited, but the end and central bearing tests provide points on each graph which confirm the average results obtained.

The scatter of results is seen to be quite high, but the average results fit a similar pattern for both bearing plates.

The effect of increasing the edge distance by a small amount is illustrated by Table 6-36.

Table 6-36
The Effect of Edge Distance on Failure Stress.

	Bearing Plate Length (ins.)												
	0.52						1.05						
Edge Distance (ins.)	0.26	0.5	0.75	1.0	1.5	5.75	.5	.75	1.0	1.5	5.75		
Failure Stress pf s.i.	*	1,250	1,570	1,800	1,960	2,200	2,300	*	1,150	1,340	1,450	1,560	1,735
% Increase	-	25	44	57	76	84	-	15	26	35.5	51		

* Taken as 100% for 0.52" and 1.05"

Thus, where lintels span into walls, or in other situations where edge stress concentrations seem likely to occur it would be beneficial to arrange the bearing so that the load cannot be concentrated at the extreme edge of the member upon which it bears. Bearing plates, mortar beds or other similar bearings **should thus** be given some edge clearance.

9.7 INITIAL CRACKING STRESS.

Approximate values of the initial cracking stress have been given in the tables of results. These values can only be approximate, as the determination of when cracking occurs is generally governed by the visibility of such cracks. The stresses given are likely to err on the high side, as it is possible for cracks and micro-cracks to form without being necessarily visible to the eye. This is particularly true where cracks have initially occurred in mortar joints. Strain measurements can indicate their presence, while they remain undetected by the eye.

An analysis of the cracking stresses indicates that apart from one or two results where loading conditions seemed initially uneven the cracking stress was not less than $2/3$ of the ultimate failure stress. In many cases initial cracking was not detected until complete failure occurred, or was about to occur. In some cases an explosive failure occurred, without prior warning, but this may be to a large extent dependent on the characteristics of the testing machine.

The formation of cracks at approximately $2/3$ of the failure stress is a useful indication that the loading is either excessive, or the brickwork defective, but the safety factors become rather low if based on a general figure of $2/3$ of the failure stress.

9.8 MODES OF FAILURE.

A general indication of the mode of failure in each test is given in the tables of results. The types of failure which occurred were generally different for the end and central bearing tests, and are discussed separately below.

i. End Bearing Tests.

The initial failure took place in several ways, the most common of which was the formation of vertical splitting cracks, in the width of the wall, below the bearing plate. This cracking was usually followed by either vertical cracking on the faces of the wall, below the centre line of the bearing plate, or by spalling on one face of the wall in the loaded zone.

In some cases vertical cracking below the centre line of the load was the first sign of failure, and this was followed by splitting in the width, and the breaking away of a wall portion, or column.

An explosive or sudden failure sometimes occurred and took the form of spalling from one face, without any other cracking.

Occasionally diagonal cracks were observed, originating at the inner edge of the bearing plate, and extending across the wall section. These cracks did not penetrate deeply into the wall, but marked the boundary of a type of surface spalling.

ii. Central Bearing Plates.

The initial failure often occurred due to the formation of a vertical crack on the centre line of the bearing plate. Sometimes this cracking appeared to originate at the base of the wall, and sometimes from just below the bearing plate. When this type of initial failure occurred at a relatively low stress it did not appear to lower the final failure stress of the wall.

The type of cracking described above was usually followed by spalling on one or both of the wall faces.

In some tests spalling was the first type of failure noticed, occurring on one or both faces. A higher failure stress was usually observed if the spalling occurred simultaneously on both faces. Examination after spalling revealed no cracking or failure of any other type. This type of failure usually occurred very rapidly.

A second type of failure, in which spalling predominated, occurred. Spalling occurred gradually, in the loaded zone, and was accompanied by diagonal surface cracking originating some distance from the bearing plate edges and occurring on both sides of the bearing plate. Examination of the specimen after failure revealed splitting cracks, occurring in the wall width, and running along the length of the wall, below and on either side of the bearing plate.

A further type of failure occurred in a few cases. This consisted of diagonal shear cracks, from the edge of the bearing plate across the wall sections. These cracks were inclined at 20° - 30° to the vertical, and passed through the full wall thickness. This type of failure, which failed the walls in shear, across several bricks, gave high failure stresses.

Plates 6-1 to 6-10 illustrate typical modes of failure.

9.9 STRAIN MEASUREMENTS.

i. End Bearing Plates.

Figs. 6-7 and 6-8 illustrate the vertical and horizontal strain distributions for a 3 ins. end bearing plate on a 1/3 rd scale wall.

Fig. 6-7 shows the typical bulb of compressive pressure directly below the bearing plate, with the maximum measured strain



1/3rd. Scale Brick Wall - End Bearing Plate -
Failures by Local Spalling, Crushing and
Vertical Cracking.

Plate 6-1

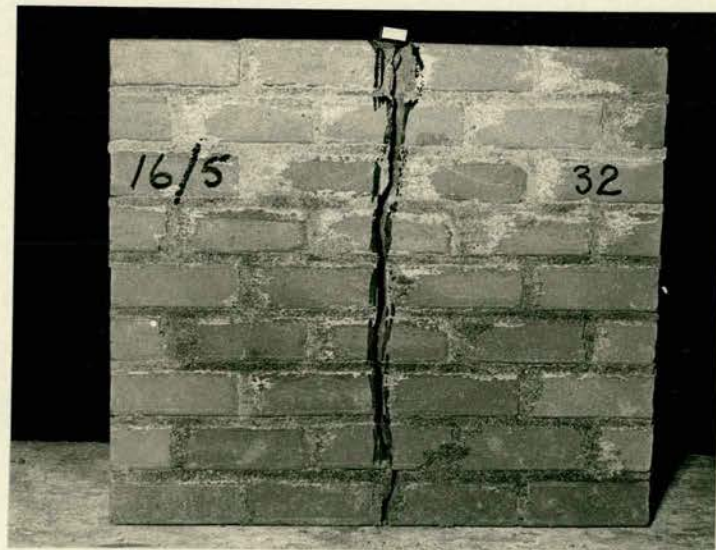


1/3rd. Scale Brick Wall - End Bearing Plate -
Failures by Local Spalling, Crushing and
Diagonal Cracking.

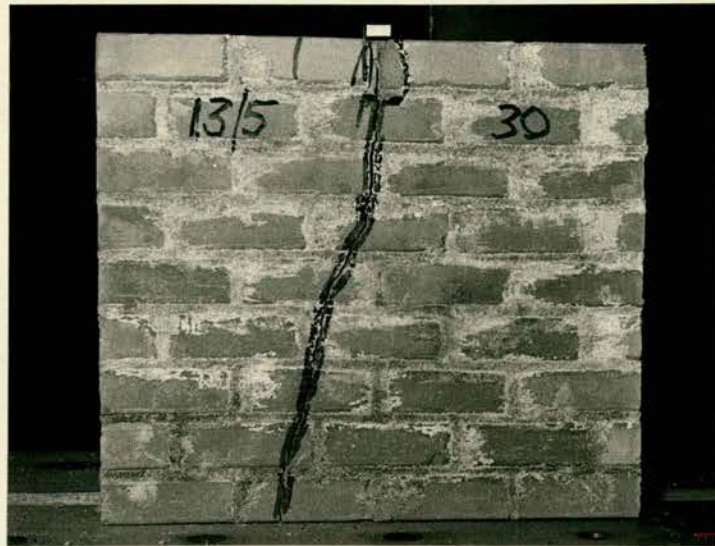
Plate 6-2



1/3rd. Scale Brick Wall - End Bearing Plate -
Failures by Vertical Cracking and Spalling.
Plate 6-3



1/3rd. Scale Brick Wall - Central Bearing Plate -
Failure by Vertical Cracking and Local Crushing.
Plate 6-4



1/3rd. Scale Brick Wall - Central Bearing Plate -
Failure by Diagonal Cracking and Local Crushing.
Plate 6-5

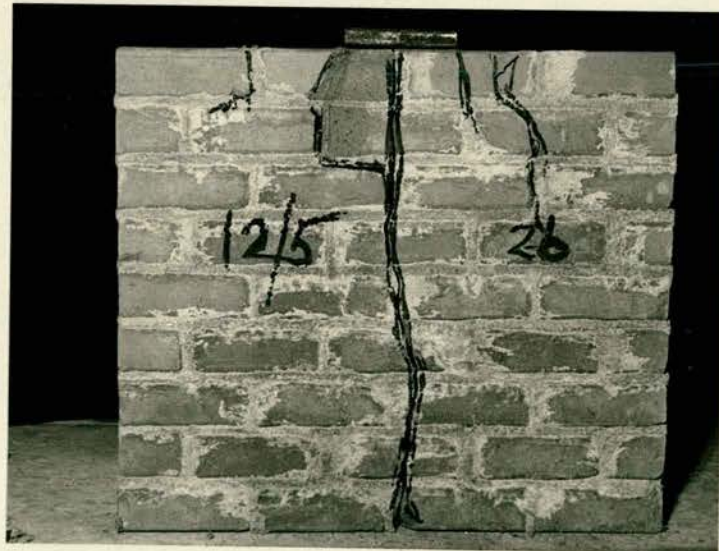


1/3rd. Scale Brick Wall - Central Bearing Plate -
Failure by Vertical Cracking and Substantial Spalling.
Plate 6-6



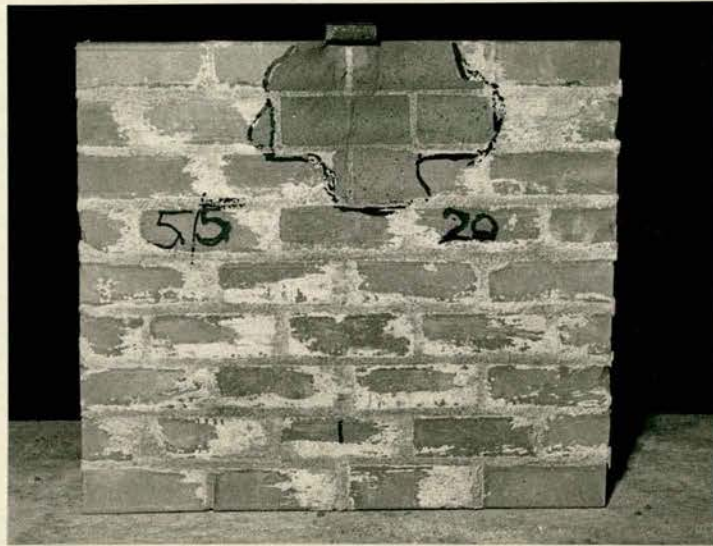
1/3rd. Scale Brick Wall - Central Bearing Plate -
Failure by Vertical Cracking, Local Spalling,
and Diagonal Shear Crack.

Plate 6 - 7



1/3rd. Scale Brick Wall - Central Bearing Plate -
Failure by Vertical Cracking, Spalling, and Surface
Cracking.

Plate 6 - 8



1/3rd. Scale Brick Wall - Central Bearing Plate -
Failure by Spalling on Both Faces.
Plate 6-9



1/3rd. Scale Brick Wall - Central Bearing Plate -
Failure by Spalling on One Face Only.
Plate 6 - 10

occurring on the centre line of the bearing plate, in the region of the bearing plate. Further down the wall section the maximum compressive strain is observed to occur on the free edge of the wall. At these levels the strain distribution across the face of the wall is observed to have become triangular, with tensile strains occurring towards the unloaded edge.

The angle of strain distribution across the section was 20° , compared with the value of 45° which is sometimes suggested as suitable.

A previous test with a 3" end bearing plate gave a strain distribution of approximately 25° , whilst one with a 1" end bearing plate gave approximately 35° . The distribution towards the base of both sections became triangular.

Fig. 6-8 illustrates the horizontal strain distribution, and indicates two distinct types of horizontal tensile strains. These may be termed "tear" tensile strains, which occur along the top surface of the wall, and "splitting" tensile strains which occur below the bearing plate.

In the zone of load application the horizontal strains are compressive, decreasing to a zero value at a certain depth, and then increasing again, until a maximum tensile strain is measured at some distance from the level of load application.

The distribution of the splitting tensile strain is that of a vertical bulb of pressure, on a section line through the bearing plate. Because of the non-homogeneous nature of brickwork the horizontal

strains generally occur in the vertical mortar joints, and for this reason plots of both the maximum tensile strains occurring, and the average strain over three readings have been presented. In fact both are similar, but the average plot evens out some of the irregularities of the single readings.

The stress levels in the other tests conducted were lower, and no significant tensile strain patterns were observed.

Strain readings taken on both faces of the wall indicated a reasonably uniform strain distribution across the width of the wall, and the strain profiles were similar.

Plate 6-11 shows the model wall before testing.

ii. Central Bearing Plates.

Figs. 6-9 and 6-10 illustrate the vertical and horizontal strain distributions in a 1/3rd scale wall, below a 1.5" central bearing plate.

Fig. 6-9 shows the vertical strain distribution to be a bulb of pressure below the bearing plate, with the maximum strain occurring directly beneath the centre line of the bearing plate. In the vicinity of the bearing plate the strain distribution is locally confined, whereas towards the base of the wall the distribution is approximately uniform.

Three vertical strain contours have been superimposed on the strain distribution, at strains of 30, 60, and 90×10^{-5} , and illustrate the bulb of pressure. These contours were constructed assuming the measured strain occurred at the mid-point of the strain interval, e.g. A-E, occurs at C.

The angle of effective strain distribution is 30° . Similar results were obtained from two other tests, with 1" and 3" central

bearing plates.

Fig. 6-10 illustrates the horizontal strain distribution beneath the bearing plate. This clearly indicates that at low stresses a compressive zone exists directly below the bearing plate (this was confirmed by other tests). However as the applied compressive stress increased the compressive zone decreased, and tensile strains predominated from the surface to the base of the section.

The relative properties of the materials incorporated in the bearing will considerably affect the degree of lateral restraint provided, and hence the strain distribution below the bearing plate.

The horizontal strains have been plotted, for a vertical section, on the bearing plate centre-line, and also the total strain (proportional to total deflection) for three adjacent vertical sections. The strain plots indicated that bulbs of horizontal tensile strain occur, with maximum values 2-3" below the bearing plate. The plot of total tensile strain evens out the individual discrepancies of the centre-line strain readings, and is geometrically similar.

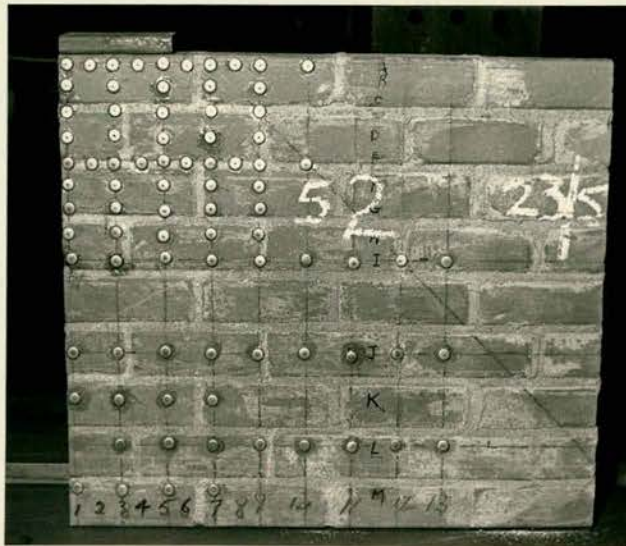
Plate 6-12 shows the model wall before testing.

iii. Comparison with Full-Scale Tests.

A comparison of Figs. 3-4 to 3-8 and Figs. 3-16 to 3-20 (in Chapter 3) shows the similarity in the strain distributions observed, for the full-scale and 1/3rd scale model tests.

10. CONCLUSIONS.

i. The behaviour of full-scale, 1/6th scale and 1/3rd scale walls is similar, when the walls are subjected to end and central concentrated loadings of various lengths.



1/3rd. Scale Brick Wall - Demec Stud
Positions for End Bearing Strain
Measurements.

Plate 6-11



1/3rd. Scale Brick Wall - Demec Stud
Positions for Central Bearing Strain
Measurements.

Plate 6-12

- ii. The failure stresses increase for both end and central bearing plates as the bearing plate size decreases.
- iii. The failure stresses of central bearing plates are higher than those of end bearing plates of the same size, and a ratio of 1.30 was found for the bearing plates from 9" - 4 $\frac{1}{2}$ " full-scale.
- iv. Modes of failure vary, and the failure stresses vary according to the mode. Statistically the results are satisfactory despite this variation.
- v. Safety factors in C.P.111:1964 are adequate at present, but further full-scale work is required, together with a more rigorous investigation of the effect of the variation of the bearing materials on the failure stress.
- vi. The effect of edge distance is significant, and it is recommended that bearings are designed to take account of this.
- vii. The strain distribution is similar in full-scale and 1/3rd scale walls, and resembles that observed in an elastic homogeneous material.

Table 6 - 1

Bearing Plate Sizes.

Full-Scale Size (ins.)	9	7	6	4.5	3	1.5
1/6th Scale Nominal (ins.)	1.5	1.167	1.00	0.75	0.5	0.25
1/6th Scale Actual (ins.)	1.516	1.187	1.029	0.76 0.74	0.52	0.279
1/3rd Scale Nominal (ins.)	3.00	2.33	2.00	1.50	1.00	0.50
1/3rd Scale Actual (ins.)	3.02	2.35	2.00	1.52	1.05	0.52

Table 6 - 2

1/6th Scale Brickwork - 1.516 End B.P. - Series I.

Wall No.	Failure Stress pf. s. i.	* Brickwork Brick	+ Brickwork Brick	Initial Cracking Stress pf. s. i.	Mode of Failure.
1	2,145	.329	.282	2,145	Split in width - Diag. cracks on faces.
1	2,210	.339	.291	2,210	Split in width - Diag. and Vert. cracks on faces - Spalling.
1a	2,050	.314	.270	2,000	Split in width - Spalling & Diag. cracks - Vert. crack on face.
1a	2,050	.314	.270	2,000	Split in width - Spalling & Diag. cracking.
1b	1,810	.278	.238	1,750	Vert. crack on face - Split in width.
1b	2,120	.325	.279	2,050	Split in width - Vert. crack on face.
34	1,700	.261	.224	1,700	Split in width - Vert. crack from edge of load.
35	1,955	.300	.257	1,690	Vert. crack below load - Split in width.
35	2,080	.319	.274	2,080	Split in width - Diag. crack & spalling on one face.
36	2,270	.348	.299	2,270	Vert. cracks - Split in width.
36	1,955	.300	.257	1,955	Sudden failure - Spalling on one face, below load.
37	1,965	.301	.259	1,965	Split in width.
Average	2,026	.311	.267	—	—

Range (1,700 - 2,270) pf. s. i., Standard Deviation = 159 pf. s. i.

Coefficient of Variation = 7.9%. Age at test, approximately 30 days.

* Brick Strength - B.S. 1257. + Dry Brick Strength.

Table 6 - 3

1/6th Scale Brickwork - 1.187 End B.P. - Series I

Wall No.	Failure Stress pf. s. i.	[*] <u>Brickwork</u> Brick	⁺ <u>Brickwork</u> Brick	Initial Cracking Stress pf. s. i.	Mode of Failure.
2	2,304	.353	.303	2,155	Split in width - Spalling on end - Spalling on one face.
3	2,330	.357	.307	2,290	Split in width - Vert. crack on one face - Diag. crack - Spalling.
3	2,805	.430	.369	2,560	Split in width - Vert. crack on face - Spalling on faces - Diag. crack.
4	2,440	.374	.321	2,330	Sudden failure - Vert. crack beneath load - Spalling - Diag. crack.
4	2,000	.307	.263	1,885	Vert. crack - Split in width - Spalling on one face.
31	2,040	.313	.269	2,000	Sudden failure - Splitting and cracking.
31	1,890	.290	.249	1,890	Vert. cracking on faces - Split in width.
32	2,145	.329	.282	2,145	Split in width - Vert. cracking on faces.
32	1,915	.294	.252	1,915	Split in width.
33	2,135	.327	.281	2,135	Vertical crack below B.P.
33	2,185	.335	.288	2,185	Split in width - Vert. crack on face.
34	2,240	.344	.295	2,075	Vert. crack below load - Split in width - Spalling.
Average	2,202	.338	.290	—	—

Range (1,890 - 2,805) pf. s. i. Standard Deviation = 253 pf. s. i.

Coefficient of Variation = 11.5%.

* Brick Strength - B.S. 1257. + Dry Brick Strength.

Table 6 - 4

1/6th Scale Brickwork - 1.029" End B.P. - Series I.

Wall No.	Failure Stress pf.s.i.	* Brickwork Brick	+ Brickwork Brick	Initial Cracking Stress pf.s.i.	Mode of failure.
5	2,120	.325	.279	2,120	Split in width - Vert. crack - Spalling on faces.
5	2,460	.377	.324	2,425	Split in width - Diag. crack - Spalling near corner.
6	2,320	.356	.305	1,710	Crack at base - Vert. crack - Spalling on face.
6	2,430	.373	.320	2,270	Vert. crack on face - Split in width - Spalling on face.
7	2,555	.392	.336	2,555	Vert. crack on face - Split in width - End column splits away.
7	2,360	.362	.311	2,360	Split in width - Spalling on face.
24	2,505	.384	.330	2,330	Vert. crack on face - Split in width - Diag. crack - Spalling.
24	2,270	.348	.299	2,270	Split in width - Diag. cracks.
29	2,270	.348	.299	2,175	Vert. crack below load - Split in width.
29	2,240	.344	.295	2,220	Split in width - Vert. cracks on faces - Spalling on end.
30	2,580	.396	.340	2,580	Vert. crack below load - Column breaks away.
30	2,365	.363	.311	2,330	Vert. crack below load.
Average	2,373	.364	.312	—	—

Range (2,120 - 2,580) pf.s.i. Standard Deviation = 138 pf.s.i.

Coefficient of Variation = 5.8%.

* Brick Strength - B.S. 1257. + Dry Brick Strength.

Table 6 - 5

1/6th Scale Brickwork - 0.76" End B.P. - Series I.

Wall No.	Failure Stress pf.s.i.	[*] Brickwork Brick	⁺ Brickwork Brick	Initial Cracking Stress pf.s.i.	Mode of Failure.
8	2,440	.374	.321	2,440	Split in width - Vert. crack - Spalling on face. Split in width - Vert. crack on face - Spalling on end.
8	2,970	.456	.391	2,970	
9	2,110	.324	.278	2,110	Split in width - Vert. crack below load - Spalling on faces.
9	2,440	.374	.321	2,440	Split in width - Vert. cracks on faces - Spalling on face.
10	2,760	.423	.363	2,525	Vert. crack below load - Split in width - Spalling on face.
10	3,200	.491	.421	2,610	Split in width - Sudden failure - Spalling on one corner.
18	2,610	.400	.344	2,610	Split in width - Slight Diag. crack - Spalling on face.
18	2,950	.452	.388	2,950	Vert. crack on faces - Spalling at one corner.
23	2,530	.388	.333	1,770	Split in width - Vert. crack on face - Diag. crack - Spalling on faces.
23	2,740	.420	.361	2,740	Vert. crack below load - Split in width - Diag. split on face.
26	2,485	.381	.327	2,190	Vert. crack below load - Split in width.
26	2,655	.407	.350	2,655	Split in width - Vert. crack below load.
Average	2,658	.408	.350	—	—

Range (2,110 - 3,200) pf.s.i. Standard Deviation = 292 pf.s.i.

Coefficient of Variation = 11.0%.

* Brick Strength - B.S. 1257. + Dry Brick Strength.

Table 6 - 6

1/6th Scale Brickwork - 0.52" End B.P. - Series 1.

Wall No.	Failure Stress pf. s. i.	[*] Brickwork Brick	⁺ Brickwork Brick	Initial Cracking Stress pf. s. i.	Mode of Failure.
11	2,710	.416	.357	2,710	Split in width - Spalling at end - Vert. crack below load.
11	3,570	.548	.470	3,570	Vert. crack below load - Split in width - Spalling on faces.
12	3,140	.482	.413	3,140	Split in width - Vert. crack on faces - Spalling on face.
12	3,380	.518	.445	3,380	Split in width - Vert. crack below load - Diag. crack - Spalling.
16	3,020	.463	.398	3,020	Spalling from one face.
16	3,440	.528	.453	3,380	Vert. crack below load - Split in width - Spalling on one face.
17	3,510	.538	.462	3,510	Vert. crack on faces - Split in width.
17	2,710	.416	.357	2,710	Vert. crack on faces - Split in width - Spalling on face.
21	2,620	.402	.345	2,620	Sudden failure - Spalling of one corner.
21	3,080	.472	.406	2,460	Spalling on one corner - Vert. crack - Split in width.
28	3,010	.462	.396	3,010	Spalling on both faces.
28	2,895	.444	.381	2,895	Vert. crack on faces - Spalling on one face.
38	2,710	.416	.357	2,710	Vert. crack below load - Split in width - Spalling on face.
38	2,400	.368	.316	2,400	Spalling on one face.
Average	3,014	.462	.397	—	—

Range (2,400 - 3,570) pf. s. i. Standard Deviation = 363 pf. s. i.

Coefficient of Variation = 12%.

* Brick Strength - B.S. 1257. + Dry Brick Strength.

Table 6 - 7

1/6th Scale Brickwork - 0.279" End B.P. - Series I.

Wall No.	Failure Stress pf. s. i.	* Brickwork Brick	+ Brickwork Brick	Initial Cracking Stress pf. s. i.	Mode of Failure.
13	3,720	.571	.490	3,720	Spalling on face - Vert. crack below B.P.
13	3,090	.474	.407	2,290	Split in width - Vert. crack below B.P. - Diag. crack - Spalling.
14	2,980	.457	.392	2,065	Vert. cracking and spalling.
14	3,610	.554	.475	3,610	Split in width - Vert. crack on face - Spalling on face.
15	3,900	.598	.513	3,900	Spalling on end and face - Vert. crack below B.P.
15	3,300	.506	.434	3,300	Spalling on end - Vert. crack below B.P.
20	3,300	.506	.434	3,300	Vert. crack below B.P. - Spalling on end.
20	3,210	.492	.423	2,980	Vert. crack below B.P. - Secondary vert. cracks.
22	4,020	.617	.529	4,020	Spalling on one face - Vert. cracking on both faces.
22	3,440	.528	.453	3,270	Vert. cracking below B.P. at corner - Spalling on faces.
25	4,240	.650	.558	4,240	Vert. cracking on faces - Spalling below B.P. and on corner.
25	3,900	.598	.513	3,900	Vert. cracking on faces - Split in width - Spalling on corner.
Average	3,559	.546	.469	—	—

Range (2,980 - 4,240) pf. s. i. Standard Deviation = 400 pf. s. i.

Coefficient of Variation = 11.2%.

* Brick Strength - B.S. 1257. + Dry Brick Strength.

Table 6 - 8

1/6th Scale Brickwork - 1.516" End B.P. - Series II.

Wall No.	Failure Stress pf. s. i.	[*] Brickwork Brick	⁺ Brickwork Brick	Initial Cracking Stress pf. s. i.	Mode of Failure.
12	2,140	.328	.282	2,140	Spalling on one face.
12	1,970	.302	.259	1,970	Splitting in width.
13	2,610	.400	.344	2,240	Splitting in width.
13	2,760	.423	.363	2,140	Splitting in width.
14	2,250	.345	.296	2,250	Sudden - Spalling on one face.
14	2,280	.350	.300	2,280	Sudden - Spalling on one face.
15	1,950	.299	.257	1,890	Split in width - Spalling on one face.
15	2,200	.337	.290	2,200	Splitting in width.
23	1,960	.301	.258	1,960	Splitting in width.
23	2,240	.344	.295	2,240	Splitting in width.
25	2,205	.338	.290	1,900	Split in width - Vert. crack on face - Spalling on face.
25	2,375	.364	.313	1,370	Vert. crack from base - Crack below load - Split in width.
30	2,420	.371	.319	2,420	Splitting in width.
30	1,865	.286	.246	1,615	Spalling on face - Further spalling.
31	2,065	.317	.272	2,065	Breaking away of corner section.
31	1,910	.293	.251	1,910	Vert. split in width - Diag. crack on face - Spalling on same face.
Average	2,200	.337	.290	—	—

Range (1,865 - 2,760) pf. s. i. Standard Deviation = 253 pf. s. i.

Coefficient of Variation = 11.5%.

* Brick Strength - B.S. 1257. + Dry Brick Strength.

Table 6 - 9

1/6th Scale Brickwork - 1.187" End B.P. - Series II.

Wall No.	Failure Stress pf.s.i.	* Brickwork Brick	+ Brickwork Brick	Initial Cracking Stress pf.s.i.	Mode of Failure.
10	2,440	.374	.321	2,440	Vert. crack from base - Local crushing.
10	2,155	.331	.284	1,480	Vert. crack from base - Split in width - Spalling on face.
11	2,490	.382	.328	2,400	Split in width - Cracking on face below B.P.
11	1,935	.297	.255	1,935	Spalling on face.
16	2,120	.325	.279	2,120	Spalling on face.
16	2,480	.380	.327	2,480	Spalling at one corner.
17	2,080	.319	.274	1,955	Vert. crack on face - Spalling on other face.
17	2,370	.363	.312	2,020	Spalling on one corner - Spalling on face.
18	2,120	.325	.279	2,120	Vert. cracking on face.
18	2,370	.363	.312	2,370	Split in width - Spalling on face.
19	2,120	.325	.279	2,120	Split in width.
19	2,285	.350	.301	2,285	Spalling on face.
28	2,410	.370	.317	2,170	Vert. crack below B.P.
28	2,260	.347	.298	2,075	Vert. crack below B.P.
34	2,220	.340	.292	2,180	Splitting in width.
34	2,250	.345	.296	2,250	Splitting in width.
Average	2,257	.346	.297	—	—

Range (1,935 - 2,490) pf.s.i. Standard Deviation = 161 pf.s.i.

Coefficient of Variation = 7.1%.

* Brick Strength - B.S. 1257. + Dry Brick Strength.

Table 6 - 10

1/6th Scale Brickwork - 1.029" End B.P. - Series II.

Wall No.	Failure Stress pf. s. i.	* Brickwork Brick	+ Brickwork Brick	Initial Cracking Stress pf. s. i.	Mode of Failure.
2	1,735	.266	.228	1,735	Splitting in width - Spalling and crushing.
2	2,460	.377	.324	2,200	Spalling on both faces.
3	1,960	.301	.258	1,960	Splitting in width - Cracks on faces.
3	1,890	.290	.249	1,890	Splitting in width - Spalling on face.
4	1,955	.300	.257	1,865	Splitting in width.
4	2,640	.405	.348	2,145	Splitting in width - Cracking on face - Spalling on face.
5	2,120	.325	.279	1,865	Spalling on face.
5	2,210	.339	.291	2,175	Splitting in width - Spalling on face.
20	2,380	.365	.313	2,050	Vert. cracking below B.P. - End section breaks away.
20	2,065	.317	.272	1,710	Vert. cracking below B.P.
21	2,180	.334	.287	2,145	Splitting in width - Spalling on face.
21	2,650	.406	.349	2,650	Splitting in width - Spalling and crushing.
26	2,570	.394	.338	2,490	Splitting in width - Spalling on face.
26	2,570	.394	.338	2,570	Splitting in width - Spalling on face.
29	2,320	.356	.305	2,320	Splitting in width - Vert. cracking on face.
29	2,575	.395	.339	2,575	Spalling on one face.
33	2,665	.409	.351	2,395	Splitting in width - Corner breaks away.
35	2,335	.358	.307	2,335	Splitting in width.
35	2,085	.320	.275	2,085	Spalling on face.
Average	2,282	.350	.300	—	—

- 166 -

Range (1,735 - 2,665) pf. s. i. Standard Deviation = 289 pf. s. i.

Coefficient of Variation = 12.6%. * Brick Strength - B.S. 1257. + Dry Brick Strength.

Table 6 - 11

1/6th Scale Brickwork - 0.74" End B.P. - Series II.

Wall No.	Failure Stress pf. s. i.	* Brickwork Brick	+ Brickwork Brick	Initial Cracking Stress pf. s. i.	Mode of Failure.
6	2,460	.377	.324	2,460	Splitting in width - Vert. crack below B.P.
6	1,580	.242	.208	1,580	Splitting in width - Crushing of section.
7	2,410	.370	.317	2,410	Spalling on face.
7	2,240	.344	.321	2,240	Vert. cracks on faces - Splitting in width.
8	2,240	.344	.321	2,240	Vert. splitting on faces - Spalling on faces.
8	2,850	.437	.375	2,850	Vert. cracking below B.P. - Spalling on faces.
9	2,280	.350	.300	2,280	Splitting away of a wall section.
9	2,220	.340	.292	2,075	Splitting in width - Vert. cracks on faces - Spalling on face.
22	2,300	.353	.303	2,300	Spalling on face - Vert. cracking on faces.
22	2,760	.423	.363	2,680	Split in width - Vert. crack on face - Spalling on face.
24	2,830	.434	.373	2,830	Vert. crack below B.P.
24	2,630	.403	.346	2,530	Splitting in width - Vert. cracking on face.
27	2,920	.448	.384	2,920	Spalling on face.
27	2,500	.383	.329	2,500	Breaking away of wall column - Vert. cracking.
32	2,500	.383	.329	2,500	Vert. cracking on face below B.P. - Breaking away of wall column.
32	1,800	.276	.237	1,800	Spalling on face.
Average	2,408	.369	.317	—	—

Range (1,580 - 2,920) pf. s. i. Standard Deviation = 365 pf. s. i.

Coefficient of Variation = 15.2%.

* Brick Strength - B.S. 1257. + Dry Brick Strength.

Table 6 - 12

1/6th Scale Brickwork - 1.516", 1.187" and 1.029" Central B.P.
- Series I.

Wall No.	Size of Bearing Plate-ins.	Failure Stress pf. s. i.	[*] Brickwork Brick	⁺ Brickwork Brick	Initial Cracking Stress pf. s. i.	Mode of Failure.
21	1.516	2,640	.405	.348	2,260	Vert. crack - Spalling over circular area - Splitting in width.
25	"	2,715	.416	.357	2,715	Spalling on both faces - No vert. cracking.
26	"	2,460	.377	.324	2,450	Off-centre vert. crack - Spalling on both faces.
27	"	2,680	.411	.353	1,055	Vert. cracking - Spalling on one face.
37	"	2,470	.379	.325	845	Diag. crack from centre line of B.P. - Spalling on one face.
Average	"	2,593	.398	.341	—	—
22	1.187	2,750	.422	.362	2,560	Diag. crack - Spalling on one face - Splitting in width.
28	"	3,280	.503	.432	2,320	Vert. crack below B.P. - Spalling on both faces.
38	"	2,460	.377	.324	2,460	Spalling on both faces.
Average	"	2,830	.434	.373	—	—
20	1.029	3,325	.510	.438	2,490	Vert. crack below load - Diag. cracks - Spalling on one face.
24	"	2,890	.443	.381	2,890	Spalling on both faces - more on one face.
33	"	2,985	.458	.393	2,985	Spalling on both faces - Diag. cracks.
Average	"	3,067	.470	.404	—	—

* Brick Strength - B.S. 1257. + Dry Brick Strength.

Table 6 - 13

1/6th Scale Brickwork - 0.74", 0.52" and 0.279" Central B.P.
- Series I.

Wall No.	Bearing Plate Length - ins.	Failure Stress pf. s. i.	* Brickwork Brick	+ Brickwork Brick	Initial Cracking Stress pf. s. i.	Mode of Failure.
18	0.76	3,370	.517	.444	2,740	Diag. cracks - Spalling on one face.
19	"	4,080	.625	.537	2,950	Vert. crack from base - Spalling on face - Diag. crack.
29	0.74	3,220	.494	.424	2,900	Diag. crack below centre-line - Spalling on faces.
30	"	3,440	.528	.453	3,440	Vert. cracks - Diag. cracks - Spalling and Splitting in width.
32	"	2,960	.454	.390	1,730	Vert. crack below B.P. - Spalling on both faces.
Average	"	3,414	.524	.450	—	—
16	0.52	4,000	.613	.526	4,000	Spalling on one face - Vert. crack below B.P.
17	"	3,140	.482	.413	2,590	Spalling on both faces - Vert. cracking.
31	"	3,910	.600	.515	3,750	Spalling on one face, followed by Spalling on other.
36	"	4,500	.690	.592	3,500	Diag. crack on face - Spalling on both faces.
Average	"	3,888	.596	.512	—	—
13	0.279	4,930	.756	.649	4,930	Vert. crack below B.P. - Spalling below B.P.
14	"	8,025	1.231	1.056	4,930	Slight crack below B.P. - Spalling on one face.
15	"	6,300	.966	.829	5,850	Diag. crack below B.P. - Vert. crack - Spalling.
Average	"	6,418	.984	.845	—	—

* Brick Strength - B.S. 1257. + Dry Brick Strength.

Table 6 - 14

1/6th Scale Brickwork - 1.516" Central B.P. - Series II.

Wall No.	Failure Stress pf. s. i.	[*] Brickwork Brick	⁺ Brickwork Brick	Initial Cracking Stress pf. s. i.	Mode of Failure.
1	2,830	.434	.373	2,425	Spalling below B.P. - Vert. splitting below B.P.
4	2,500	.383	.329	2,320	Vert. crack below B.P. - Spalling in width.
5	2,230	.342	.294	1,690	Vertical cracking.
6	2,510	.385	.330	2,430	Vert. cracking - Splitting in width.
7	3,050	.468	.402	2,320	Vert. cracking - Split in width - Spalling on faces.
8	3,320	.509	.437	2,270	Vert. crack from base - Spalling on face - Split in width.
20	1,985	.304	.261	1,690	Off centre cracking - Top courses break up.
26	2,765	.424	.364	2,500	Vert. cracking - Spalling on both faces - Split in width.
32	2,395	.367	.315	2,320	Vert. cracking - Spalling on one face.
34	2,830	.434	.373	2,215	Vertical cracking below B.P.
Average	2,642	.409	.351	—	—

Range (1,985 - 3,320) pf. s. i. Standard Deviation = 410 pf. s. i.

Coefficient of Variation = 15.4%.

* Brick Strength - B.S. 1257. + Dry Brick Strength.

Table 6 - 15

1/6th Scale Brickwork - 1.187" Central B.P. - Series II.

Wall No.	Failure Stress pf. s. i.	* <u>Brickwork</u> Brick	+ <u>Brickwork</u> Brick	Initial Cracking Stress pf. s. i.	Mode of Failure.
9	2,905	.446	.382	2,905	Off-centre vert. crack - Spalling on faces.
11	3,360	.515	.442	2,940	Off-centre diag. crack, from B.P. - Spalling on face.
16	3,120	.479	.411	2,670	Off-centre vert. crack - Splitting in width.
17	2,220	.340	.292	2,220	Diag. crack from B.P.
18	2,500	.383	.329	2,450	Vert. crack below B.P. - Spalling on face.
19	3,640	.558	.479	2,695	Vert. crack below B.P. - Spalling on both faces.
21	2,700	.414	.355	2,370	Vert. crack below B.P. - Spalling on face - Diag. crack.
35	3,540	.543	.466	2,535	Vert. crack below B.P. - Spalling on both faces.
Average	2,998	.460	.395	—	—

Range (2,220 - 3,640) pf. s. i. Standard Deviation = 501 pf. s. i.

Coefficient of Variation = 16.7%.

* Brick Strength - B.S. 1257. + Dry Brick Strength.

Table 6 - 16

1/6th Scale Brickwork - 1.029" Central B.P. - Series II.

Wall No.	Failure Stress pf. s. i.	* Brickwork Brick	+ Brickwork Brick	Initial Cracking Stress pf. s. i.	Mode of Failure.
2	2,750	.422	.362	2,425	Vert. crack below B.P. - Spalling on faces - Splitting in width.
3	2,800	.429	.369	2,800	Diag. crack from below B.P.
10	2,870	.440	.378	901	Diag. cracks below B.P.
22	2,715	.416	.357	2,675	Vert. crack below B.P. - Spalling - Splitting in width.
28	3,660	.561	.482	3,295	Vert. crack below B.P.
29	3,440	.528	.453	3,250	Vert. crack below B.P. - Splitting in width.
30	3,110	.477	.409	2,425	Vert. crack below B.P.- Splitting in width.
31	2,585	.396	.340	2,585	Spalling on one face.
35	3,465	.531	.456	2,920	Vert. crack below B.P. - Spalling on both faces.
Average	3,043	.473	.405	—	—

Range (2,585 - 3,660) pf. s. i. Standard Deviation = 309 pf. s. i.

Coefficient of Variation = 12.8%.

* Brick Strength - B.S. 1257. + Dry Brick Strength.

Table 6 - 17

1/6th Scale Brickwork - 0.74" Central B.P. - Series II.

Wall No.	Failure Stress pf. s. i.	* Brickwork Brick	+ Brickwork Brick	Initial Cracking Stress pf. s. i.	Mode of Failure.
12	2,995	.459	.394	2,160	Spalling on one face - Splitting in width.
13	4,340	.666	.571	4,040	Spalling on both faces - Splitting in width.
14	3,820	.585	.503	3,050	Off-centre vert. crack - Spalling on face - Split in width.
15	3,440	.528	.453	3,440	Vert. crack below B.P.- Splitting in width.
23	3,010	.462	.396	3,010	Crushing below B.P. - Brick fails locally.
24	3,250	.498	.560	2,550	Spalling on both faces - Splitting in width.
25	3,315	.508	.436	3,000	Diag. crack from B.P. - Cracks widen considerably.
33	3,715	.570	.489	3,715	Vert. crack below load - Spalling and Crushing on face.
Average	3,486	.535	.459	—	—

Range (2,995 - 4,340) pf. s. i. Standard Deviation = 455 pf. s. i.

Coefficient of Variation = 13.1%.

* Brick Strength - B.S. 1257. + Dry Brick Strength.

Table 6 - 18

1/6th Scale - 1" Mortar Cube Strengths.

Series	Age-Days.	No. of Cubes.	Ave. Compr. Strength pf. s. i.
Series I	30	9	2,000
Range (1,750 - 2,330) pf. s. i. Standard Deviation = 183 pf. s. i. Coefficient of Variation = 9.2%.			
Series I	90	8	2,348
Range (1,815 - 3,070) pf. s. i. Standard Deviation = 405 pf. s. i. Coefficient of Variation = 17.2%.			
Series I	60	9	2,888
Range (1,815 - 3,470) pf. s. i. Standard Deviation = 540 pf. s. i. Coefficient of Variation = 18.7%.			
Series I	40	3	1,988
Series II	360	14	2,985
Range (2,220 - 3,740) pf. s. i. Standard Deviation = 531 pf. s. i. Coefficient of Variation = 17.8%.			

Table 6 - 19

1/3rd Scale Brickwork - 3.02" End B.P. - Series I.

Wall No.	Age at Test-Days.	Failure Stress pf. s. i.	* Brickwork Brick	Initial Cracking Stress pf. s. i.	Mode of Failure.
1	35	923	.317	790	Vert. crack on face - Split in width.
1	35	1,174	.403	854	Vert. crack from base - Split in width - Spalling.
2	35	803	.276	695	Vert. crack at base - Splitting in width - Spalling.
2	35	753	.259	750	Vert. crack below load - Spalling.
43	47	959	.329	790	Split in width - Diag. crack - Spalling on one face.
43	47	1,089	.374	870	Splitting in width - Diag. crack - Vert. crack - Split.
44	47	1,029	.353	820	Split in width - Spalling on one face.
44	47	1,104	.379	1,100	Splitting in width - Vert. crack on face - Spalling on face.
45	48	1,018	.350	905	Splitting in width - Crack on face - Spalling.
45	48	1,126	.387	1,100	Split in width - Vert. crack on faces - Diag. crack from B. P.
Average	—	998	.343	—	—

Range (753 - 1,174) pf. s. i. Standard Deviation = 127 pf. s. i.

Coefficient of Variation = 12.7%.

* Brick Strength - B.S. 1257.

Table 6 - 20

1/3rd Scale Brickwork - 2.35" End B.P. - Series I.

Wall No.	Age at Test-days	Failure Stress pf. s. i.	* Brickwork Brick	Initial Cracking Stress pf. s. i.	Mode of Failure.
3	34	1,052	.361	1,052	Vert. crack below B.P. - Split in width - Spalling.
3	34	1,052	.361	1,052	Split in width - Vert. crack on faces.
4	34	1,019	.350	1,000	Splitting in width - Vert. crack on faces.
4	34	984	.338	870	Splitting in width - Vert. crack on faces - Spalling.
30	80	1,145	.393	1,145	Vert. crack below B.P. - Splitting in width - Spalling on one face.
41	46	1,086	.373	855	Split in width - Vert. crack on faces - Diag. cracks - Spalling.
41	46	1,053	.362	855	Splitting in width - Vert. crack on faces.
42	37	1,144	.393	790	Slight vert. crack on one face - Split in width - Spalling on end.
42	37	1,100	.378	855	Splitting in width - Vert. crack on face - Spalling.
Average	—	1,071	.368	—	—

Range (984 - 1,145) pf. s. i. Standard Deviation 53 pf. s. i.

Coefficient of Variation = 4.9%.

* Brick Strength - B.S. 1257.

Table 6 - 21

1/3rd Scale Brickwork - 2.0" End B.P. - Series I.

Wall No.	Age at Test-Days.	Failure Stress pf. s. i.	* Brickwork Brick	Initial Cracking Stress pf. s. i.	Mode of Failure.
5	34	1,029	.353	1,010	Split in width - Vert. crack below B.P. - Spalling of a column.
5	34	1,082	.372	905	Split in width - Vert. crack below B.P. - Spalling of a column.
6	35	981	.337	965	Split in width - Vert. crack on faces - Section breaks away.
6	35	989	.340	980	Vert. crack below B.P. - Splitting in width.
39	35	1,237	.425	1,120	Vert. crack on one face - Splitting in width - Spalling.
39	35	1,300	.446	1,005	Split in width - Vert. crack on face - Diag. cracks - Spalling.
40	37	827	.284	710	Vert. crack on faces, from base - Column splits away.
40	37	1,105	.379	835	Vert. crack below B.P. - Splitting in width.
Average	—	1,068	.366	—	—

Range (827 - 1,300) pf. s. i. Standard Deviation = 150 pf. s. i.

Coefficient of Variation = 14%.

* Brick Strength - B.S. 1257.

Table 6 - 22

1/3rd Scale Brickwork - 1.52" End B.P. - Series I.

Wall No.	Age at Test Days	Failure Stress pf.s.i.	* Brickwork Brick	Initial Cracking Stress pf.s.i.	Mode of Failure.
7	35	896	.308	810	Splitting in width - Vert. crack below B.P. - Column breaks away.
7	35	1,060	.364	1,025	Split in width - Vert. crack below B.P. - Spalling.
8	35	1,132	.389	955	Vert. crack on faces - Split in width.
8	35	969	.333	955	Splitting in width - Spalling of a large portion.
37	43	976	.335	945	Split in width - Vert. cracks on face - Spalling.
37	43	1,087	.373	1,015	Split in width - Vert. crack on faces below load - Spalling.
38	44	1,261	.433	860	Split in width - Vert. cracks on faces - Spalling at end.
38	44	1,169	.401	1,015	Split in width - Vert. cracks on faces - Diag. cracks - Spalling.
Average	—	1,069	.367	—	—

Range (896 - 1,261) pf.s.i. Standard Deviation = 119 pf.s.i.

Coefficient of Variation = 11.2%.

* Brick Strength - B.S. 1257.

Table 6 - 23

1/3rd Scale Brickwork - 1.05" End B.P. - Series I.

Wall No.	Age at Test Days	Failure Stress pf. s. i.	* Brickwork	Initial Cracking Stress pf. s. i.	Mode of Failure.
			Brick		
9	36	1,134	.389	1,090	Splitting in width - Vert. cracks on faces.
9	36	1,208	.415	1,180	Splitting in width.
10	37	1,149	.395	1,030	Splitting in width - Vert. cracks on face.
10	37	1,076	.370	880	Split in width - Vert. crack below B.P.
35	43	1,017	.349	910	Splitting in width - Vert. crack on faces.
35	43	1,163	.399	1,163	Split in width - Vert. cracking below B.P. - Spalling.
36	44	1,258	.432	1,250	Split in width - Vert. cracks on faces - Spalling.
36	44	1,163	.399	1,163	Split in width - Cracking on faces - Spalling.
Average	—	1,146	.394	—	—

Range (1,017 - 1,258) pf. s. i. Standard Deviation = 74 pf. s. i.

Coefficient of Variation = 6.5%.

* Brick Strength - B.S. 1257.

Table 6 - 24

1/3rd Scale Brickwork - 0.52" End B.P. - Series I.

Wall No.	Age at Test Days	Failure Stress pf. s. i.	* Brickwork Brick	Initial Cracking Stress pf. s. i.	Mode of Failure.
27	80	1,220	.385	1,220	Local Spalling.
33	43	1,159	.398	1,130	Split in width - Cracking on face - Spalling from end.
33	43	1,188	.408	1,155	Cracking and spalling below load.
34	43	1,161	.399	1,130	Local spalling below load.
34	43	1,292	.444	1,155	Vert. crack on one face - Split in width - Local Spalling.
48	49	1,220	.419	1,200	Vert. crack on face - Split in width - Spalling.
48	49	1,515	.520	1,485	Vert. crack on faces - Spalling from end.
Average	—	1,251	.430	—	—

Range (1,159 - 1,515) pf. s. i. Standard Deviation = 125 pf. s. i.

Coefficient of Variation = 9.9%.

* Brick Strength - B.S. 1257.

Table 6 - 25

1/3rd Scale Brickwork - 3.02" End B.P. - Series II.

Wall No.	Failure Stress pf. s. i.	[*] Brickwork Brick	Initial Cracking Stress pf. s. i.	Mode of Failure.
49	1,437	.493	1,260	Spalling on one face - Vertical crack on faces - Spalling on both faces.
49	1,290	.443	1,080	Spalling of corner - Spalling on both faces.
52	1,390	.477	1,010	Vertical splitting - Spalling.
52	1,140	.391	1,010	Vertical Splitting - Spalling.
54	1,023	.351	755	Splitting in width - Spalling on one face.
54	1,025	.352	910	Splitting in width - Spalling of corner.
56	1,180	.405	1,000	Vertical crack below B.P., from base upwards - Splitting - Spalling.
56	1,265	.434	1,010	Splitting in width - Diag. cracks from B.P.
58	800	.275	730	Spalling on one face.
58	1,172	.402	705	Spalling on one face.
60	1,310	.450	935	Splitting in width, causes failure.
60	832	.286	805	Spalling on one face.
62	966	.332	830	Splitting in width - Spalling on one face.
62	1,070	.367	1,060	Splitting in width - Spalling on one face.
Average	1,136	.390	—	—

Range (800 - 1,437) pf. s. i. Standard Deviation = 194 pf. s. i.

Coefficient of Variation = 17.1%.

* Brick Strength - B.S. 1257.

Table 6 - 26

1/3rd Scale Brickwork - 2.5" and 1.52" End B.P. - Series II.

Wall No.	Bearing Plate Length ins.	Failure Stress pf. s. i.	* Brickwork Brick.	Initial Cracking Stress pf. s. i.	Mode of Failure.
50	2.5	1,595	.548	914	Splitting in width - Vert. cracks on faces - Spalling near base.
50	2.5	1,062	.365	1,050	Splitting in width - Spalling on one face.
Average	—	1,284	.441	—	—
53	1.52	1,180	.405	800	Splitting in width - Spalling on corner column.
53	"	1,355	.465	1,000	Splitting in width - Vert. cracks on faces - Spalling on one corner.
55	"	1,185	.407	1,150	Splitting in width - Spalling on both faces.
55	"	977	.374	977	Spalling from one corner.
57	"	1,173	.403	1,100	Splitting in width.
57	"	1,200	.412	920	Spalling at one corner - Spalling on faces.
59	"	1,170	.385	950	Splitting in width - Spalling on one face.
59	"	880	.302	880	Splitting in width - Spalling on one face.
61	"	1,268	.442	1,150	Splitting in width.
61	"	1,645	.565	1,200	Spalling on one face - Vert. cracking on faces.
Average	—	1,203	.413	—	—

Range (880 - 1,645) pf. s. i. Standard Deviation = 227 pf. s. i.

Coefficient of Variation = 18.9%.

* Brick Strength - B.S. 1257.

Table 6 - 27

1/3rd Scale Brickwork - 3.02" and 2.35" Central B.P. - Series I.

Wall No.	Age at Test Days	Bearing Plate Size ins.	Failure Stress pf. s. i.	*Brickwork		Initial Cracking Stress pf. s. i.	Mode of Failure,
				Brick			
8	80	3.02	1,350	.464	1,150	Vert. crack below B.P. - Spalling on face - Split in width.	
11	36	"	1,489	.487	1,060	Vert. crack - Diag. cracks on one side of B.P.	
12	36	"	1,326	.455	-	Vert. crack below B.P. - Diag. cracks - Spalling.	
13	36	"	1,052	.361	920	Vert. crack below B.P. - Diag. cracks - Split in width.	
28	46	"	1,168	.401	930	Vert. crack on face - Spalling on one face.	
29	45	"	1,018	.350	820	Vert. crack below B.P. - Spalling below B.P. on faces.	
Average	—	—	1,234	.424	—	—	
14	36	2.35	1,522	.523	1,250	Vert. cracking below load - Spalling on both faces.	
15	36	"	1,313	.451	355	Vert. cracking (Low load) - Diag. cracks - Spalling on faces.	
26	43	"	1,190	.409	1,005	Vert. cracking below load - Spalling on one face.	
27	43	"	1,158	.398	1,130	Vert. cracking below load - Spalling on one face.	
39	80	"	1,250	.429	920	Vert. cracking below load - Spalling on both faces.	
Average	—	—	1,287	.442	—	—	

- 183 -

Ranges - 3.02" (1,018 - 1,489) pf. s. i. - 2.35" (1,158 - 1,522) pf. s. i.

* Brick Strength - B.S. 1257.

Table 6 - 28

1/3rd Scale Brickwork - 2.0" and 1.52" Central B.P. - Series I.

Wall No.	Age at Test Days	Bearing Plate Length ins.	Failure Stress pf.s.i.	* Brickwork Brick	Initial Cracking Stress pf.s.i.	Mode of Failure.
9	80	2.0	1,830	.628	1,420	Vert. crack below B.P. - Shear cracks from B.P.
16	35	"	1,190	.409	1,120	Vert. crack below B.P. - Spalling below B.P., both faces.
17	36	"	1,777	.610	1,210	Vert. crack below B.P. - Diag. cracks - Spalling both faces.
24	43	"	1,152	.396	1,010	Vert. crack below B.P. - Spalling below B.P.
25	43	"	1,128	.387	1,128	Spalling causes failure - No vert. cracking.
38	80	"	1,275	.438	1,105	Vert. cracking below B.P. - Spalling on one face.
Average	—	—	1,392	.478	—	—
18	36	1.52	1,420	.488	1,420	Vert. crack below B.P. - Local Spalling - Shear cracks.
19	39	"	1,524	.523	1,524	Vert. cracks below B.P. - Local Spalling on both faces.
22	43	"	1,240	.426	1,100	Vert. crack below B.P. - Spalling on both faces.
23	43	"	1,372	.471	1,372	Vert. cracking below B.P. - Spalling on faces.
36	80	"	1,635	.561	1,565	Vert. crack below B.P. - Diag. cracking - Spalling on faces.
Average	—	—	1,438	.494	—	—

Ranges - 2.0" (1,128 - 1,830) pf.s.i. - 1.52" (1,155 - 1,635) pf.s.i.

* Brick Strength - B.S. 1257.

Table 6 - 29

1/3rd Scale Brickwork - 1.05" and 0.52" Central B.P. - Series I.

Wall No.	Age at Test Days	Bearing Plate Size ins.	Failure Stress pf. s. i.	* Brickwork Brick	Initial Cracking Stress pf. s. i.	Mode of Failure.
20	48	1.05	1,850	.635	1,470	Local spalling on one face - No vert. cracking. Vert. crack below load - Spalling below load, both faces. Spalling below load - Vert. crack below load. Vert. crack below load - Spalling on both faces. Vert. crack below load - Spalling both faces. Vert. crack below load - Spalling on both faces.
21	43	"	1,620	.556	1,250	
22	43	"	1,790	.615	1,790	
35	80	"	1,685	.579	1,685	
37	80	"	1,785	.613	1,785	
48	40	"	1,678	.576	1,545	
Average	—	—	1,735	.596	—	—
30	45	0.52	2,110	.725	2,080	Vert. crack below load - Diag. cracks - Spalling on both faces. Spalling below load on one face - Vert. crack below load. Vert. crack below load - Spalling below load both faces. Diag. crack - Spalling on one face - Vert. cracking. Vert. crack below load - Diag. crack - Spalling.
31	45	"	2,440	.838	2,440	
32	45	"	2,080	.714	2,080	
33	43	"	2,200	.755	2,200	
34	43	"	2,642	.907	2,640	
Average	—	—	2,294	.788	—	—

Ranges - 1.05" (1,620 - 1,850) pf. s. i. - 0.52" (2,080 - 2,642) pf. s. i.

* Brick Strength - B.S. 1257.

Table 6 - 30

1/3rd Scale Brickwork - 3.02" and 1.52" Central B.P. - Series II.

Wall No.	Bearing Plate Length ins.	Failure Stress pf. s. i.	[*] Brickwork Brick	Initial Cracking Stress pf. s. i.	Mode of Failure.
53	3.02	1,400	.481	730	Vert. crack below B.P. - Diag. cracks - Spalling on one face.
55	"	1,485	.510	860	Vert. crack below B.P. - Spalling mainly on one face.
57	"	1,580	.543	1,135	Off-centre crack - Spalling - Diag. cracks.
59	"	1,300	.446	1,120	Off-centre crack - Spalling - 2nd off-centre crack.
60	"	1,440	.495	1,185	off-centre crack.
61	"	1,575	.541	1,210	Vert. crack below B.P. - Spalling on both faces.
Average	-	1,463	.502	-	—
46	1.52	1,563	.537	1,500	Vert. crack below B.P. - Spalling on one face.
49	"	1,775	.610	1,705	Diag. crack below B.P. - Vert. crack below B.P.
52	"	1,663	.571	1,605	Vert. crack below B.P. - Spalling on both faces.
54	"	1,710	.587	1,400	Vert. crack below B.P. - Spalling on both faces.
56	"	1,850	.635	1,150	Slightly off-centre crack - Spalling on one face.
58	"	1,625	.558	1,615	Vert. crack below B.P. - Spalling on both faces.
Average	-	1,698	.583	-	—

Ranges - 3.02" (1,300 - 1,580) pf. s. i. - 1.52" (1,563 - 1,850) pf. s. i.

* Brick Strength - B.S. 1257.

Table 6 - 31

1/3rd Scale - 1" Mortar Cube Strengths.

Series	Age-Days.	No. of Cubes.	Ave. Compr. Strength - pf. s. i.
Series I	40	10	2,565
Range (1,860 - 3,495) pf. s. i.			Standard Deviation = 533 pf. s. i.
Coefficient of Variation = 20.8%.			
Series I	60	10	2,276
Range (1,700 - 2,840) pf. s. i.			Standard Deviation = 349 pf. s. i.
Coefficient of Variation = 15.3%.			
Series II	360	14	2,985
Range (2,220 - 3,740) pf. s. i.			Standard Deviation = 531 pf. s. i.
Coefficient of Variation = 17.8%.			

Table 6 - 32

1/3rd Scale Brickwork - 1.05" B.P. : Position Variable - Series I(a).

Wall No.	Edge Distance d-ins.	L/a	L/d	Failure Stress pf. s.i.	* Brickwork	Initial Cracking Stress pf. s.i.	Mode of Failure.
					Brick		
23	0.75	5.2	7.3	1,528	.525	1,528	Vert. crack below B.P. - Spalling on faces.
25	0.75	10.5	14.7	1,140	.391	955	Diag. crack below B.P., towards end - Spalling at end.
28	1.0	5.5	5.5	1,520	.522	1,515	Vert. crack below load - Split in width - Spalling on faces.
23	1.0	4.8	5.0	1,445	.496	1,400	Vert. crack below B.P. - Spalling on faces.
22	1.0	10.5	11.0	1,675	.575	1,660	Slightly diag. crack from B.P. - Spalling on faces.
22	1.0	7.9	8.3	1,135	.390	1,120	Diag. crack from B.P. to end face - Spalling one face.
28	1.375	5.5	4.2	1,325	.455	1,310	Spalling one face - Vert. crack below load.
24	1.50	5.5	3.8	1,860	.639	1,860	Vert. crack below B.P. - Section breaks away at end.
20	1.5	10.5	7.3	1,420	.488	1,400	Vert. crack below B.P. - Spalling.
25	1.5	10.5	7.3	1,415	.486	1,415	Vert. crack below B.P. - Split in width - Diag. cracks - Spalling.
30	2.0	3.6	1.9	1,720	.591	1,720	Vert. crack below load.
32	2.75	5.2	2.0	1,490	.512	1,480	Vert. crack below B.P. - Spalling on one face.
37	2.75	5.2	2.0	1,785	.613	1,785	Vert. crack below B.P. - Spalling on both faces.
33	2.8	4.8	1.8	1,610	.553	1,485	Vert. crack below B.P. - Spalling on one face.
35	3.75	9	2.5	1,685	.579	1,685	Vert. crack below B.P. - Spalling on both faces.

L = Specimen Length; a = Bearing Plate Length; d = Edge Distance to Centre-Line of Bearing Plate.

* Brick Strength - B.S. 1257.

Table 6 - 33

1/3rd Scale Brickwork - 0.52" B.P. : Position Variable - Series I (a).

Wall No.	Edge Distance d - ins.	L/a	L/d	Failure Stress pf. s. i.	* Brickwork	Initial Cracking Stress pf. s. i.	Mode of Failure.
					Brick		
26	0.51	11.1	11.3	1,650	.567	1,650	End section shears from centre of B.P. Vert. crack below B.P. - Spalling on one face.
21	0.51	11.1	11.13	1,515	.520	1,040	
24	0.76	11.1	7.6	1,515	.520	1,190	Spalling on one face - Diag. crack from B.P. to edge.
26	1.01	11.1	5.7	1,930	.663	1,930	Vert. crack below B.P., becomes Diag. at depth to edge - Spalling.
27	1.26	11.1	4.6	1,665	.572	1,635	Vert. crack below B.P.
28	1.36	8.7	3.3	1,945	.668	1,900	Diag. cracks - Spalling on one face - Vert. crack below B.P.
29	1.37	10.6	4.0	2,260	.776	2,260	Vert. crack below B.P. - Spalling on one face.
27	1.37	10.6	4.0	2,160	.742	2,160	Vert. crack below B.P.
29	1.37	10.6	4.0	2,320	.797	2,080	Vert. crack below B.P. - Spalling on faces.

L = Specimen Length; a = Bearing Plate Length; d = Edge Distance to Centre-Line of Bearing Plate.

* Brick Strength - B.S. 1257.

Table 6 - 34

Allowable Stresses in Brickwork - C.P.111 : 1964.

Type of Brick.	Full Scale	1/6th Scale	1/3rd Scale Type I.
Unit Compressive Strength pf. s. i.	6,675 [*]	6,520 [*]	2,912 [*]
Unit Basic Stress pf. s. i. - Table 3	460.5	451.2	234.7
Reduction Factor ⁺ for Area	0.865	0.823	0.825
Reduction Factor for Slenderness	1.0	0.964	0.964
Factor for Concentrated Loading	1.5	1.5	1.5
Combined Factor	1.3	1.191	1.195
Final Allowable Stress - pf. s. i.	577	537	280
Allowable Brickwork/Brick	0.086	0.082	0.096
5 x Allowable Brickwork/Brick	0.432	0.412	0.481

* Brick Strength - B.S. 1257.

+ Areas for 1/6th and 1/3rd Scale were actual areas.

x 36 and 9 respectively.

Table 6 - 35

Safety Factors for Brickwork - C.P.111 : 1964.

Brick Type		1/6th Scale.											
Bearing Plate Type		End B.P.						Central B.P.					
Bearing Plate Size - ins.*		9	7	6	4.5	3	1.5	9	7	6	4.5	3	1.5
Series I	Ave.	3.8	4.1	4.4	5.0	5.6	6.7	4.2	4.5	4.9	5.5	6.2	10.3
	Min.	3.2	3.5	4.0	4.0	4.5	5.6	4.0	4.0	4.6	4.8	5.0	7.9
Series II	Ave.	4.1	4.2	4.3	4.5	-	-	5.0	5.6	5.8	6.5	-	-
	Min.	3.5	3.6	3.2	2.9	-	-	3.7	4.1	4.8	5.6	-	-
		1/3rd Scale.											
Series I	Ave.	3.6	3.8	3.8	3.8	4.1	4.5	4.4	4.6	5.0	5.1	6.2	8.2
	Min.	2.7	3.5	3.0	3.2	3.6	4.1	3.6	4.1	4.0	4.1	5.8	7.4
Series II	Ave.	4.1	-	-	4.3	-	-	5.2	-	-	6.1	-	-
	Min.	2.9	-	-	3.1	-	-	4.6	-	-	5.6	-	-
		Full-Scale.											
	Ave.	4.3	4.9	4.5	5.3	-	-	4.7	-	-	8.4	-	-
	Min.	3.2	3.8	3.8	4.8	-	-	4.7	-	-	7.1	-	-

* Based on Full-Scale B.P. Sizes.

CHAPTER 7.

CAVITY WALLS - AN INTRODUCTION.

1. GENERAL CONSIDERATIONS.

The cavity wall is a very widely used form of construction in Great Britain, for single and two storey dwellings and for this form of construction the loads applied are such that there is no question of the limiting strength of the wall being reached.

The thermal insulation and weathering properties of cavity walls have led to their adoption as structural members in load-bearing brickwork structures of a multi-storey type. In Switzerland, where many multi-storey load-bearing brickwork structures have been built, solid brick walls, rendered on the outside, have been utilised, and test programmes have concentrated on the properties of single leaf walls of varying thicknesses and dimensions.

The theoretical analysis of single leaf walls incorporated into load-bearing structures has been investigated by Sven Sahlin⁽⁵⁶⁾ and others, and suggestions have been proposed for the design of masonry members subject to axial and eccentric compressive forces. Many tests have also been conducted, to check the validity of the theories developed, and reasonable correlation has been found.

Special attention was paid in Sahlin's tests to the interaction between the floor slabs, and the two leaves of a cavity wall, which is particularly important when assessing the load bearing capacity of the cavity wall subjected to the normal loads associated with a structural member.

The assessment of the load distribution between the two leaves of a cavity wall, when the floor slab or edge beam bears onto the leaves is difficult, and will depend on such factors as the relative stiffnesses of the members, the degree of fixity of the slab to wall junction, and the dimensional accuracy of the construction of the two leaves.

For design purposes it has been necessary to make certain assumptions about the behaviour and load distributing properties of cavity walls. C.P.111:1964⁽¹⁾ gives very little information on how cavity walls should be considered from a load distribution point of view, and considers two possible cases of loading. The first is when the load is shared between the leaves, and the code recommends using a permissible stress based on a slenderness ratio calculated from an effective thickness of $2/3$ of the sum of the individual leaf thicknesses. Such an approach leaves the designer to assess the distribution of load between the two leaves when floor loadings are included in the analysis.

The second case is when one leaf only is considered as load bearing, and here the permissible stress is based on the slenderness ratio of this leaf. The load bearing member is similar to a single leaf wall, and provision has only to be made for the lateral stability of the unloaded leaf. However the provision of lateral restraint can lead to the transfer of load in the form of bending moment.

It is known that thermal changes can cause differential expansion between the two leaves, but the magnitudes of the stresses caused by such differential movement are unknown and are usually ignored.

With the increasing use of load-bearing brickwork construction

the need for experimental research on the load distribution characteristics of cavity walls has become obvious, and certain test programmes have been initiated.

2. PREVIOUS EXPERIMENTAL INVESTIGATIONS.

2.1 WALL TIE TESTS.

As far as the author is aware there have been only two investigations of cavity wall behaviour up to the present date, although further work is proceeding.

F.G. Thomas ⁽⁵⁷⁾ has described tests carried out at the Building Research Station, to investigate the efficiency of metal wall ties in ensuring the equal lateral deflection of both leaves of a cavity wall, when the load is applied eccentrically to one leaf only.

In some tests the load was applied in such a way that the wall ties were subjected to compression, and the loaded leaf deflected in such a way as to exert a thrust on the unloaded leaf. In other tests the eccentric load caused the wall ties to be subjected to tension, and the unloaded leaf to be pulled into the same deflected shape as the loaded leaf.

The wall ties used in the construction of the cavity walls were of two types. Both were Butterfly types, but one was 9. S.W.G. steel wire, and the other 12 S.W.G. copper wire, complying with the minimum requirements of B.S. 1243, "Metal Wall Ties".

The results of the tests conducted clearly showed that wall ties of the types traditionally used are sufficient to ensure that any bending moments induced by eccentric loading, on one or both of the

leaves, will be shared by the leaves in proportion to the stiffnesses (EI) of the leaves. Thus, if the cavity leaves are similar the provision of wall ties allows the "eccentric moment" to be equally shared by the leaves.

Unfortunately the provision of wall ties of this type can lead to rather unexpected results if the load is applied eccentrically to only one leaf, Fig. 7-1. The strength of the two types of wall tie are such that very little, if any, direct compressive load can be transferred from the loaded to the unloaded leaf by shear action, and hence the unloaded leaf is subject only to bending moment. As is well known, the tensile strength of brickwork is low, and rather an unknown quantity, and hence the unloaded leaf may crack, well before the loaded leaf has attained its full load potential. It is possible that the sudden transference of load, from the unloaded to the loaded leaf, on the cracking of the unloaded leaf may cause the premature failure of the loaded leaf.

From the above it is evident that it is desirable that both leaves should sustain at least some portion of the compressive load. This is of course more economic in terms of the utilisation of the full strength potential of the cavity system, although it complicates the analysis of the system.

Experience and tests have indicated that the provision of wall ties as indicated by the Code gives a reasonable margin of safety against the structural failure of the ties, even when the lightest ties permitted are used. For multi-storey construction it is recommended

that strip metal ties are used. Tests have shown that a strip metal tie can transfer at least 800 lbf. in direct compression.

These tests, whilst providing valuable information on the behaviour of wall ties, have not considered the distribution of load between the two leaves, when the load is applied through the floor slab to both leaves.

2.2 LOAD DISTRIBUTION TESTS.

i. Scope of the Tests Conducted.

R. Bradshaw ⁽⁵³⁾ carried out a series of tests on single leaf walls, investigating the strain distribution on the wall faces, with axially and eccentrically applied loads. As part of a long term series of tests on cavity walls he investigated two axially loaded walls, the load being applied through 6" reinforced concrete slabs.

The object of the tests was to determine the actual stress distribution in the leaves of a cavity wall, when the wall was axially loaded through a 6" floor slab, 10' - 6" long, and simply supported at its free end. The walls tested were 10.5" cavity constructions, 8'-2" high, and 4'-6" wide. The bricks used had a compressive strength of 3,710 pf. s.i., and the walls were constructed in stretcher bond, with galvanised strip metal wall ties. The mortar joints were 3/8" nominal, and a 1:3 cement to sand mix was used.

ii. Test Results.

The results obtained are of considerable interest. The failure stresses were 770 pf. s.i., and 855 pf. s.i., giving brickwork/brick ratios of 0.208 and 0.230 respectively, which compare with 0.26-0.47

for single leaf walls constructed using bricks with a compressive strength of 6,235 pf. s.i.

iii. Discussion of Results.

(a) Strength Factors.

The results obtained confirmed the work of Haller⁽¹⁰⁾, who has shown that single leaf walls are considerably stronger than bonded walls.

Why a cavity wall should be weaker than two similarly constructed single leaf walls is not immediately clear, but can be explained when a number of factors are considered. Despite the fact that nominally the walls were constructed so that the load would be axially applied, the strain readings obtained on each face showed that in fact the load was being eccentrically applied, particularly in the lower stress ranges. In fact, the results obtained indicated that at no stress level did the more highly stressed leaf carry less than 70% of the applied load, if the loads are computed directly from the strain readings, assuming no bending stresses. This corresponds to a strain ratio of 2.3 for the two leaves. If bending is allowed for in the calculation then the load ratio is 1.63:1.

From the point of view of the safety of the cavity wall as a whole, it is the highest stress or strain which is important and taking the stress ratio as 2.3:1 then this leads to a failure load of 0.72 compared with the axially loaded wall. Thus a reduction of 28% compared with the axial failure load would be observed.

(b) Strain Measurements.

It is interesting to note that the strains on each face were measured using vertical extensometers attached to both wall faces and measuring over a gauge length of 72 ins. The extensometers consisted of a rod, fixed at one end, the other end being clamped to the spindle of a dial gauge, which was itself fixed to the wall. The wall fixings consisted of pieces of angle section, which were screwed onto the brickwork face.

The type of strain measurement indicated above suffers from the disadvantage that the dial gauge and rod are fixed about 2" from the wall surface, and hence any rotation of the bracket due to lateral deflection of the wall will produce corresponding deflection readings of the dial gauge, which do not represent the strain on the actual surface of the wall. The magnitude of this effect is unknown, but casts doubt on the validity of the readings obtained. This suggests that further dial gauges are required, positioned on the centre line of each leaf, or on the internal faces of the leaves.

The 72" gauge length chosen has certain disadvantages, as only the average strain can be computed. Bradshaw conducted three single leaf wall tests, in which an 8" Demec gauge was employed to determine the distribution of horizontal and vertical strains on the two faces. The results obtained indicated that "there appeared to be no clear pattern of horizontal and vertical strains over the wall face and a more detailed study is required. Uneven bedding of the top slab may have a considerable influence on this". In much of the work described in this thesis Demec gauges have been used for the measurement of

strains, and significant results have been obtained.

(c) Workmanship Factors.

The uneven distribution of strain in a seemingly axially loaded member may have been caused by one or more failures in maintaining the dimensional accuracy of the wall construction.

If the wall was constructed off plumb, then the resulting eccentricity is obvious. Similarly, if one leaf is constructed appreciably higher than the other uneven load distribution will result although the magnitude of such an effect is unknown.

If the floor slab is unevenly bedded then non-uniform load distribution will occur. As the method of fixing the slab consisted of lowering it 1/2" onto a bed of mortar, and allowing the bed to squeeze out, until the desired thickness was reached, then such unevenness is a possibility.

(d) Modulus of Elasticity.

The modulus of elasticity calculated was the Secant modulus, and was found to vary, decreasing with increasing stress. Typical of the results obtained were moduli of 1×10^6 pf.s.i. at 100 pf.s.i. and 0.53×10^6 pf.s.i. at 500 pf.s.i. The modulus was calculated from the average stress and strain values.

(e) Mode of Failure.

The failures in both cavity tests were initiated by vertical hair cracks, followed by spalling and load crushing of the brickwork.

(f) Design Considerations.

The load factors, based on C.P.111:1964 were 3.8 and 4.4.

These values are rather low, a factor of six being considered suitable, and are only about half the load factors obtained for the single leaf walls tested. However, it seems likely that the mortar strengths, which at the times of testing were only 335 pf. s. i. and 670 pf. s. i. respectively, were at least partly responsible for the low strengths.

(g) Rate of Loading.

It is evident that in the testing of all materials subject to creep strain, a time factor plays an important part. The plastic flow of mortar under load is known to be quite considerable, and research conducted by Lenczner has shown that whilst instantaneous strain plays an important role in the deformation of a brick structure, creep strain also occurs, fairly rapidly in the first instance. The rate of creep deformation then slows down, either continuing at a fairly uniform rate, or stopping altogether.

In some controlled tests, structures subject to sustained loading, at a high stress level, have continued to deform, and have eventually collapsed more than a year after the application of the load. Such collapses due to creep were noticed particularly when the original loading was applied eccentrically. The creep deformation under load increased this eccentricity, thus increasing the applied stress. Such a system is unstable, and is likely to collapse ultimately. The precise point at which such a structure becomes unstable is not known, and has been shown to vary from structure to structure. Identically constructed and loaded specimens subjected to sustained loadings have been found to behave differently. For example, one will deform

under load instantaneously, continue to deform due to creep, and then stabilise, with a cessation of movement. Another will not attain a stabilised condition, and will continue to deform steadily, ultimately failing.

This knowledge of the non-elastic deformation properties of brickwork leads to the conclusion that even in short term testing the time factor is important. If a series of gauge readings have to be taken at each load increment, then some delay is inevitable, and creep strain can be observed. This phenomenon is particularly evident at higher stresses, and the extra strain can lead to failure at a lower stress than would otherwise have been observed.

Bradshaw⁽⁵³⁾ has concluded that there is no noticeable reduction in the strength of otherwise identical walls, when the time of testing is prolonged within normal limits.

For specimens such as brickwork cubes it seems reasonable that a standard rate of loading should be specified in order that a uniformity of results between different sets of specimens may be obtained. The 2,000 pf. s. i. /minute generally agreed on seems reasonable, and should enable the standardisation of the testing of brickwork control specimens.

In conducting a series of tests of a relatively new nature, in order to determine the basic strength properties of single leaf or cavity walls it would seem essential that the tests are conducted at such a rate of loading that the failure stress is not overestimated.

Certain time limitations exist for obvious practical reasons,

but where possible sufficient time should be allowed for instantaneous deformation, and initial creep strain to take place. Initial creep strain is rather a vague term, and cannot be precisely defined, but is that creep which takes place relatively quickly after the application of the load. Very slow rates of loading would be acceptable, if these were necessary to allow readings to be taken, as this could lead to only a lower failure stress. High rates of loading can only cast doubts on the validity of the results obtained.

3. A THEORETICAL INVESTIGATION OF THE STRESS DISTRIBUTION IN A CAVITY WALL.

3.1 ASSUMPTIONS.

(a) The load is applied to the cavity wall through a floor slab which absorbs no moment, so that all the eccentric moment is distributed to the two cavity wall leaves. In practice, in wall and slab construction, the stiffness of the floor slab will be such that it is capable of resisting applied moments.

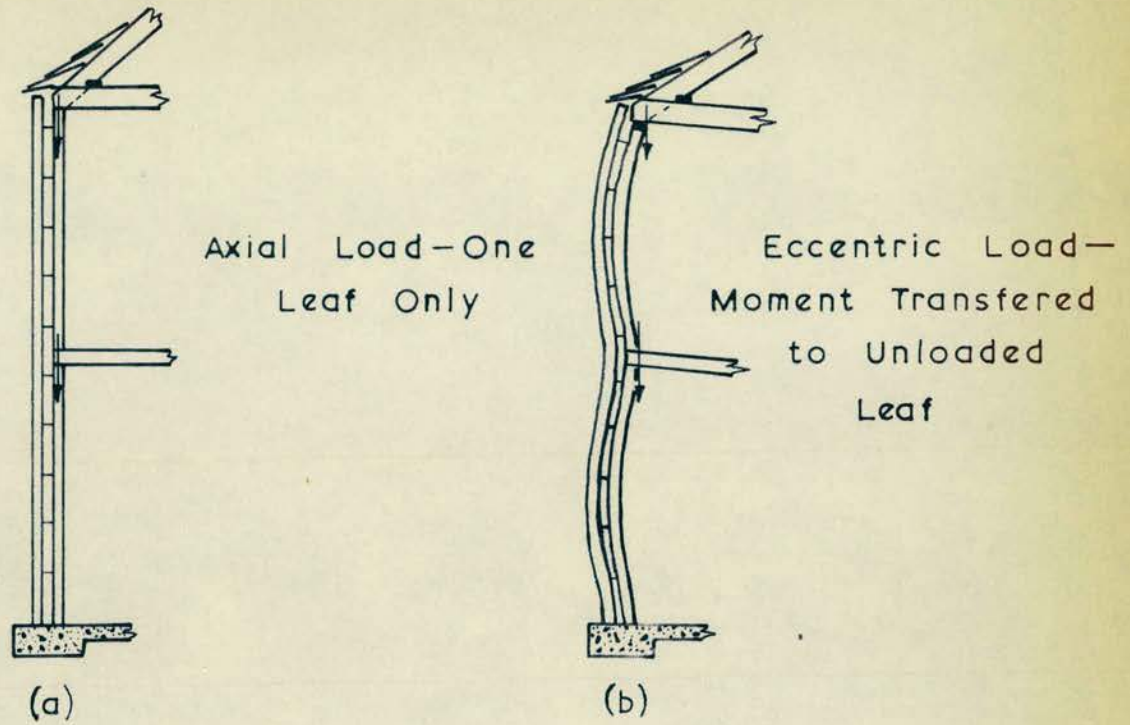
(b) The leaves act together, bending about their combined neutral axis, and the eccentricity of loading is considered as constant down the wall section.

(c) The stress intensity in each leaf will be calculated on the basis of a direct stress, combined with a bending stress.

(d) The stress ratio will be calculated from the stresses, as indicated in (c), in the first instance.

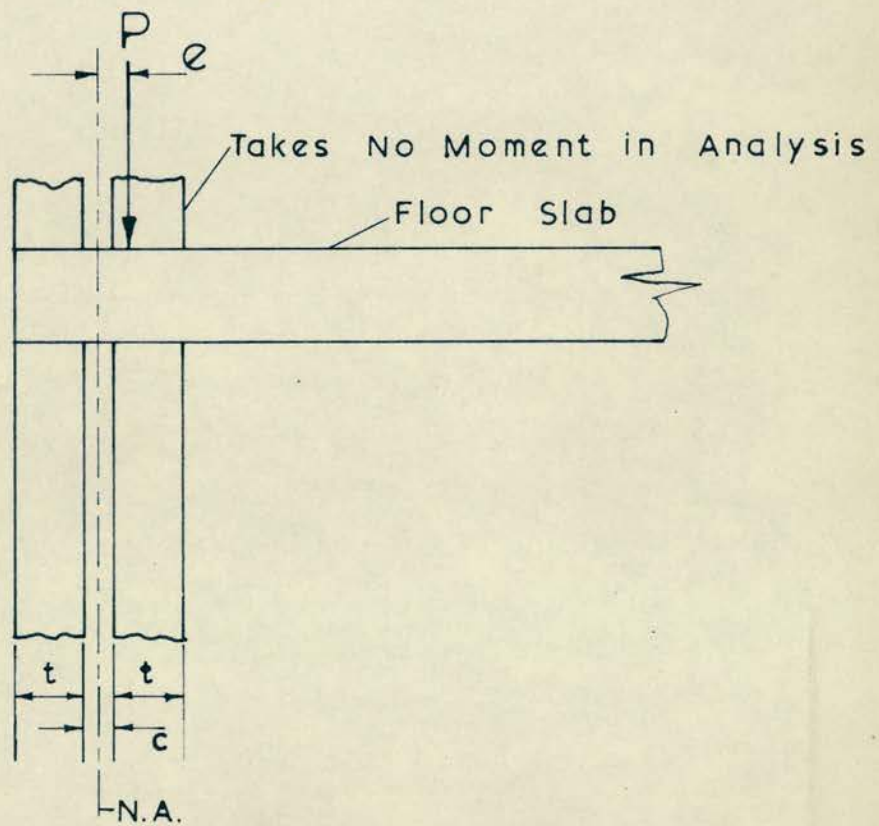
3.2 CALCULATION OF STRESSES.

Referring to Fig. 7-2, and taking P as the applied load/in.



The Effect of Eccentricity of Load & Wall Ties

Fig. 7-1



Loading System for Cavity Wall

Fig. 7-2

along the slab.

The direct stress = $P/2t$

The bending stresses are $\frac{\pm P.e (t + c/2)}{I N.A.}$

where $I N.A. = 2 \left\{ \frac{t^3}{12} + t \left\{ t/2 + c/2 \right\}^2 \right\}$

∴ The combined stresses are,

$$\frac{P}{2t} \pm \frac{P.e (t + c/2)}{I N.A.}$$

The edge stress ratio is therefore,

$$\frac{\frac{P}{2t} + \frac{P.e (t + c/2)}{I N.A.}}{\frac{P}{2t} - \frac{P.e (t + c/2)}{I N.A.}}$$

When the denominator of the expression is zero, then the leaf subject to the tensile bending stress has a zero edge stress, and any further increase in the load eccentricity will lead to tensile stresses being developed in this leaf.

The theoretical edge stress ratios are given in Table 7-1.

Table7 - 1

Theoretical Load Distribution in a Cavity Wall.

Eccentricity - ins.	Eccentricity Factor - F	Stress [*] Ratio	% Load on Higher Stressed Leaf
0	∞	1	50
0.05	74	1.13	51.7
0.075	49.3	1.21	53.0
0.10	37	1.29	53.8
0.125	29.6	1.37	54.8
0.15	24.7	1.46	55.9
0.20	18.5	1.67	57.8
0.30	12.33	2.2	62.0
0.40	9.25	2.99	65.5
0.50	7.40	4.3	69.7
0.60	6.17	6.94	73.5
0.70	5.29	14.7	77.2
0.80	4.62	713.0	80.5

* Assumes both leaves bend about their combined axis.

CHAPTER 8.

THE CAVITY WALL TEST PROGRAMME.

1. THE OBJECTIVE OF THE TEST PROGRAMME.

The test programme was performed in order to:

- (a) Discern the nature of the load distribution between the two leaves of a cavity wall, when the load is applied both axially and eccentrically to the floor slab above the wall.
- (b) Investigate the stress distribution in the individual leaf, both horizontally and vertically, and at varying positions on the wall. In reality the strain distribution has been investigated.
- (c) Investigate the stress/strain relationship when an axial or eccentric concentrated load is applied to the floor slab.
- (d) Investigate the elastic properties of the cavity wall.
- (e) Check the correlation between the theoretical analysis suggested, and the experimental results.

2. THE MATERIALS USED.

2.1 BRICKS.

The brick chosen for the wall construction was a 1/3rd scale model brick, which has the physical properties as given in Table 5-1, Chapter 5. The brick was Type II.

2.2 MORTAR.

The mortar used was a 1:3 mortar by volume, using Leighton Buzzard sand No.21, and rapid hardening Portland cement. All mortar joints were nominally 1/8".

2.3 FLOOR SLAB OR LINTEL.

The slab for the wall was cast using aggregate 3/8" dia., Leighton Buzzard sand, and rapid hardening Portland cement in a 1: 1½ : 3 mix, cement : sand: aggregate. The slab contained considerable M.S. reinforcement of tensile, compressive and shear types. The nominal lintel size was 15" long x 3.5" wide and 2" deep.

2.4

WALL TIES.

Wall ties of a Butterfly type were incorporated in the wall construction. They were made from M.S. wire of B.S.W.G. No.16 (0.064"), and were placed in every fourth course, using three per course. The positioning was staggered, as suggested in C.P.111 : 1964 (1).

2.5

WALL CONSTRUCTION.

The cavity walls were constructed on a M.S. base 1" thick, fitted with side lugs to facilitate handling.

The nominal dimensions of the wall were 15" long x 3.5" thick x 32" high.

To facilitate construction a wooden frame was built, of the required dimensions, and with a movable spacing board between the two leaves. The spacing board, which had the thickness of the cavity required, had courses of brick and mortar joints marked on it, to enable dimensional accuracy to be maintained. By withdrawing the board as the wall was constructed it was possible to place the ties in position. Plate 8-1 shows a typical stage in the construction.

Before construction the frame and the spacing board were greased, using cube mould oil.

1" mortar cubes were cast during construction from several of the batches of mortar used.

After the construction and curing of the wall, under damp sacks, the lintel was mortared into position, using a 2:1 cement: sand mortar.

After a further 30 days curing an overhead crane was utilised to transport the wall and supporting frame into position on the loading beam of an Avery testing machine. The frame was then stripped off, and the wall was then ready for testing.

3. THE SCOPE OF THE INVESTIGATION.

3.1 NATURE OF THE TEST PROGRAMME.

The aim of the investigation was to conduct a series of non-destructive tests on 1/3rd scale cavity walls. As the tests were to be non-destructive then a direct comparison of the results obtained could be made.

The tests were conducted in two distinct phases, and two nominally identical 1/3rd scale cavity walls were constructed as detailed in section 2.5, and one utilised for each series.

The first phase involved taking detailed strain readings on the two exposed leaf faces, referred to as X and Y. In these tests only a central deflection reading was taken at the top of the wall.

The second phase concentrated on taking strain readings across the leaf width, on the two exposed ends, referred to as α and β . A detailed series of lateral deflection tests was carried out as part of this series.

For practical reasons of accessibility it was impossible to combine both series of tests.

The results of phase one and phase two of the test programme

are discussed in Chapters 9 and 10 respectively.

3.2 DISTRIBUTED LOAD INVESTIGATION.

The effect of applying uniformly distributed load to the lintel was investigated, varying the eccentricity of the resultant load from 0 - 0.5" from the longitudinal axis of the lintel.

3.3 CONCENTRATED LOAD INVESTIGATION.

The effect of applying concentrated load to the cavity wall through the lintel was investigated for various types of concentrated load, as follows.

- i. A concentrated load, 3" x 3", positioned on the transverse axis of the lintel, whose eccentricity from the longitudinal axis varied from 0 - 0.5".
- ii. A concentrated load, 3" x 3", positioned with one of its axes parallel to, and 3" from the transverse axis of the lintel. The eccentricity of loading from the longitudinal axis was varied from 0 - 0.5".
- iii. A concentrated load, 3" x 3", placed in certain other positions, with various eccentricities from the longitudinal axis.

3.4 LATERAL DEFLECTION PROFILES.

The lateral deflections of both leaves of the cavity were measured for various types of load application, taking deflections measured using dial gauges.

Certain dial gauge readings were taken onto the lintel, to check the rotation (if any) and to check if any torsion occurred under eccentric loading.

4. METHOD OF STRAIN MEASUREMENT.

A simple, cheap, and reasonably accurate method of ascertaining the horizontal and vertical strains was chosen, that utilised three Demec gauges, of gauge lengths 2", 8" and 12", with strain sensitivities of 2.48×10^{-5} , 1.01×10^{-5} and 6.6×10^{-6} , per dial gauge division, respectively.

The use of the three gauges enabled readings of a local nature, beneath say a concentrated load, to be made, and also readings of a more general nature, some distance from the point of load application. Thus an overall pattern of the strains on both leaves of the cavity was obtained.

The positioning of Demec studs is detailed in Plate 8-2.

In some tests only vertical readings were taken, as it was judged that little information could be obtained from horizontal readings taken at relatively low applied stress.

5. EXPERIMENTAL DETAILS.

5.1 TEST ARRANGEMENT.

The wall under test was positioned centrally on the beam of an Avery testing machine. (Plate 8-2). The maximum load capacity was 100^T , and a suitable load range was chosen for each test.

5.2 LOAD APPLICATION.

The testing machine was of the rigid head type, but in the preliminary tests the platen was free to move in a horizontal lateral direction, being restrained only by friction.

To ensure an even load distribution it was essential that the



A Typical Stage in the 1/3rd. Scale
Cavity Wall Construction.

Plate 8-1



1/3rd. Scale Cavity Wall in Testing Machine
Demec Stud Positions.

Plate 8-2

lintel should be as nearly horizontal as possible. Although care was taken in construction, some misalignment of the lintel was noted on positioning in the Avery. A portion of "I" section joist (Plate 8-2) was required to distribute the load from the head of the machine to the full width of the wall, for the distributed loadings. This section was packed, with a shaved sheet of plywood, giving a horizontal surface. When the load was applied the strain distribution was found to be uniform.

For the 3" x 3" concentrated loading the provision of 1/8" plywood sheets above and below the bearing plate was found to be satisfactory.

The actual lintel dimensions were found to be 15.3" long and 3.7" wide (nominally 15" x 3.5"), but the load was positioned accordingly to give the required eccentricities.

The Avery machine had an arrangement for holding the load steady at any one load, so that a series of strain readings could be taken at any particular load, without assistance.

5.3 LOAD RANGE.

Because of the essentially non-destructive nature of the tests conducted the range of loading chosen had to be such that there was no risk of cracking the specimen within the range.

The brick strength was approximately 5,800 pf.s.i., and the cavity wall strength was anticipated as being from 0.2 to 0.3 of the brick strength, i.e. 1,160 - 1,740 pf.s.i. The lower limit at which initial cracking might occur was taken as 0.4 times the failure stress,

giving a minimum value of 460 pf.s.i. For the preliminary tests the maximum applied stress was taken as 460 pf.s.i., allowing some safety factor. In later tests loadings up to 470 pf.s.i. were allowed, and no cracking was observed.

For concentrated loadings the nature of the load distribution was assumed to be at 45° , through the lintel, and the load applied was quite low. In later tests an estimate of the allowable load was made, based on the observed vertical strains in the uniformly distributed loading tests. Strains were calculated, as the tests proceeded, and checked to see they did not exceed the limit. The safe vertical strain limit was taken as $10 - 12 \times 10^{-4}$.

For eccentric loadings the strain limit was particularly valuable, as the average applied stress had little meaning.

5.4 ZERO READINGS.

An initial compressive load was applied to the wall, before the zero Demec gauge readings were taken. This load was applied in order that the zero readings could be taken without any risk of damage to the wall, caused by lateral deflection.

The initial load was noted, so that a correction to the stress to strain relationship could be made, and the initial tangent modulus calculated.

CHAPTER 9.

PRELIMINARY INVESTIGATIONS OF THE STRAIN
DISTRIBUTION IN A CAVITY WALL.

1. THE CAVITY WALL UNDER TEST.

A 1/3rd scale cavity wall (No. 1) was constructed, as detailed in Chapter 8.

2. TYPES OF LOADING.

2.1 UNIFORMLY DISTRIBUTED LOAD.

Tests were conducted with the load application over the full length of the lintel, with the eccentricities of loading of 0", 0.2", 0.3", 0.4", and 0.5" from the longitudinal axis of the cavity.

2.2 CONCENTRATED CENTRAL LOADINGS.

Tests were conducted with the load applied through a 3" x 3" M.S. bearing plate, 1" thick, positioned symmetrically on the lateral axis of the wall. Eccentricities of 0", 0.2", 0.3", 0.4" and 0.5" were investigated.

2.3 CONCENTRATED ECCENTRIC LOADINGS.

Tests were conducted with a 3" x 3" bearing plate, positioned on the lintel, with one axis parallel to and 3" from the lateral axis of the wall.

Eccentricities of 0", 0.2", 0.3", 0.4", and 0.5" from the longitudinal axis were investigated.

Two tests were conducted with eccentricities of 4" and 6" from the lateral axis of the lintel, but no eccentricity from the longitudinal centre line.

3. MEASUREMENTS TAKEN.

3.1 STRAIN MEASUREMENTS.

Demec gauge readings were taken on the two exposed faces of the leaves, X and Y, using 2", 8", and 12" Demec gauges. The main interest was in the vertical strains, but some horizontal readings were taken, below concentrated loadings, and in the test to failure. Readings were taken at various horizontal levels, across the wall faces.

Plate 9-1 shows the three gauges used.

3.2 LATERAL DEFLECTION MEASUREMENTS.

One complete lateral deflection test was performed, taking readings at the 1/4 points, the mid-height, and at the top of the wall, on both faces, using dial gauges.

In the other tests conducted only the deflection below the load centre-line was taken.

4. RESULTS OF THE TEST PROGRAMME.

4.1 STRESS/STRAIN CHARACTERISTICS WITH DISTRIBUTED APPLIED LOAD.

i. Vertical Strain.

Figs. 9-1, 9-2 and 9-3 indicate the distribution of vertical compressive strain on the faces of both leaves, with eccentricities of loading of 0", 0.3" and 0.5", corresponding to eccentricity factors of $t/12$, and $t/7.5$. The eccentricity factor is designated F (Chapter 7-3, Table 7-1).

Results are not presented for eccentricities of 0.2" and 0.4",



2", 8" and 12" Demec Gauges
Plate 9-1

as they are similar, and are summarised in other figures.

ii. Horizontal Strain.

Figs. 9-4 and 9-5 show the horizontal strain distribution plotted in two different ways, for an axially applied load. The strain distribution is only plotted in the portion of the wall adjacent to the area of load application.

iii. Stress/Strain Relationships.

Figs. 9-6 to 9-8 indicate the Stress/Strain relationships for eccentricities of 0", 0.2" and 0.5", at various positions on the walls. Vertical and horizontal strains are illustrated.

iv. Modulus of Elasticity.

Values of Young's Modulus(E) have been calculated, based on a 30" gauge length. A correction was applied for a non-zero load at the initial Demec readings, and was calculated on the basis of a linear Stress/Strain relationship. The "E" values calculated have been plotted against applied stress in Fig. 9-9.

E values at level F-H, where the moment was observed to be zero are plotted in Fig. 9-10, as a check on the values obtained using a 30" gauge length.

v. Strain Ratios.

Figs. 9-11 to 9-13 show the variations in the % edge strains in each leaf, based on the average strains at the corresponding levels. The figures have been plotted to show the variation in the % strain in the leaf for both the variation of eccentricity and the variation of applied stress.

4.2 STRESS/STRAIN CHARACTERISTICS WITH CONCENTRATED APPLIED LOAD.

i. Vertical Strain Distribution.

Figs. 9-14 to 9-21 show the vertical strain distribution on the faces of both leaves for various applied stresses, and for eccentricities of loading of 0", 0.3" and 0.5" from the longitudinal axis, and 0", 3", 4" and 6" from the transverse axis.

Results for eccentricities of 0.2" and 0.4" were of a similar form, and are not presented in this way.

ii. Horizontal Strain Distribution.

Figs. 9-22 and 9-23 illustrate the horizontal strain distribution in the zone of the concentrated loading, for an axially applied load. The strain distribution has been plotted in two ways. Fig. 9-22 shows the variation in strain down the wall section, and Fig. 9-23 the variation in the strain, on different horizontal sections. The distribution is given for both faces.

iii. Stress/Strain Relationships.

Fig. 9-24 illustrates the Stress/Strain relationship for an eccentricity of 0.5" (vertical strain), and a zero eccentricity (horizontal strain), plotted from the average strains (vertical) or the individual strain (horizontal).

iv. Modulus of Elasticity.

Values of Young's Modulus (E) have been calculated as indicated in 4.1 .iv. above. Values have been plotted in Fig. 9-9 against applied stress.

v. Strain Ratios.

Fig. 9-25 shows the edge strain ratios, plotted as the % in each leaf, for various positions on the leaf.

The effect of increasing eccentricity is shown, but the increase of stress was found to make little difference, and has not been plotted.

4.3 LATERAL DEFLECTION PROFILE.

Fig. 9-26 gives the lateral deflection profiles for both leaves of the cavity wall, for a concentrated eccentric loading. The profiles are plotted for various loads.

5. DISCUSSION OF TEST RESULTS.

5.1 DISTRIBUTED LOADINGS.

i. Vertical Strain Distribution.

Figs. 9-1, 9-2 and 9-3 indicate that although the strain distribution beneath the lintel has certain local irregularities, particularly in the upper portion of the wall, which is susceptible to any uneven bedding, of the lintel, the distribution is generally of a uniform nature along the wall.

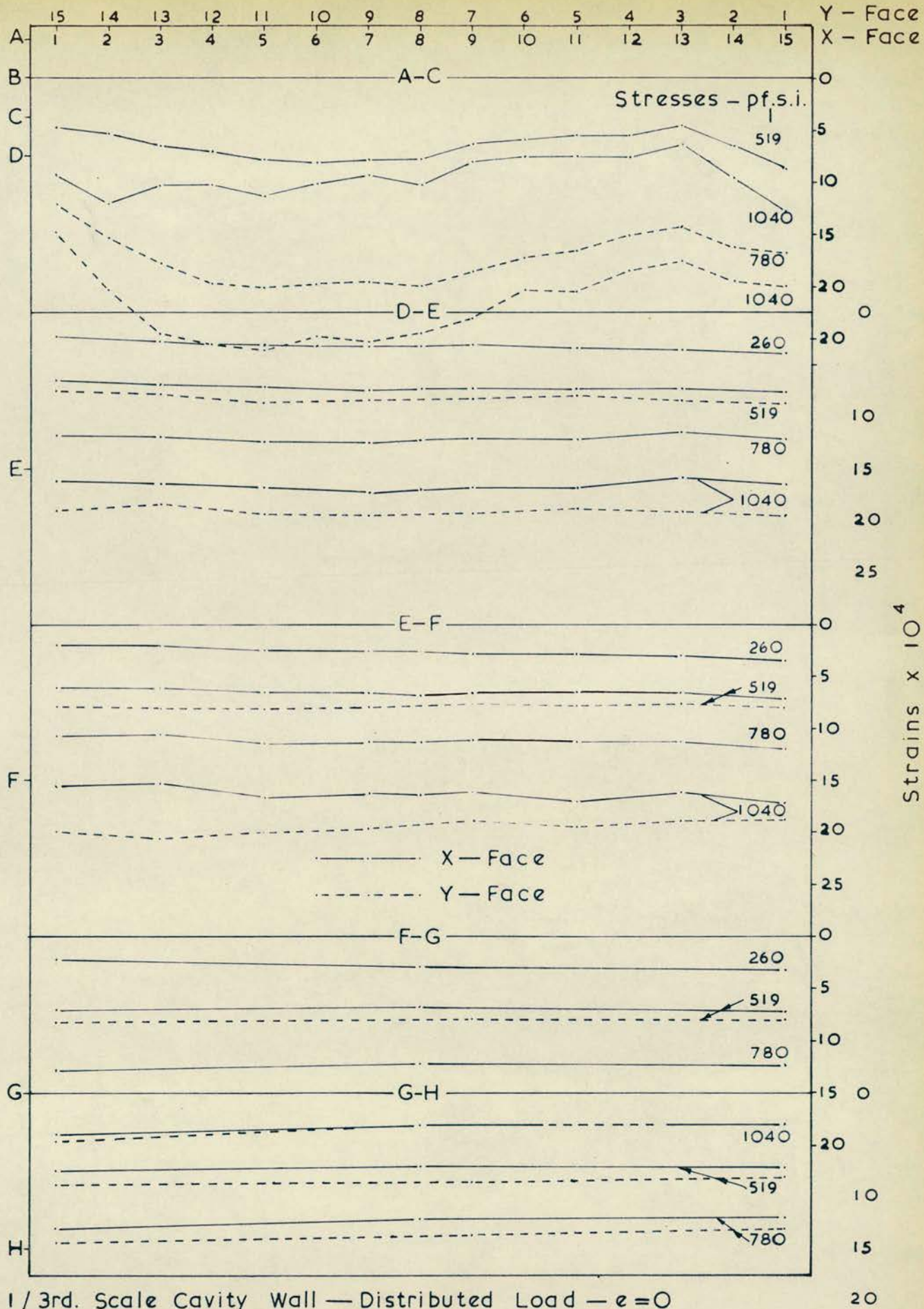
The nature of the strain distribution is the same in both leaves, although the strain magnitudes are not necessarily the same.

A comparison of Figs. 9-11 to 9-13 indicates that as the eccentricity of loading increases the strain ratio also increases.

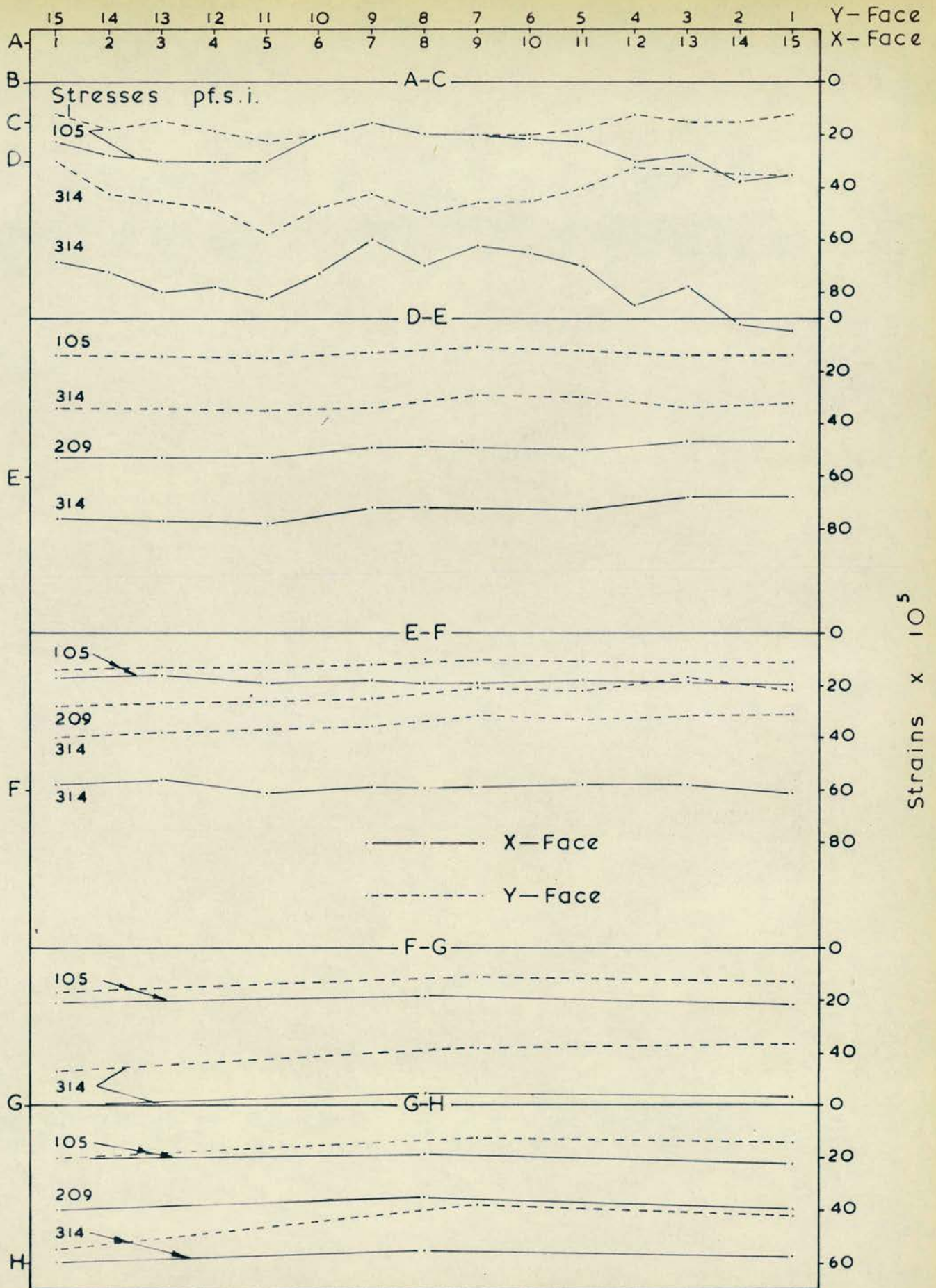
Towards the base of the wall the strain magnitudes are similar in both leaves.

The strain ratio is seen to increase with increasing stress.

ii. Horizontal Strain Distribution.



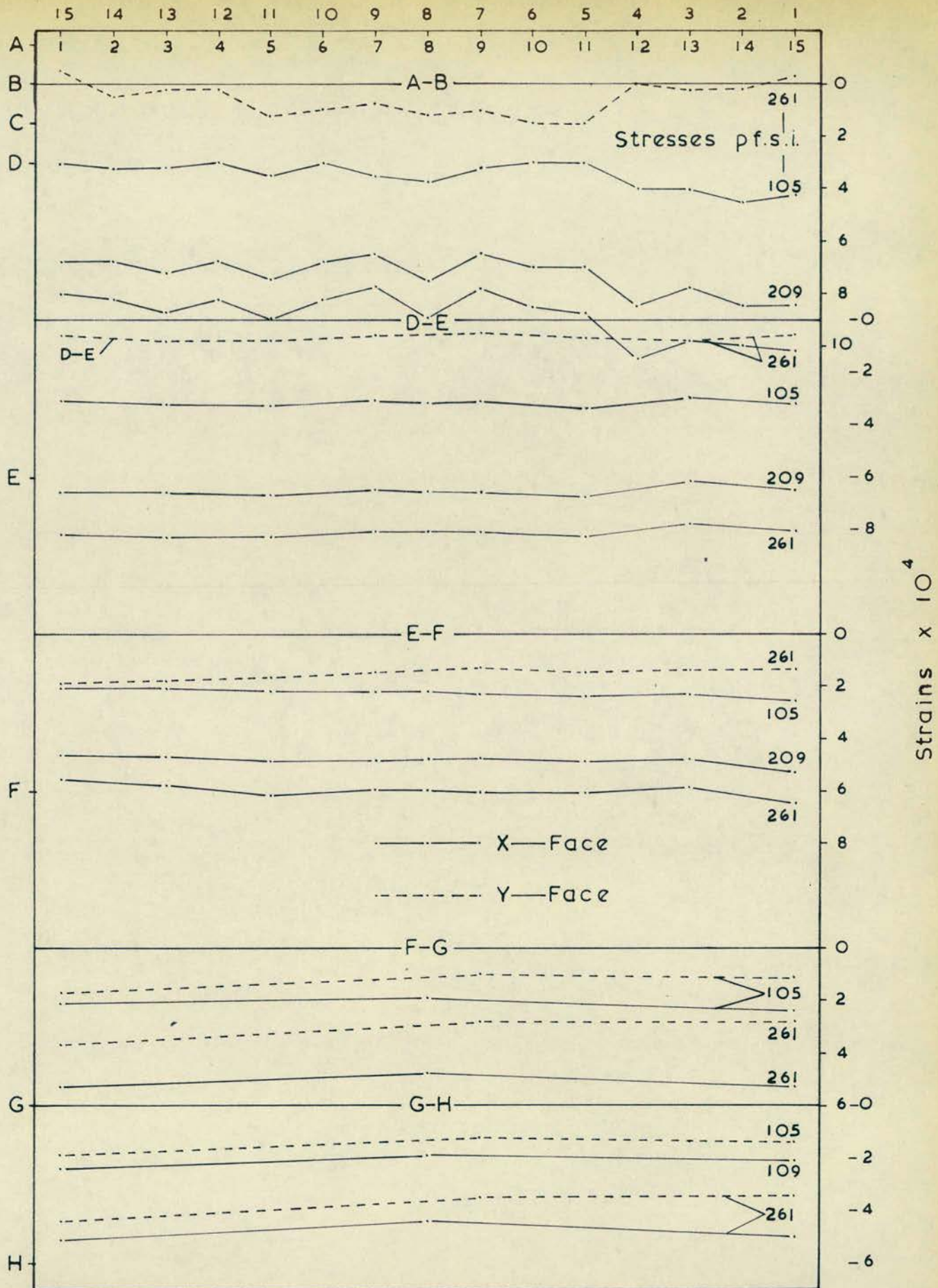
The Strain Distribution on the Faces of a Cavity Wall.



1/3rd. Scale Cavity Wall—Distributed Load — $e=0.3''$

The Strain Distribution on the Faces of a Cavity Wall

Fig. 9-2



1/3rd. Scale Cavity Wall — Distributed Load — $e = 0.5''$
 The Strain Distribution on the Faces of a Cavity Wall

Fig. 9-3

The nature of the horizontal strain distribution (Figs. 9-4 and 9-5) is one of horizontal tensile strains across the whole wall face, and no particular variation, on different vertical sections, is noted. Similar results were obtained for both leaf faces.

Fig. 9-8 illustrates the Average compressive stress/Horizontal strain relationship, which is non-linear, particularly at higher stresses.

Most horizontal strain readings were taken across vertical joints, and it is suspected that where high strain readings were obtained the movement occurred mainly in the vertical joint. Readings taken on individual bricks indicated little strain.

Results obtained showed that the magnitude of the horizontal strains decreased with distance from the line of load application. Strains at level E, 8" below D, were considerably lower than those at levels A, B, C, and D. Some strain below the lintel may be caused by the bending deflection of the lintel, or uneven bedding conditions.

iii. Stress/Strain Relationships.

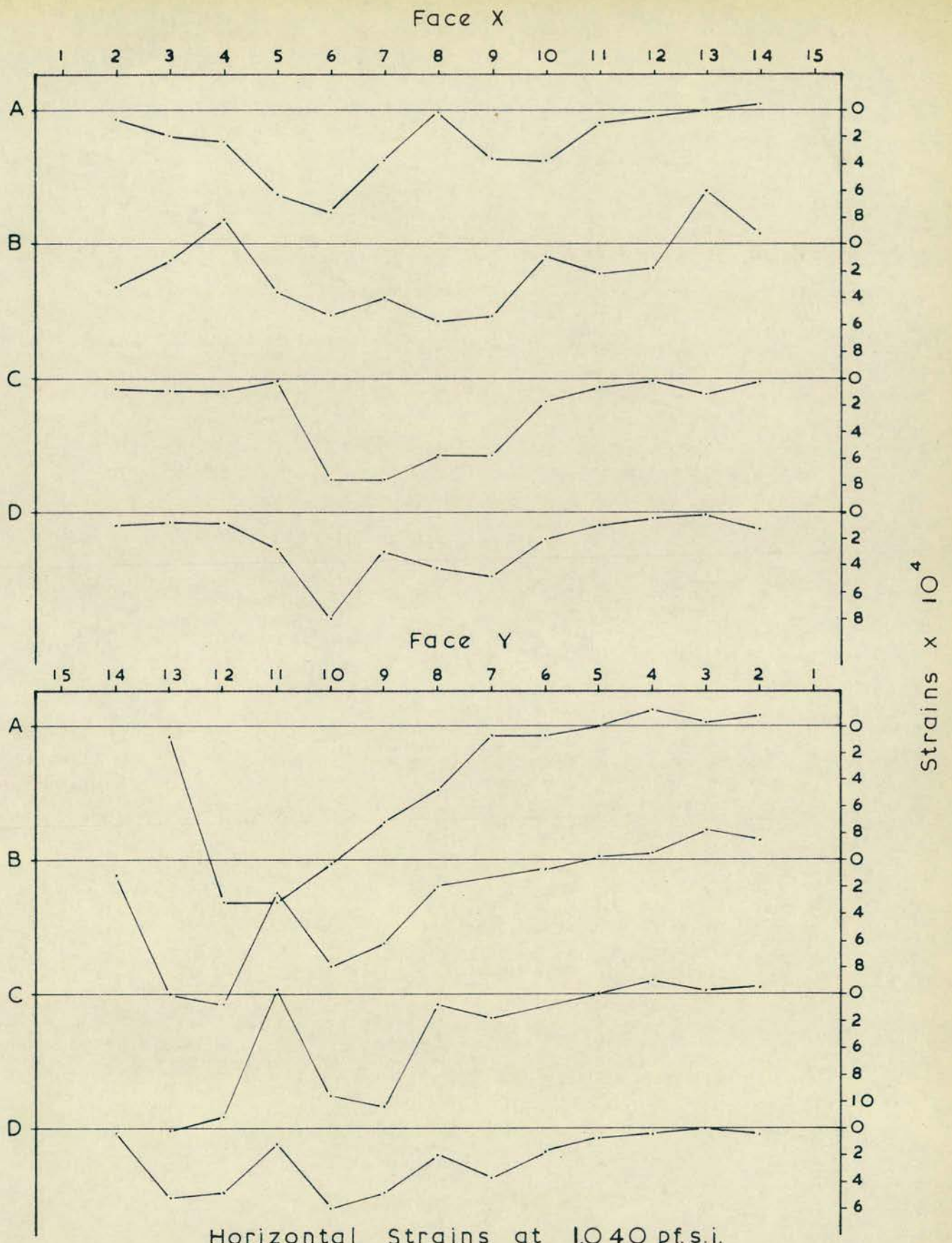
a) Vertical Compressive Strain.

Figs. 9-6 and 9-7 indicate the nature of the Stress/Strain relationship along lines parallel to the direction of loading.

Figs. 9-6 and 9-7 show that when the eccentricity of loading is 0" and 0.2", then the relationship is linear in the stress interval 100-500 pf. s. i.

Readings were not taken below 100 pf. s. i., and hence certain assumptions were made.

The origin, at zero stress, and zero strain, should lie on the



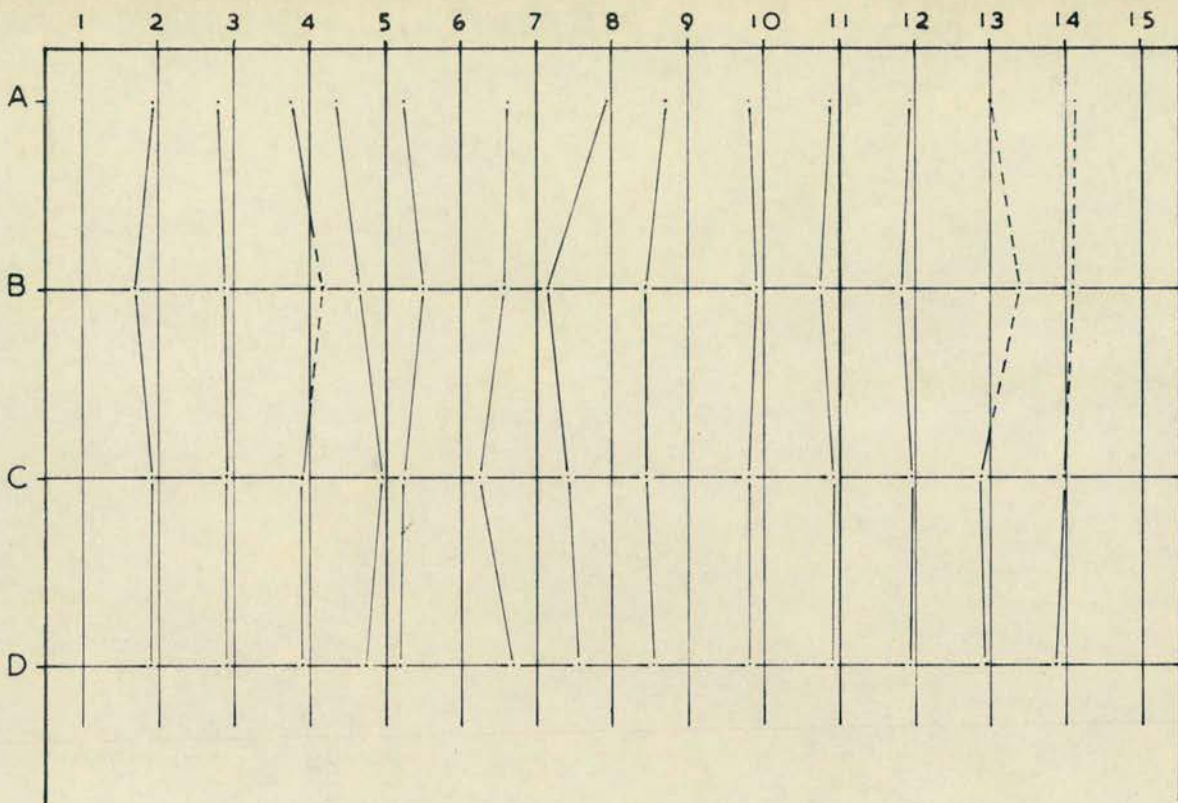
Horizontal Strains at 1,040 p.f.s.i.

1/3rd. Scale Cavity Wall—Distributed Load— $e=0$

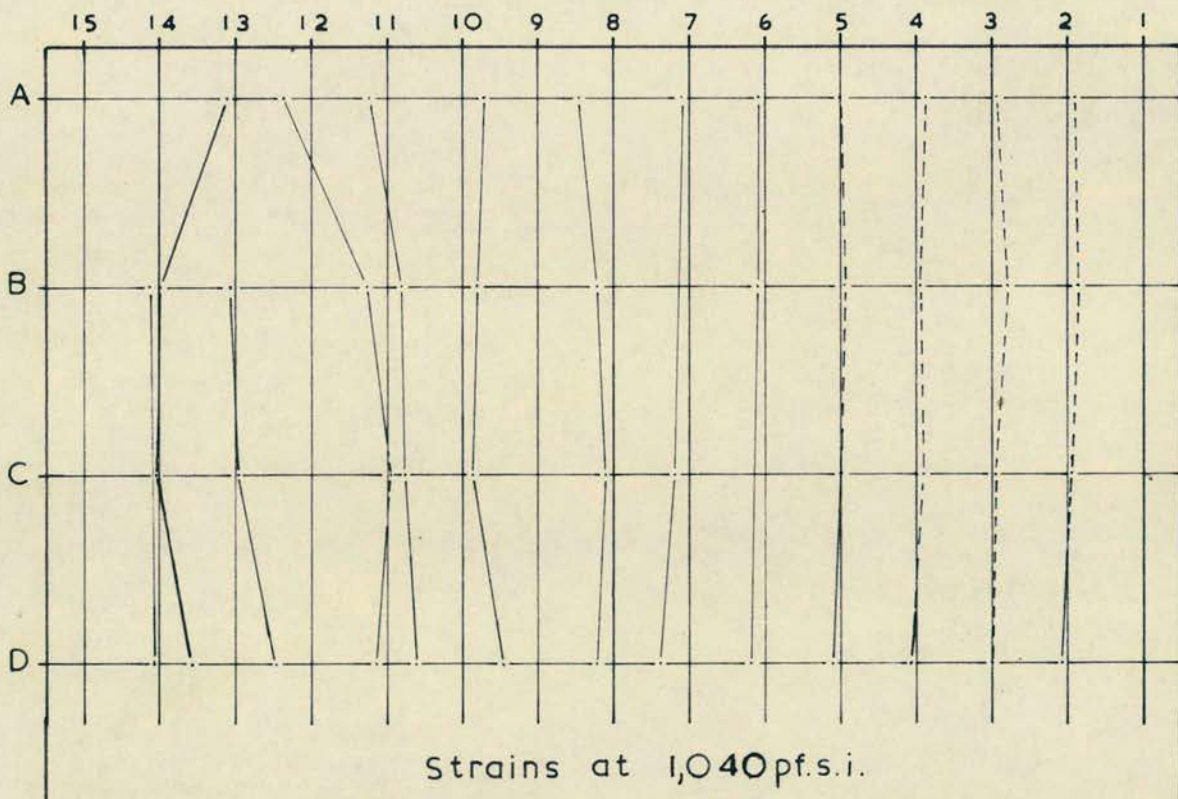
The Horizontal Strain Distribution on the Faces of a Cavity Wall
Horizontal Sections

Fig. 9-4

Face X



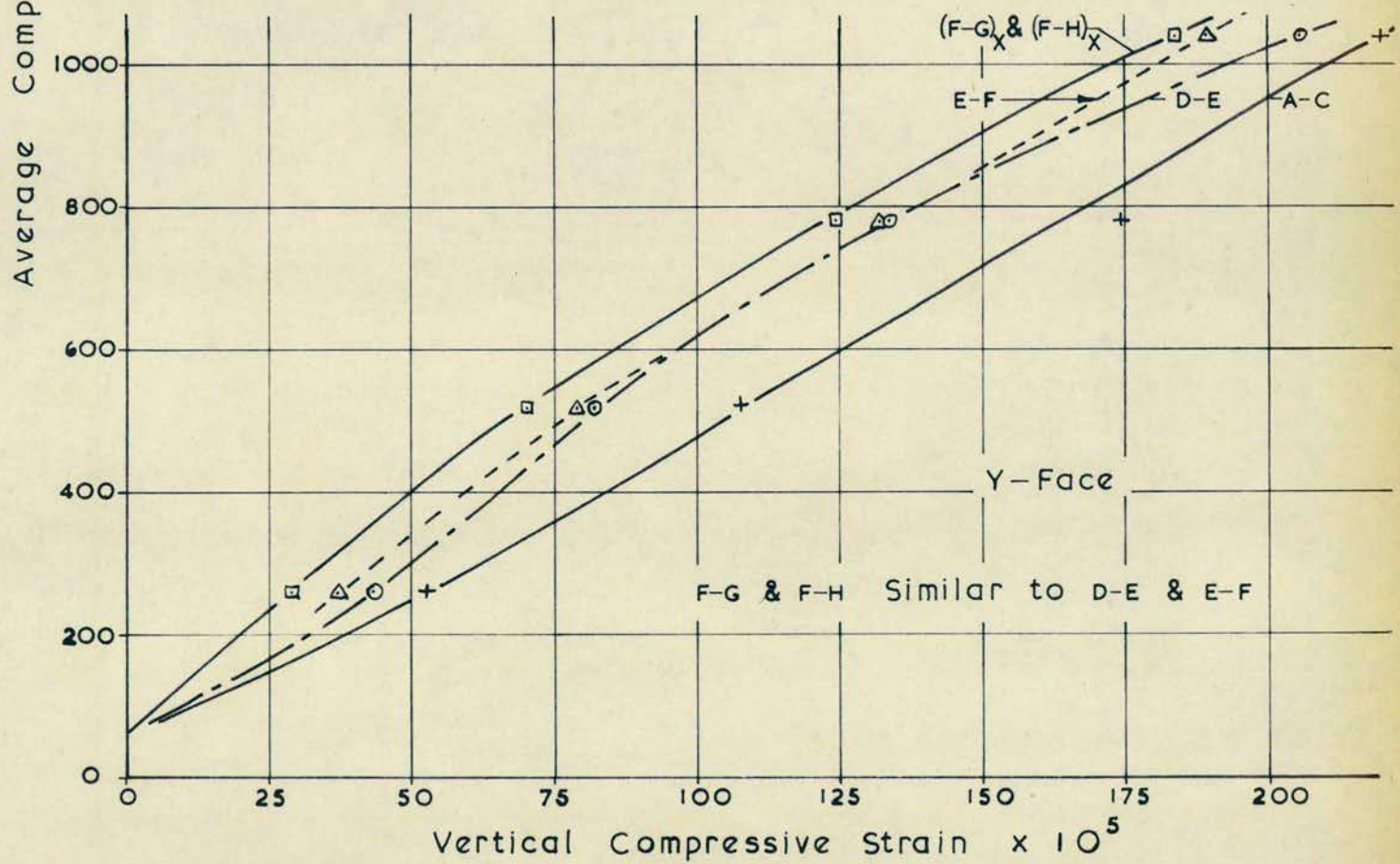
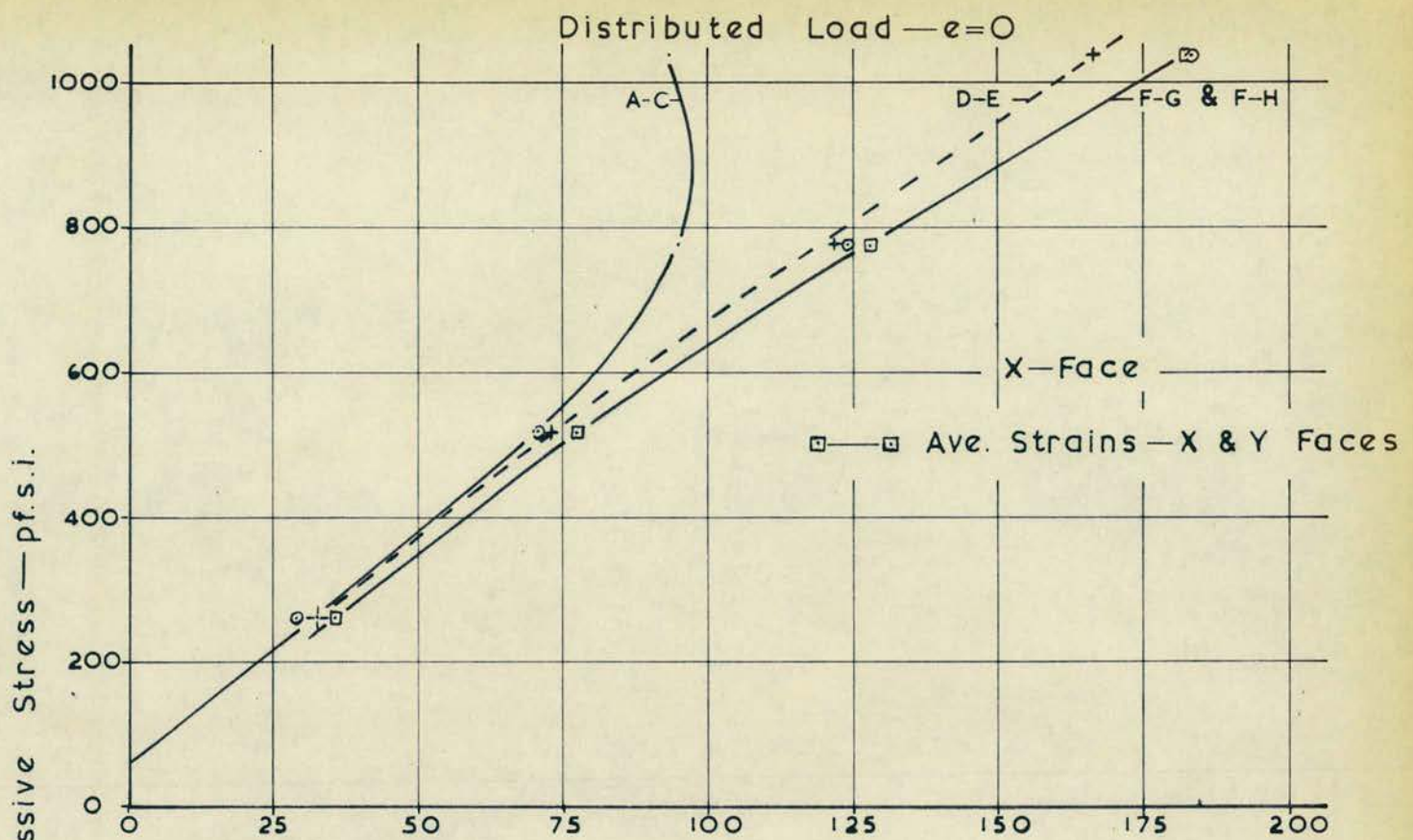
Face Y



Strains at 1,040 p.s.i.

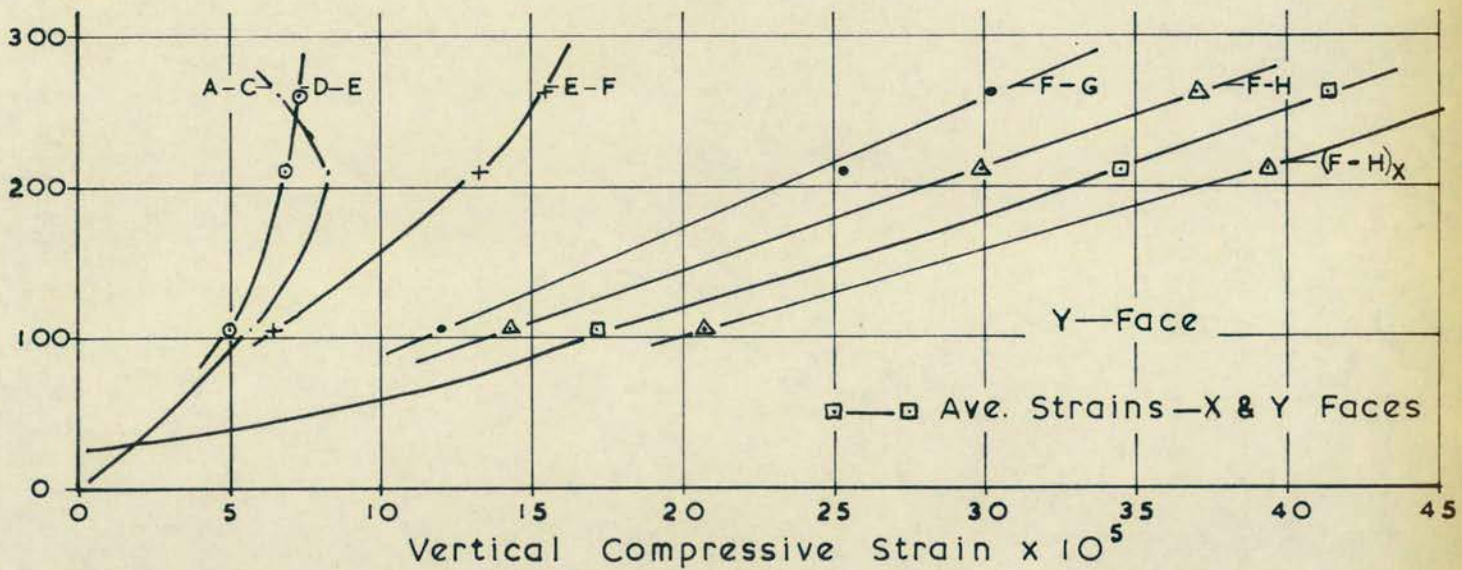
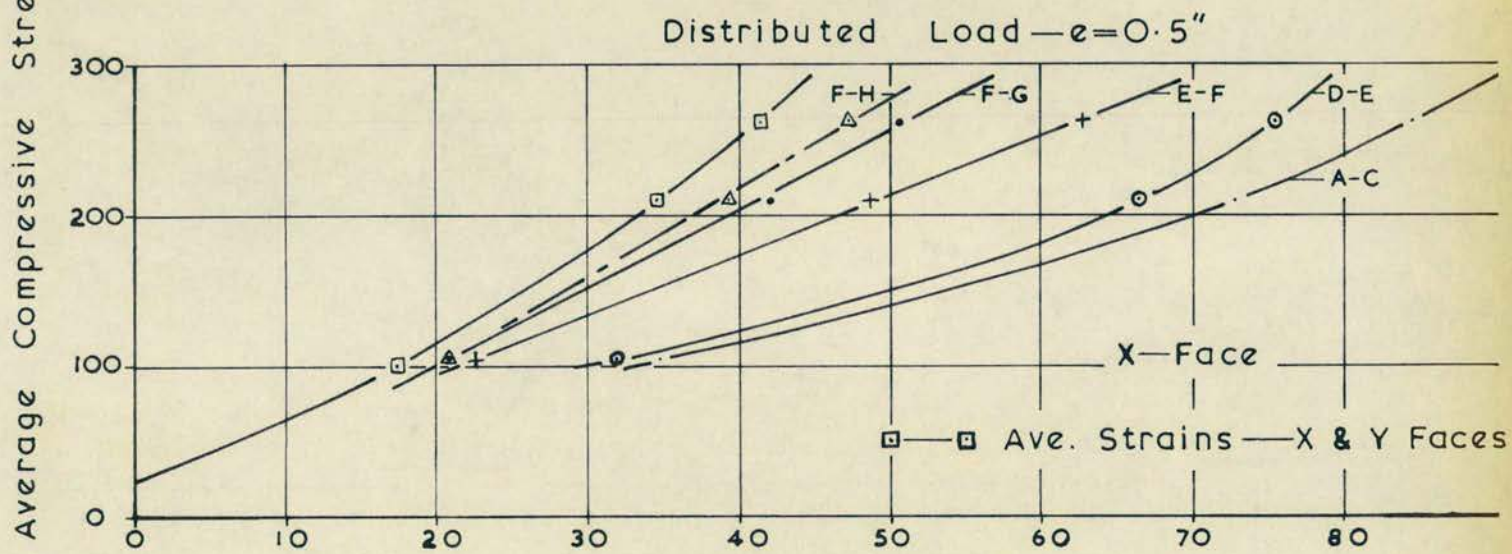
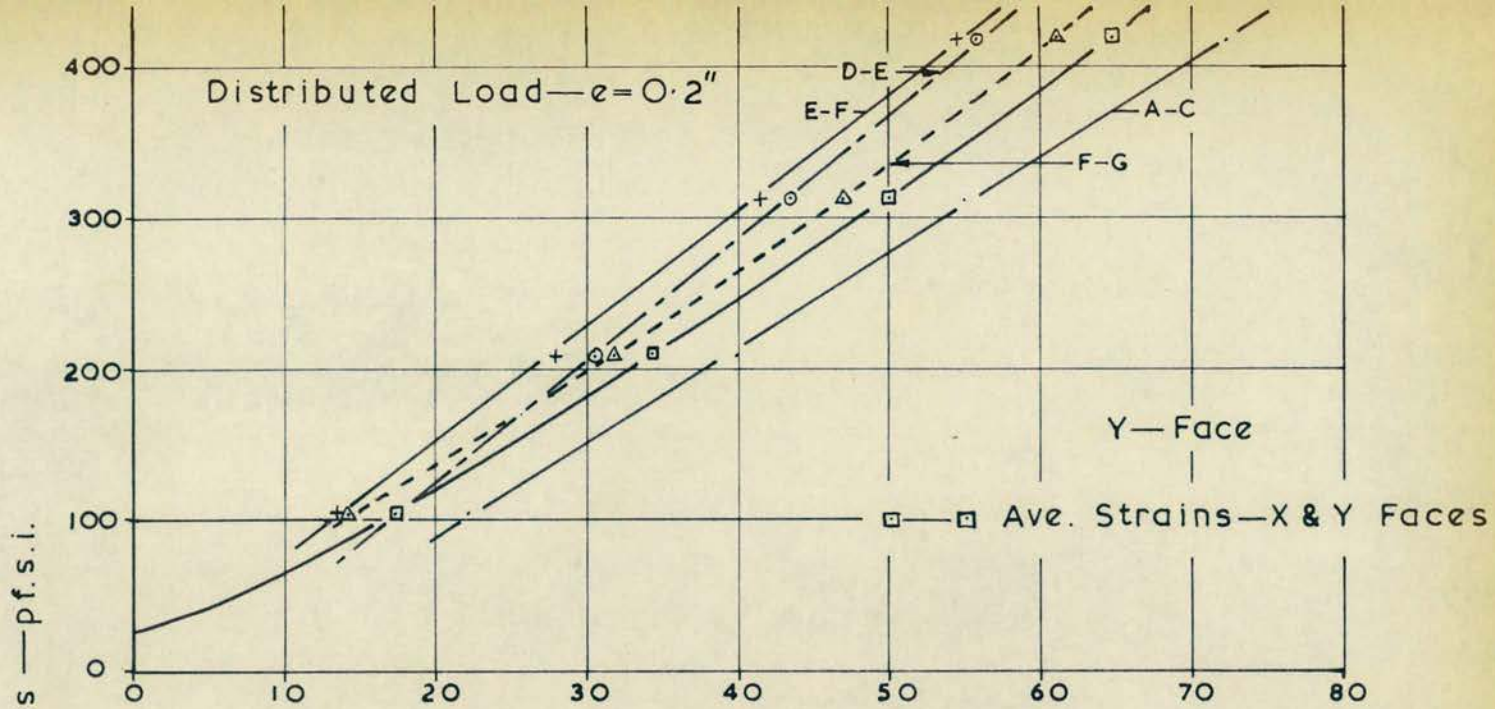
Strain Scale $\frac{2}{1} \text{ } 0 \times 10^3$ Tension $\leftarrow + \text{---} \rightarrow$ Compression
 1/3rd. Scale Cavity Wall — Distributed Load — $e=0$
 Horizontal Strain Distribution — Vertical Sections.

Fig. 9-5



Average Stress/Ave. Strain Relationship—Vertical—for Various Pos.^{ns.}

Fig. 9-6



Ave. Stress / Ave. Strain Relationship—Vertical—for Various Pos.^{ns.}

Fig. 9-7

plot, when a correction has been made to allow for the initially applied stress. With the exception of the failure test, Fig. 9-6, the plots do not pass through the corrected origin, indicating that at low applied stress the Stress/Strain relationship is non-linear. Non-linearity might be expected at low stress, if account is taken of the evening out of the mortar joint bedding, and any other irregularities.

A stress higher than 500 pf. s. i. was only applied in the final failure test, and the Stress/Strain relationship, Fig. 9-6, indicates a non-linear decrease in the E value above this stress.

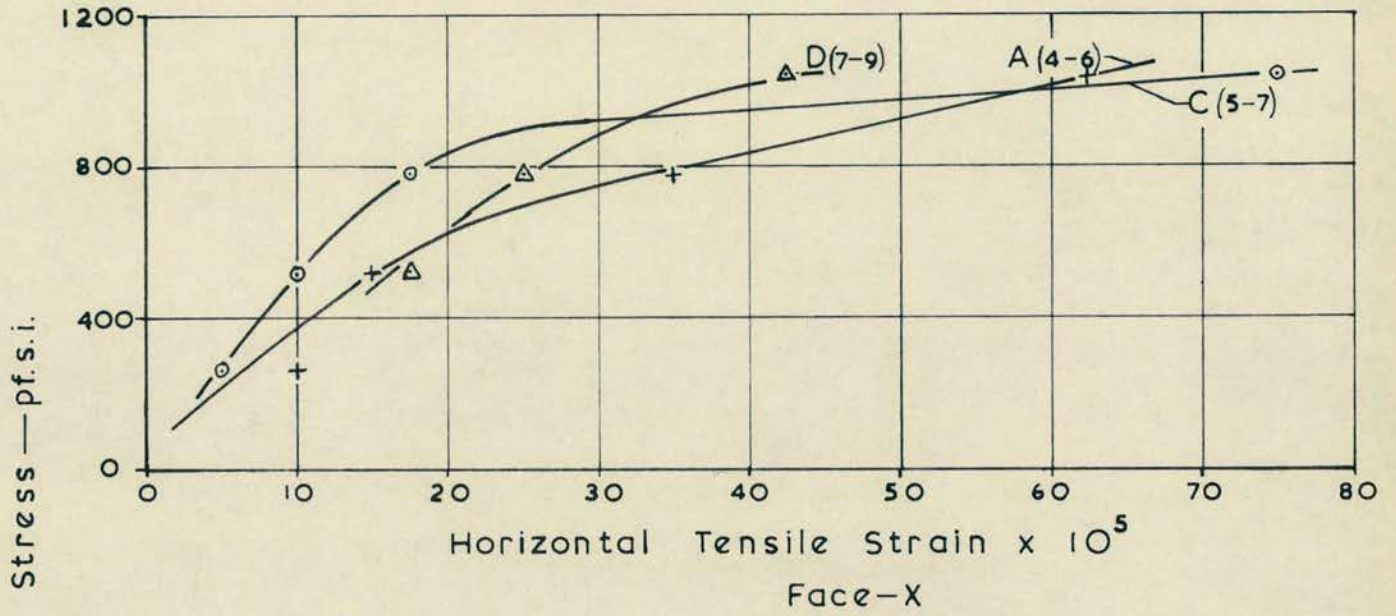
For an eccentric loading, Fig. 9-7, the behaviour of the two leaves differs. The more heavily stressed leaf (at the top) has a linear Stress/Strain relationship above 100 pf. s. i., whereas the lesser stressed leaf behaves non-linearly particularly in the region of the application of the eccentric load, where the moment is high.

For all loading cases the average surface strain has been calculated on each leaf, over a gauge length of 30", and the average stress plotted against the average strain, on the figures giving the Stress/Strain relationships. The E value is seen to be either constant or increasing in the stress zone investigated (0-500 pf. s. i.).

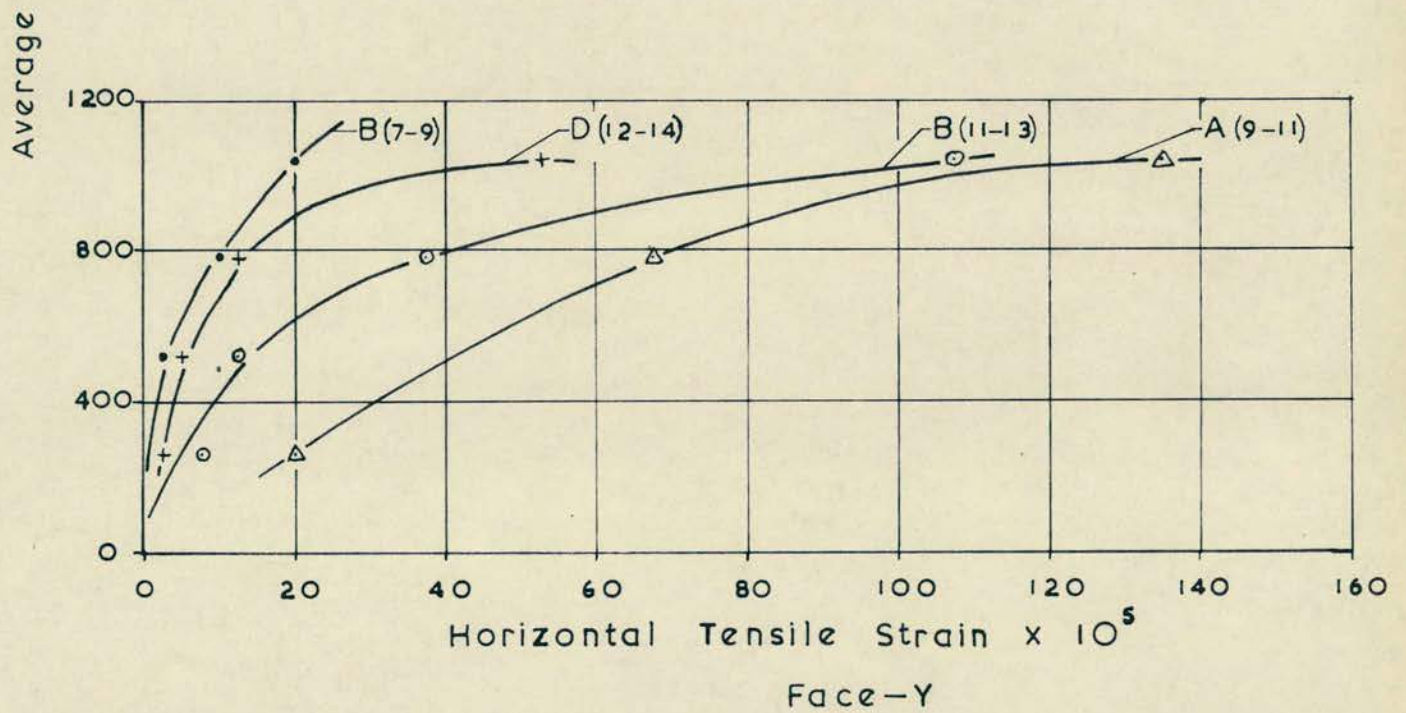
b) Horizontal Strain.

Fig. 9-8 indicates that the Average compressive stress/Horizontal strain relationship is non-linear, and irregular.

The first tensile cracks were observed at approximately 700-800 pf. s. i., and the apparent limit of elastic tensile strain was approximately 15×10^{-5} .



Uniformly Distributed Load — $e=0$



Average Compressive Stress / Horizontal Tensile Strain—Relationships for Various Positions.

Fig. 9-8

iv. Modulus of Elasticity.

a) Method of Calculation.

The modulus of elasticity, E , may be calculated in a number of ways.

The Initial Tangent modulus may be taken, by drawing a tangent to the Stress/Strain curve at the origin. However, if there are irregularities at low stress, then this modulus is unlikely to be representative of the modulus which prevails for most of the stress range, up to the failure stress .

From Figs. 9-6 and 9-7 it is clear that the initial tangent modulus gives an unrepresentative and low value.

The Tangent modulus, which is obtained from the calculation of the slope of the curve at any point, varies along the Stress/Strain plot, unless the relationship is linear. This modulus represents the relationship prevailing at any particular stress, and hence gives a good idea of the mode of behaviour of the material. Unfortunately, for calculation the tangent has to be drawn, and this is subject to error. Consideration of Figs. 9-6 and 9-7 indicates that the tangent modulus varies from the initial tangent modulus, which has a low value, to a higher value at approximately 500 pf. s. i. The modulus decreased above 500 pf. s. i., but this may have been due to the formation of micro-cracks in the initial failure zone.

The Secant modulus, which is calculated from the slope of the chord drawn from the origin to any particular point on the curve, gives values which vary from the initial tangent modulus to higher

or lower values, depending on the nature of the Stress/Strain relationship. From Figs. 9-6 and 9-7 the Secant modulus is seen to increase with increasing stress, but is never as large as the tangent modulus. The modulus increases with increasing stress, even if the Stress/Strain relationship becomes linear. Where values of the strain have been tabulated, at various stresses, the Secant modulus may be calculated simply, and for this reason is the modulus calculated from the test results.

The "E" value has been calculated from the average applied stress, and the average overall strains on faces X and Y of the two leaves, based on a gauge length of 30". The strain profile has been assumed to be linear across the leaves considering both leaves to bend about the combined neutral axis.

A full investigation of the actual distribution of bending stress is detailed in Chapter 10. The Stress/Strain relationship, and the strain ratios indicate that the actual behaviour of the eccentrically loaded cavity wall is complex.

b) The Variation of the Elastic Modulus with the Applied Compressive Stress.

From Fig. 9-9 E is seen to increase non-linearly as the stress increases. The E value reached a maximum of $0.6 - 0.65 \times 10^6$ pf.s.i. at a stress of approximately 500 pf.s.i. This value compares with an E value, for the bricks used for construction, of $0.63 - 0.79 \times 10^6$ pf.s.i. The 1 : 3 mortar used had a modulus of approximately 2.2×10^6 pf.s.i.

As a check on the E values obtained from the 30" gauge lengths, the modulus was calculated at level F-H, where the strain ratio obtained indicated that there was little bending moment. The values obtained are plotted against the average compressive stress in Fig. 9-10, and the result is similar to that of Fig. 9-9.

In the final test, to failure, the modulus decreased above 500 pf. s. i., having a value of 0.54×10^6 pf. s. i. at 1,050 pf. s. i.

v. Strain Ratios.

a) Variation with Position on Wall.

Figs. 9-11, 9-12 and 9-13 show that the strain ratio decreases from a maximum value, at or near the point of load application, to a minimum near the base.

The variation of the strain ratio indicates that the wall is not behaving as originally assumed, which would have given a uniform strain ratio, independent of position on the wall, (Chapter 7-3).

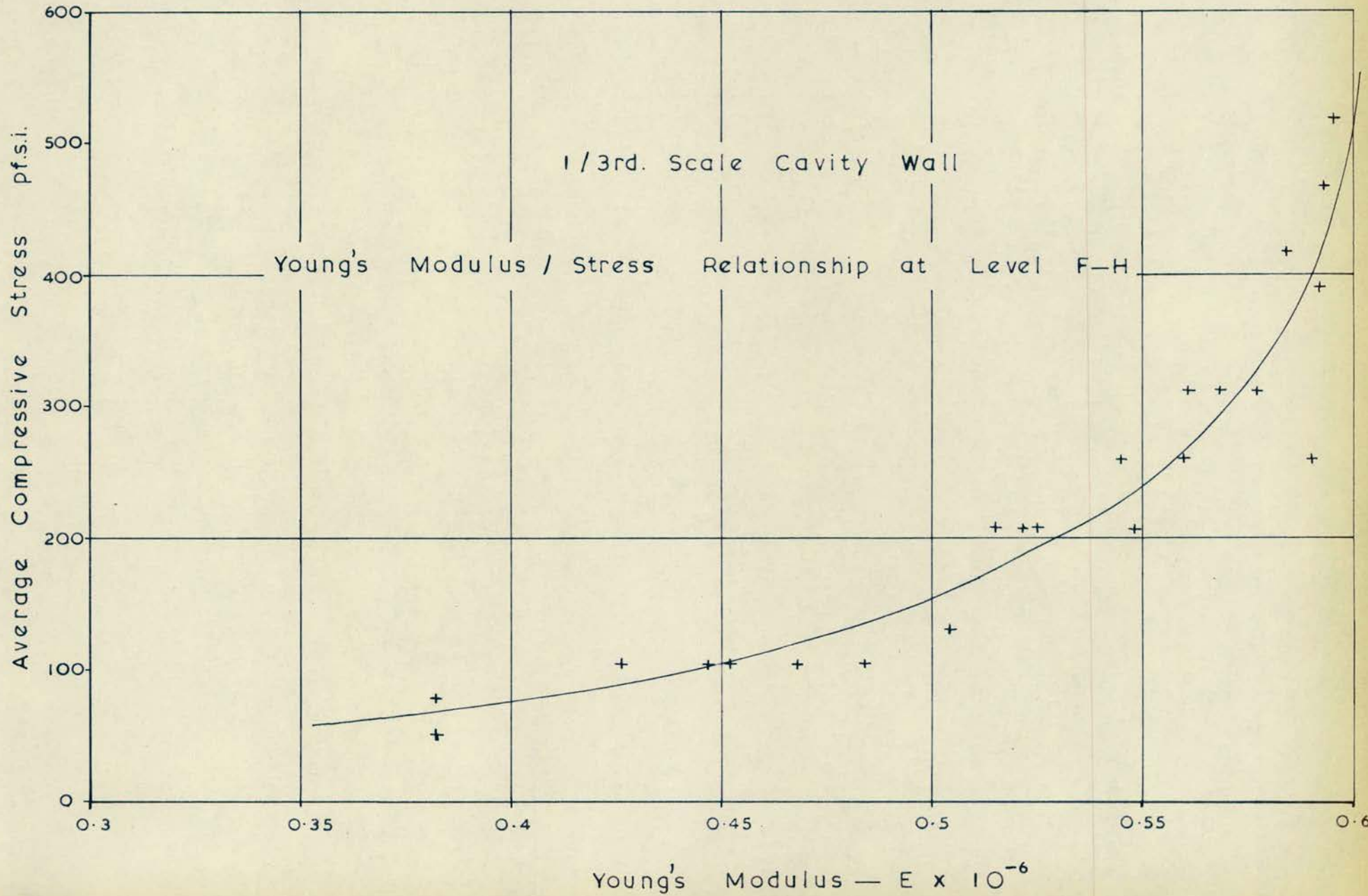
b) Variation with Stress.

The effect of increasing the applied stress was to increase the strain ratio, and % strains on the exposed leaf faces are given in Figs. 9-12 and 9-13. The increase in applied stress also varied the mode of behaviour of the wall, as the strain ratio changed from >1 to <1 at the base, in three of four tests, indicating a point of contra-flexure near the base of the wall.

c) Varying the Load Eccentricity.

The effect of increasing the eccentricity is shown in Fig. 9-11. The strain ratio increased with increasing eccentricity.

Fig. 9-10



Eccentricity Towards X-Face .

Strain Variation with Load Eccentricity and Applied Stress
 1/3rd Scale Cavity Wall—Uniformly Distributed Load

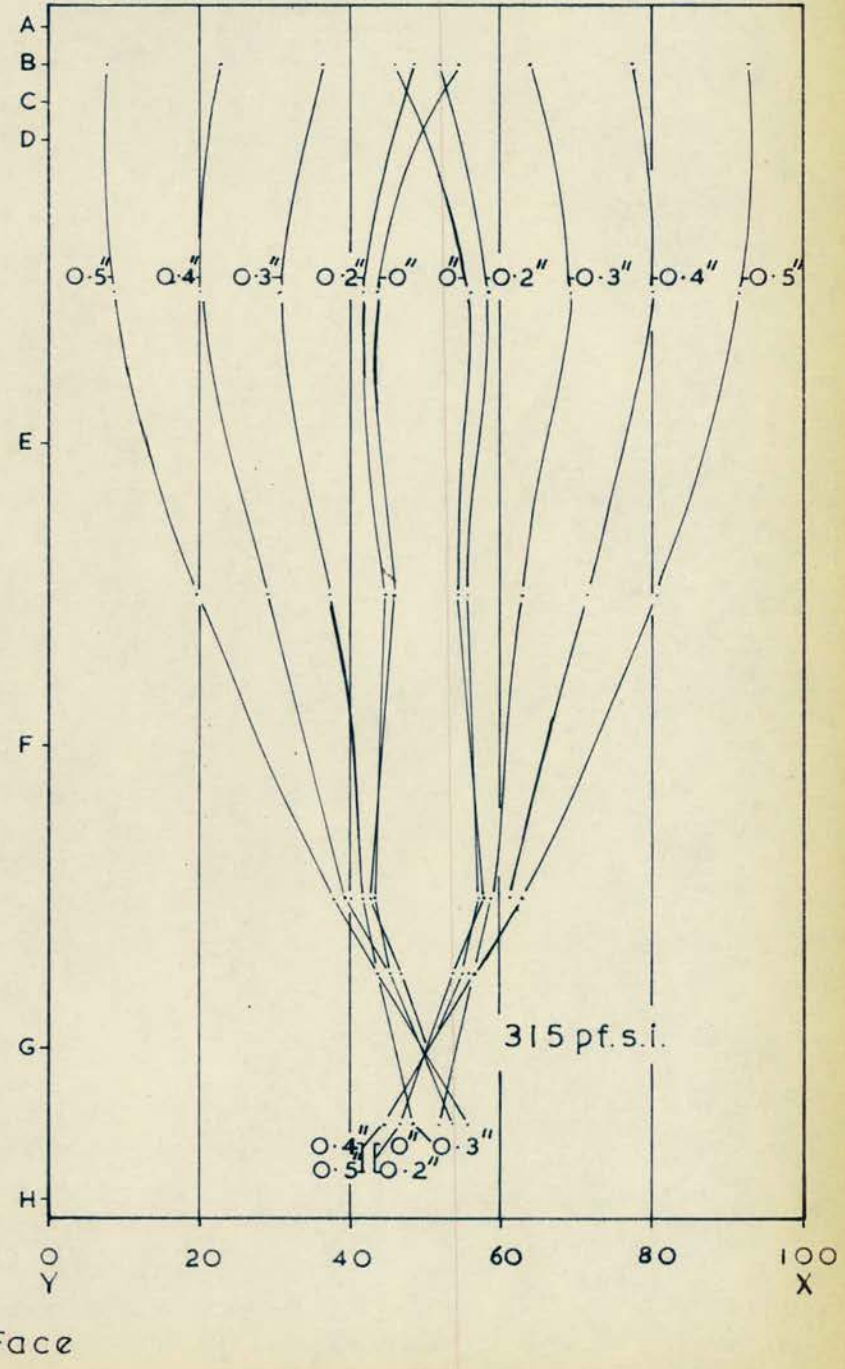
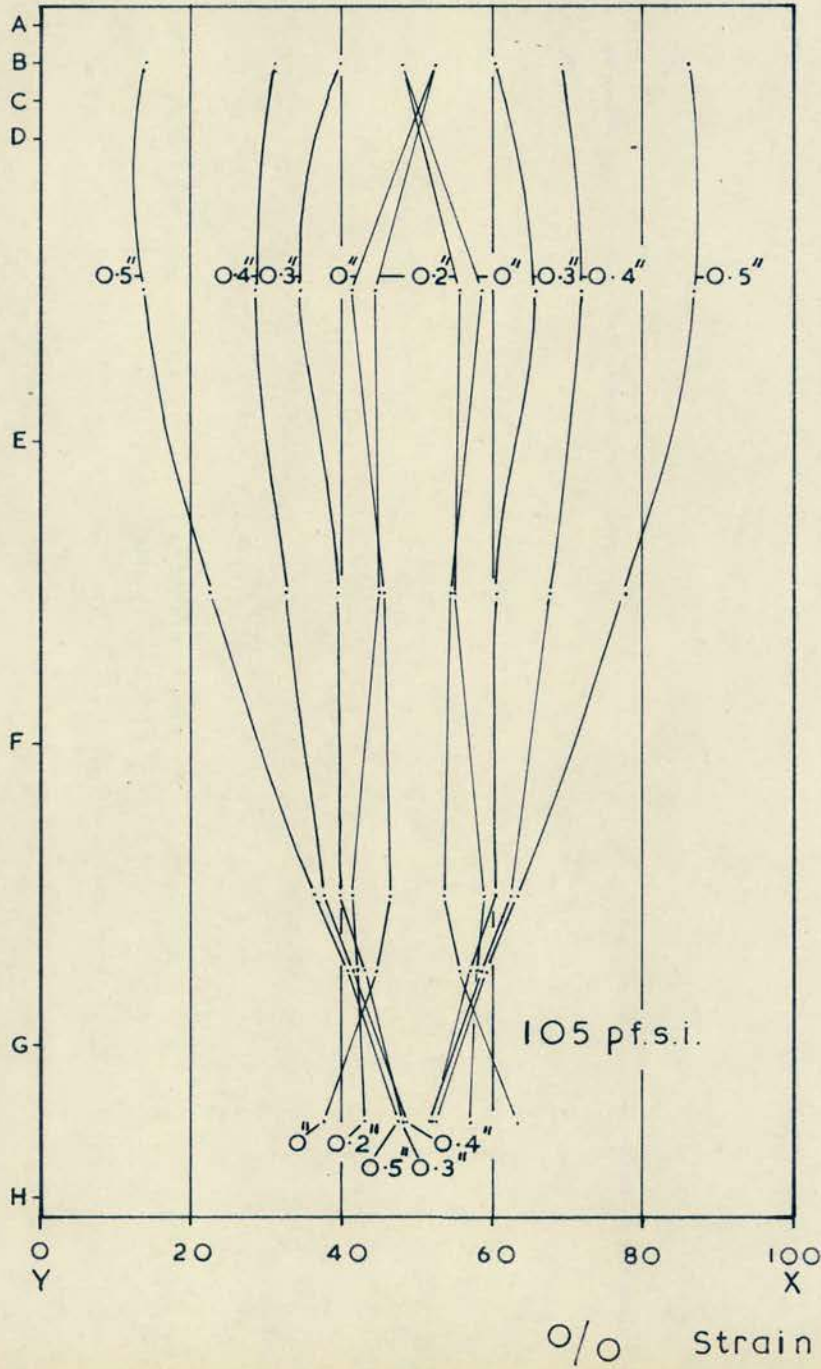
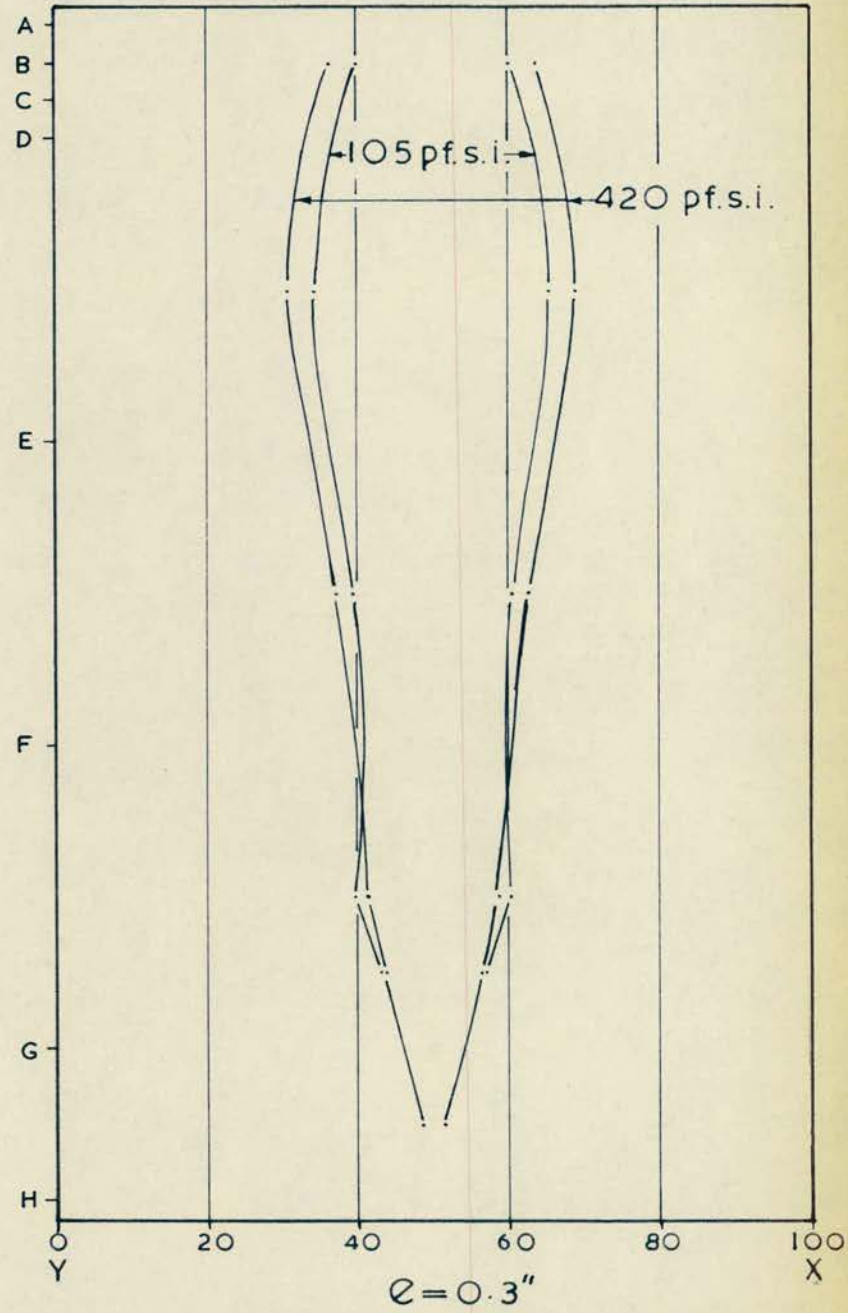
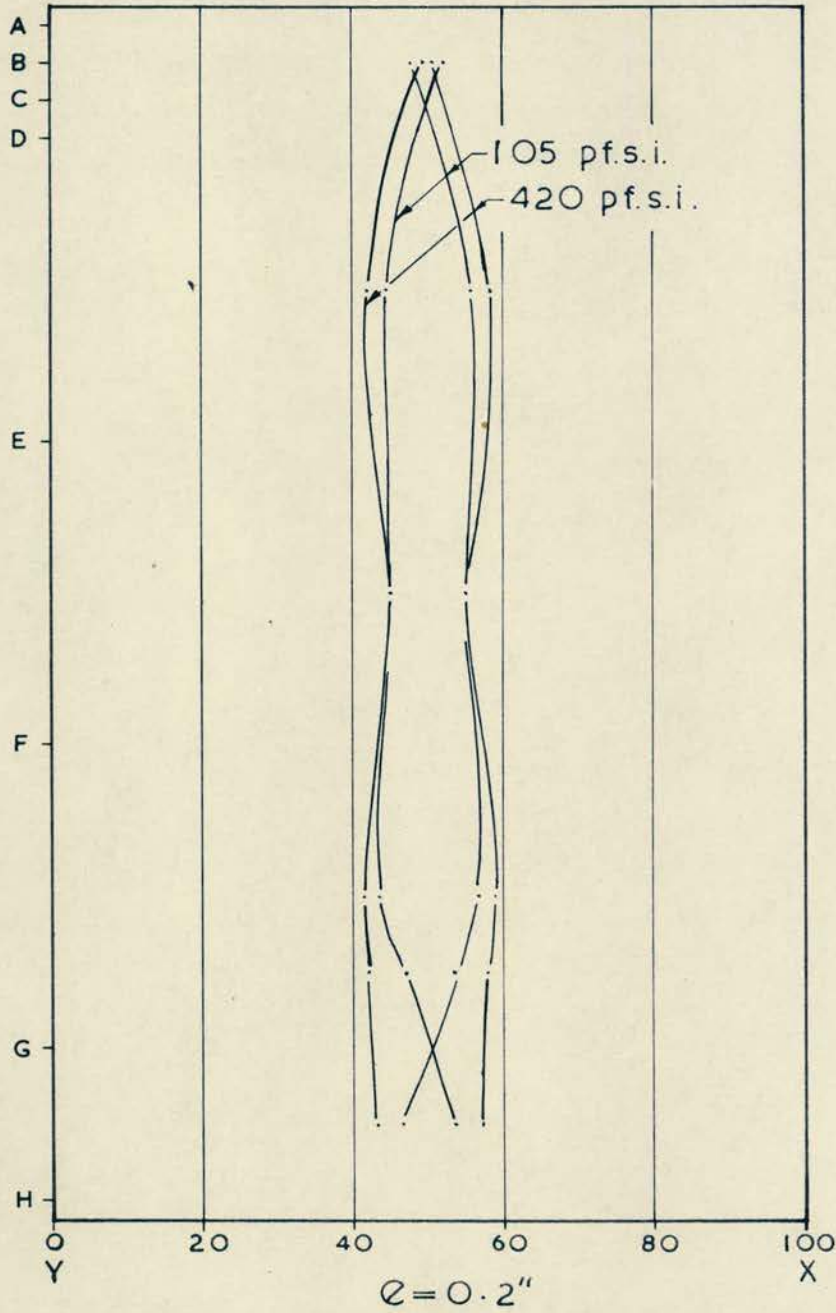


Fig. 9-11

Uniformly Distributed Load

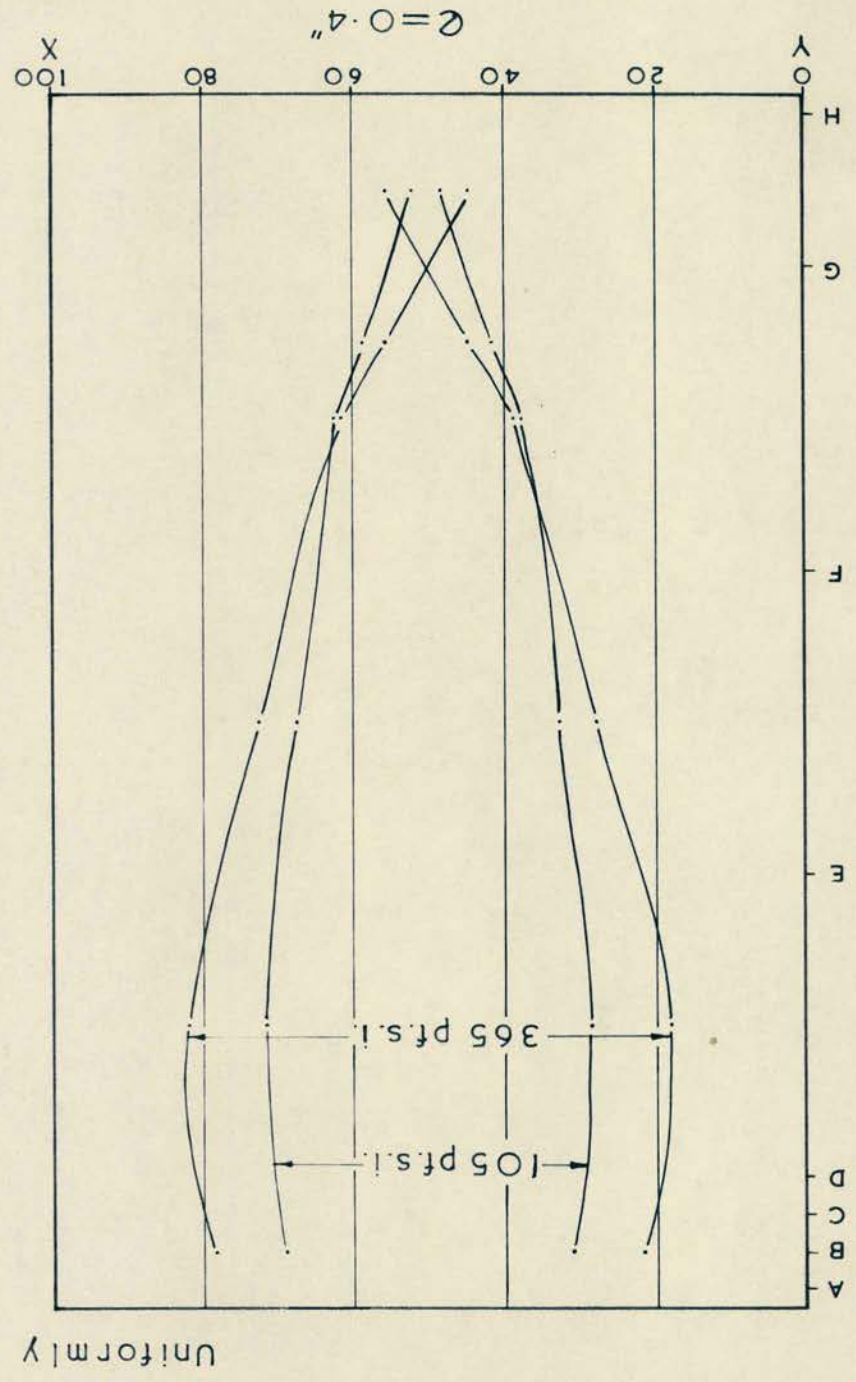
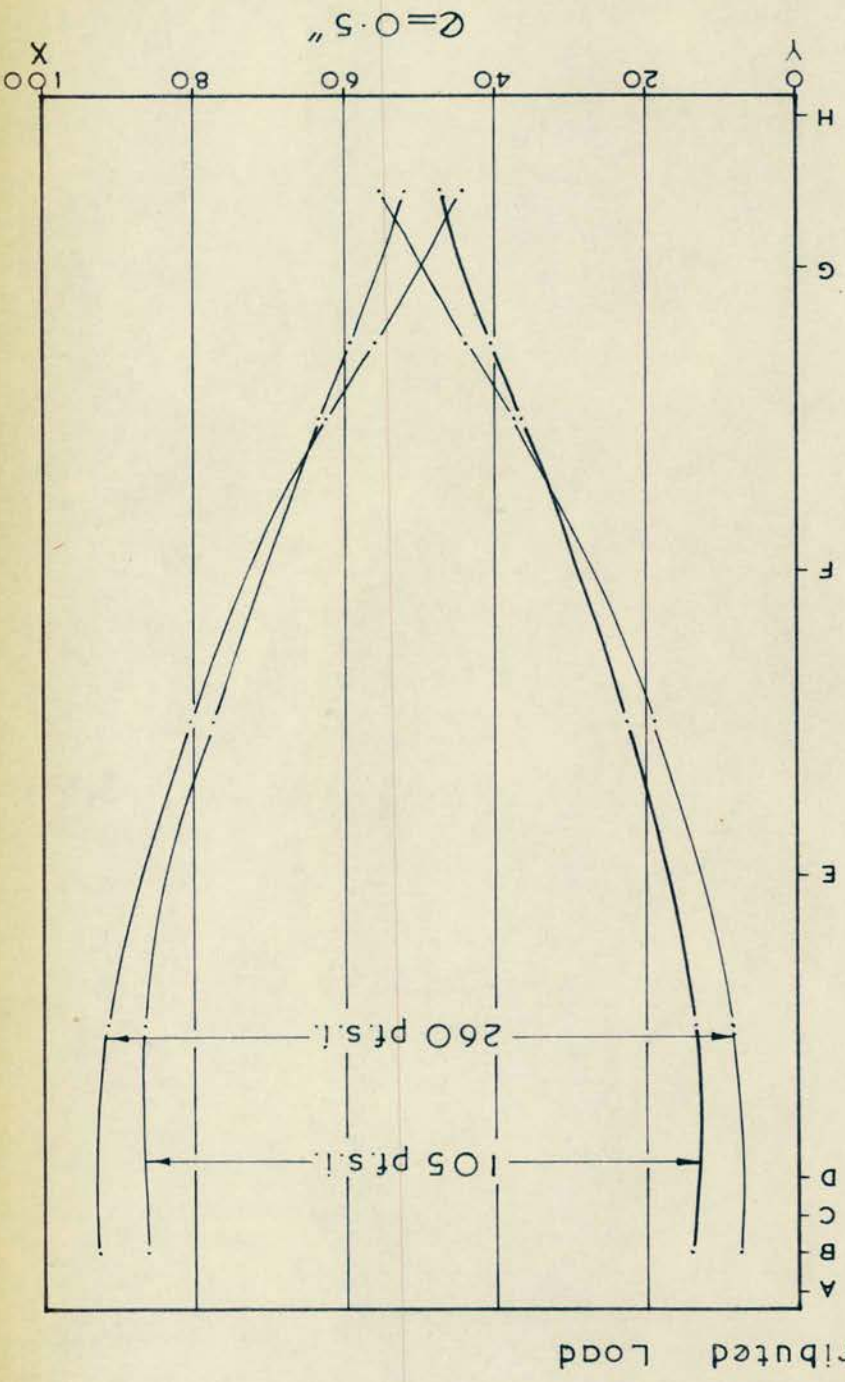


0/0 Strain on Leaf Faces

1/3rd. Scale Cavity Wall—Eccentric Distributed Load
Strain Variation with Applied Stress and Load Eccentricity

Fig. 9-12

0/0 Strain on Left Faces



1/3rd. Scale Cavity Wall—Eccentric Distributed Load
Strain Variation with Applied Stress and Eccentricity

Fig. 9-13

The strain ratios for axial loading indicate that the wall had a built in eccentricity. Results obtained were similar to those from the test with an intentional eccentricity of 0.2".

d) Implications of the Strain Ratios.

The information about the cavity walls mode of behaviour that can be obtained from the strain ratios is discussed in Chapter 10.

5.2 CONCENTRATED LOADINGS.

i. Vertical Strain Distribution.

a) Central Loadings.

Figs. 9-14, 9-15 and 9-16 illustrate the vertical strain distributions on both faces, X and Y of the cavity wall, for varying eccentricities of loading.

The maximum vertical strain occurs below the centre-line of the bearing plate.

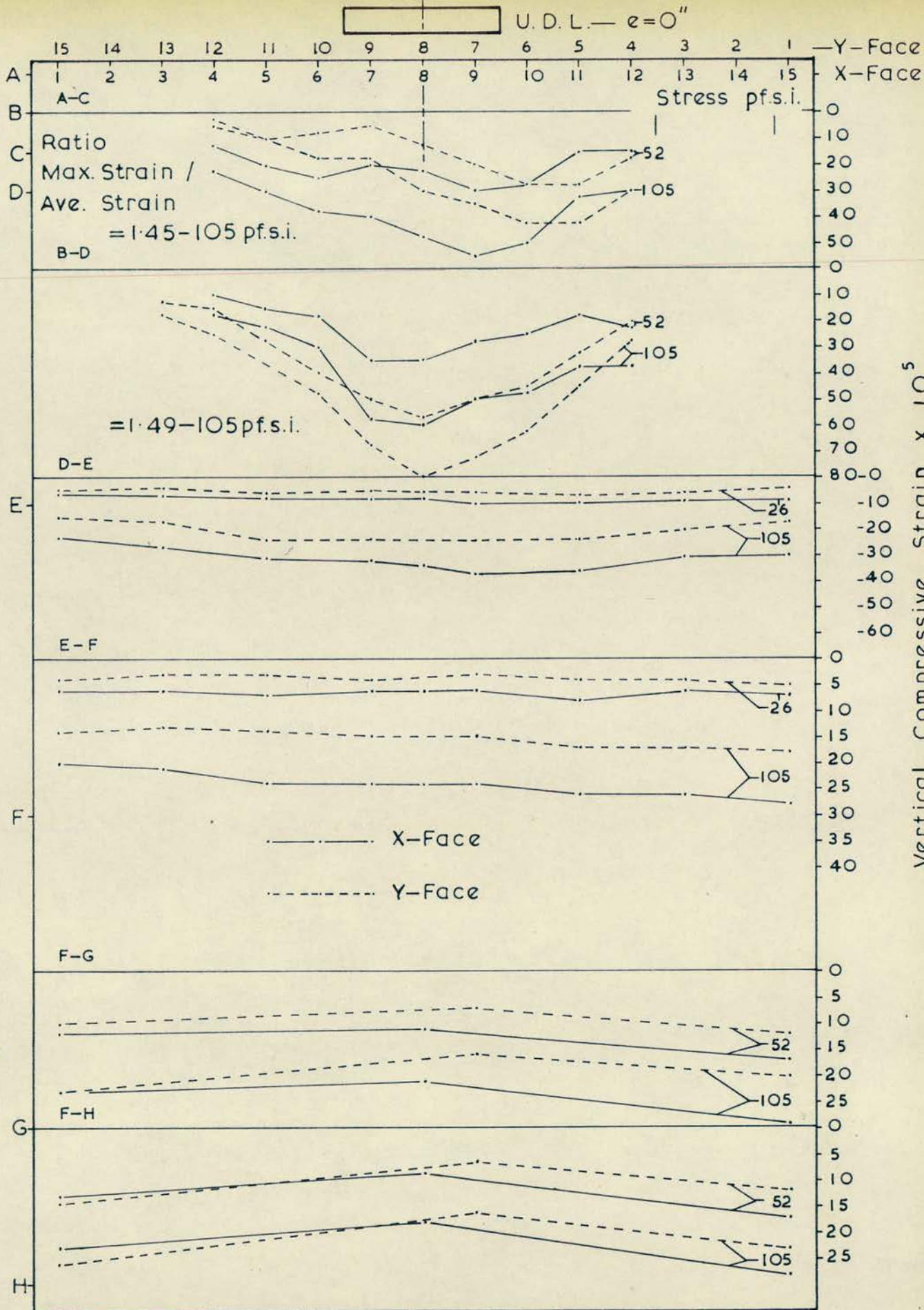
The strain distribution at the top of the leaves is geometrically similar in both leaves, and indicates a high degree of strain concentration at this level.

The average ratio of the Maximum strain/Average strain is 1.9 at level A-C. The average value of the ratio is taken from values ranging from 1.86 - 1.97 and includes those values from the tests with eccentricities of 0.2" and 0.4", whose full results are not presented.

At level D-E the strain distribution is still non-uniform across the leaf face, but is more uniform than at level A-C.

At level E-F, and at levels below, the distribution is uniform.

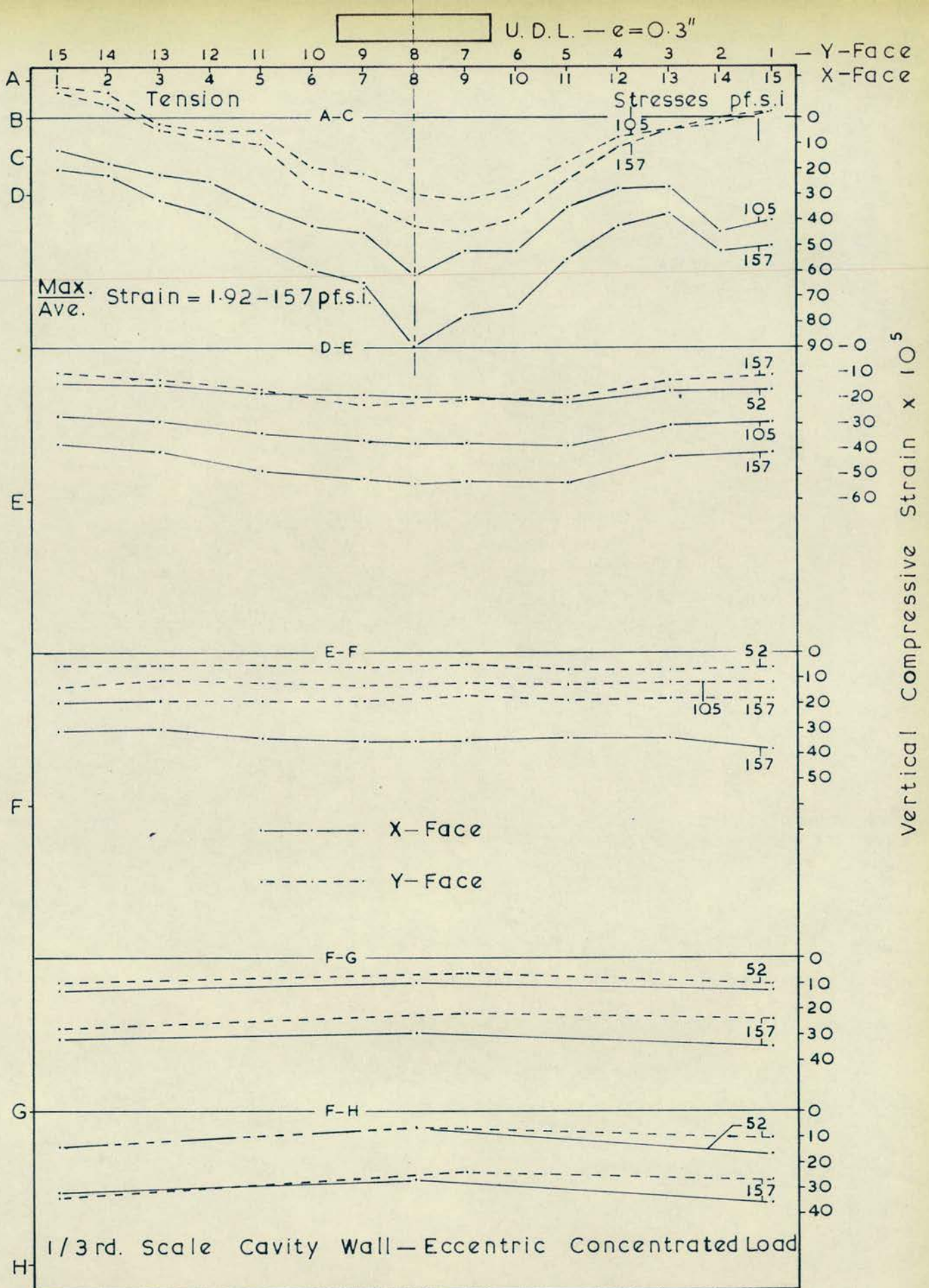
b) Loadings 3" Eccentric from the Transverse Axis.



1/3rd. Cavity Wall — Concentrated Load — $e=0''$

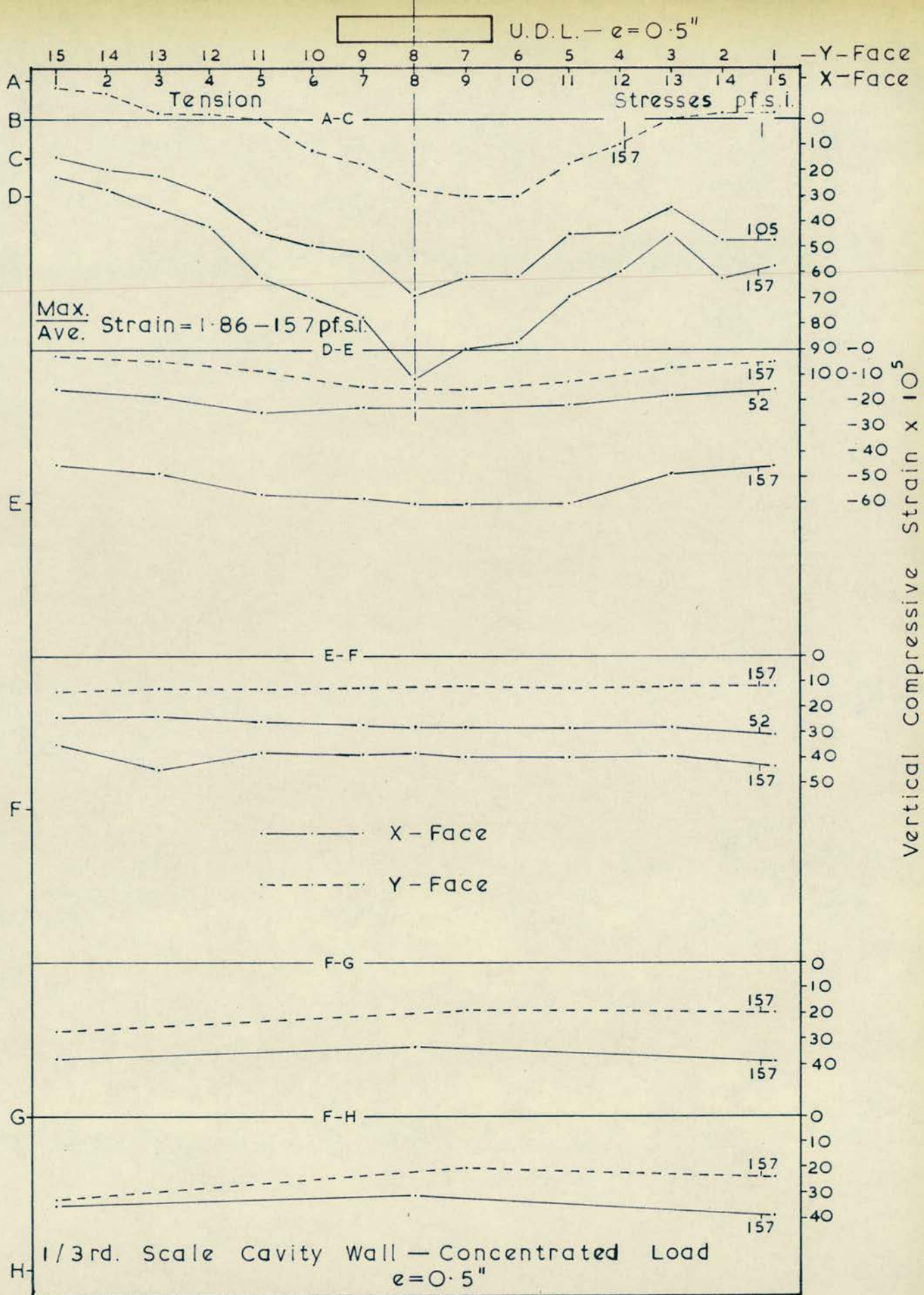
The Strain Distribution on the Faces of a Cavity Wall

Fig. 9-14



The Strain Distribution on the Faces of a Cavity Wall

Fig. 9-15



The Strain Distribution on the Faces of a Cavity Wall

Fig. 9-16

Figs. 9-17, 9-18 and 9-19 illustrate the vertical strain distributions on faces X and Y for various eccentricities of loading. A "pressure bulb" of strain is observed in each case.

The average ratio Maximum strain/Average strain is 1.9, and is taken from values ranging from 1.81 - 2.03, for level A-C. The average ratio includes values from tests with eccentricities 0.2" and 0.4", that are not fully presented.

In the lesser stressed leaf Y, the bending moment about the centre-line of the wall face causes the resultant strain to be tensile, at level A-C, where the compressive stress has not been distributed across the section. This effect increases with eccentricity of loading. As the eccentricity is increased tensile strains are also noted at level D-E, towards the edge of the lesser stressed leaf.

From level D-E downwards the strain distribution becomes generally more uniform.

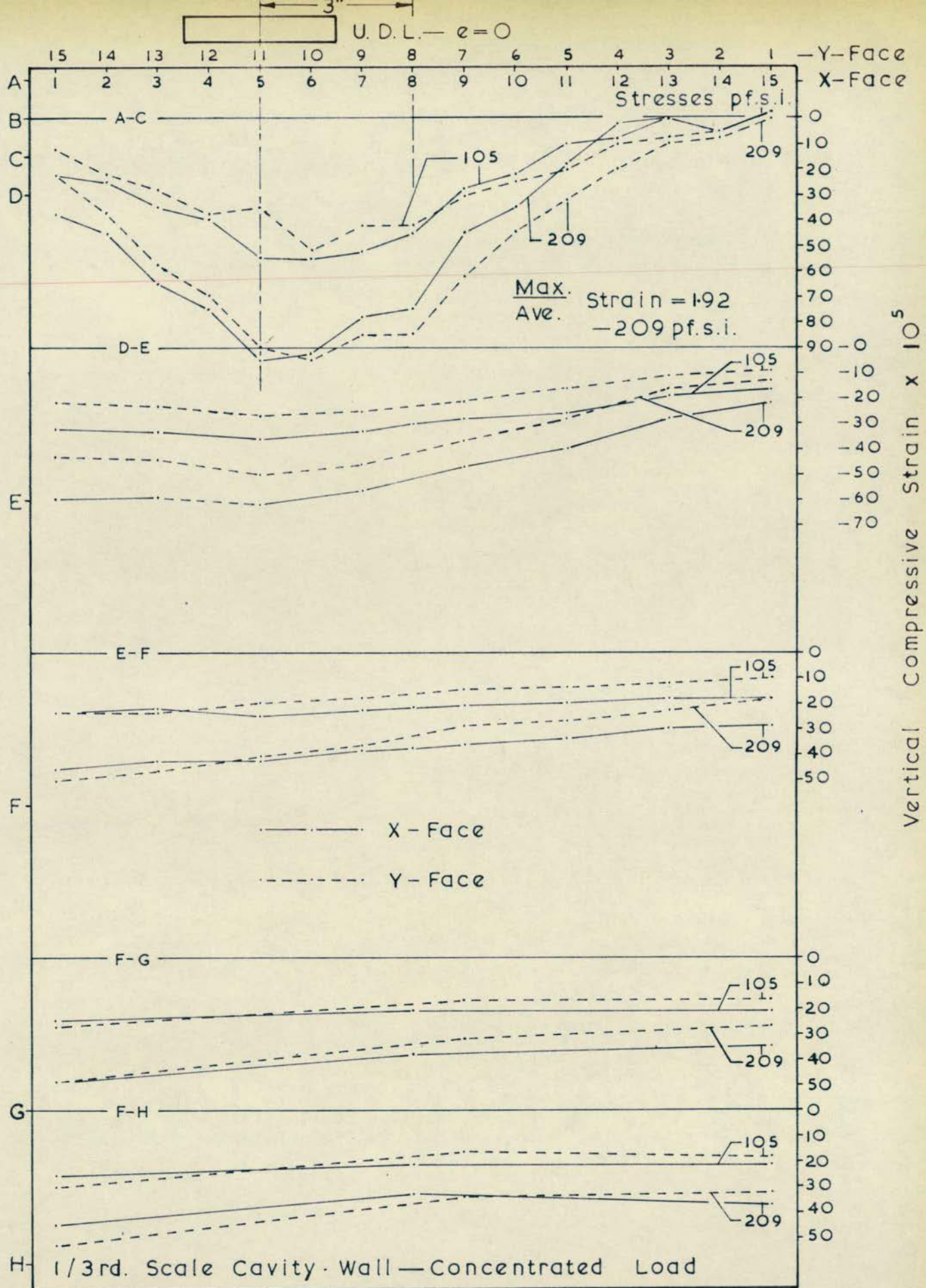
The strain distribution is geometrically similar on both faces.

c) Loadings 4" & 6" from the Transverse Axis.

Figs. 9-20 and 9-21 illustrate the vertical strain distributions when the bearing plates are positioned as indicated, with zero eccentricity from the longitudinal axis.

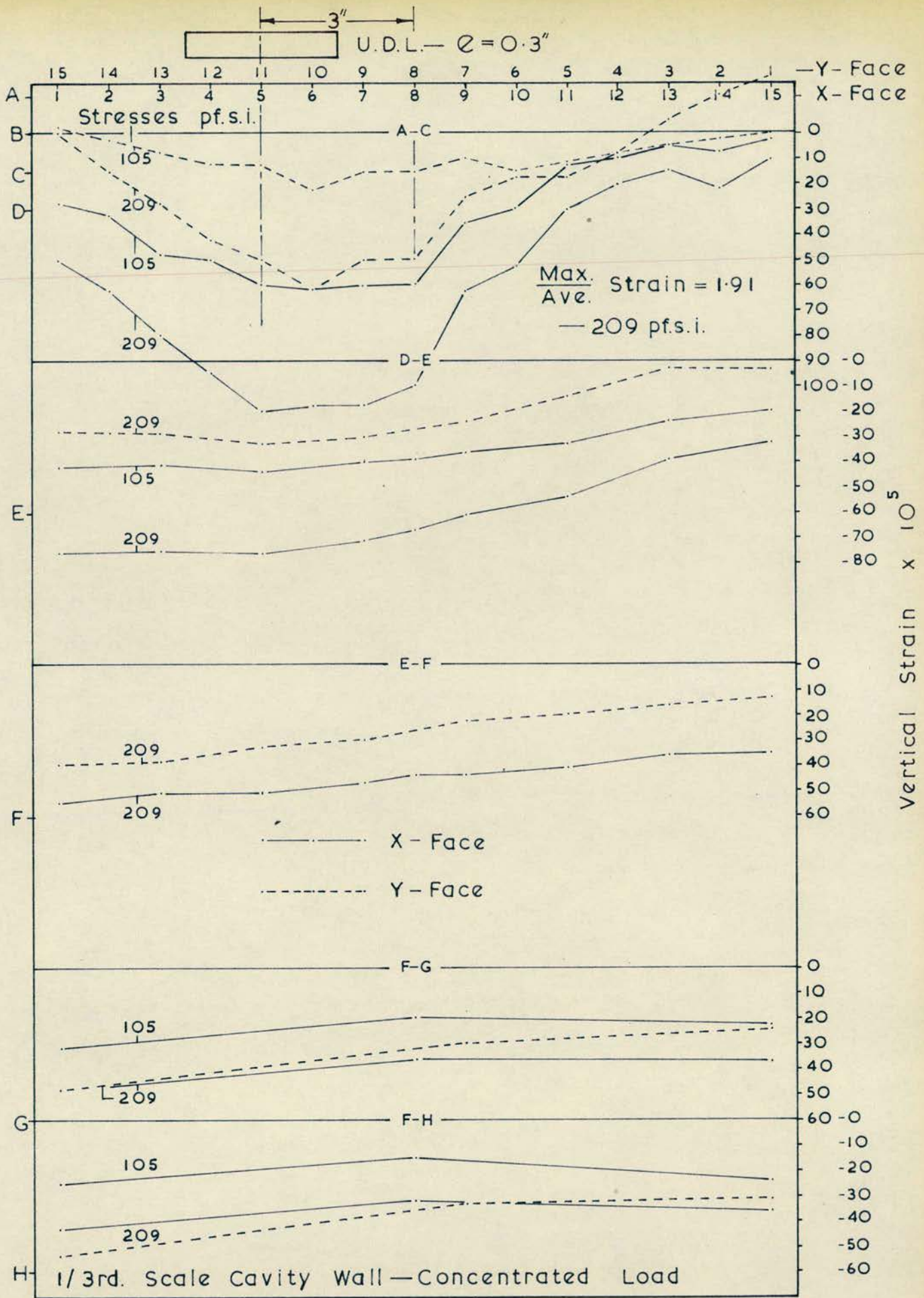
Ideally the load should be uniformly shared, but the strain distributions indicate that the bearing plates were transferring unequal amounts of load.

The strain distribution for the 4" eccentric bearing plates shows that the maximum vertical strain occurs below the bearing



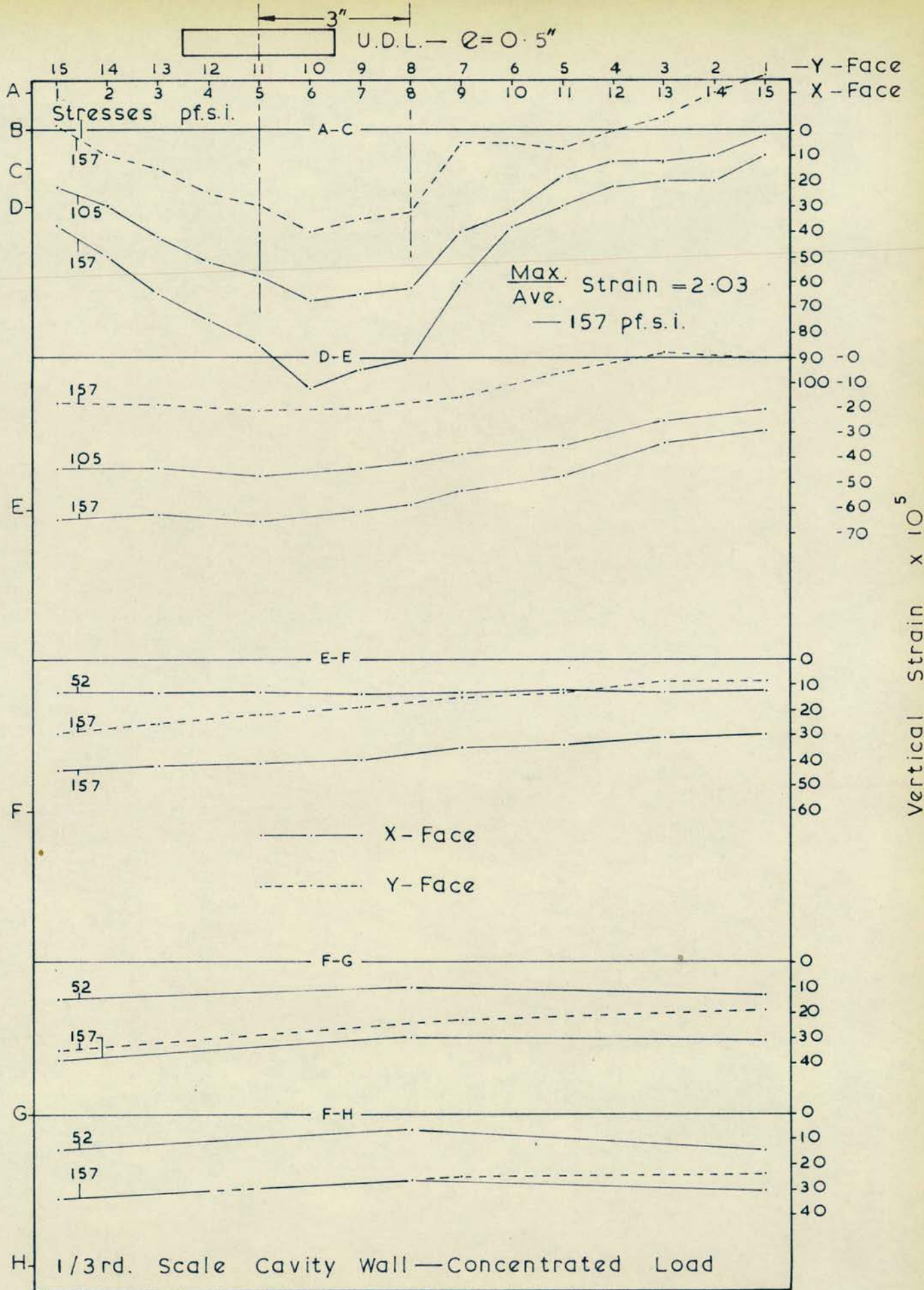
The Strain Distribution on the Faces of a Cavity Wall

Fig. 9-17

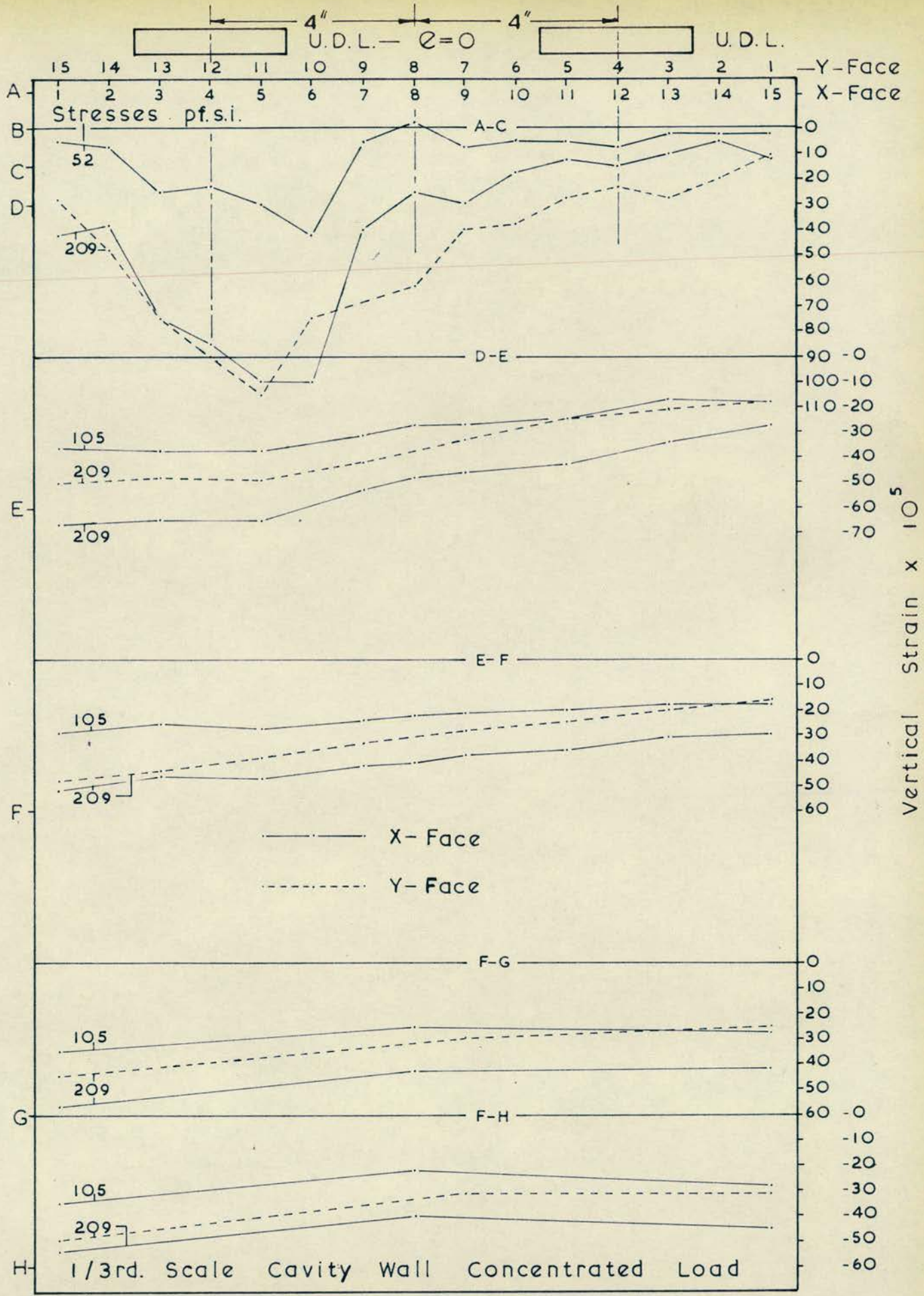


The Strain Distribution on the Faces of a Cavity Wall

Fig. 9-18

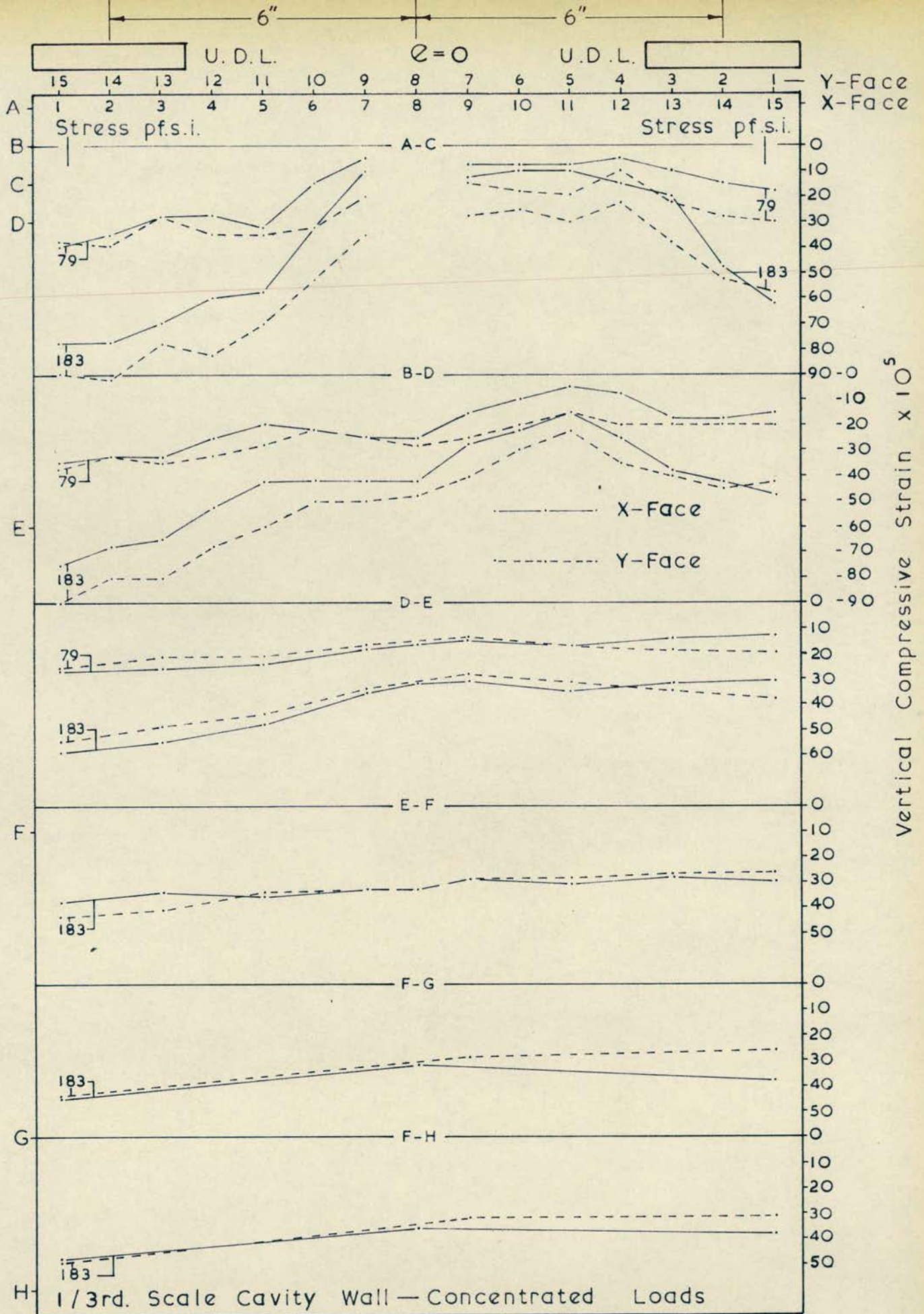


The Strain Distribution on the Faces of a Cavity Wall
 Fig. 9-19



The Strain Distribution on the Faces of a Cavity Wall

Fig. 9-20



The Strain Distribution on the Faces of a Cavity Wall

Fig. 9-21

plate, and the strains are similar on both faces X and Y.

The strain distributions for the edge bearing plates Fig. 9-21 indicate that the applied load is reasonably shared by the two bearing plates, but the difference in strains on the two faces indicates some initial eccentricity. At the top of the wall the maximum strains occur at the end edge of the leaves, whereas, towards the base the strain distribution is nearly uniform across the face, and the strain ratio has also decreased.

ii) Horizontal Strain Distribution.

Figs. 9-22 and 9-23 indicate the horizontal strain distribution, beneath a concentrated axial load, for an average applied stress of 105 pf. s. i.

The strain variation is plotted in two ways.

Fig. 9-22 shows the strain variation along vertical sections, for both wall faces. The strain pattern is confused, and obviously affected by the vertical jointing of the structure.

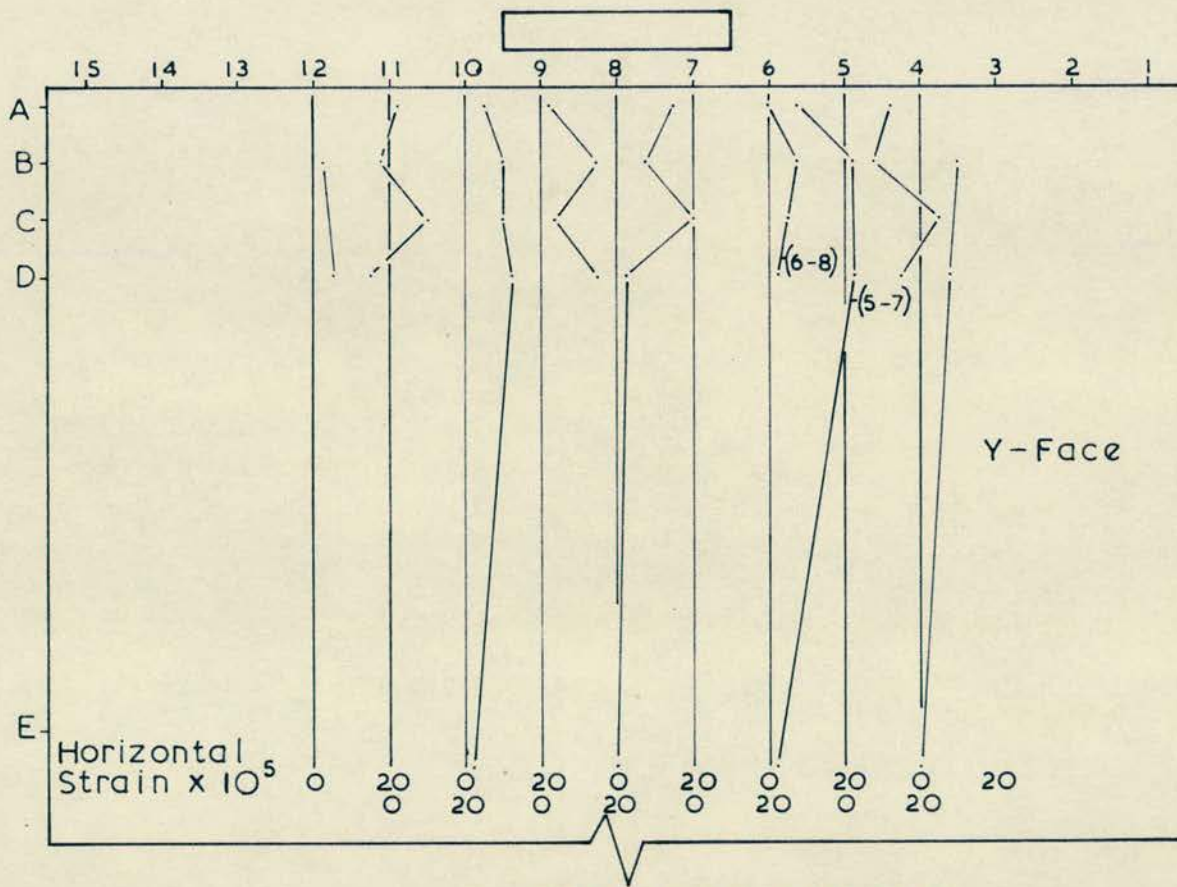
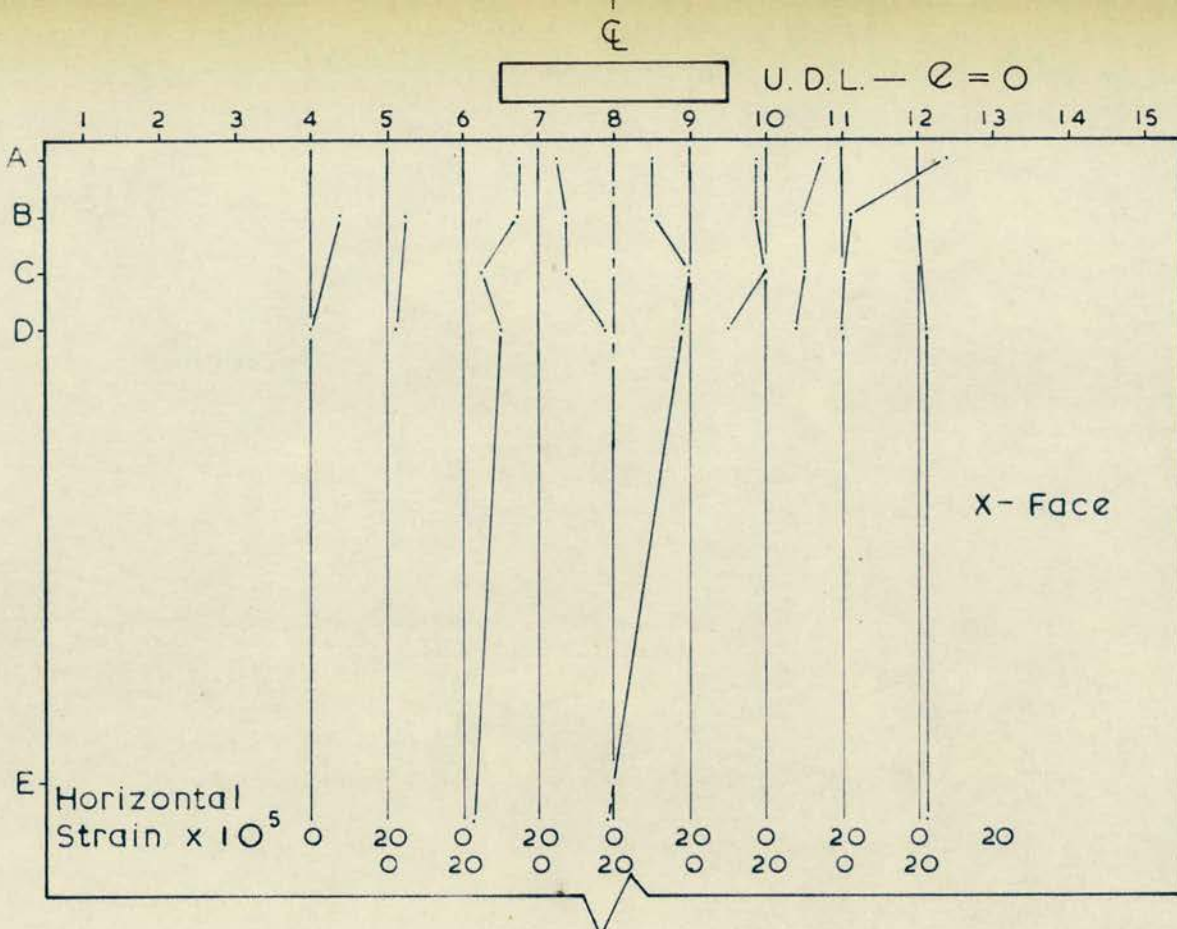
The maximum strains generally occur at levels B and C, and little discernible strain is noted at level E.

Fig. 9-23 shows the variation in horizontal strain along horizontal sections. The strain patterns are similar on both faces, as are the strain magnitudes, the maximum values occurring below the centre-line of the load.

iii. Stress/Strain Relationships.

a) Vertical Compressive Strain.

Fig. 9-24 indicates the Stress/Strain relationship along lines

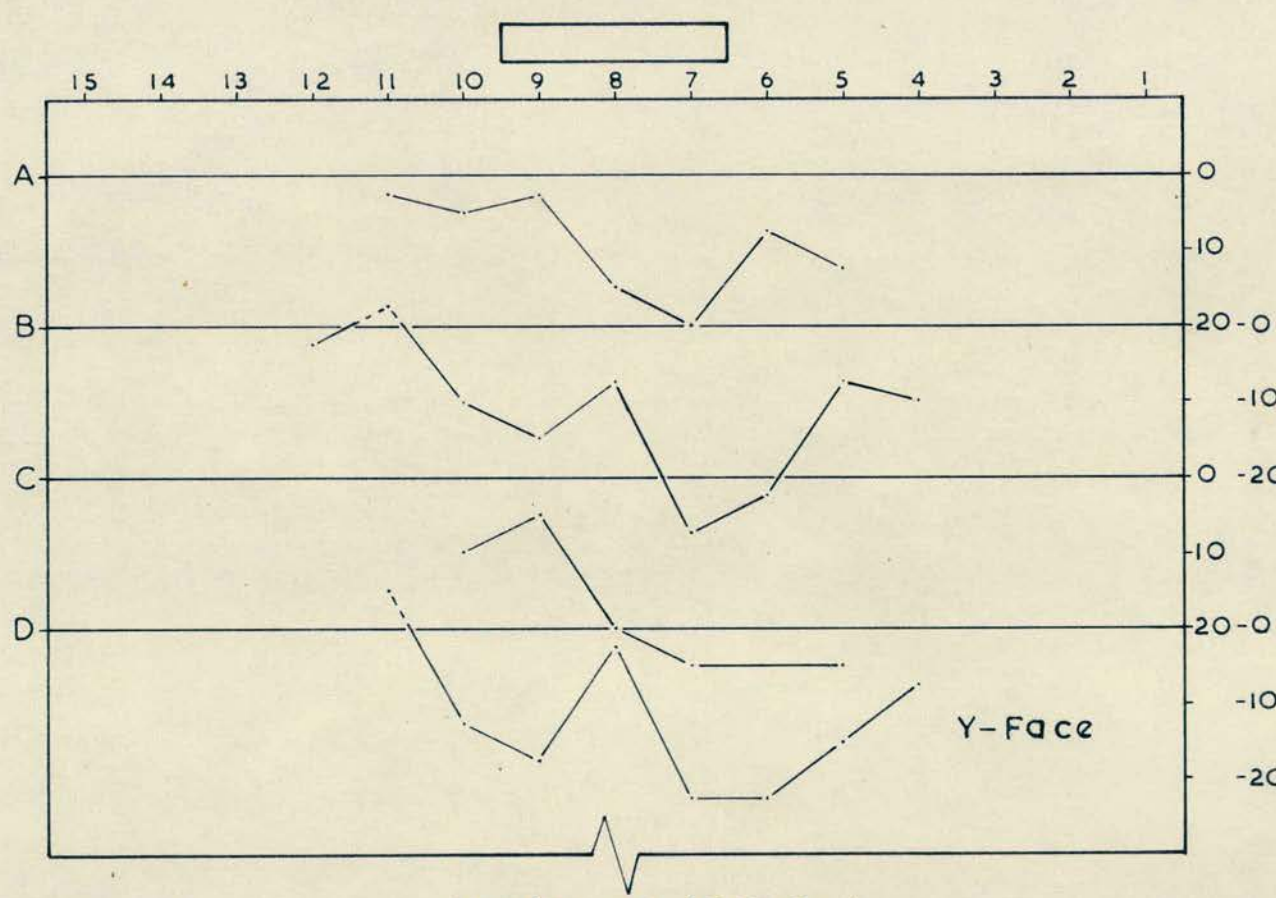
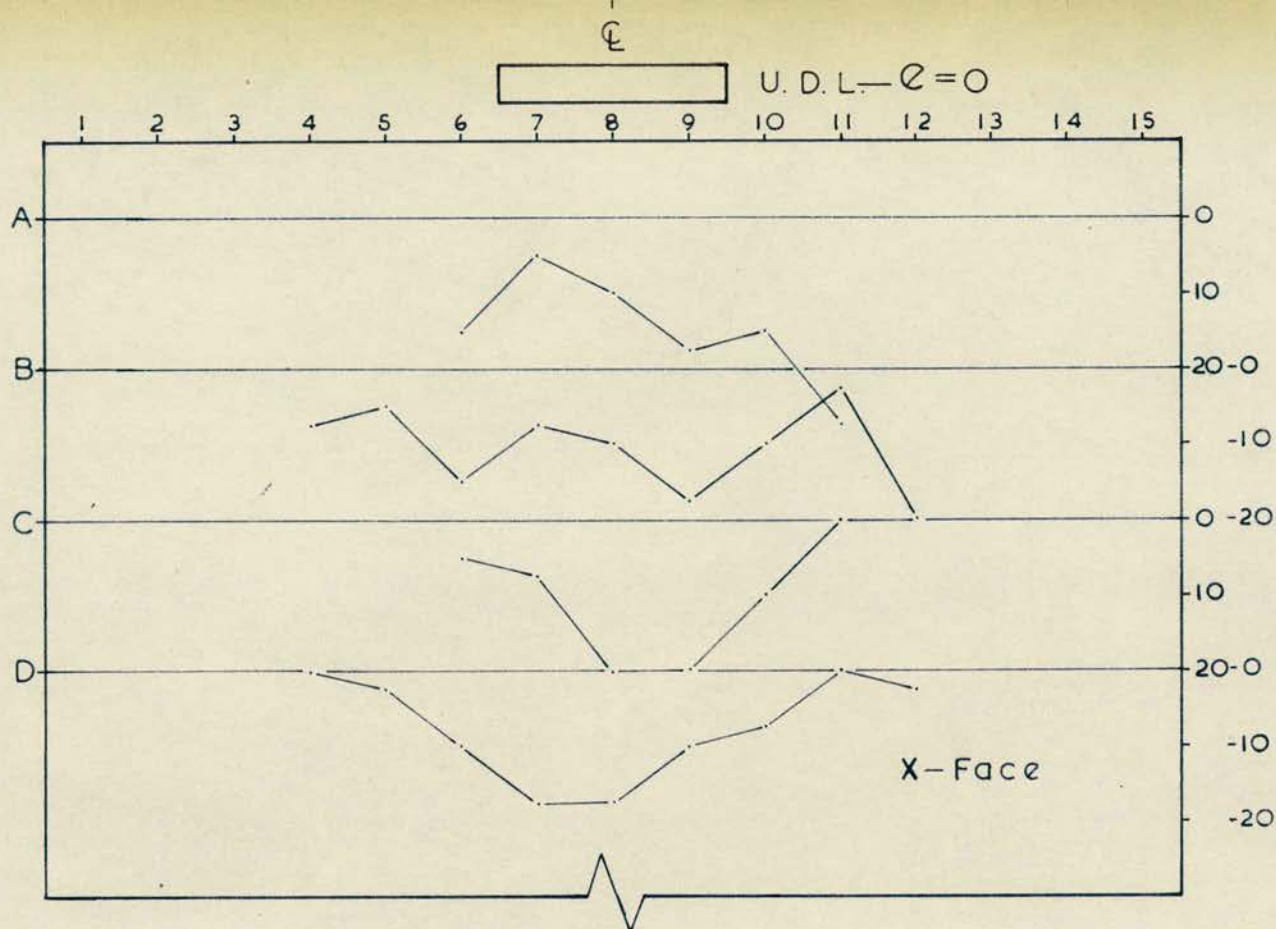


Strains at 105 pf.s.i.

1/3rd. Scale Cavity Wall — Concentrated Load

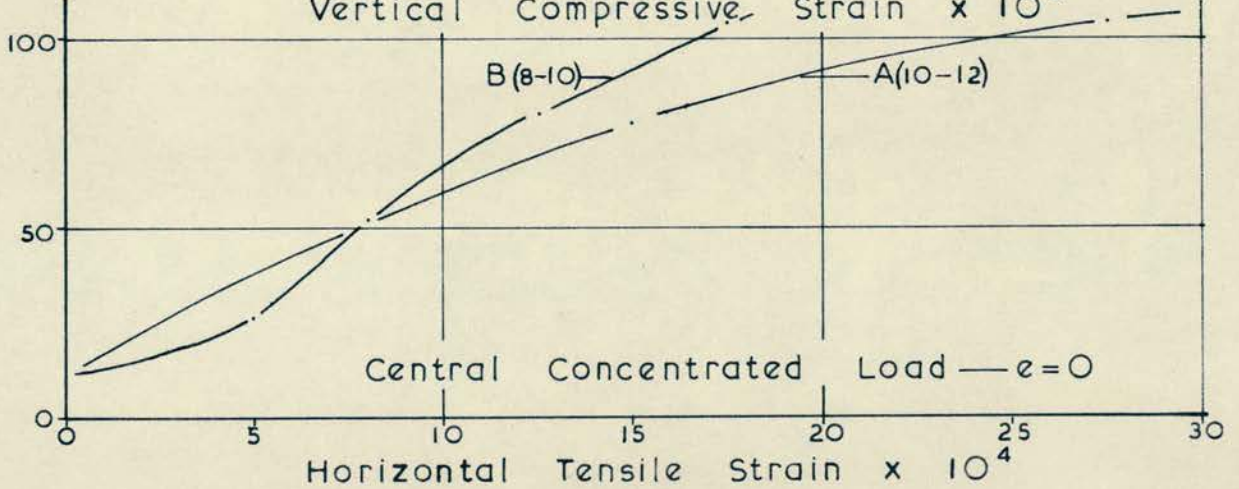
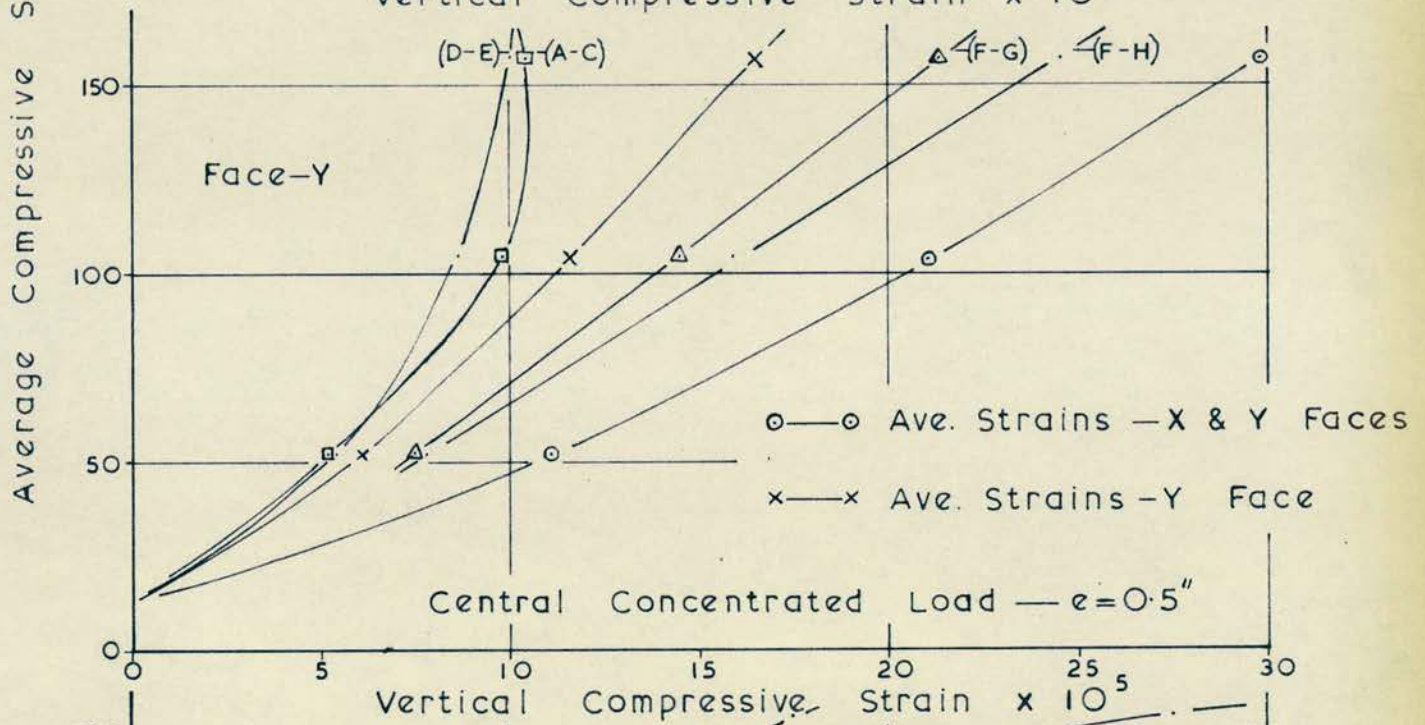
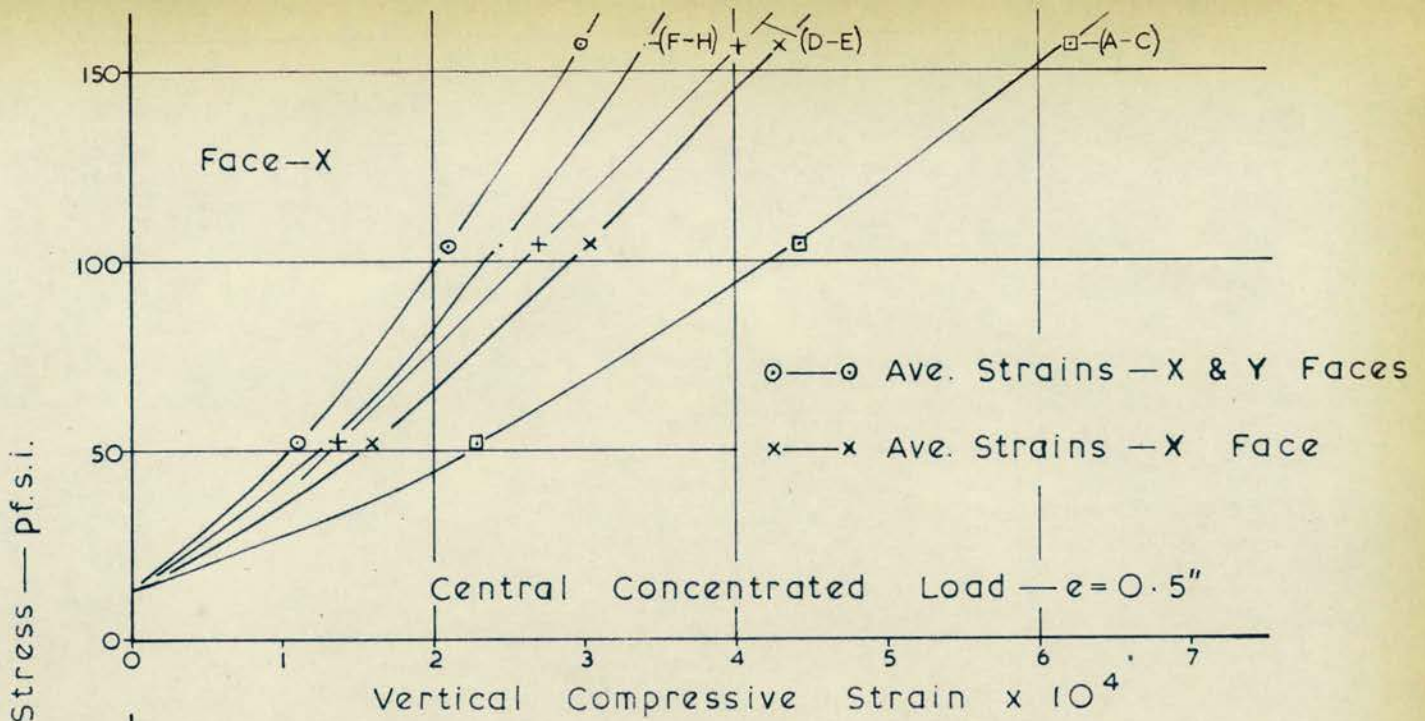
The Horizontal Strain Distribution on the Faces of a Cavity Wall

Fig. 9-22



1/3 rd. Scale Cavity Wall — Concentrated Load

The Horizontal Strain Distribution on the Faces of a Cavity Wall
Fig. 9-23



1/3rd. Scale Cavity Wall — Concentrated Load
 Stress / Strain Relationships

Fig. 9-24

parallel to the direction of loading. The relationship is not linear, and the average strain for both faces, plotted against the average applied stress indicates an increasing E value with increased stress.

For zero eccentricity of loading the average strains were similar on both faces (not illustrated).

b) Horizontal Strain.

Fig. 9-24 shows the Average compressive stress/Horizontal strain relationship, for two positions on the wall face. The relationship is generally non-linear, and very variable.

The maximum measured "tear" tensile strain was 27.5×10^{-5} , compared with a measured maximum compressive strain of 55×10^{-5} on the same face, at the same level, and occurred at level A.

The maximum "splitting" tensile strain, shown in Fig. 9-23 was 27.5×10^{-5} and corresponded in position with the maximum compressive strain measured, which was 80×10^{-5} .

iv. Young's Modulus.

a) Method of Calculation.

As indicated in 4.1.iv. above.

b) Variation with Applied Stress.

From Fig. 9-9 E can be seen to increase non-linearly with stress. The points plotted for the concentrated stresses fit the general pattern of the results for the distributed loadings.

An investigation of the E values at higher stresses was not possible, as the safe strain limit was considered to have been reached. The calculated stress was based on the full wall area, as the nature

of the load distribution through the lintel was unknown.

v. Strain Ratios.

Fig. 9-25 gives the variation in the edge strain ratio for several positions on the leaf, for different stresses and eccentricities of loading.

a) Position on Leaf.

Fig. 9-25 shows that the strain ratio decreased from a maximum near the top of the wall, to a minimum near the base. In some loading cases the strain ratios indicate a point of contra-flexure near the base of the wall.

Similar results were obtained for both positions of concentrated loading.

b) Varying Stress.

The effect of varying the stress was found to be slight within the applied stress range.

c) Varying Eccentricity.

Fig. 9-25 indicates that the strain ratio increased with increasing eccentricity of loading.

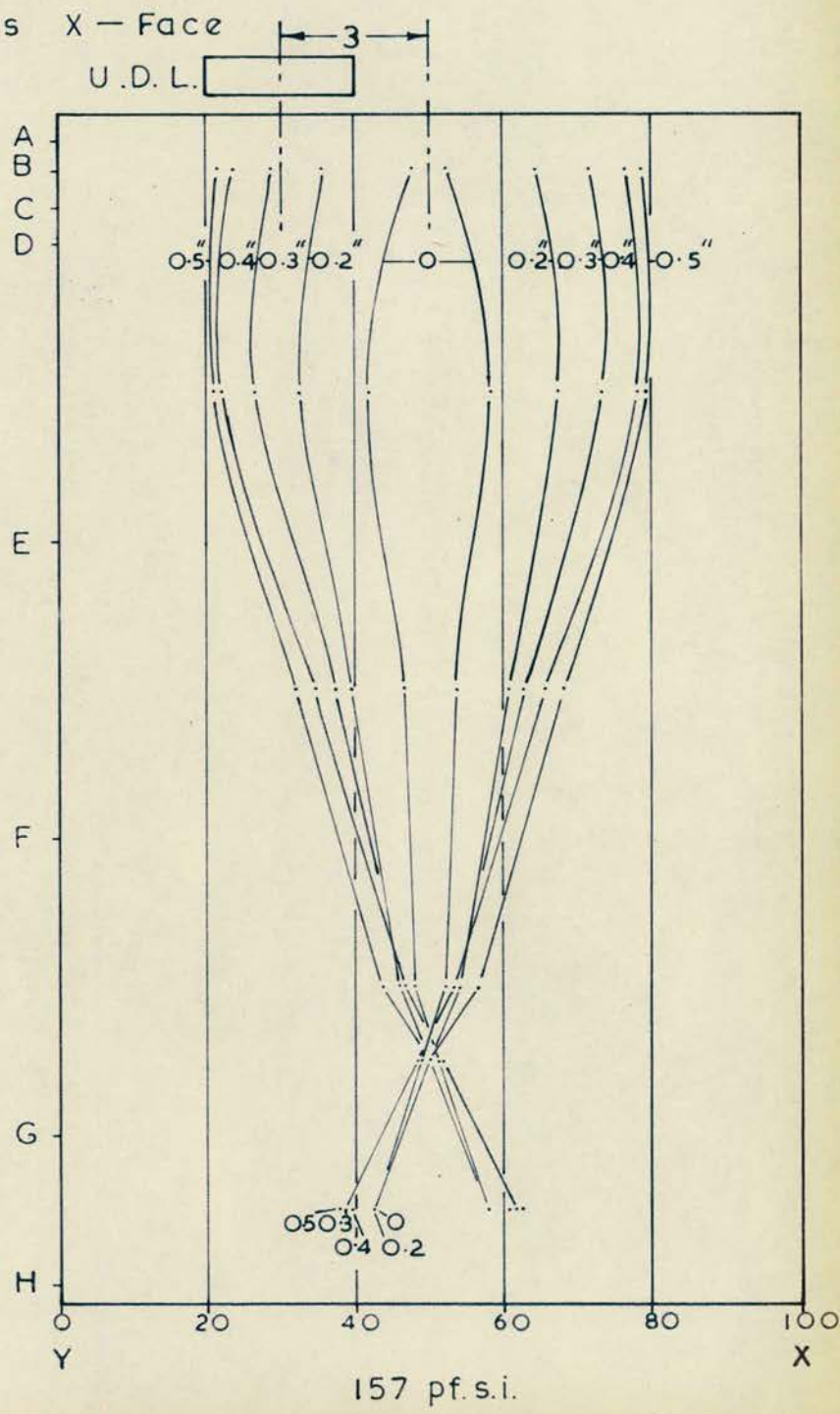
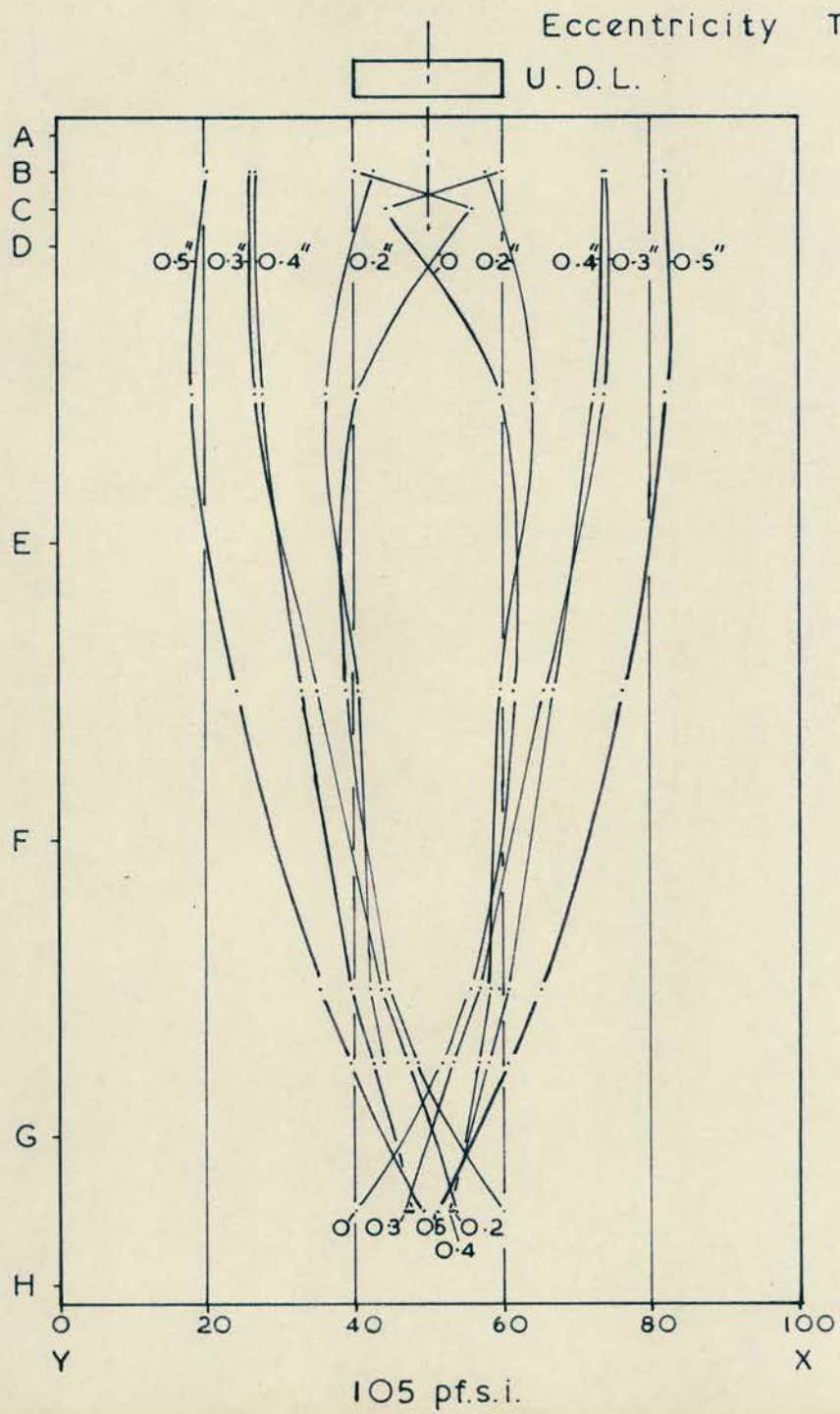
The strain ratios are less than those for the distributed loadings.

The behaviour for the two types of concentrated loading is similar.

5.3 LATERAL DEFLECTION PROFILE.

Fig. 9-26 illustrates the lateral deflection profiles for both leaves of the cavity wall, when an eccentric loading is applied to the wall. The loading case illustrated was a 3" x 3" bearing plate, 3" and 0.5" eccentric.

1/3rd. Scale Cavity Wall — Concentrated Load
 Strain Variation with Load Eccentricity and Load Position
 Fig. 9-25



0/100 Strain on Leaf Faces

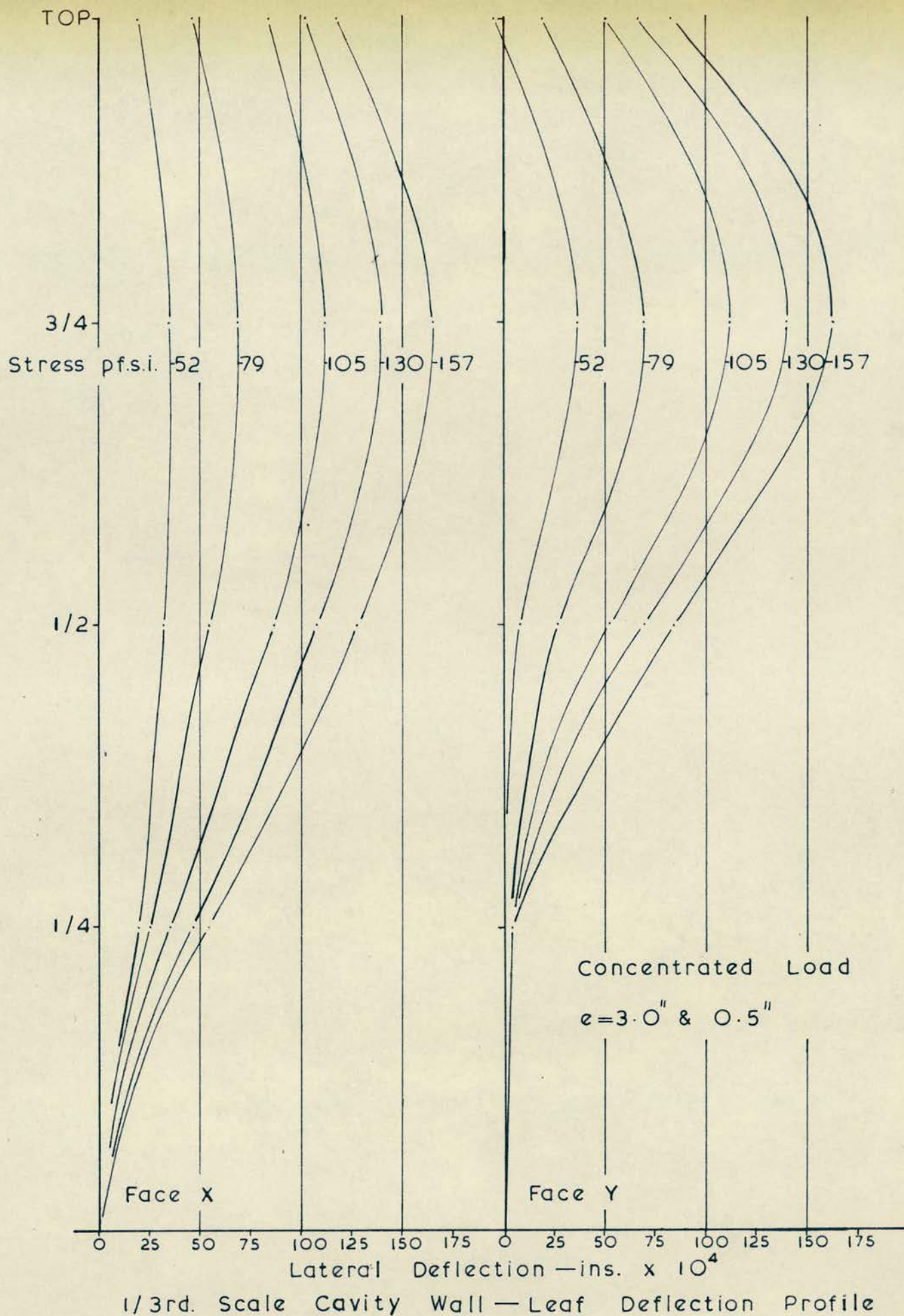


Fig. 9-26

Both leaves have a similar deflection profile, and the maximum deflections measured were approximately the same in both leaves.

The eccentricity of load application was towards the X face, and the deflection profiles are therefore of the expected shape.

Points of interest are the apparent degree of fixity at the base, and the pinned condition at the top of the wall.

The movement of the top of the wall, away from X is surprising especially when the strain ratios are considered. This is discussed in Chapter 10.

The movement of the top of the wall, measured in each test, indicated no definite mode of behaviour, some loadings producing movement in one direction, and others movement in the other direction.

6. CONCLUSIONS.

After this test series certain conclusions can be reached.

6.1 TRANSFER OF BENDING MOMENT.

The measured strains, in all the types of test conducted indicated the transference, by the loading system, of bending moments to the leaves of the wall.

The measured strain ratios indicate that at higher eccentricities and stresses the leaves may have been bending about arbitrary axes, rather than the combined axis of the wall.

The strain ratios obtained indicate that the behaviour of the wall was similar to that of a partially or fully propped cantilever.

6.2 STRAIN DISTRIBUTION.

Strain readings showed that a distributed loading applied to the

lintel was dispersed uniformly to the cavity wall, and only slight local stress concentrations were noted.

Concentrated loadings, applied to the lintel, were distributed to some extent by the lintel, but strain concentrations of the pressure bulb type were measured on the brickwork faces.

Horizontal strain measurements failed to produce conclusive results, as the applied stress levels were low, in all but the final test.

The maximum splitting tensile strains were measured below the centre-line of the concentrated loadings.

6.3 ELASTIC PROPERTIES.

The value of Young's modulus of elasticity was found to increase in the stress range 0 - 500 pf. s. i. A similar result was obtained for the bricks of which the wall was constructed. The E values for the brick and the brickwork are also similar in the stress range where E is constant.

CHAPTER 10.

A DETAILED INVESTIGATION OF THE STRAIN DISTRIBUTION
IN THE LEAVES OF A CAVITY WALL.

1. THE CAVITY WALL UNDER INVESTIGATION.

A 1/3rd scale cavity wall was constructed (No.2), as detailed in Chapter 8. The reinforced concrete lintel from the preliminary test was undamaged, and reused for this wall.

Before testing the wall the 1" mortar cubes, cast at the time of wall construction, were crushed to ensure the mortar had reached the desired strength.

2. TYPES OF LOADING.

2.1 UNIFORMLY DISTRIBUTED LOAD.

Three tests were conducted, applying load over the full lintel length, and with eccentricities of loading of 0", 0.3" and 0.5" from the longitudinal axis of the wall.

2.2 CONCENTRATED LOADINGS.

Concentrated loadings were applied to the lintel through a 3" x 3" mild steel bearing plate, 1" thick.

Various positions of loading were investigated, with eccentricities, from the lateral centre-line of the wall, of 0", 3" and 6", the last being the end bearing condition.

In two tests two bearing plates were used, one at each end of the wall, as this prevented excess vertical tensile strains occurring at the unloaded end.

The following tests were performed, the eccentricity from

the lateral centre-line being stated first.

- i) One 3" x 3" B.P. ; e = 0" and 0.5".
- ii) One 3" x 3" B.P. ; e = 3" and 0.5".
- iii) One 3" x 3" B.P. ; e = 6" and 0".
- iv) Two 3" x 3" B.P.s ; e = 6" and 0.3".
- v) Two 3" x 3" B.P.s ; e = 6" and 0.5".

3. THE STRAIN MEASUREMENTS MADE.

3.1 MEASUREMENTS ON THE FACES OF THE LEAVES.

Certain strain measurements were made on the two exposed leaf faces, X and Y, using 2" and 8" Demec gauges. These measurements were made mainly to allow a comparison of this series of tests with those previously conducted (Chapter 9). Readings were not taken as extensively across the surface of the leaves, but the number of horizontal sections, at which the vertical strain was measured was increased.

3.2 MEASUREMENTS ON THE LEAF ENDS.

Extensive strain measurements were made on the end faces of the cavity wall, α and β , using a 2" Demec gauge. Four strain measurements were made at each level, taking two on each leaf. These four readings were judged sufficient to enable the full strain distribution across the leaf to be plotted.

Measurements were made from the top to the bottom of the wall in order to obtain the full bending moment distribution. The positions of Demec gauge studs are shown in Plate 10-1.

4. LATERAL DEFLECTION MEASUREMENTS.

A series of tests were conducted to determine the lateral deflection profiles of both leaves of the cavity wall.

Four tests were conducted, two having uniformly distributed loading, with eccentricities of 0" and 0.5", and two with a 3" x 3" concentrated loading, having eccentricities of 0" and 0.5", and 3" and 0.5", the first eccentricity denoting the distance of the bearing plate from the lateral centre line of the lintel, and the second from the longitudinal axis.

Mechanical movement dial gauges were positioned to read onto both leaves of the wall, at the quarter points, the mid-height and the top of the wall. Three gauges were positioned at the top, reading onto one face, to indicate any torsional rotation of the wall in plan.

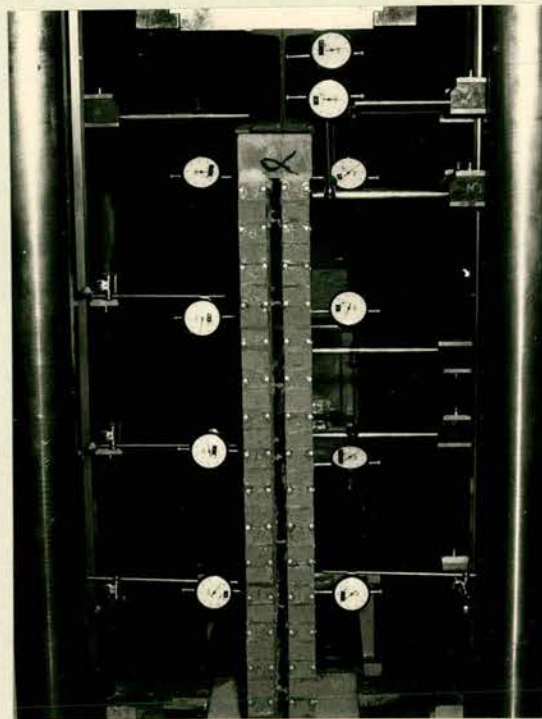
Dial gauges were also arranged to read both onto the web of the "I" section, through which the load was transmitted to the wall, and onto a piece of flat glued to the lintel. The latter reading was not taken when the load was uniformly distributed. These gauges were positioned to determine any rotation in elevation of either the "I" section, or the lintel.

The typical arrangement of the dial gauges is illustrated in Plates 10-1 and 10-2.

5. THE RESULTS OF THE TEST PROGRAMME.

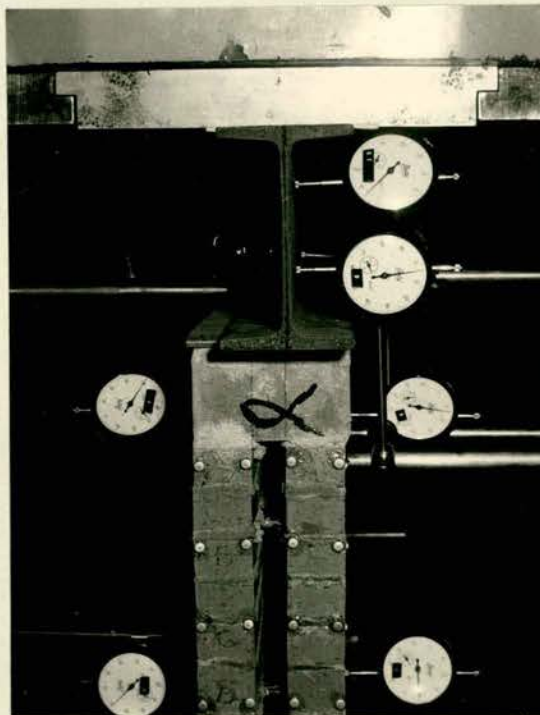
5.1 STRAIN MEASUREMENTS ON THE FACES OF THE LEAVES.

Details of the strain distributions on the faces are not presented, as they were found to be similar to those obtained in the preliminary tests.



1/3rd. Scale Cavity Wall - Demec Stud Positions on The End of the Leaves, and Dial Guages.

Plate 10-1



1/3rd. Scale Cavity Wall - Dial Gauges on I Section and Leaves.

Plate 10-2

The strain distributions for two types of eccentric end loadings are presented in Figs. 10-1 and 10-2, as these types of loading were not investigated in the preliminary series.

The % surface strain on the more heavily stressed leaf is shown in Fig. 10-3 for eccentricities of 0.3" and 0.5" (uniformly distributed load). In this test series the load eccentricity was towards the Y face.

The comparable results from the preliminary test series are also presented in Fig. 10-3.

The variation of vertical strain with position on the more heavily stressed leaf is shown in Fig. 10-4, for eccentricities of distributed load of 0.3" and 0.5", and for various applied loads.

5.2 STRAIN MEASUREMENTS ON THE ENDS OF THE LEAVES.

The strain distribution across the wall leaves, for different types of loading, eccentricity of loading, and applied load, are shown in Figs. 10-5 to 10-9.

The variation of vertical strain on several vertical sections is shown in Fig. 10-10.

5.3 LATERAL DEFLECTION PROFILES.

The lateral deflection profiles of both leaves are presented in Figs. 10-11 to 10-14.

The deflection profiles have been replotted, to show suggested bases for the bending moment diagrams, allowing an explanation of the end strains measured. These bending moment diagrams are shown in Figs. 10-15 and 10-16.

6. DISCUSSION OF RESULTS.

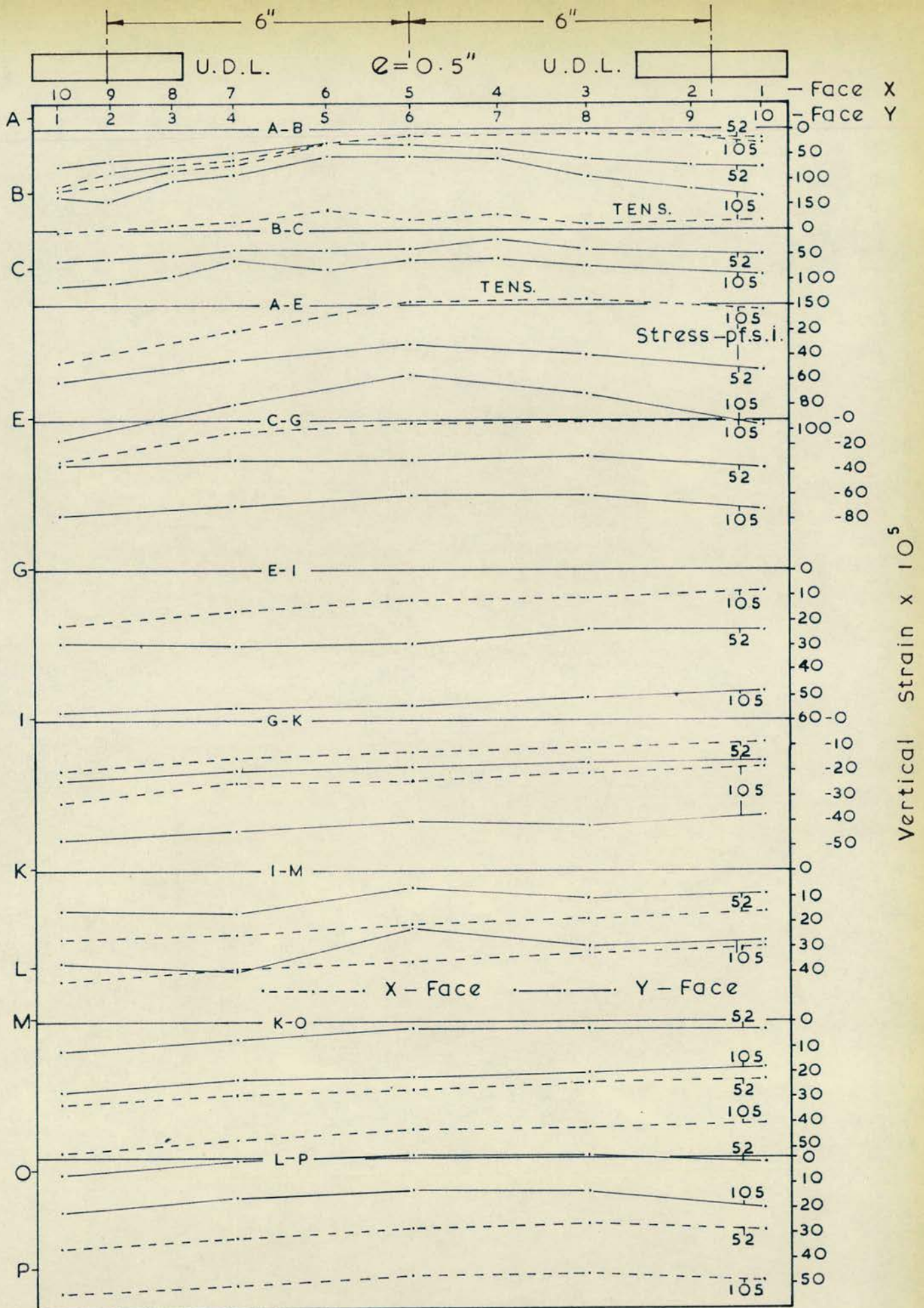
6.1 STRAINS ON THE FACES OF THE LEAVES.

Figs. 10-1 and 10-2 show the vertical strain distributions below the concentrated loadings. Strain concentrations are evident in the regions below the bearing plates. Where the load was applied through two bearing plates the distribution has become uniform by the base of the wall, Fig. 10-1. For the single end bearing plate, Fig. 10-2, the distribution is triangular at the base of the wall.

For the single stress concentration considerable tensile strains were noted at the opposite end of the wall to the loading, indicating the transfer of the eccentric moment. Further down the wall the transfer of the direct stress across the section has countered any tensile stresses, and the strains are purely compressive.

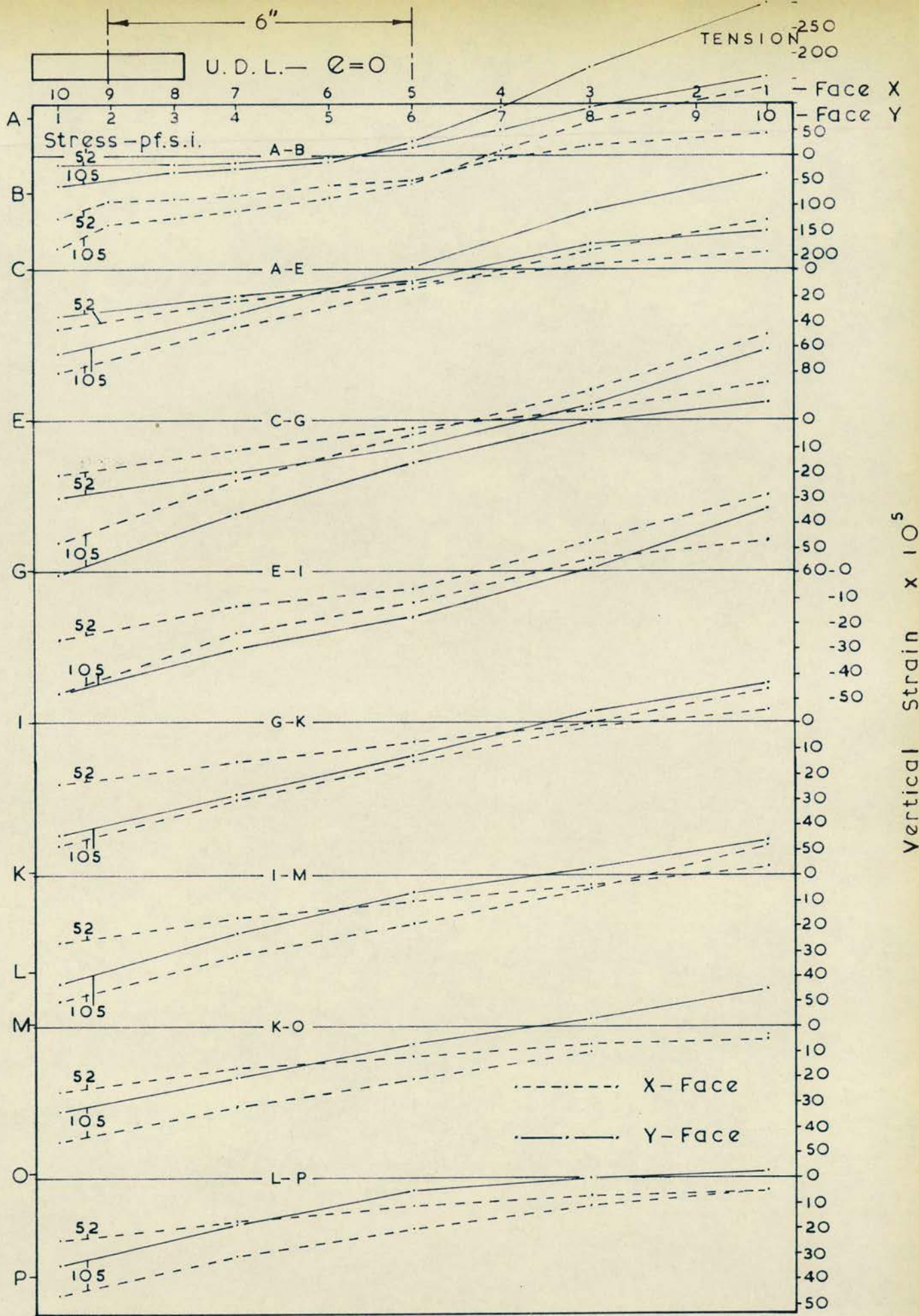
The correlation between the preliminary test series, and the series described in this chapter, shown in Fig. 10-3 is reasonably clear. The % of strain on the faces is similar, where measurements were taken at the same horizontal levels. The second series of tests should have presented a more detailed explanation of the behaviour of the cavity wall, as readings were taken at smaller vertical intervals.

The mode of behaviour at the top of the wall was different for the two walls. In the first test series the wall was aligned in the testing machine in such a way that the platen of the machine was free to move horizontally, as the wall deflected, being restrained only by friction. In the second series the wall was positioned at 90° to the position of the wall in the first series, and the platen was not free to move.



Strain Distribution — 1/3 rd. Scale Cavity Wall

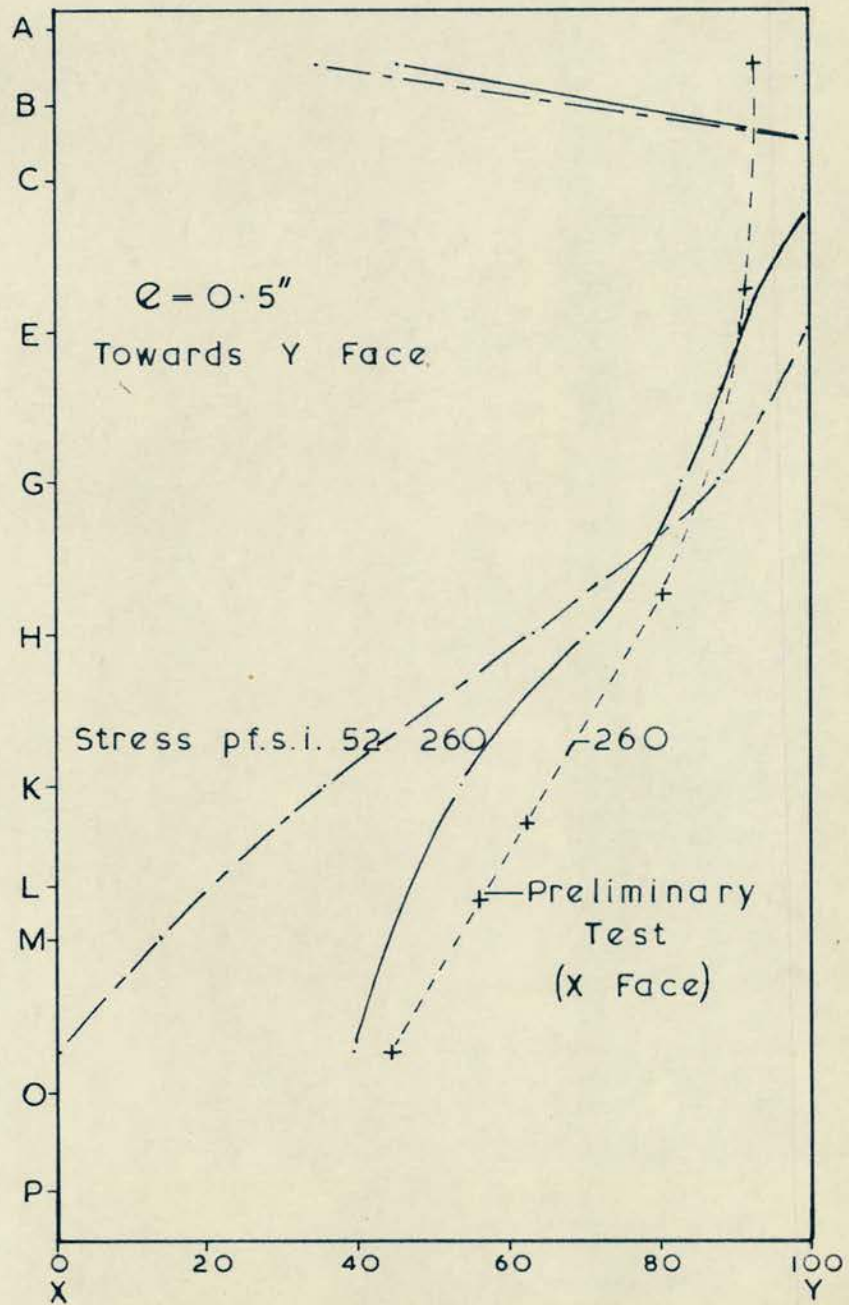
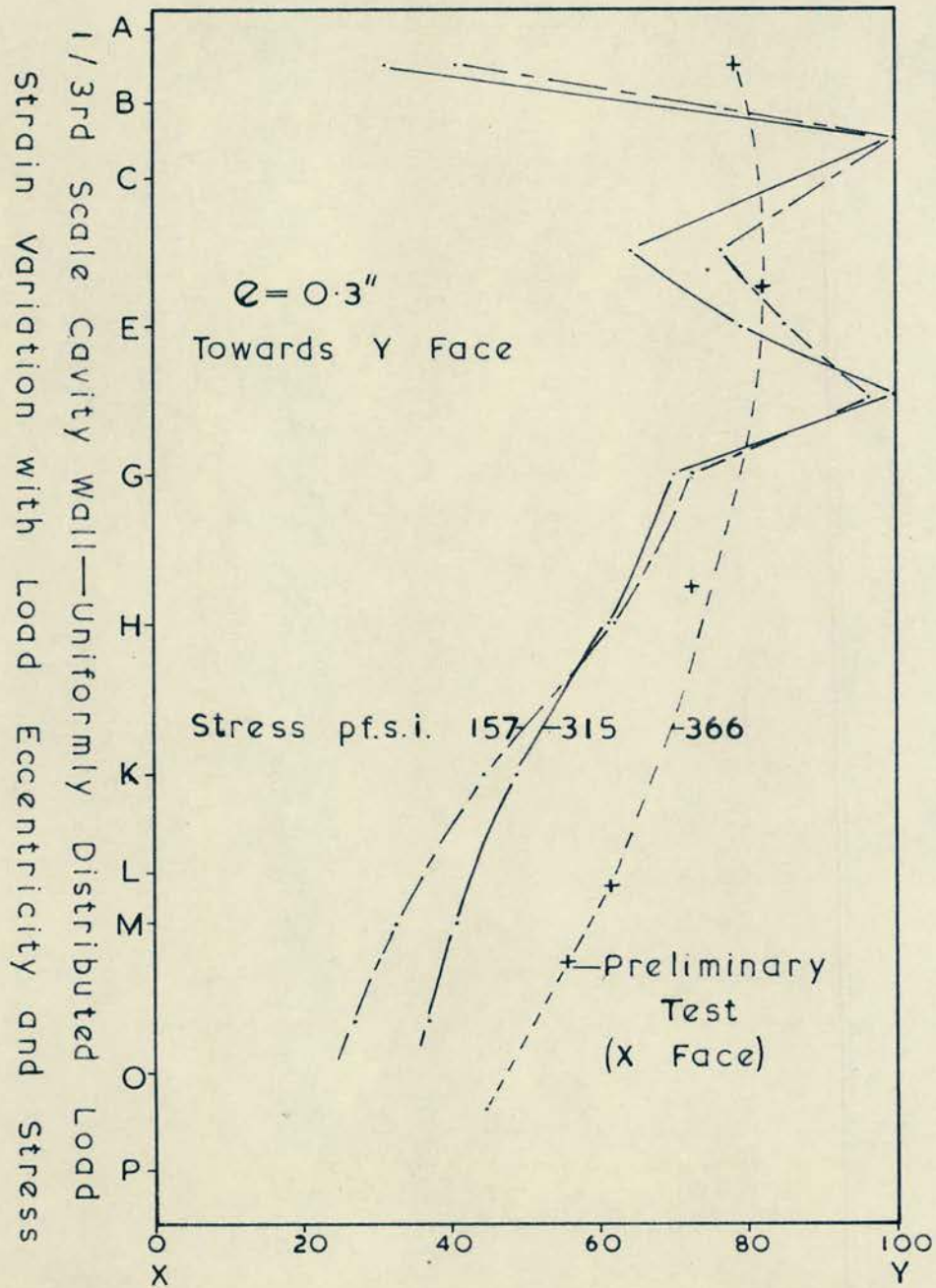
Fig. 10-1



Strain Distribution — 1/3rd. Scale Cavity Wall

Fig. 10-2

Distributed Load



0/0 Strain on Leaf Face Y

Fig. 10-3

Distributed Load — Eccentricity Towards Y Face

Average Vertical Strain Distribution — Face Y

1/3rd. Scale Cavity Wall

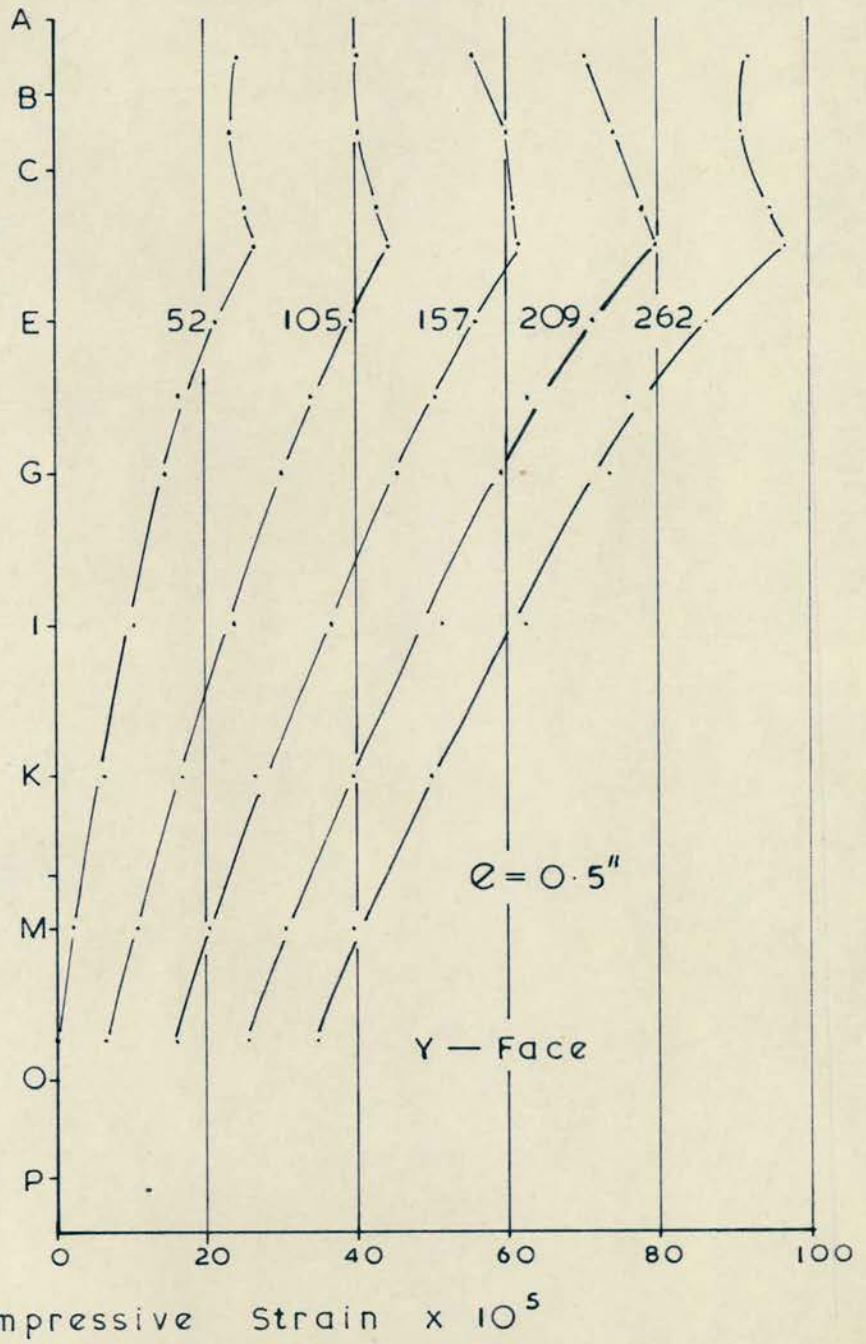
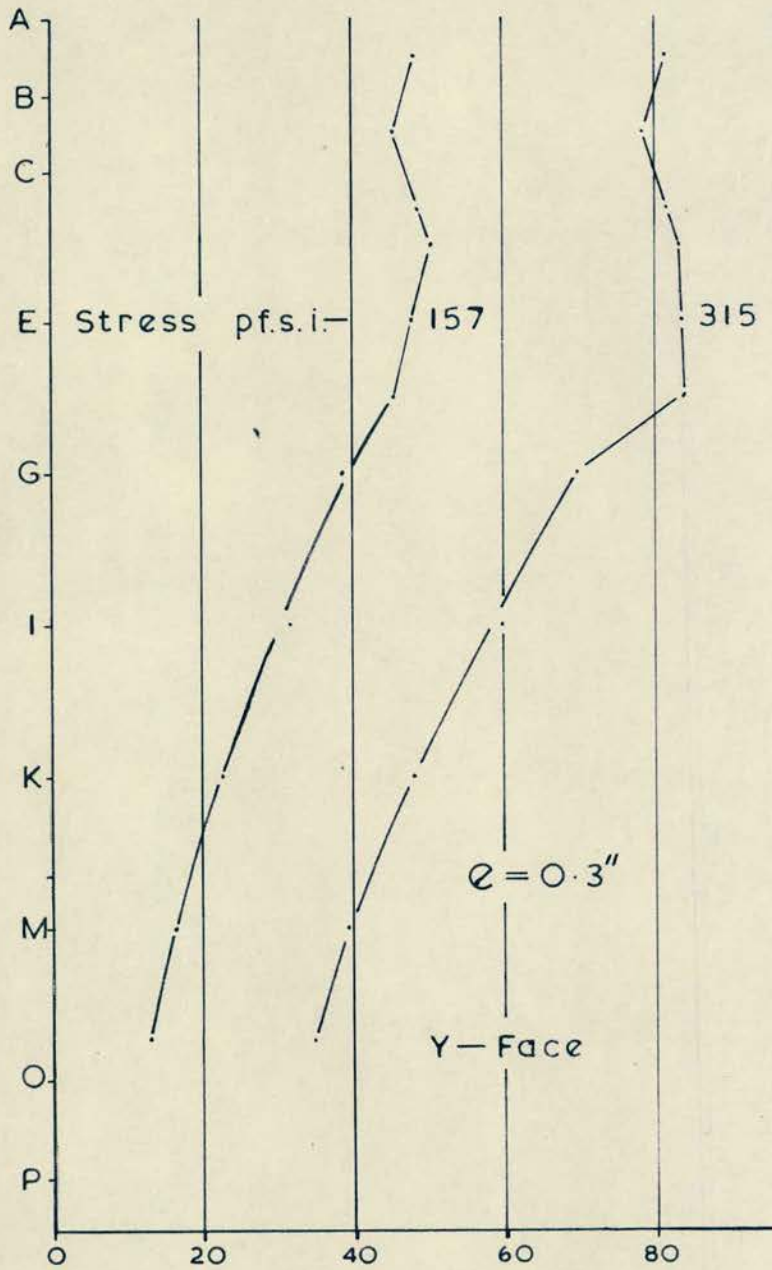


Fig. 10-4

From the strain ratios in the second test series, the maximum moment is seen to occur not at the top of the wall, but at some small distance from it.

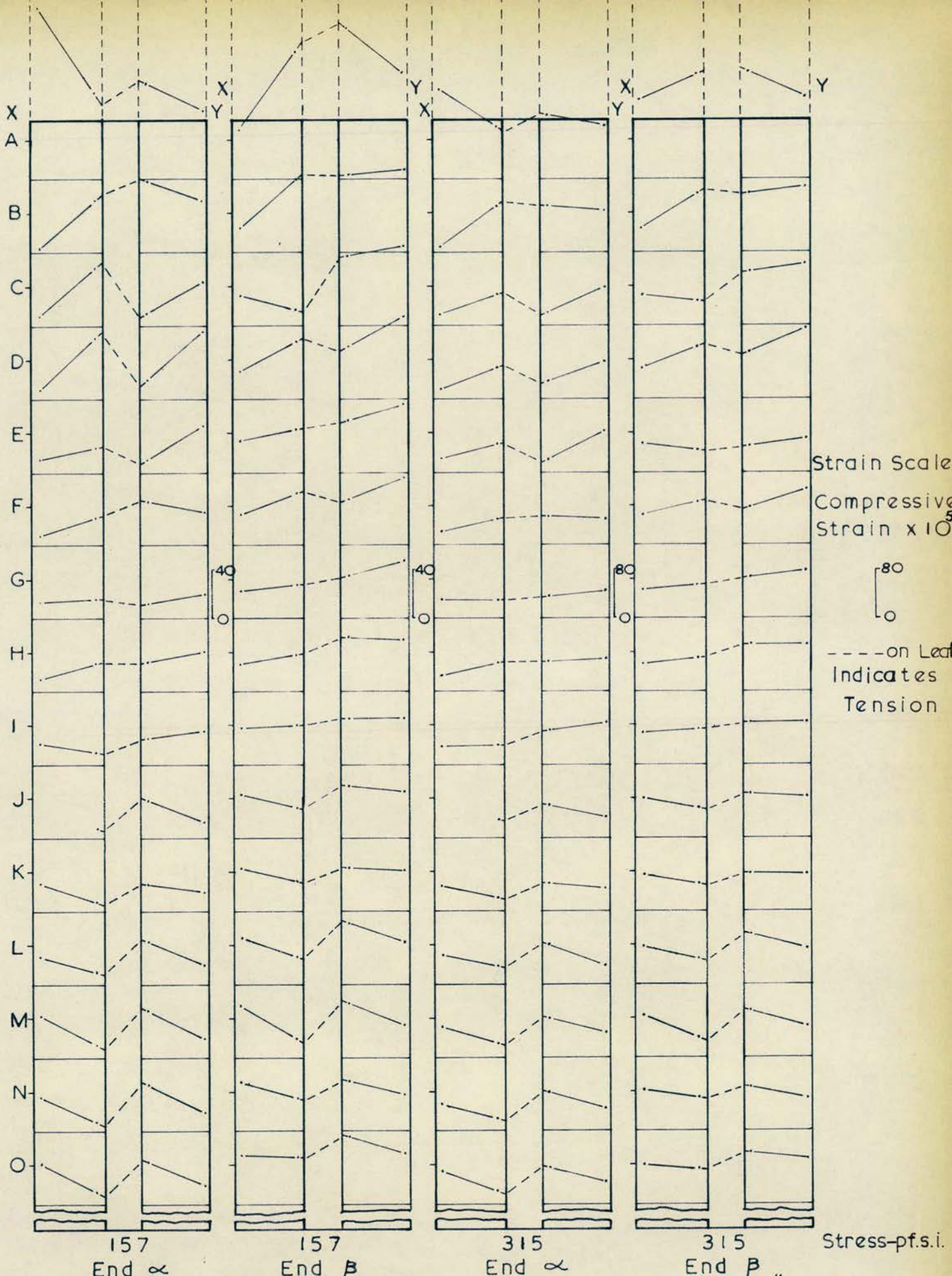
6.2 STRAINS ON THE ENDS OF THE LEAVES.

Figs. 10-5 to 10-9 illustrate the strain distribution on the end faces of the leaves.

The most significant and common factor of all the strain distributions is that the individual leaves of the cavity wall are bending about axes which are distinct for each leaf, rather than the neutral axis of the combined wall unit. This is true irrespective of the level of stress, and the position on the wall.

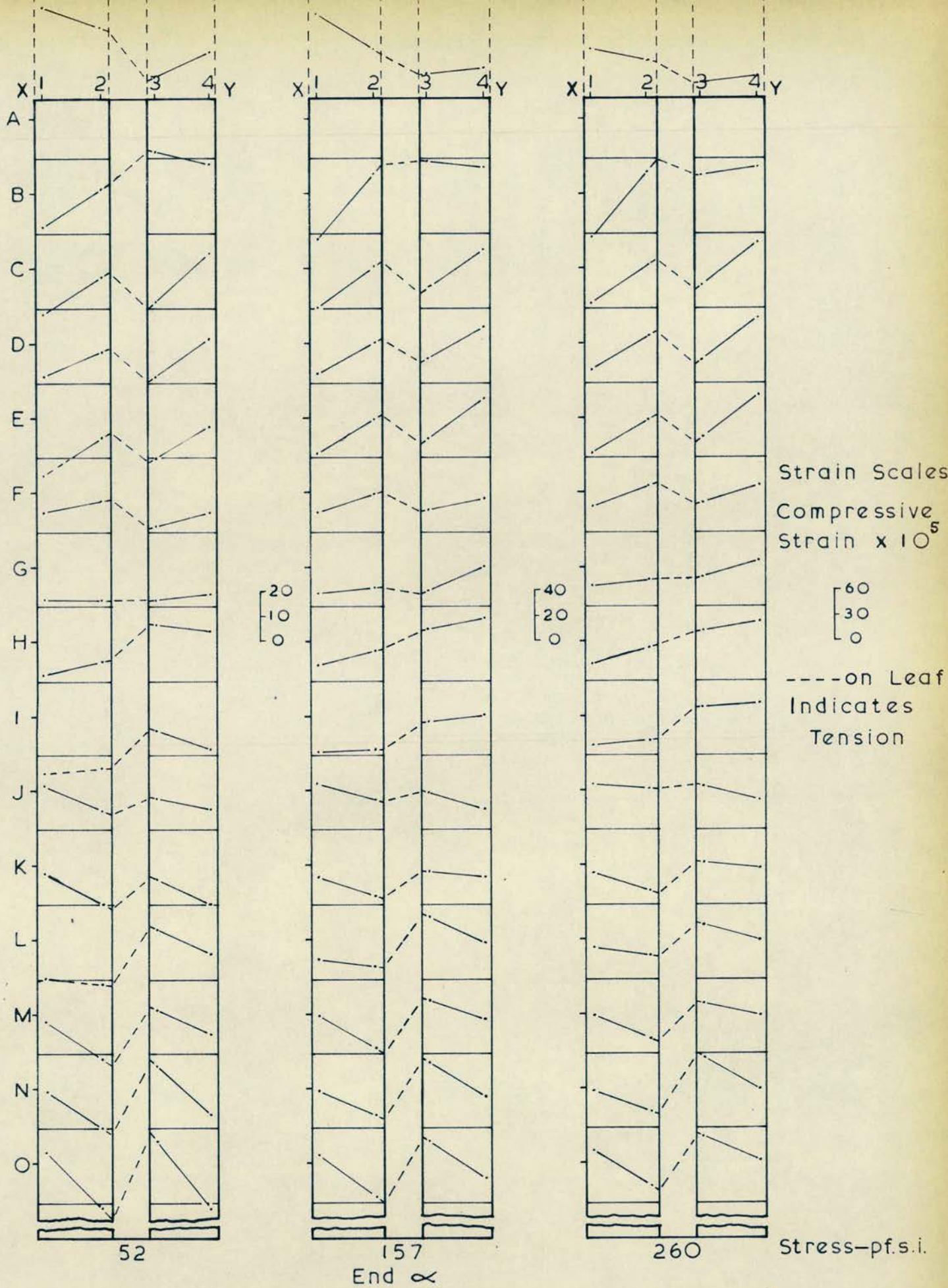
The axes about which the leaves are bending are difficult to determine, as the bending moment transmitted to the wall may not be the full value of the Applied load X the nominal eccentricity. If the leaves were bending about their own axes, and the full moment was transmitted, then tensile strains would occur for even small eccentricities. From the experimental results tensile strains are not observed under these conditions, and so either the transmitted moment is smaller than intended, or the leaves are bending about intermediate axes, in between the combined axis and their own axes. The axes of bending appear to be parallel, confirming the efficiency of the wall ties as tie or strut members.

The bending moment distribution in the wall, from the lintel to the base can be ascertained from the variation of the strains on the end faces. The strains indicate a point of inflection, and hence



The Strain Distribution on the Leaf Ends

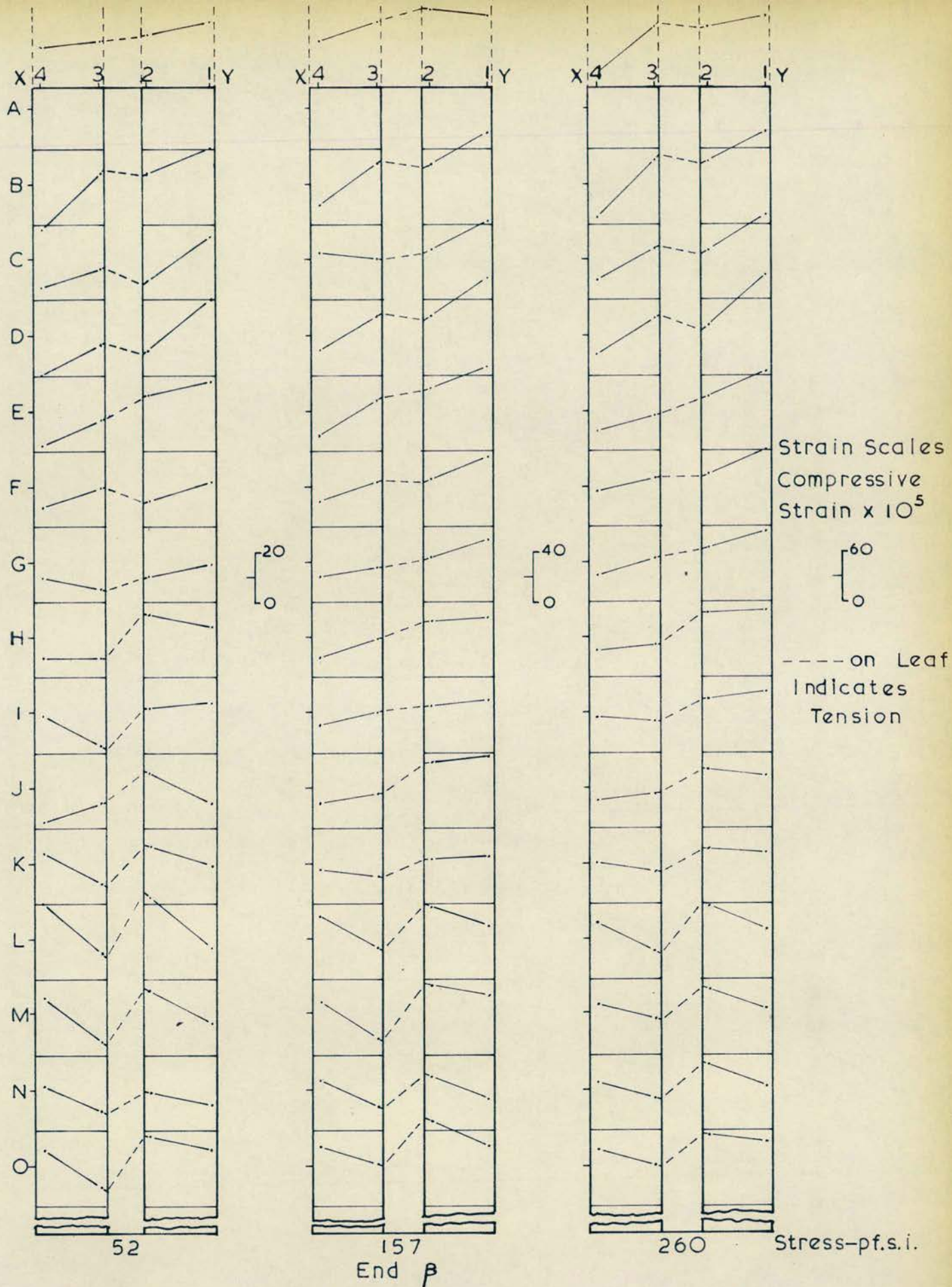
Fig. 10-5



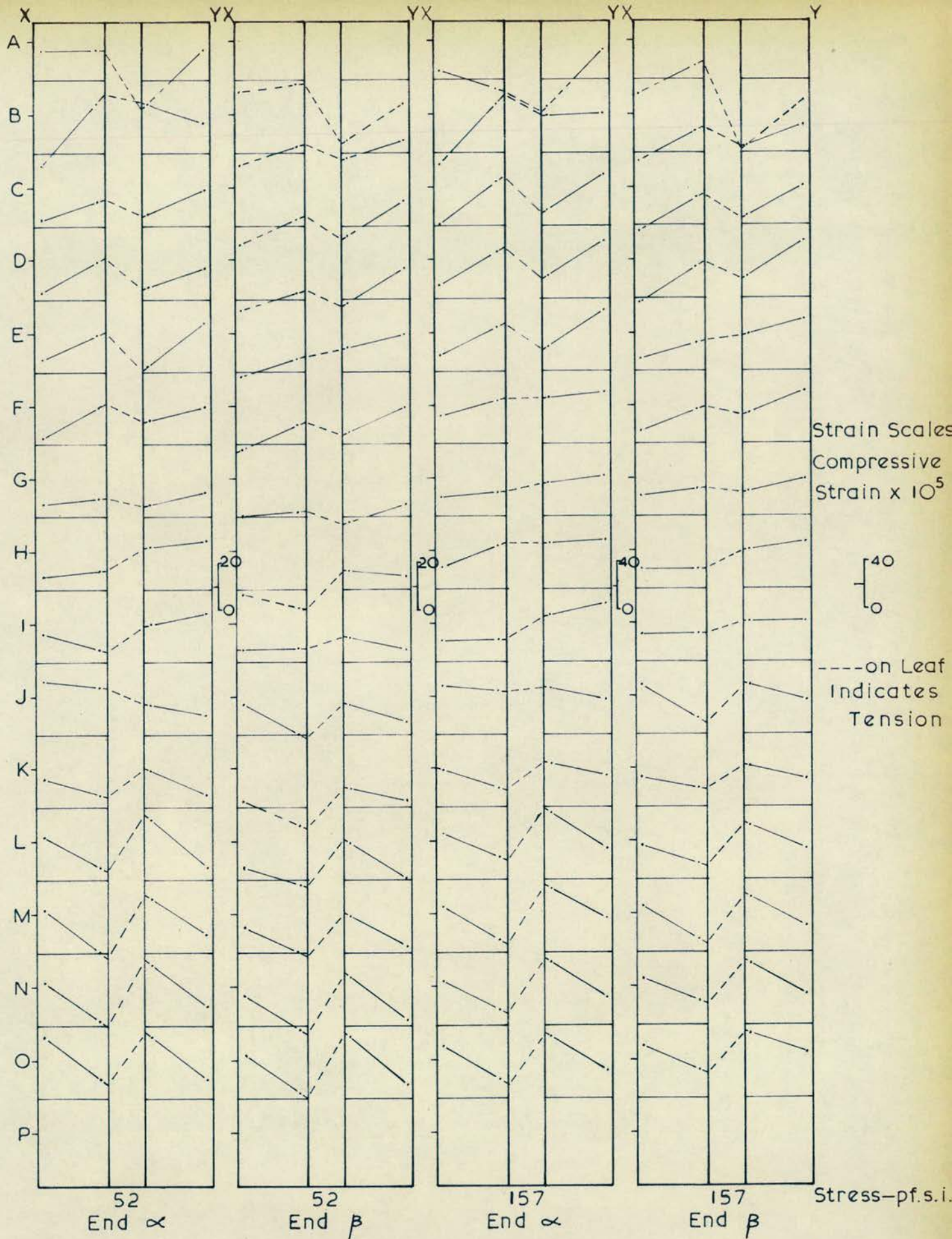
1 / 3rd. Scale Cavity Wall — Distributed Load — $e = 0.5'' \rightarrow Y$

The Strain Distribution on the Leaf End

Fig. 10-6

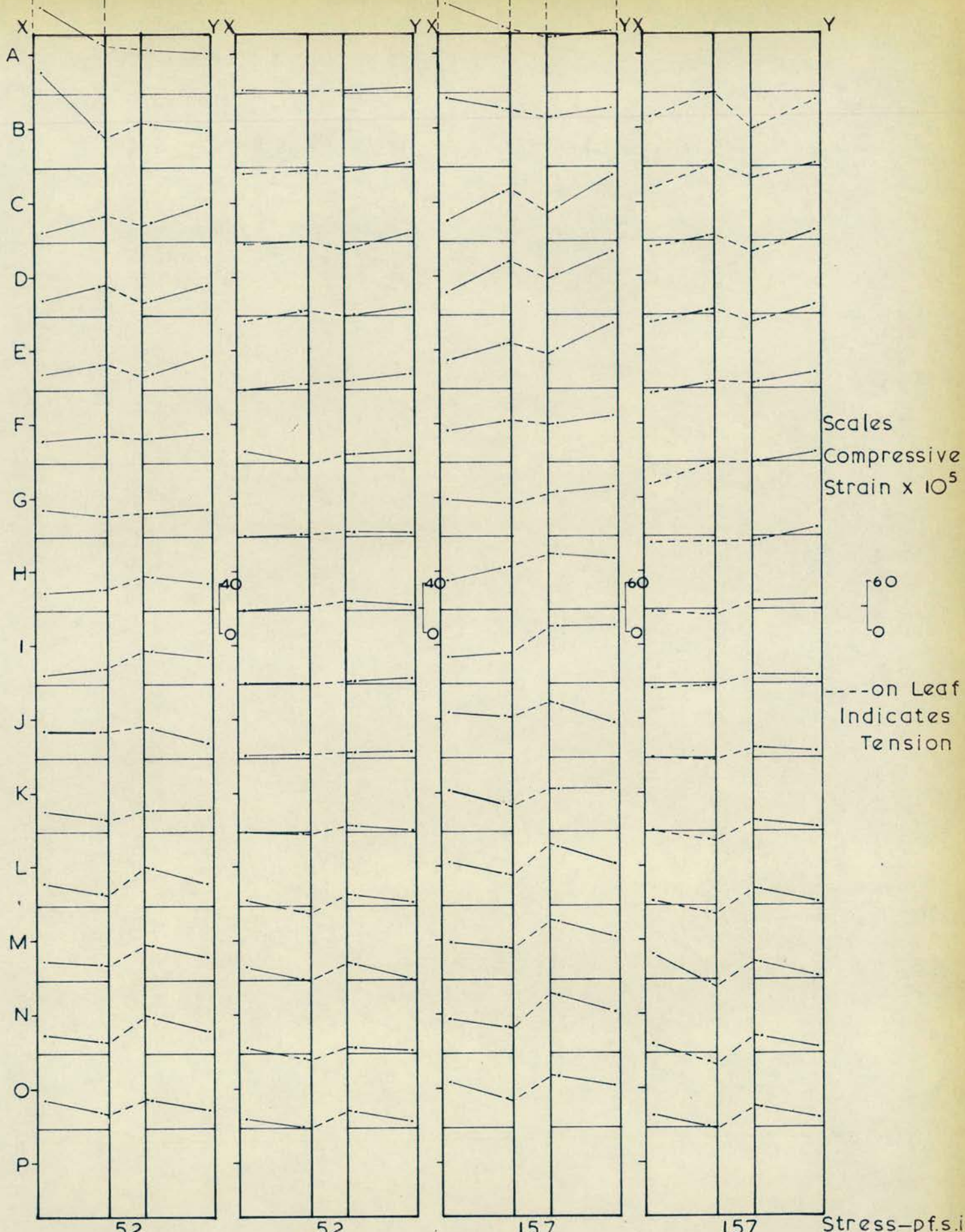


1/3rd. Scale Cavity Wall — Distributed Load — $e = 0.5'' \rightarrow Y$
 The Strain Distribution on the Leaf End
 Fig. 10-7



1/3rd. Scale Cavity Wall—Central Concentrated Load — $e=0.5'' \rightarrow Y$
The Strain Distribution on the Leaf End

Fig. 10-8



1/3rd. Scale Cavity Wall—Eccentric Concentrated Load— $e=3.0'' \rightarrow \alpha$, & $0.5'' \rightarrow Y$
 The Strain Distribution on the Leaf End

Fig. 10-9

zero moment, at the approximate position I-J.

A second point of zero bending moment was observed, in some tests, near the lintel.

Fig. 10-9 indicates the tendency for tensile strains to develop, when the load is applied eccentrically with respect to both axes of the wall. Tensile strains exist at some point of the lesser loaded ends for all vertical sections.

Fig. 10-10 presents the vertical strain distributions, for one leaf, considering both ends, α and β . The positions investigated, α -4 and β -1 are for the leaf near face Y, and α -3 and β -2 for the same leaf, near the cavity.

The strain distribution is similar for ends α and β , although strains were higher for the end β , in both positions, and particularly near the top of the leaf. The higher strain is probably due to some initial unevenness of load distribution.

The strains at the top of the leaves are high, for both the ends α and β , and for both sides of the leaf. Consultation of the end strain distributions indicates that the leaves are behaving independently and erratically at this level.

6.3 LATERAL DEFLECTION PROFILES.

Figs. 10-11 to 10-16 illustrate the lateral deflection profiles.

In all cases a large lateral deflection was noted, when only a small load was applied, and this has been considered as the initial settling deflection, and arbitrary stresses were chosen, from which the further deflection under load could be measured.

Fig. 10-11 shows the lateral deflection profile for a uniformly distributed load, with a zero eccentricity. Deflection readings plotted were taken at the centre-line of each leaf face. The deflection profiles indicate that at low loads deflection is taking place, without any bending moment being transferred to the wall. At higher loads the deflection profiles become less linear, indicating that moment has been introduced by the lateral deflection of the wall.

The deflection profiles of both leaves are similar, and readings taken at the ends α and β of the faces indicated deflections little different from the centre-line values.

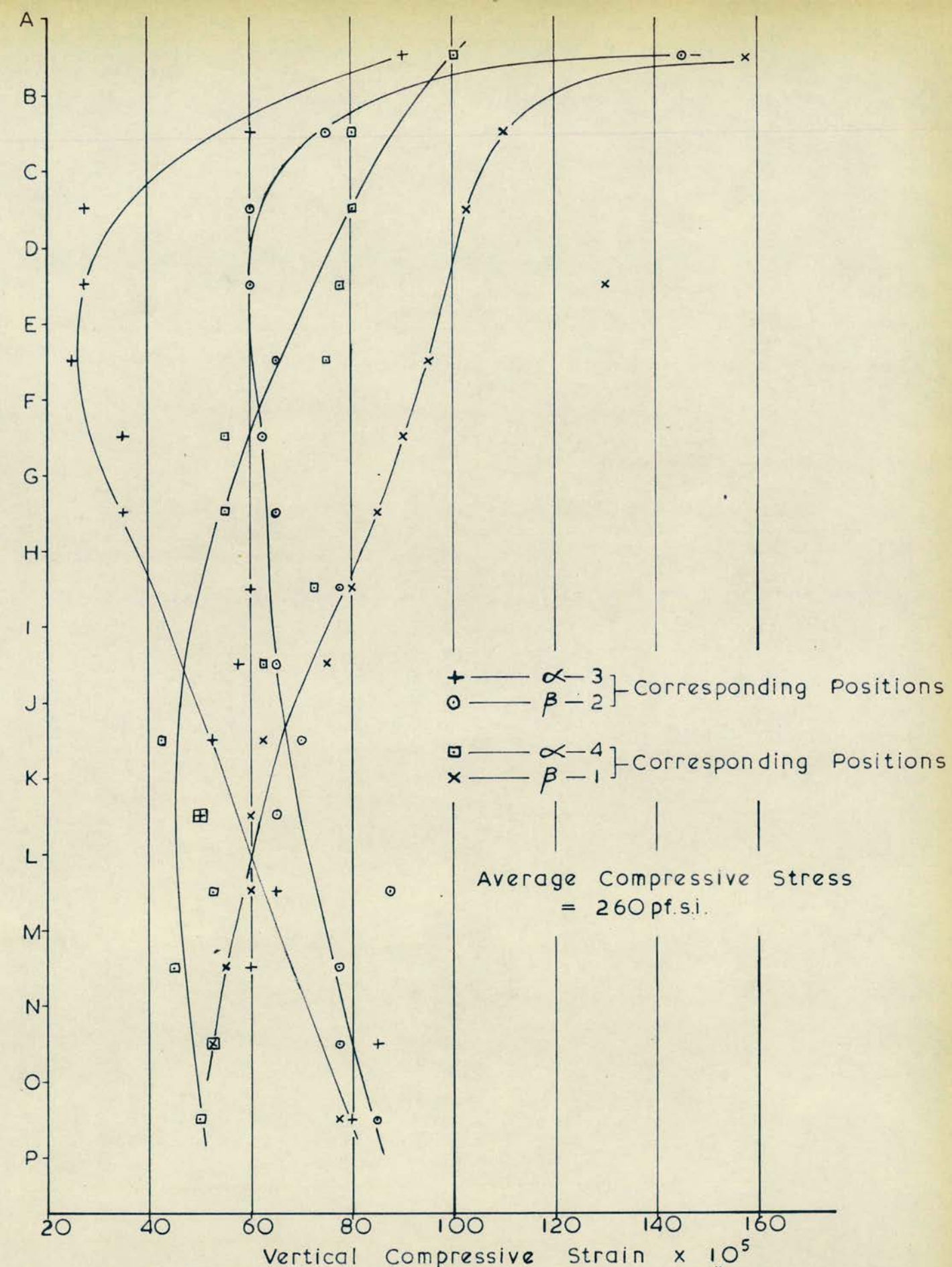
Figs. 10-11 to 10-14 indicate considerable variation in the type of deflection profile obtained.

Fig. 10-12 indicates that the wall ties are not ensuring equal lateral deflections in this test, although in the other tests the deflections of both leaves were approximately equal.

Fig. 10-13 indicates a change in the shape of the deflection profile as the load was increased.

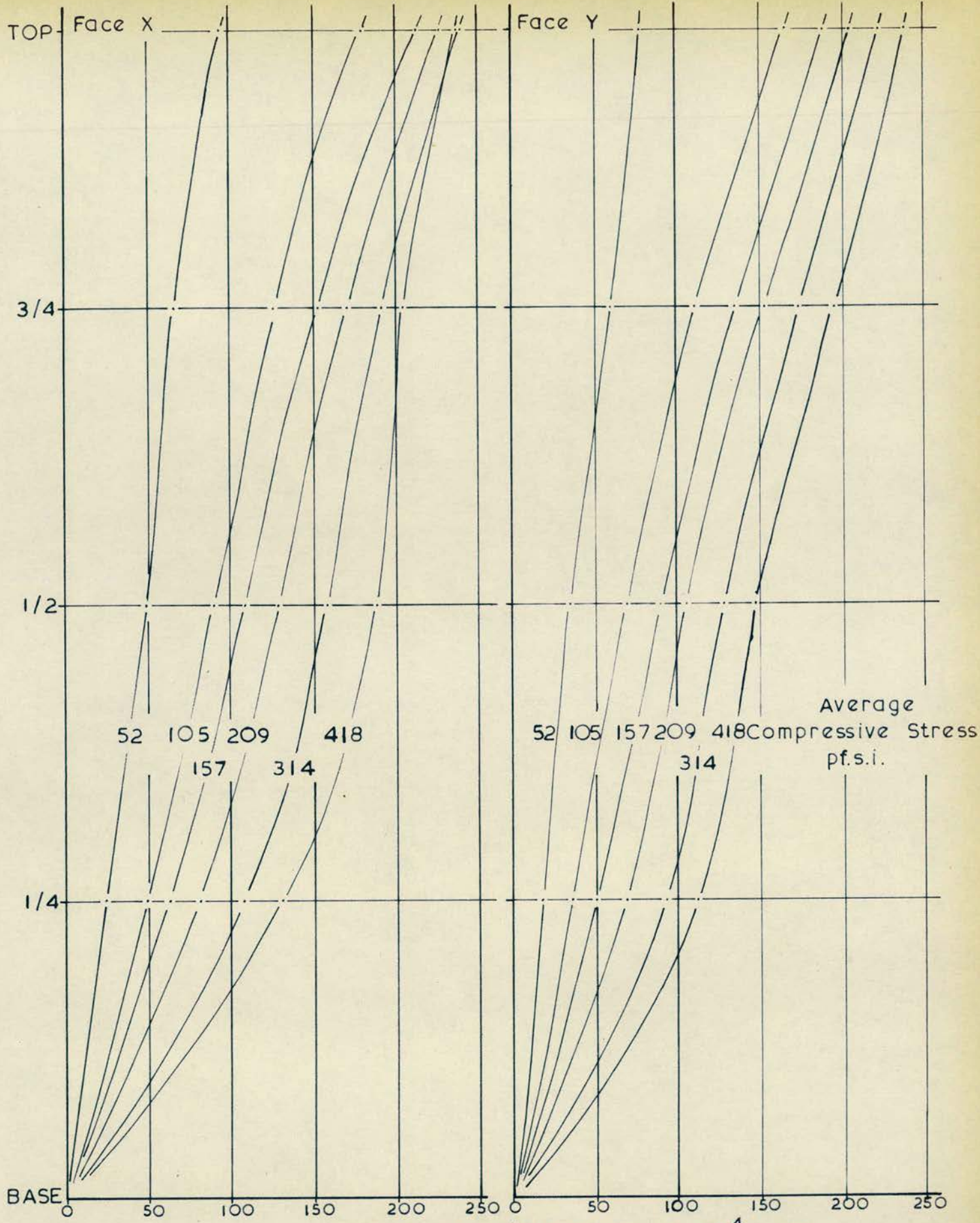
The lateral deflection profiles generally give a good idea of the behaviour of the cavity wall under different types of loading, and Figs. 10-15 and 10-16, replotted for clarity illustrate how base lines may be drawn on the lateral deflection profiles to give bending moment diagrams, which produce stresses which agree with those obtained from the end strains.

An analysis of the dial gauge readings onto the I section, and the lintel reveals that after the initial settling of the wall the angle of



1/3rd. Scale Cavity Wall—Distributed Load— $e=0.5'' \rightarrow Y$
 The Vertical Strain Variation with Position on the Leaf

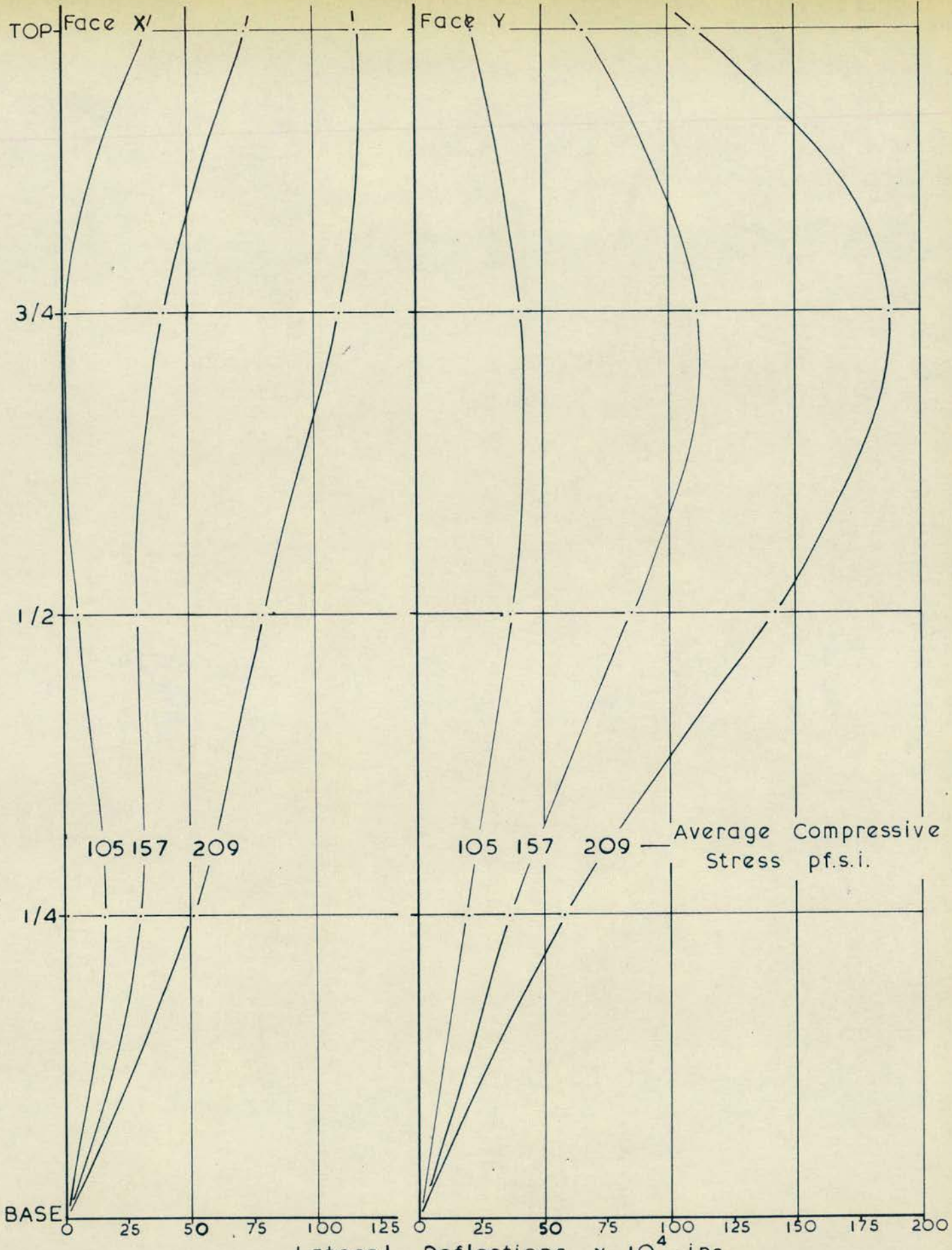
Fig. 10-10



Lateral Deflections $\times 10^4$ — ins.
 1/3rd. Scale Cavity Wall — Distributed Load — $e=0$

Lateral Deflection Profiles

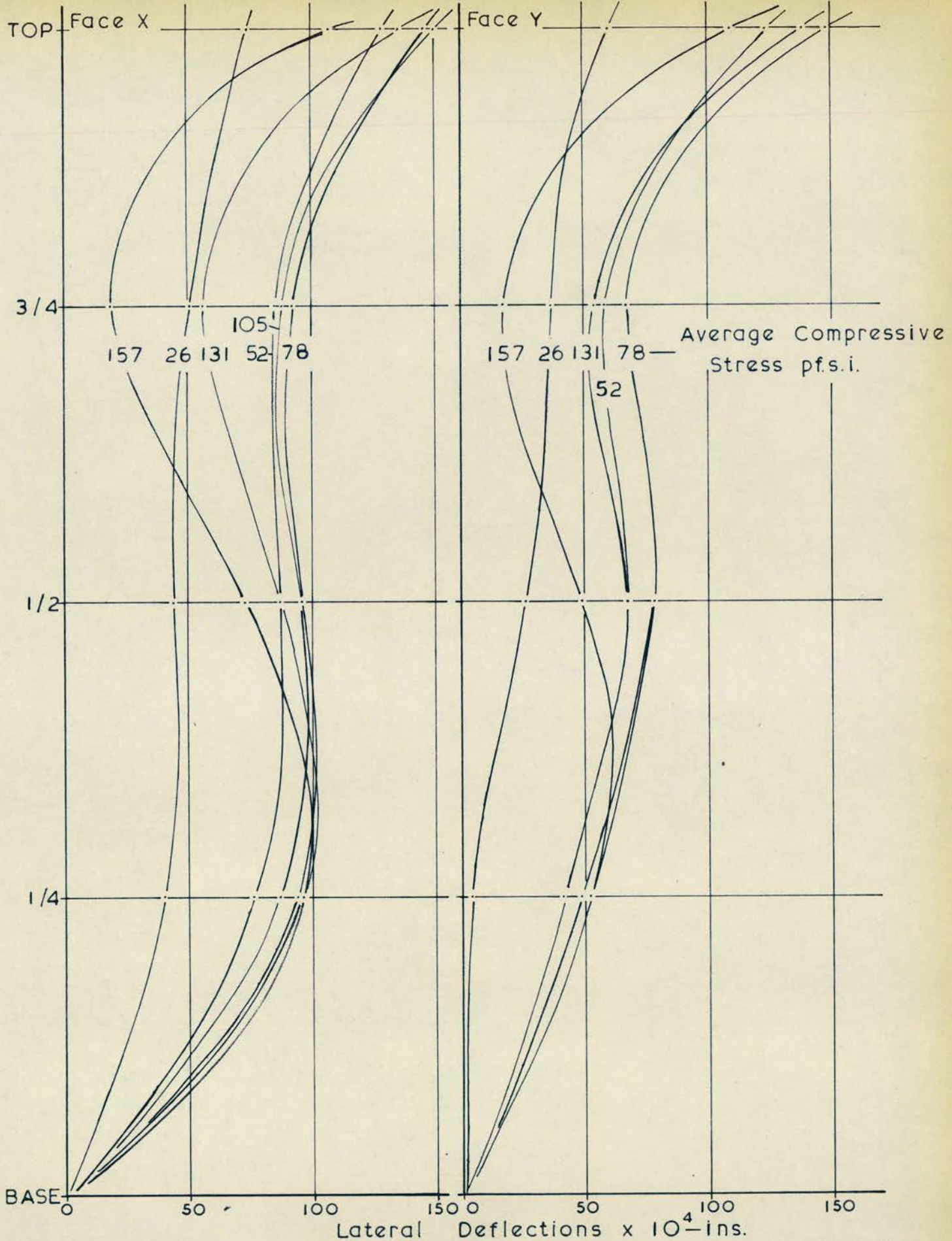
Fig. 10-11



1/3rd. Scale Cavity Wall - Distributed Load - $e = 0.5'' \rightarrow Y$

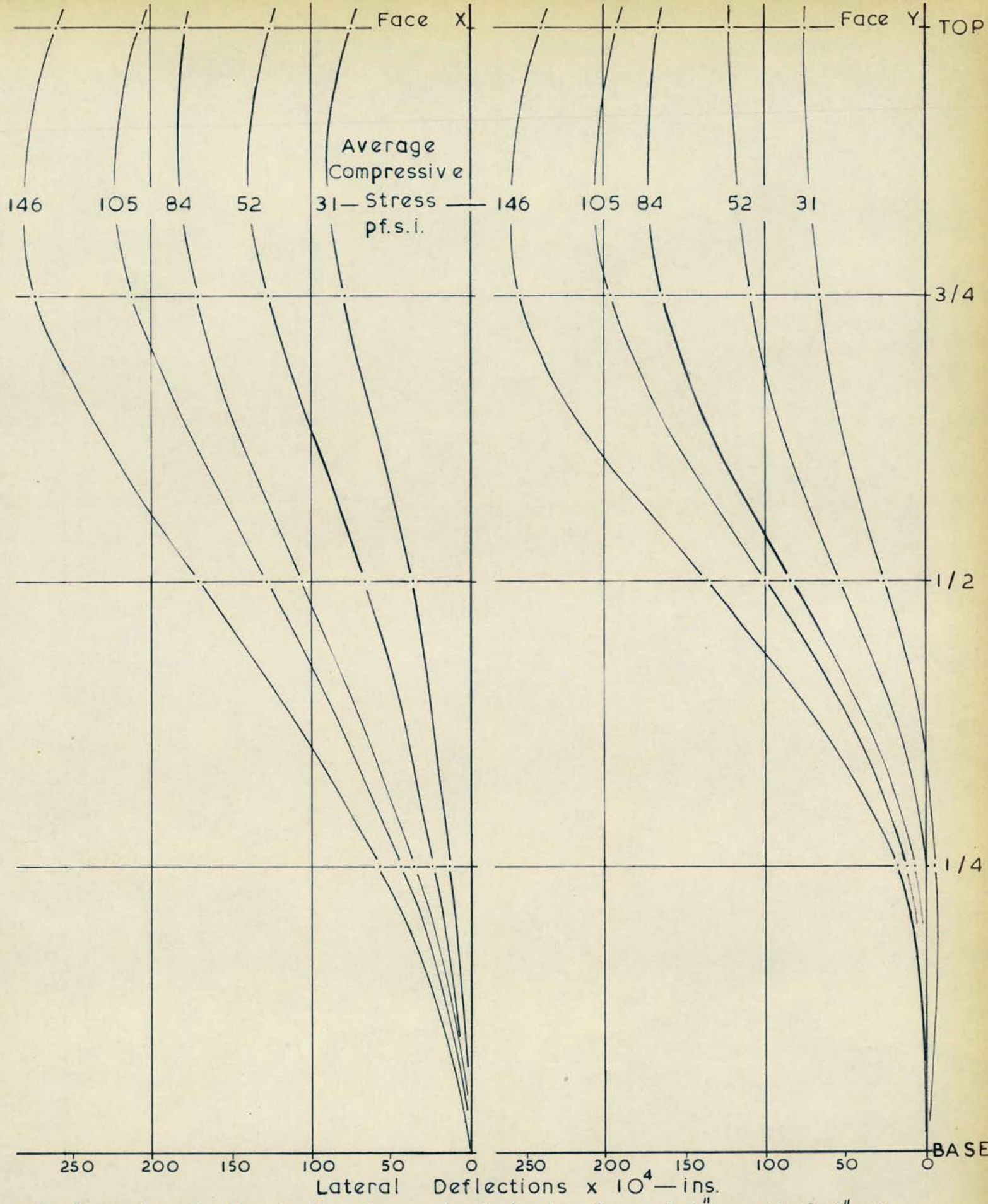
Lateral Deflection Profiles

Fig. 10-12



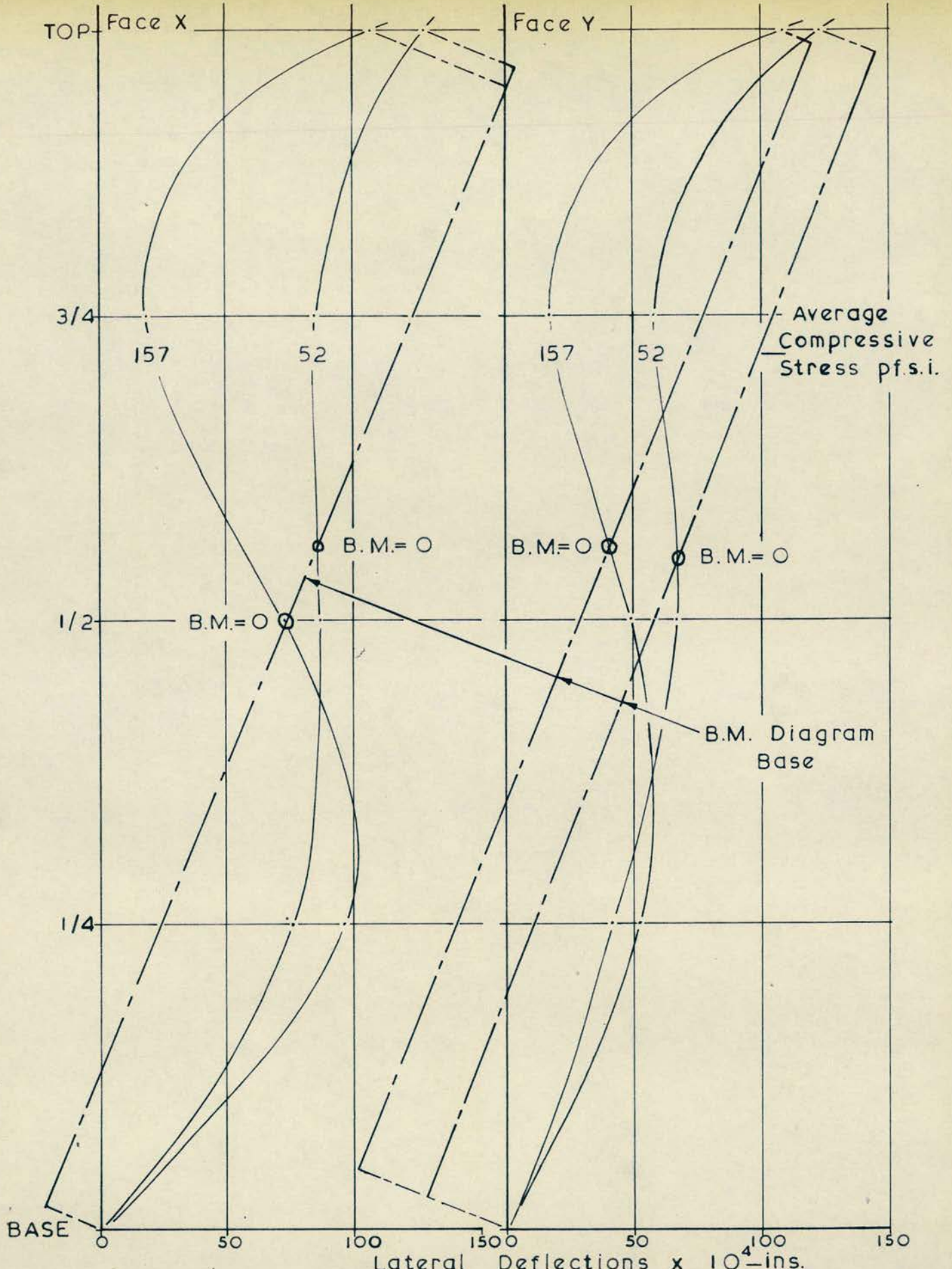
1/3rd. Scale Cavity Wall — Central Concentrated Load — $e = 0.5'' \rightarrow Y$
 Lateral Deflection Profiles

Fig. 10-13



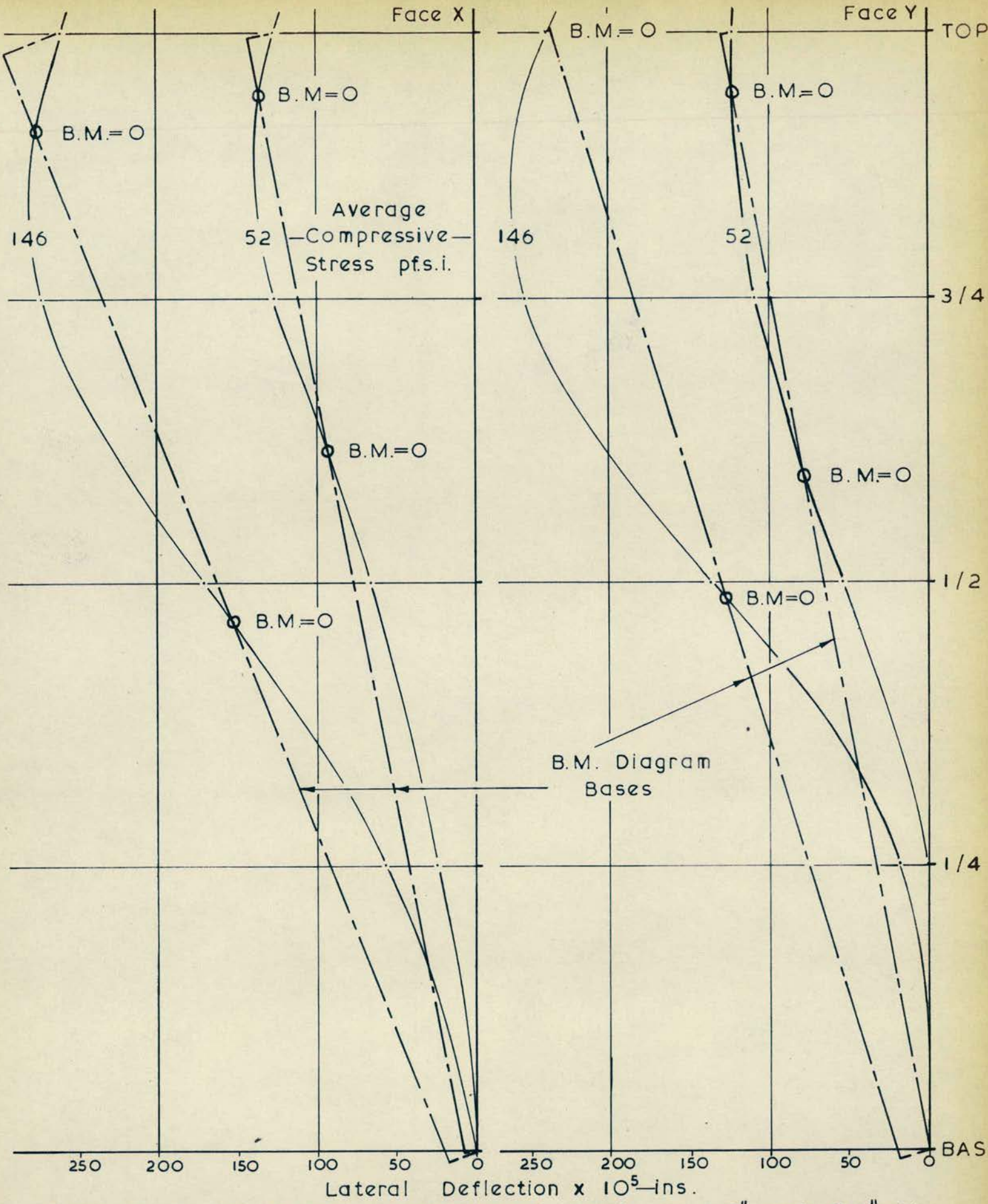
1/3rd. Scale Cavity Wall — Concentrated Load — $e = 3.0'' \rightarrow$ & $0.5'' \rightarrow Y$
 Lateral Deflection Profiles

Fig. 10-14



1/3rd Scale Cavity Wall—Central Concentrated Load— $e=0.5'' \rightarrow Y$
 Estimated Bending Moment Form from Deflections & End Strains

Fig. 10-15



1/3rd. Scale Cavity Wall—Concentrated Load — $e = 3.0'' \rightarrow X$ & $0.5'' \rightarrow Y$
 Estimated Bending Moment Form from Deflections & End Strains

Fig. 10-16

rotation is very small indeed - maximum $1/8^{\circ}$.

7. AN ANALYSIS OF THE BEHAVIOUR OF THE CAVITY WALLS TESTED.

A discussion of the results of the preliminary tests, and the detailed investigation is given in this section.

7.1 THE NEUTRAL AXIS OF THE CAVITY WALL.

From the observed strain ratios in the preliminary tests, at higher eccentricities, and from the detailed end strain measurements of the second series of tests it can be concluded that the leaves of the cavity wall were not bending about the neutral axis of the wall.

The axes about which the leaves bent are unknown, but probably intermediate between the leaf's own axis and the axis of the wall. Generally the leaves appeared to bend about parallel axes, confirming the efficiency of the wall ties as compression and tension members (one test cast some doubt on this). However, the wall ties appear to be incapable of transferring any shear from one leaf to the other and hence of ensuring bending about the combined axis. The relatively small cross-sectional area of the wall ties (0.003 ins.^2) confirms this conclusion.

7.2 THE BEHAVIOUR OF THE WALLS AS UNITS.

From the strain distributions and lateral deflection profiles observed some comments can be made on the mode of behaviour of the cavity walls tested.

The modes of behaviour of the walls in the two test series were slightly different, and may be explained as follows.

In the tests in the first series, and in some of the tests of the

second series, the walls behaved as propped cantilevers, subjected to both an axial compressive load, and a pure moment. In these tests the bending moment diagrams indicated one zero position of B. M., and this was near the base of the wall. This B. M. distribution corresponds to that of a propped cantilever, with some sinking or movement of the prop, and the moment applied at the point of propping. Fig. 10-17 indicates the various possible modes of behaviour of a propped cantilever, showing the corresponding bending moment distributions.

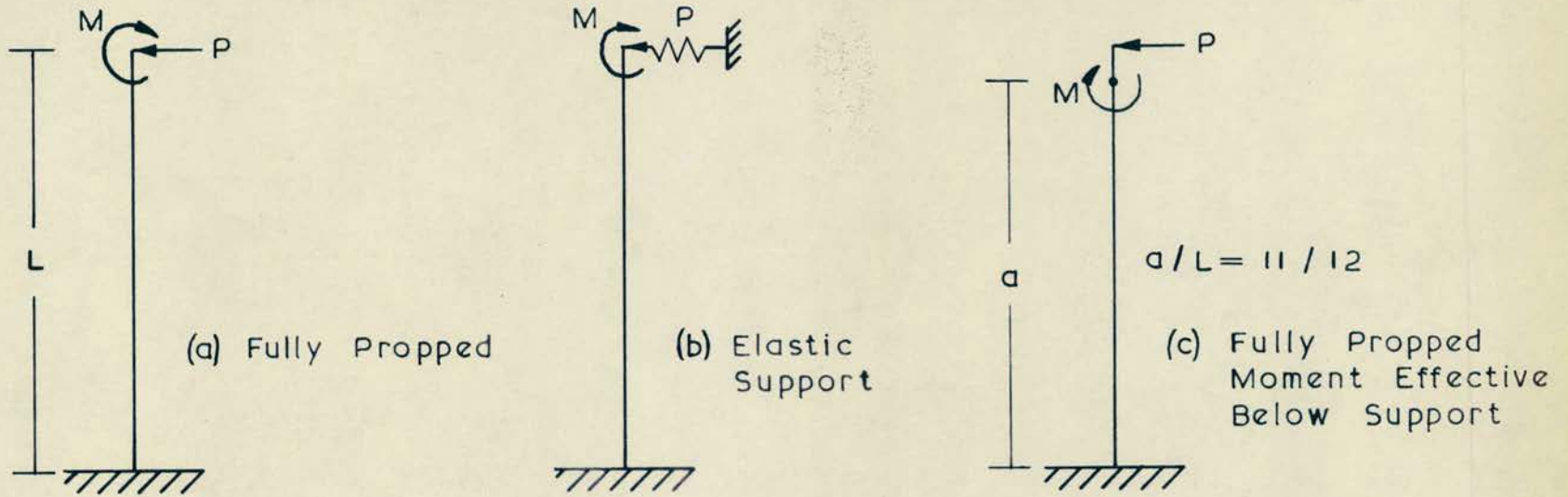
The elastic support condition can be explained by the consideration that the platen of the testing machine was free to move horizontally in the test machine, restrained only by friction.

In the second test series, where the loading was uniformly distributed, the mode of behaviour of the wall was observed to be different from that of the first series.

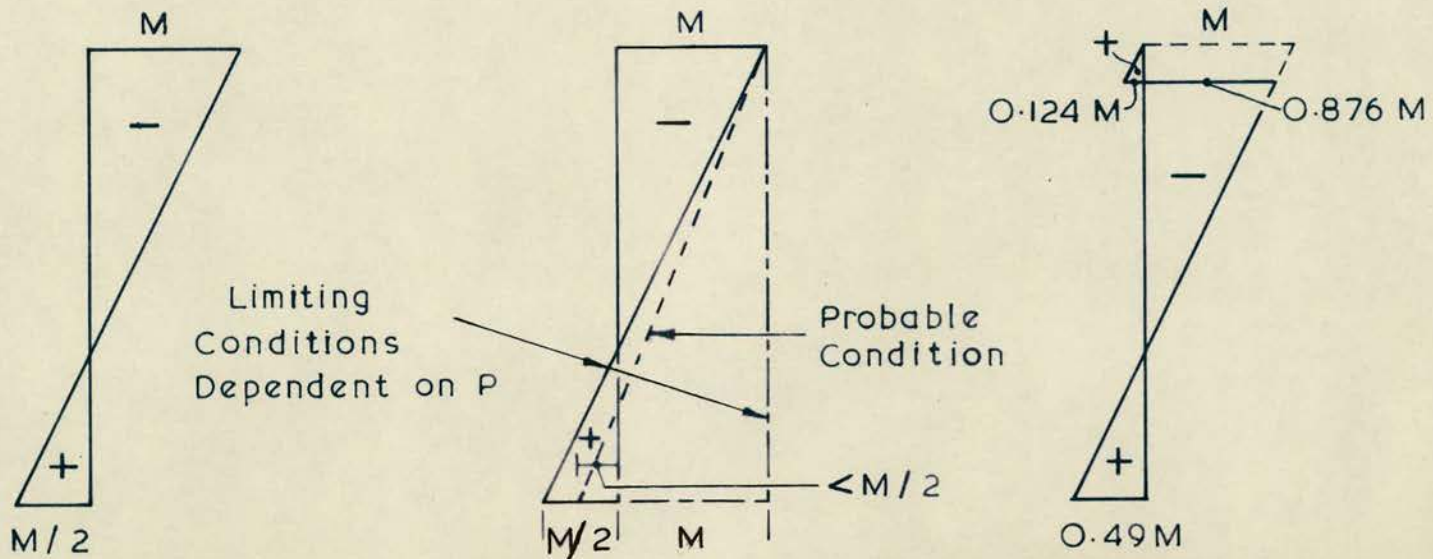
In this series a greater rigidity existed at the point of load application, as the wall had been rotated through 90° , and the platen was no longer free to move laterally. This led to a more fixed end condition, and the wall behaved as a built in beam, subject to an applied moment, and an axial load.

Rotation measurements taken onto the I section, through which the load was applied, and onto the wall lintel, indicated very little rotation in elevation, and hence it seems likely that the moment is effectively applied at the level B, approximately. Fig. 10-18 shows the loading condition, and the resulting B. M. distribution, for the

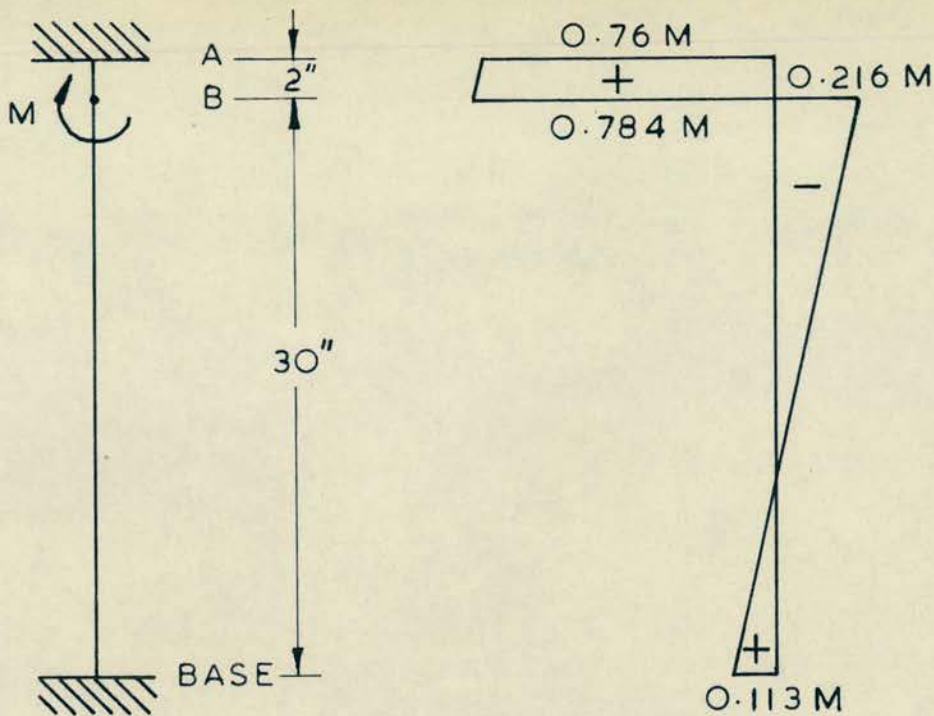
Possible Bending Moment Distributions for a Propped Cantilever Subject to an Applied Moment



Loading Conditions

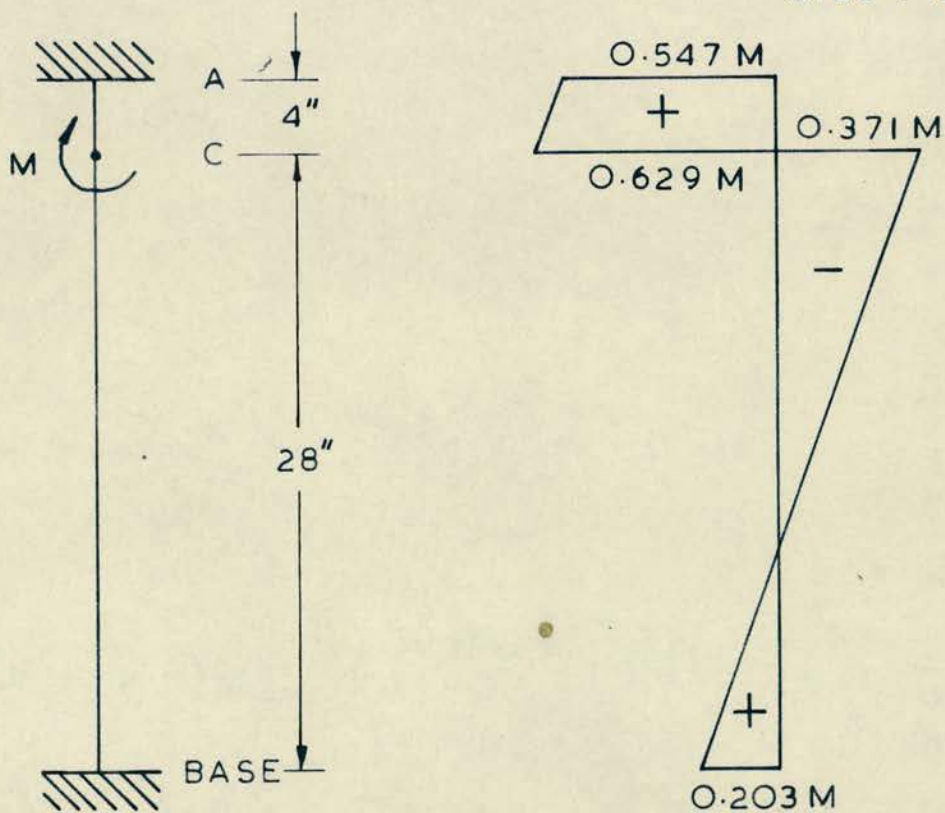


Bending Moment Diagrams



(a) Moment Effective at B

+ve Compression on Side Plotted



(b) Moment Effective at C

Loading Conditions Bending Moment Distributions
Bending Moment Distributions for a Built-in Beam

moment effective at either B or C.

The end strains measured indicated that in the case of the uniformly distributed load, when maximum support rigidity occurs, a change of B. M. sign occurs not only near the base of the wall, but also near the lintel, in the region of level B.

The high level of strains measured in the A-B region is explained by the bending moment distribution for the built in beam case, where the maximum B. M. occurs at the top.

The strains at ends α and β , Figs. 10-6 and 10-7 indicate different modes of behaviour at the two ends, but both show changes in the B. M. profile near the top of the wall. Fig. 10-3 indicates a change of B. M. sign near the top of the wall, and is based on the average strains across the wall face.

The mode of behaviour is clearly complex, and all the factors observed cannot be explained.

8. CONCLUSIONS.

In the eccentrically loaded cavity wall tests the leaves of the walls were observed to bend about separate axes, and not about the combined axis of the wall. If full-scale tests give similar results, and it is likely that with the same types of wall ties the behaviour will be similar, the design implications are important.

The bending moment applied appeared to be shared equally by the leaves, and their lateral deflections were generally similar, indicating the effectiveness of the wall ties in tension and compression.

The basic modes of behaviour of the cavity walls were those

of either a propped cantilever, or a built in beam, subject to axial load and applied moment, and hence the bending moment varied with position on the leaf. The different modes of behaviour observed were thought to depend on the end conditions of the wall.

CHAPTER 11.

CONCLUSIONS.

1. INTRODUCTION.

The aim of the experimental work performed, and described in this thesis, was to investigate stress concentrations in brickwork members.

The investigation was divided into basically two parts. One was an investigation of bearing failure stresses, and the other an investigation of the load distribution in different brickwork members, subject to load concentrations of various types. Allied to the second aim, the deformation properties of several types of brickwork member were investigated.

2. BEARING STRESSES.

2.1 EXPERIMENTAL RESULTS.

- i. The behaviour of full-scale, 1/3rd. scale and 1/6th. scale walls was found to be similar.
- ii. The end loading position produced the lowest failure stresses, and the central loading position the highest failure stresses, for a bearing plate of a particular length. A ratio of approximately 1.3 was found for the Central failure stress/End failure stress, for bearing plate lengths from 9" - $4\frac{1}{2}$ " (full-scale size).
- iii. The failure stress increased with decreasing bearing plate length for both end and central loadings. The increase was rapid with decreasing bearing plate length for central bearing plates $< 4\frac{1}{2}$ " long (full-scale size).

- iv. The effect of the edge distance of the bearing plate was found to be significant, and the failure stress increased rapidly as the edge distance was increased.
- v. Initial cracking stresses were rarely found to be less than $2/3$ of the failure stress, and in the few cases where this occurred, uneven loading was suspected.
- vi. Modes of failure varied, and included vertical cracking below the load, spalling on one or both faces, splitting along the length of the wall, and diagonal cracking away from the zone of load application.
- vii. Increased age of the specimens tested in Series II led to only a small increase in the failure stresses.
- viii. The allowable stresses given by C.P. 111:1964 are adequate, providing satisfactory load factors. In the tests conducted a minimum load factor of 2.7 was found, for one case of end loading, and this value was the same based on either the ultimate or the initial cracking stress, for this failure.

The allowable stresses, based on the codes requirements, are not however based on a rational approach to the problem of a stress concentration, and the load factors in the tests conducted increased as the a'/a factor decreased (bearing plate length/wall length).

In many reinforced and prestressed concrete codes of practice the permissible bearing stress is related to the $\sqrt[3]{a/a'}$. This relationship leads to an increase of 50% in the permissible bearing stress if the a/a' ratio is increased by a factor 3.38, and an increase of 100% if the ratio is increased by a factor 8. (These codes consider

only the axial loading of members).

Considering the experimental results obtained, the following factors emerge, and are presented in tabular form, Table 11-1.

Table 11-1
The Relation Between Failure Stress and $\sqrt[3]{a/a'}$

Bearing Plate Length-ins.	a/a'	$\sqrt[3]{a/a'}$	Failure Stress as a Factor of 9" Failure Stress		
			Full Scale	1/3rd Scale	1/6th Scale
9	k	k1	1	1	1
2.67	3.38k	1.5k1	1.9	1.54	1.61
1.1	8k	2k1	> 2.0	2.0	> 2

k, k1, constants.

Thus for the full-scale (only a limited number of test results available) the 1/3rd scale, and the 1/6th scale brickwork tests the results either gave an increase in bearing stress equal to, or exceeding that indicated on a basis of $\sqrt[3]{a/a'}$.

The range of bearing plate size considered, 9" - 1.1" (full-scale) covers the practical range to be encountered. Hence it would be suitable to adopt a clause into the code allowing an increase in the permissible bearing stress when the bearing plate size is decreased. The permissible stress for the 9" bearing plate is suitable, leading to reasonable load factors.

For the particular size of wall tested in this experimental investigation, and for the range of bearing plates tested, the bearing stress increased in proportion to the $\sqrt[3]{a/a'}$.

Before a definite proposal can be made for the code, giving

a formula relating the permissible bearing stress to the a/a' ratio, further full-scale tests are required.

The failure stress for end bearing tests increased as a/a' increased, but not sufficiently to warrant any increase in the permissible bearing stress, within the range of normal bearing plate size.

2.2 THE CORRELATION OF TEST RESULTS WITH THEORETICAL CONCEPTS AND OTHER EXPERIMENTAL WORK.

i. Theoretical Concepts and Experimental Tests on Concrete.

Various theories have been proposed for determining the stress distribution in, and the failure stresses of elements subject to stress concentrations.

Experimental investigations of the strain distributions in axially loaded concrete blocks have indicated the applicability of many of the theories to practical cases.

The Bleich-Sievers theory was found to give results which correlated best with experimental observations in the range of a/a' values investigated. Unfortunately the range of a/a' values investigated, both experimentally and theoretically, was outside that of the tests described in this thesis.

Guyon's theory, for axial concentrated loadings, was however found to give values of the horizontal transverse tensile stress which were approximately $1/2$ of the experimental results obtained, and stress values for different horizontal sections were plotted, for a'/a ratios from 0 to 1.0. Guyon's stresses may be corrected using certain factors, and the Guyon values, and corrected values are given

in Table 11-2.

The experimental results for 1/3rd and 1/6th scale walls are compared with the theoretical values, in Table 11-2. For various plate sizes the a^1/a ratios, and the theoretical stresses are presented, in terms of $P/2a$, where P is the total applied load.

Assuming failure occurs by tensile splitting, then the theoretical stresses, f_y , may be equated to the brick tensile strength, f_t , and hence the value of P , to cause failure, may be calculated. Hence the bearing stress at failure is obtained ($P/2a^1$), in terms of f_t .

Comparing the theoretical and experimental bearing failure stresses, the value of f_t may be obtained, for a particular bearing plate length, and was calculated for the largest bearing plates for the 1/3rd scale and 1/6th scale tests. The initial cracking stress is considered as the failure stress.

For the 1/3rd scale walls the tensile strength was calculated to be 197.5 pf. s. i., giving an f_c/f_t value of 14.6 (f_c , the brick compressive strength). For the 1/6th scale wall the tensile strength was calculated to be 380 pf. s. i., giving an f_c/f_t value of 17.1. Sinha obtained f_c/f_t values of 13.6 and 15.6 respectively for bricks of the same compressive strengths.

Having calculated the tensile strength of the brickwork, the theoretical bearing stresses at failure may be calculated, and are given in Table 11-2, as factors of f_t , and in pf. s. i., together with the experimental failure stresses.

From Table 11-2 the theoretical and experimental failure

stresses are seen to follow the same pattern of increased failure stress with decreasing a^1/a ratios. The theoretical stresses increase more rapidly however, and for the smallest bearing plates considered the theoretical failure stress is higher than the brick compressive strength, indicating that failure would have occurred in compression. Considering Table 6-29, it is significant that the initial cracking stress practically coincides with the failure stress, indicating that tensile cracking only occurred after failure.

The 1/6th scale tests gave results which were nearer to the theoretically suggested values than the 1/3rd scale results.

In conclusion it may be said that the theoretical values for the horizontal stresses, and the variation in these values together with the bearing stress values at failure, do not provide a suitable analysis for the brickwork structure subject to axial concentrated load, when compared with all the experimental results obtained. The general pattern indicated for the relationship between failure stress and a^1/a ratio does however correspond with that obtained experimentally.

ii. A Comparison with Photo-Elastic Tests.

The photo-elastic tests described in Chapter 2, section 18 provide values for the horizontal splitting stresses, for various a^1/a ratios.

The stresses are given in terms of the applied stress intensity q

For central bearings typical values are $0.04q - a^1/a = 0.1$;
 $0.026q - a^1/a = 0.06$; $0.021q - a^1/a = 0.033$.

If these tensile stresses cause failure, then the bearing stresses,

at the initial failure, are 25 ft, 38.4 ft, and 42.4 ft, respectively for the cases above.

These values, obtained from a test on an araldite plate, are such that for brickwork, where ft is likely to be $(1/12.5 - 1/24) f_c$, where f_c varies from 1,000 - 14,500 p.f.s.i. (Sinha), compression failure will occur in all cases before the brickwork tensile strength is reached, bearing in mind the compressive strength of the bricks used.

By plotting the bearing capacities indicated above, against the a'/a ratios, intermediate values of the bearing capacity can be determined for different a'/a ratios within the range.

Considering the 1/3rd scale test results, and bearing plates 1.05" and 0.52" long, with a'/a ratios of 0.091 and 0.045, the bearing capacities are determined as 42.5q and 28q, with a ratio of 1.52. The experimental results have a ratio of 1.44, based on the initial cracking stress.

Hence, the quantitative results of the photo-elastic tests are not applicable to brickwork, but the trend of increased bearing capacity with increasing a/a' ratio agrees with the experimental results, as does the nature of the strain distribution obtained.

3. THE LOAD DISTRIBUTION AT A STRESS CONCENTRATION.

3.1 SINGLE LEAF WALLS.

- i. In the full-scale and 1/3rd scale tests the strain distributions due to end or central loadings, with zero eccentricities, were found to be similar.

- ii. The strain distributions were as might be expected for a homogeneous material, with bulbs of compressive or tensile strain on horizontal or vertical sections respectively, below the bearing plate.
- iii. The degree of load distribution was effectively less than 45° , as when it extended to 45° the maximum strains were still measured below the bearing plate.
- iv. For end loadings a triangular strain distribution was noted, towards the base, and tensile strains were often found towards the unloaded end.
- v. A series of full-scale tests, in which the position of the bearing plate was varied indicated that two types of tensile strains exist in a stress concentration. These are splitting and tear tensile strains. The relative magnitude of the two was found to vary with load position, and the variation was found to correlate with photo-elastic tests conducted, and described in Chapter 2. The strain magnitudes could not be correlated however, and individual brickwork tests gave widely differing strain magnitudes.
- vi. The brickwork loading tests in v. above indicated that the end edge strains were only high when the load was actually at the end of the wall. Once positioned even a small distance from the edge of the wall, the vertical strain distribution is similar to that of a central loading.

3.2 CAVITY WALLS.

- i. Load that was uniformly distributed along the lintel produced strains which were generally uniform across the wall faces, indicating

only slight local concentrations of stress.

- ii. Eccentric distributed load produced strains of different magnitudes on the leaf faces, and these strains varied from the lintel to the base of the wall.

Increased eccentricity of load had a clear effect on the relative strains on the two faces, the surface strain ratios increasing with increasing eccentricity.

Increased stress had only a slight effect and increased the strain ratios.

- iii. Concentrated loadings produced bulbs of pressure, similar to those observed with the concentrated loadings without a lintel.

The effect of increased eccentricity of load, and increased stress was as in ii. above.

- iv. End concentrated loadings were found to produce tensile strains of considerable magnitude at the unloaded end, and high compressive edge strains at the loaded edge. At some depth the distribution was triangular across the leaf faces, and the tensile edge stresses disappeared.

- v. Vertical strains measured on the ends of the leaves indicated that for all types of loading the behaviour of the walls was essentially the same, and the leaves were found to bend about independent axes. The axes of bending appeared to be parallel, and the applied moment equally shared by the two leaves.

- vi. Lateral deflection measurements indicated that generally speaking both leaves assumed the same deflected profile, indicating

the efficiency of the wall ties.

- vii. From the strain ratios on the faces, the end strains, and the lateral deflection profiles the mode of deformation of the wall could be determined. Some variance was noticed between the two test series, and was judged to be due to slightly different end conditions.

The mode of behaviour was either that of a propped, or partially propped cantilever, in the first test series, and part of the second test series, or of a built in beam in the other tests of the second series. In both cases the loading consisted of an applied moment, and an axial load.

- viii. One failure test with distributed axial stress gave a failure by vertical splitting (many vertical hair cracks were observed) followed by spalling on the faces (not directly beneath the lintel), and finally a complete collapse.

In this test the horizontal strains were large enough to be measured, and indicated the formation of the vertical cracks before they were visible.

4. THE DEFORMATION CHARACTERISTICS OF BRICKWORK.

- i. The Young's Moduli determined for the bricks used for the model construction were similar to those of the brickwork walls constructed.

- ii. The Stress/Compressive strain relationship for the walls constructed was such that Young's modulus (tangent) increased with increasing stress at low stresses. The value was then constant, over a large stress range, and eventually decreased, at higher stress in the

failure zone.

- iii. The Stress/ Horizontal strain relationship was non-linear, or linear over only a very low stress range, and indicated that cracking occurred at low tensile strains, when the horizontal stress exceeded the tensile strength of the bricks. The stress/strain plots clearly indicated the cracking of the section.
- iv. The strain readings on the brickwork cubes indicated the irregularity of the stress distribution before cracking occurred. The early formation of vertical cracks was also indicated. The failure stress was not however affected by the initial unevenness, and consistent failure stresses were obtained.

The average vertical strain plotted against compressive stress indicated much irregularity at low stress, but a linear relationship at higher stresses.

Horizontal strains measured did not indicate any capacity for brickwork to sustain tensile strains of any magnitude before cracking occurred.

5. SUMMARY.

The behaviour of brickwork walls, loaded to failure by concentrated loadings, of various sizes, and variously positioned has been determined. The results justified the adoption of the model technique.

The requirements of C.P. 111 : 1964 were found to be adequate, the minimum load factor being 2.7, based on the initial cracking stress of the specimen. For central loadings of the smaller sizes tested the

load factors were considerably higher, and the tests conducted point to a relationship of the form $f_b = k \sqrt[3]{a/a'}$, where f_b is the bearing stress when the first cracks form, and k is a constant dependent upon the brick and mortar properties, or more generally the brickwork strength.

The strain distributions in the brickwork, and the deformation properties of the brickwork units indicated a mode of behaviour similar to that of an elastic homogeneous body, except where the material was subject to tensile stress.

The behaviour of eccentrically loaded cavity walls indicated that the resistance to bending depended on the bending resistance of each leaf, rather than that of the system as a unified structure.

Table 11-2

The Correlation Between Experimental and Theoretical
Failure Stresses

	Bearing Plate Size - ins.	a'/a	Transverse Tensile Stress - f_y (Guyon) - Factor of $P/2a$	Corrected f_y - Factor of $P/2a$	Bearing Failure Stress - f_b - Factor of f_t	f_b pf. s. i.	f_b Experimental pf. s. i.
1/3rd Scale Series I	3.0	0.261	0.33	0.776	4.94	975	975
	2.0	0.174	0.39	0.870	6.6	1,305	1,165
	1.05	0.091	0.45	0.954	11.5	2,270	1,585
	0.52	0.045	0.475	0.978	22.7	4,480	2,285
1/6th Scale Series I	1.52	0.262	0.33	0.776	4.94	1,865	1,865
	1.03	0.174	0.39	0.870	6.6	2,500	2,790
	0.52	0.091	0.45	0.954	11.5	4,180	3,460
	0.28	0.045	0.475	0.978	22.7	8,600	5,235

REFERENCES.

1. Br. Standards C.P. C.P. 111:1964 Structural Recommendations for Loadbearing Walls.
2. Monk, C.B. Jr. Old & New Research on Clay Masonry Bearing Walls - Proc. National Brick & Tile Bearing Wall Conference - Sponsored by S.C.P.I. - N.W. Washington - 1965.
3. Davey, N. & Thomas, F.G. The Structural Uses of Brickwork - Structural & Building Paper No. 24 - London - Institution of Civil Engineers - 1950.
4. Various Report on Bearing Pressures on Brick Walls - The Structural Engineer - Aug. 1938.
5. S.C.P. Research Foundation European Clay Masonry Load Bearing Buildings - S.C.P.R.F. - Geneva, Illinois.
6. Hast, N. Measuring Stresses and Deformations in Solid Materials.
7. Wood, R.H. The Composite Action of Brick Panel Walls Supported on Reinforced Concrete Beams - Nat. Bldg. Studies - Res. Paper No. 13 - H. M.S. O.
8. Roberts, A. The Photo-elastic Glass Insertion Stressmeter - Paper Presented to Groupement pour L'Avancement des Methodes d'Analyse des Contraintes - Dec. 1964.
9. Vogt, H. Consideration and Investigations of the Basic Properties of Model Tests for Brickwork and Masonry Structures - Libr. Commun. No. 932. D.S.I.R., B.R.S. - Garston - Jan. 1960.

10. Haller, P. The Properties of Load Bearing Brickwork in Perforated Fired Bricks for Multi-Storey Buildings - Libr. Comn. 870 - B.R.S., Garston - Feb. 1959.
11. Sinha, B.P. Splitting Failure of Brickwork as a Function of the Deformation Properties of Bricks and Mortar - S.C.R.U. - Res. Report - Feb. 1966.
12. Onishchik, L.I. Masonry Structures - Stroizdat - 1939.
13. Polyakov, S.V. Masonry in Framed Buildings - Moscow - 1956 - Trans. by B.R.S., D.S.I.R.
14. Sementsov, S.A. & Kameiko, V.A. The Strength and Stability of Large-Panel Constructions - Trans. by W.L. Goodman & Edited by Br. Cer. Res. Assoc.
15. S.C.P.I. Technical Notes on Brick & Tile Construction - Nov. - Dec. 1964.
16. Iyengar, K.T. & Yogananda, C.V. A 3-D Stress Distribution Problem in the Anchorage Zone of a Post-tensioned Concrete Beam - Mag. of Concrete Res. - Vol.18.No.55 - June 1966.
17. Boussinesq, J.V. Application des Potentiels à l'Etude de l'Equilibre et du Mouvement des Solides Élastiques - Paris - Gauthier - Villars - 1885.
18. Flamant Compt. Rend. - Vol. 114, p.1465 - Paris - 1892.
19. Michell, J.H. Proc. London Math. Soc. - Vol.34, p. 134 - 1902.
20. Coker, E.G. & Filon, L.N.G. A Treatise on Photo-elasticity - Cambr. Univ. Press - 1931.
21. Shepherd, W.M. Stress Systems in an Infinite Sector - Proc. Royal Soc. (London) - Vol.148, p. 284 - 1935.

22. Gerstner, R.W.
& Zienkiewicz, O.C. A Note on Anchorage Zone Stresses -
Journal Amer. Conc. Instit. - June,
1962 - Proceedings, 1959.
23. Iyengar, K.T. 2-D Theories of Anchorage Zone
Stresses in Post-Tensioned
Prestressed Concrete Beams -
Journal Amer. Conc. Instit.
Proceedings - Vol. 59, No. 10,
p. 1443-1466 - 1962.
24. Ross, A.D. Some Problems in Concrete
Construction - Mag. of Conc. Res.
- Vol. 12, No. 34 - March, 1960.
25. Douglas, D.J.
& Trahair, N.S. An Examination of the Stresses in
the Anchorage Zone of a Post-
Tensioned Prestressed Concrete
Beam - Mag. of Conc. Res. -
Vol. 12. No. 34 - March, 1960.
26. Christodoulides, S.P. 3-D Investigation of the Stresses
in the End Anchorage Blocks of
a Prestressed Concrete Gantry
Beam - The Struct. Eng. - Vol. 1.
35, No. 9, p. 349-356 - Sept. 1957.
27. Christodoulides, S.P. A 2-D Investigation of the End
Anchorages of Post-tensioned
Concrete Beams - The Struct.
Eng. - Vol. 33, No. 4, p. 120-133 -
April, 1955.
28. Ban, S, Nugurama, H.,
& Ogaki, Z. Anchorage Zone Stress Distributions
in Post-tensioned Concrete Members
- Proceedings of the World
Conference on Prestressed Concrete
at San Francisco - p. 16-1 -16-14
- July, 1957.
29. Zielinski, J.
& Rowe, R.E. An Investigation of the Stress
Distribution in the Anchorage Zones
of Post-tensioned Concrete Members
- Cem. and Concr. Assoc. -
Research Report 9 - 1960.
30. Meyerhof, G.G. The Bearing Capacity of Concrete
and Rock - Mag. of Conc. Res. -
Vol. 4 - April, 1953.

40. Br.St. Instit. B.S. 1257 : 1945 - Methods of Testing, Clay Building Bricks.
41. Br. St. Instit. B.S. 1200:1955 - Concrete Aggregates and Building Sands.
42. Br. St. Instit. B.S. 12 : 1958 - Portland Cement, Ordinary and Rapid Hardening.
43. S.C.P. Research Foundation National Testing Programme - Structural Clay Products Research Foundation - Geneva - Illinois.
44. B.C.R.A. The Effect of the Testing Method on the Results of the Nine Inch Cube Test for the Strength of Brickwork - British Ceramic Research Association - March, 1965.
45. Zellerer, E. von & Thiel, H. Uber das Kraftfeld einer Tragawrd auf Zwei Stutzenmit Drei Tueroffnungen bei Unsymmetrischer Einzelbelastung - Die Bautechnik - March, 1959.
46. Sinha, B.P. Model Studies Relating to Load-Bearing Brickwork - Ph. D. Thesis - University of Edinburgh - May, 1967.
47. Benjamin, J. R. and Williams, H. A. The Behaviour of One Storey Brick Shear Walls - Proc. A.S.C.E. - Vol. 84, No.ST.4, Paper No. 1723 - 1958.
48. Murthy, C.K. Model Studies Related to Load-Bearing Brickwork - Ph. D. Thesis - University of Liverpool - 1964.
49. Prasan, S. Structural Interaction of Reinforced Concrete Floor Slabs and Single Leaf Brick Walls - M.Sc. Thesis - University of Liverpool - 1963.
50. Stedham, M.E.C. Quality Control of Load-Bearing Brickwork. Part 1. 9ins. Cubes. Preliminary Results - Transactions of the British Ceramic Society - Vol. 64 - Jan. 1965.

51. Stedham, M.E.C. Quality Control for Load-Bearing Brickwork. Part 2. 9 ins. Cubes. Further Results. Proceedings of the British Ceramic Society - July, 1965.
52. Lenczner, D. Strength and Elastic Properties of Brickwork Cubes - Transactions of the British Ceramic Society - Vol. 65 - June, 1966.
53. Bradshaw, R.E. Load Bearing Brickwork Walls - M.Sc. Thesis - University of Edinburgh - Mar. 1966.
54. Bradshaw, R.E. and Hendry, A.W. The Influence of Mortar Joint Thickness on the Strength of Brickwork. Part 2. Theoretical Investigation - S.C.R.U. - Sept. 1966.
55. West, H.W.H. Everill, J.B. and Beech, D.G. Development of a Standard 9 ins. Cube Test for Brickwork - Transactions of the British Ceramic Society - Feb. 1966.
56. Sahlin, H. The Structural Interaction of Walls and Floor Slabs - Stockholm - 1959.
57. Thomas, F.G. The Strength of Brickwork - The Structural Engineer - Feb. 1953.